DIC
SOCIEDADE BRASILEIRA DE CARDIOLOGIA • SBC 1943

ABC Imagem Cardiovascular

Volume 36 | Number 2
April/May/June 2023

Sociedade Brasileira de Cardiologia
ISSN-2675-312X

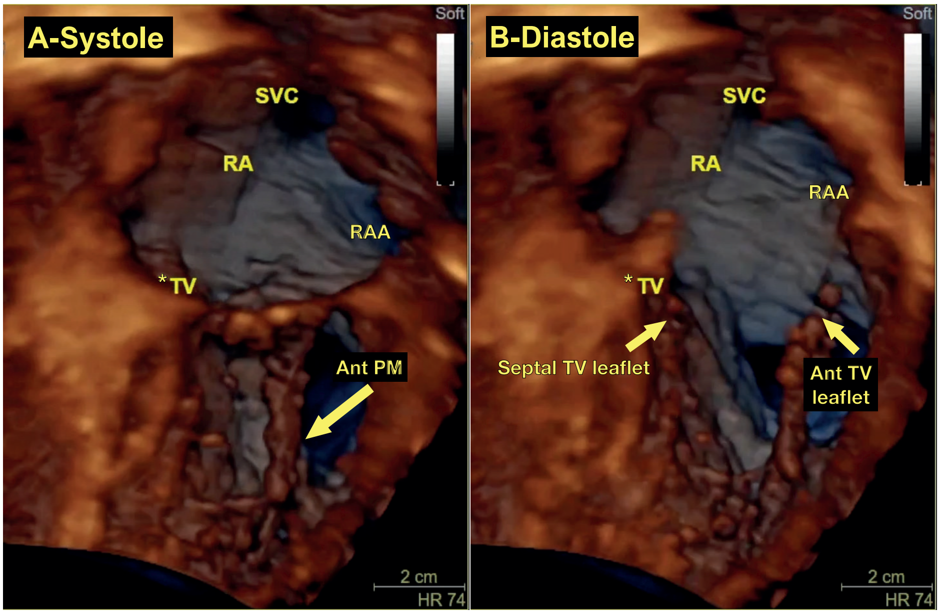

Figure 1 of the article: My Approach to Three-Dimensional Echocardiography for Pathophysiological Classification of Tricuspid Regurgitation

ABC Imagem Cardiovascular

Contents

Click on the title to read the article

Review Article

Case Report

Case Report

Image

Review Article

ABC Imagem Cardiovascular

ABC Imagem Cardiovascular

Volume 36, Nº 2, April/May/June 2023

Indexing: Lilacs (Latin American and Caribbean Health Sciences Literature), Latindex (Regional Cooperative Online Information System for Scholarly Journals from Latin America, the Caribbean, Spain and Portugal) and DOAJ (Directory of Open Access Journals)

Address: Av. Marechal Câmara, 160 - 3º andar - Sala 330
20020-907 • Centro • Rio de Janeiro, RJ • Brazil
Phone.: (21) 3478-2700
E-mail: abcimaging@cardiol.br
https://www.abcimaging.org/

Commercial Department
Phone: (11) 3411-5500
E-mail: comercialsp@cardiol.br

Editorial Production
SBC - Scientific Department

Graphic Design and Diagramming
SBC - Scientific Department

Editorial

How to Manage a Cardiovascular Imaging Journal? Reflections and Ideas

Gerald Maurer[1,2]

Medical University of Vienna,[1] Wien – Austria

European Heart Journal Cardiovascular Imaging,[2] Oxford - United Kingdom

Cardiovascular Imaging is a rapidly growing field with an increasing impact on clinical practice. Each imaging modality has undergone remarkable development in recent years, requiring a very specialized understanding not only of physiology and disease processes, but also of technical aspects and physics. This has been reflected not only in the number but also in the complexity of published papers (as in most fields of medicine). While just two or three decades ago, cardiovascular imaging topics could be adequately covered in the major general cardiology journals, this is no longer the case and has led to the establishment of journals specializing in the field.

When managing a scientific journal, several issues need to be considered. These include its overall goals, its target audience, affiliation to an academic society, and relationship to other journals. The European Heart Journal Cardiovascular Imaging[1] is the official journal of the European Association of Cardiovascular Imaging, which is a branch of the European Society of Cardiology. The journal's goals are, to a great extent, influenced by these affiliations and by their policies. As stated in its title, it is a European journal, but it nevertheless aims to serve the international community, including readers, editorial board, and authors. Indeed, at this point, a large percentage of our readers are from outside Europe and we receive many submissions from other continents. Similarly, the American College of Cardiology and the American Heart Association publish dedicated imaging journals in conjunction with their more general journals. It is therefore important that a large and vital country like Brazil, with its excellent and active cardiological community, publish a journal such as ABC Imagem Cardiovascular on behalf of the Brazilian Society of Cardiology.

Until some years ago scientific journals were printed only. With the advent of the internet there has been a move toward online publications. Currently, many journals follow a hybrid approach, with simultaneous print and online publication. While some demand for printed hardcopies continues, most readers have preferred the online versions and some journals abandoned the print issues. Obviously, the online version has the advantage of being published more promptly and better disseminated, and more easily accessible. In addition, in view of the proliferation of publications in the medical literature, physical storage space for paper journals becomes an issue. Any imaging journal requires the ability to provide high quality images to the reader. While still frames images can be delivered in print, dynamic video material can only be viewed online (the use of supplementary CDs and DVDs for this purpose has largely been abandoned).

Open Access publication is an important issue peer-reviewed academic journals are confronted with. Traditionally the cost of publishing has been paid by the reader, either in form of a subscription fee (personal or institutional), site license, or by purchasing individual articles. This model has hampered the accessibility to scientific research, especially in poorer countries. Thus, to an increasing degree many funding or governmental agencies that sponsor and finance scientific research require open access publication.[2] This has led to the evolution toward open-access journals, which are characterized by funding models that do not require the reader to pay for accessing the journal's contents. Instead, fees are paid by the author or via funding from other sources, such as public funding, subsidies and grants. In the hybrid model, there is a combination of the traditional approach, where some articles are available for subscribers or by purchase, with the online access, paid for by the author. There are, however, increasing initiatives toward publishing research sponsored by state-funded institutions in journals that are freely available. In Europe the so-called Plan S initiative was initiated by a consortium of national research agencies and funders from twelve European countries. Plan S pushes for publishing in truly open access journals, that are freely available to all. Hybrid journals are not considered to be compliant with Plan S unless they are part of a transformative agreement. However, there are also clear downsides to the open access model. For many authors, the publication fee can be a considerable financial burden, particularly when trying to publish smaller studies with limited funding. On the publishing side, even some prestigious journals have experienced an immediate and drastic drop in the number of submissions after switching to a fully open access model.[3]

Importantly, the rating of journals deserves mention, and different metrics have been used. The most popular is the impact factor,[4] calculated as the ratio between the number of citations received in a year and the total number of citable items published in that journal during the two preceding years. The impact factor receives a lot of criticism for its shortcomings,[5] which include flawed statistical validity, inapplicability to individual scientists and between-discipline differences. Despite many concerns, the impact factor continues to be the most widely followed metric by the

Keywords

Cardiovascular therapy; medical publishing; journal ranking; open access.

Mailing Address: Gerald Maurer •
Department of Cardiology, Medical University of Vienna. Spitalgasse 23, 1090. Vienna, Austria.
E-mail: gerald.maurer@meduniwien.ac.at

Manuscript received March 13, 2023; revised manuscript March 13, 2023; accepted March 20, 2023.
Editor responsible for the review: Daniela do Carmo Rassi Frota

DOI: https://doi.org/10.36660/abcimg.20230030i

public. Some alternative metrics have been proposed, like the Eigenfactor,[6] which weights citations from highly ranked journals to count more than those from poorly ranked journals, and the Citescore that reflects the yearly average number of citations to recent articles published in a journal. A very different type of measure, the Altmetrics score[7] has gained widespread as a complement to more traditional metrics, to assess impact based on diverse online research output, such as social media, online news media, and online reference managers. Also, the importance of other measures, such as the number of downloads, content engagement, and total number of citations needs to be recognized. There can be striking discrepancies: some papers may have a relatively small number of citations but a very large number of downloads, as often seen for publications that are highly relevant for routine practice but perhaps not for cutting-edge research.

So, what determines the true success of a journal? Which path should an editor pursue? There are differences between various journals' objectives and missions, but what ultimately counts are integrity, scientific quality, and, most importantly, usefulness to its readers.

References

1. Taylor J. A New ESC Journal for All Cardiac Imaging Modalities. European Heart Journal. 2012;33:281–289.
2. Brainard J. Open Access Takes Flight. Science. 2021;371(6524):16-20. doi: 10.1126/science.371.6524.16.
3. van Noorden R. Open-Access Plan S to Allow Publishing in Any Journal. Nature. 2020 Jul 16. doi: 10.1038/d41586-020-02134-6.
4. Hoeffel C. Journal Impact Factors. Allergy. 1998;53(12):1225. doi: 10.1111/j.1398-9995.1998.tb03848.x.
5. Callaway E. Beat it, Impact Factor! Publishing Elite Turns Against Controversial Metric. Nature. 2016;535(7611):210-1. doi: 10.1038/nature.2016.20224.
6. Bergstrom CT, West JD, Wiseman MA. The Eigenfactor Metrics. J Neurosci. 2008;28(45):11433-4. doi: 10.1523/JNEUROSCI.0003-08.2008.
7. Chavda J, Patel A. Measuring Research Impact: Bibliometrics, Social Media, Altmetrics, and the BJGP. Br J Gen Pract. 2016;66(642):e59-61. doi: 10.3399/bjgp16X683353.

Editorial

Contrast Echocardiography in Real Life: Practicality, Safety, and Cost-Effectiveness

Márcio Silva Miguel Lima[1,2]
Instituto do Coração (InCor), Faculdade de Medicina, Universidade de São Paulo,[1] São Paulo, SP – Brazil
Grupo Fleury,[2] São Paulo, SP – Brazil

After approximately 2 decades of use in practice, based also on several clinical studies, it can be stated that ultrasound enhancing agents (UEA) are extremely safe, following recommendations for their preparation and administration.[1-5] Severe adverse events are very rare, with an approximate prevalence of around 1 in every 10,000 administrations, anaphylactoid reactions being the most frequent.[1,6-8] Specifically with the contrast SonoVue® (sulfur hexafluoride) used in Brazil, Furtado, Rassi, et al., in their safety study, reported a very low incidence of only 0.6% of allergic reaction in their population of 1,099 patients who received this agent.[9] In general, allergic reactions occur immediately or within 30 minutes after administration; they are of mild intensity and transitory. The most common presentation is the appearance of erythematous skin lesions and urticaria. In this scenario, however, special attention should be paid to respiratory signs and symptoms, such as dyspnea, laryngeal stridor, and bronchospasm, as well as signs and symptoms of progression to eventual circulatory collapse, such as dizziness, paleness, and hypotension, as these are warning signs for the onset of anaphylactic shock. Patients must be carefully evaluated and observed, and measures aimed at anaphylaxis should be promptly instituted with antihistamines, corticosteroids, and epinephrine, following the care protocol of the institution, whose personnel must be very well trained.[3]

In October 2007, the United States Food and Drug Administration (FDA) issued a general contraindication ("black box") for the use of Definity® and Optison® agents in acutely ill patients after analysis of 11 deaths potentially related to the use of these UEA. This restriction was later withdrawn after subsequent clinical studies provided extensive evidence of safety. Advanced pulmonary disease and pulmonary hypertension initially represented contraindications, but clinical trials confirmed their safety.[10-12] Additionally, in relation to the suspicion or presence of significant intracardiac shunt, also a previous contraindication, it was suspended by the FDA in 2016.[2,12] Currently, only history of allergic reaction to any component of UEA constitutes an absolute contraindication to their use.

Keywords

Echocardiography; Safety; Cost-Benefit Analysis.

Mailing Address: Márcio Silva Miguel Lima •
Instituto do Coração (InCor HCFMUSP). Av Dr Eneas de Carvalho Aguiar, 44. Postal code: 05.403-000. São Paulo, SP – Brazil
E-mail: marcio.lima@incor.usp.br

DOI: https://doi.org/10.36660/abcimg.20230033i

Further supporting their safety, there is also the fact in which clinical scenarios UEA are used, often in technically more difficult exams of severely ill patients. Even so, multiple studies have not demonstrated an increase in morbidity and mortality outcomes. Additionally, in these adverse scenarios, it is also valid to argue that UEA can provide important definitions, such as assessment of left ventricular (LV) systolic function in critically ill patients with marked limitation of the echocardiographic window or search for intracavitary thrombus, making intervention possible, with improved evolution and prognosis.

In medical practice, we must always base our conduct on what is known as "evidence-based medicine," on well-conducted and reliable studies. The medical literature is extremely important and must be followed. Nonetheless, I recognize that we must also consider the knowledge generated by the application of the various techniques in "real life," a genuine translation of theory into practice with the challenges we face on a daily basis. A good example would be the use of UEA in stress echocardiography (SE), which is one of the main applications of contrast. Classically, its use is formally indicated when there is no clear visualization of at least 2 contiguous LV myocardial segments, but, in "real life" practice, it is justified in all exams in which the echocardiographer does not feel confident and judges the acoustic window suboptimal for interpretation, which is fundamental in this type of examination.[2,13] UEA, in addition to increasing the sensitivity of the method, are also associated with an increase in the reproducibility of the wall motility score.[14-16] In this field, I highlight an interesting study conducted by Larsson et al. The authors reported that, in 83 unenhanced exams, with acoustic windows considered adequate (with no formal indication for the use of UEA) and concluded as negative for the presence of myocardial ischemia, 46 patients (55%) showed evidence of myocardial ischemia (positive) when analyzed after the use of UEA and were reclassified.[17] Finally, I quote another situation that is not uncommon for those who routinely perform SE. Eventually, an exam with an adequate resting echocardiographic window may become suboptimal in the peak stage as cardiac imaging becomes more difficult to acquire. This certainly causes difficulties and can lead to inaccurate interpretation, especially in a context where there are symptoms suggestive of ischemia and electrocardiographic changes. Undoubtedly, UEA can be of great help at this crucial moment.

The association with real-time myocardial perfusion (RTMP) adds even more in terms of sensitivity and positive predictive value for the presence of obstructive coronary artery disease and as a prognostic predictor, as demonstrated by Tsutsui et al.[18,19] However, this technique, in addition to still being considered "off-label" by various medical societies, requires an additional expertise of the echocardiographer, who must have experience in this analysis in multiple exams. This is a fact that makes RTMP less widely used; moreover, it is better applied in stress tests with a vasodilator, such as dipyridamole, which is known to be less frequently used than dobutamine. The observation of a "darkened" zone (perfusion deficit), without myocardial refilling with contrast after a pulse with a high mechanical index ("flash"), assists with eventual doubts regarding worsening of segmental contractile function (Figure 1). On the other hand, a bright myocardial segment denotes adequate flow in the microcirculation, and this may help to define normal local contraction.

In relation to cost-effectiveness, UEA also have a favorable profile. A cost-effectiveness analysis of a diagnostic test considers the cost of the method itself compared to what results from it, in other words, how much the test, based on a diagnostic definition that it provides, reduces or eliminates the need for additional tests for the same purpose, promoting or modifying a conduct. In this sense, UEA have been shown to be cost-effective in different scenarios of cardiology. This is mainly evident in critical medicine and in SE.[1,2,20]

Technically difficult echocardiograms, with limited and suboptimal ultrasound windows in the emergency room and intensive care units are very common in daily care routine. This fact may be related to patient positioning, limited access to the thorax, inappropriate local lighting, among others. In these cases, for example, there may be a significant impairment or even impossibility of assessing the LV systolic function, leading to inconclusive tests, and sometimes requiring the use of another imaging method in the diagnostic process, which might eventually be more expensive, for example, cardiac magnetic resonance (CMR). Within this adverse scenario, an accurate definition of LV volumes and calculation of the ejection fraction become possible with the aid of UEA, without requiring other methods. The use of contrast makes the echocardiographic examination more accurate and reproducible, similar to CMR, considered the gold standard. This will guide medical management, confirming its favorable cost-effectiveness profile.[14,17] This is very evident, for example, in patients with morbid obesity. In these patients, due to the limited acoustic window, an eventual search for intracavitary thrombi may be inaccurate, especially in the apical region of the LV, which is more difficult to visualize. The use of UEA makes this exam possible, eliminating the need to complement it with CMR and guiding the conduct regarding anticoagulation for the patient, with an evident impact on cost.[21] Finally, contrast echocardiography is virtually the only diagnostic method to confirm myocardial rupture in a critically ill patient at the bedside.

In chest pain units, even though it is not included in several protocols at different services, the integration of SE with the aid of UEA to assess LV segmental contractility, with or without assessment by RTMP, can be an interesting alternative compared to other more expensive tests, such as tomography angiography of the coronary arteries and myocardial scintigraphy.[22] Echocardiography with UEA may represent a cheaper, more accurate alternative, without radiation. When there is a positive result for myocardial ischemia, it is also more definitive regarding the need to refer the patient for coronary angiography, reinforcing its favorable cost-effectiveness profile.[23,24]

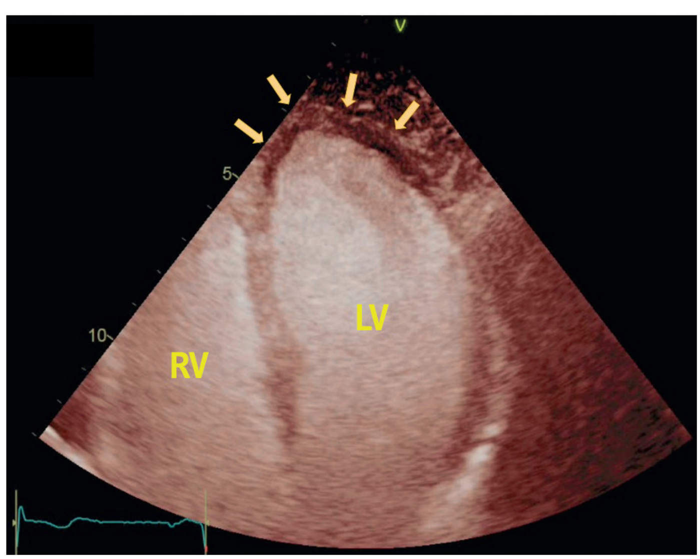

Figure 1 – *A 60-year-old woman undergoing contrast-enhanced echocardiography with pharmacological stress with dobutamine. She had chest discomfort and presented a ST-segment depression in precordial leads on the electrocardiographic tracing. An area of hypoperfusion was identified in the apical region of the LV associated with local hypokinesia (arrows). Positive test for the presence of myocardial ischemia. LV: left ventricle; RV: right ventricle.*

Similarly, when it does not reveal myocardial ischemia, it is possible to discharge the patient safely. Exams without evidence of ischemia are associated with a very low risk, with an annual cardiovascular event rate of less than 1%.[18,25,26]

In the general field of SE, whether using physical or pharmacological stress, UEA have also been shown to be cost-effective. As shown by Mathias et al., SE with suboptimal windows in resting images can be "saved" using UEA, thus optimizing cost, given that it eliminates the need to add another method in the diagnostic process (Figure 2).[27]

In conclusion, over the years contrast echocardiography has shown its value in theory and in "real life" practice. Theory provides the basis for practice. Practice feeds theory and provides the foundation for experience. In the words of the historian Thomas Fuller (1608 to 1661): "Knowledge is a treasure, but practice is the key to it."

Author contributions

Writing of the manuscript: Lima MSM

Potential Conflict of Interest

No potential conflict of interest relevant to this article was reported.

Sources of Funding

There were no external funding sources for this study.

Study Association

This study is not associated with any thesis or dissertation work.

Ethics Approval and Consent to Participate

This article does not contain any studies with human participants or animals performed by any of the authors.

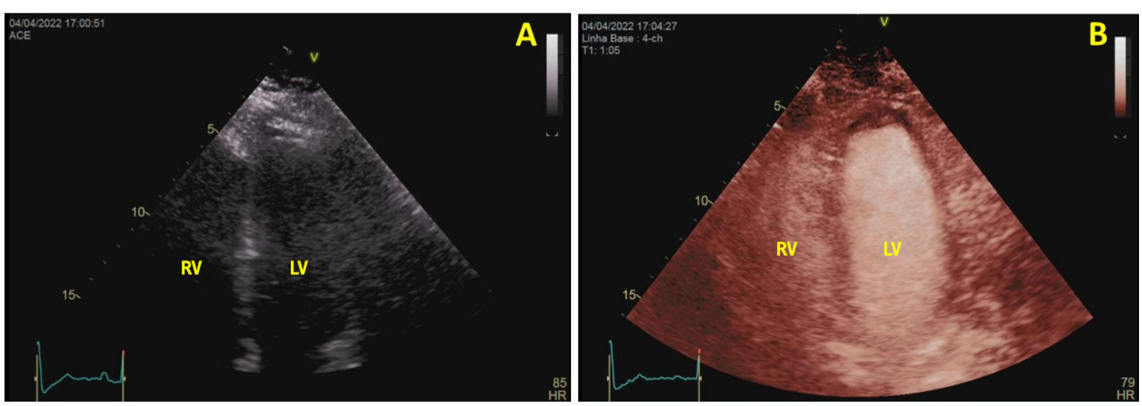

Figure 2 – *A 60-year-old man with obesity and chronic obstructive pulmonary disease. An elective dobutamine stress echocardiogram was ordered. A) Suboptimal resting acoustic window for the exam. B) Echocardiographic contrast (sulfur hexafluoride; SonoVue®) was used, making the exam possible.*

References

1. Senior R, Becher H, Monaghan M, Agati L, Zamorano J, Vanoverschelde JL, et al. Clinical Practice of Contrast Echocardiography: Recommendation by the European Association of Cardiovascular Imaging (EACVI) 2017. Eur Heart J Cardiovasc Imaging. 2017;18(11):1205-1205af. doi: 10.1093/ehjci/jex182.

2. Porter TR, Mulvagh SL, Abdelmoneim SS, Becher H, Belcik JT, Bierig M, et al. Clinical Applications of Ultrasonic Enhancing Agents in Echocardiography: 2018 American Society of Echocardiography Guidelines Update. J Am Soc Echocardiogr. 2018;31(3):241-74. doi: 10.1016/j.echo.2017.11.013.

3. Porter TR, Feinstein SB, Senior R, Mulvagh SL, Nihoyannopoulos P, Strom JB, et al. CEUS Cardiac Exam Protocols International Contrast Ultrasound Society (ICUS) Recommendations. Echo Res Pract. 2022;9(1):7. doi: 10.1186/s44156-022-00008-3.

4. Kusnetzky LL, Khalid A, Khumri TM, Moe TG, Jones PG, Main ML. Acute Mortality in Hospitalized Patients Undergoing Echocardiography with and without an Ultrasound Contrast Agent: Results in 18,671 Consecutive Studies. J Am Coll Cardiol. 2008;51(17):1704-6. doi: 10.1016/j.jacc.2008.03.006.

5. Main ML, Ryan AC, Davis TE, Albano MP, Kusnetzky LL, Hibberd M. Acute Mortality in Hospitalized Patients Undergoing Echocardiography with and without an Ultrasound Contrast Agent (Multicenter Registry Results in 4,300,966 Consecutive Patients). Am J Cardiol. 2008;102(12):1742-6. doi: 10.1016/j.amjcard.2008.08.019.

6. International Collaborative Study of Severe Anaphylaxis. Risk of Anaphylaxis in a Hospital Population in Relation to the Use of Various Drugs: An International Study. Pharmacoepidemiol Drug Saf. 2003;12(3):195-202. doi: 10.1002/pds.822.

7. Wei K, Mulvagh SL, Carson L, Davidoff R, Gabriel R, Grimm RA, et al. The Safety of deFinity and Optison for Ultrasound Image Enhancement: A Retrospective Analysis of 78,383 Administered Contrast Doses. J Am Soc Echocardiogr. 2008;21(11):1202-6. doi: 10.1016/j.echo.2008.07.019.

8. Muskula PR, Main ML. Safety with Echocardiographic Contrast Agents. Circ Cardiovasc Imaging. 2017;10(4):e005459. doi: 10.1161/CIRCIMAGING.116.005459.

9. Furtado RG, Rassi DDC, Melato LH, Oliveira ACR, Nunes PM, Baccelli PE, et al. Safety of SF6(SonoVue®) Contrast Agent on Pharmacological Stress Echocardiogram. Arq Bras Cardiol. 2021;117(6):1170-8. doi: 10.36660/abc.20200475.

10. Abdelmoneim SS, Bernier M, Scott CG, Dhoble A, Ness SA, Hagen ME, et al. Safety of Contrast Agent Use During Stress Echocardiography in Patients with Elevated Right Ventricular Systolic Pressure: A Cohort Study. Circ Cardiovasc Imaging. 2010;3(3):240-8. doi: 10.1161/CIRCIMAGING.109.895029.

11. Wever-Pinzon O, Suma V, Ahuja A, Romero J, Sareen N, Henry SA, et al. Safety of Echocardiographic Contrast in Hospitalized Patients with Pulmonary Hypertension: A Multi-Center Study. Eur Heart J Cardiovasc Imaging. 2012;13(10):857-62. doi: 10.1093/ehjci/jes057.

12. Parker JM, Weller MW, Feinstein LM, Adams RJ, Main ML, Grayburn PA, et al. Safety of Ultrasound Contrast Agents in Patients with Known or Suspected Cardiac Shunts. Am J Cardiol. 2013;112(7):1039-45. doi: 10.1016/j.amjcard.2013.05.042.

13. Mulvagh SL, DeMaria AN, Feinstein SB, Burns PN, Kaul S, Miller JG, et al. Contrast Echocardiography: Current and Future Applications. J Am Soc Echocardiogr. 2000;13(4):331-42. doi: 10.1067/mje.2000.105462.

14. Nayyar S, Magalski A, Khumri TM, Idupulapati M, Stoner CN, Kusnetzky LL, et al. Contrast Administration Reduces Interobserver Variability in Determination of Left Ventricular Ejection Fraction in Patients with Left Ventricular Dysfunction and Good Baseline Endocardial Border Delineation. Am J Cardiol. 2006;98(8):1110-4. doi: 10.1016/j.amjcard.2006.05.038.

15. Hoffmann R, von Bardeleben S, Kasprzak JD, Borges AC, ten Cate F, Firschke C, et al. Analysis of Regional Left Ventricular Function by Cineventriculography, Cardiac Magnetic Resonance Imaging, and Unenhanced and Contrast-Enhanced Echocardiography: A Multicenter Comparison of Methods. J Am Coll Cardiol. 2006;47(1):121-8. doi: 10.1016/j.jacc.2005.10.012.

16. Plana JC, Mikati IA, Dokainish H, Lakkis N, Abukhalil J, Davis R, et al. A Randomized Cross-Over Study for Evaluation of the Effect of Image Optimization with Contrast on the Diagnostic Accuracy of Dobutamine Echocardiography in Coronary Artery Disease The OPTIMIZE Trial. JACC Cardiovasc Imaging. 2008;1(2):145-52. doi: 10.1016/j.jcmg.2007.10.014.

17. Larsson MK, Silva C, Gunyeli E, Ilami AA, Szummer K, Winter R, et al. The Potential Clinical Value of Contrast-Enhanced Echocardiography Beyond Current Recommendations. Cardiovasc Ultrasound. 2016;14:2. doi: 10.1186/s12947-015-0045-0.

18. Tsutsui JM, Elhendy A, Anderson JR, Xie F, McGrain AC, Porter TR. Prognostic Value of Dobutamine Stress Myocardial Contrast Perfusion Echocardiography. Circulation. 2005;112(10):1444-50. doi: 10.1161/CIRCULATIONAHA.105.537134.

19. Senior R, Moreo A, Gaibazzi N, Agati L, Tiemann K, Shivalkar B, et al. Comparison of Sulfur Hexafluoride Microbubble (SonoVue)-Enhanced Myocardial Contrast Echocardiography with Gated Single-Photon Emission Computed Tomography for Detection of Significant Coronary Artery Disease: A Large European Multicenter Study. J Am Coll Cardiol. 2013;62(15):1353-61. doi: 10.1016/j.jacc.2013.04.082.

20. Kurt M, Shaikh KA, Peterson L, Kurrelmeyer KM, Shah G, Nagueh SF, et al. Impact of Contrast Echocardiography on Evaluation of Ventricular Function and Clinical Management in a Large Prospective Cohort. J Am Coll Cardiol. 2009;53(9):802-10. doi: 10.1016/j.jacc.2009.01.005.

21. Siebelink HM, Scholte AJ, Van de Veire NR, Holman ER, Nucifora G, van der Wall EE, et al. Value of Contrast Echocardiography for Left Ventricular Thrombus Detection Postinfarction and Impact on Antithrombotic Therapy. Coron Artery Dis. 2009;20(7):462-6. doi: 10.1097/mca.0b013e328330d58f.

22. Tong KL, Kaul S, Wang XQ, Rinkevich D, Kalvaitis S, Belcik T, et al. Myocardial Contrast Echocardiography versus Thrombolysis In Myocardial Infarction Score in Patients Presenting to the Emergency Department with Chest Pain and a Nondiagnostic Electrocardiogram. J Am Coll Cardiol. 2005;46(5):920-7. doi: 10.1016/j.jacc.2005.03.076.

23. Shah BN, Zacharias K, Pabla JS, Karogiannis N, Calicchio F, Balaji G, et al. The Clinical Impact of Contemporary Stress Echocardiography in Morbid Obesity for the Assessment of Coronary Artery Disease. Heart. 2016;102(5):370-5. doi: 10.1136/heartjnl-2015-308796.

24. Jeetley P, Burden L, Stoykova B, Senior R. Clinical and Economic Impact of Stress Echocardiography Compared with Exercise Electrocardiography in Patients with Suspected Acute Coronary Syndrome But Negative Troponin: A Prospective Randomized Controlled Study. Eur Heart J. 2007;28(2):204-11. doi: 10.1093/eurheartj/ehl444.

25. Wyrick JJ, Kalvaitis S, McConnell KJ, Rinkevich D, Kaul S, Wei K. Cost-Efficiency of Myocardial Contrast Echocardiography in Patients Presenting to the Emergency Department with Chest Pain of Suspected Cardiac Origin and a Nondiagnostic Electrocardiogram. Am J Cardiol. 2008;102(6):649-52. doi: 10.1016/j.amjcard.2008.05.008.

26. Lerakis S, Kalogeropoulos AP, El-Chami MF, Georgiopoulou VV, Abraham A, Lynch SA, et al. Transthoracic Dobutamine Stress Echocardiography in Patients Undergoing Bariatric Surgery. Obes Surg. 2007;17(11):1475-81. doi: 10.1007/s11695-008-9425-y.

27. Mathias W Jr, Arruda AL, Andrade JL, Orlando C Filho, Porter TR. Endocardial Border Delineation During Dobutamine Infusion Using Contrast Echocardiography. Echocardiography. 2002;19(2):109-14. doi: 10.1046/j.1540-8175.2002.00109.x.

Editorial

How to Proceed in a Multimodality Analysis for the Diagnosis and Risk Stratification of Pulmonary Hypertension?

Pedro Gutiérrez-Fajardo[1]

Cardiotest, Laboratorio de Ecocardiografia, Hospital de Especialidades San Francisco de Asís, Guadalajara,[1] *Jalisco – Mexico*

Pulmonary hypertension (PH) is a complex multiorgan system disease defined as mean pulmonary artery pressure (mPAP) $\geq$ 20 mmHg. The etiologies related to pathological changes in pulmonary vasculature leading to PH are wide. Hemodynamic categorization considers precapillary PH, represented by pulmonary arterial hypertension (PAH), pulmonary vascular resistance (PVR) $\geq$ 3 Woods units (WU), and pulmonary arterial wedge pressure $\leq$ 15 mmHg. Postcapillary PH, represented by left heart disease, involves PVR $\geq$ 3 WU and pulmonary arterial wedge pressure $\geq$ 15 mmHg. Clinical categorization considers 5 groups. Incidence per group is not well known; however, group 2 (associated with left heart disease) is the most common cause of PH. PAH (group 1) is still a highly devastating condition causing limited quality of life and high mortality, mostly related to right ventricle (RV) failure. Group 3 refers to PH associated with lung diseases and or hypoxia. Group 4 corresponds to PH associated with pulmonary artery obstructions, and group 5 to PH with unclear and or multifactorial mechanisms.[1] Currently, the diagnostic algorithm for PH considers a 3-step approach, from clinical suspicion by first-line physicians considering vital signs, functional class, etc.; non-invasive RV parameters by transthoracic echocardiography (TTE), cardiac magnetic resonance imaging (CMRI), computed tomography (CT), and pulmonary vascular assessment by ventilation perfusion (V/Q) scan. For diagnostic confirmation, however, right heart catheterization is necessary, preferably in PH centers.[2,3]

In PH, a multimodality approach involves the use of multiple diagnostic tests to evaluate the various aspects of the disease, from suspecting to determining its etiology.[4] It provides a comprehensive assessment for prognosis and can assist in guiding treatment decisions and evaluating response to therapy.

Transthoracic echocardiography

TTE is considered a highly useful, inexpensive, safe, and available imaging modality for initial approach to differential diagnosis of PH. Although a normal TTE does not rule out diagonsis, it decreases the likelihood of PH. Neither CT nor CMRI are part of the initial line of PH; however, in selected patients they can provide additional information before proceeding to right heart catheterization.[1,2]

It is important to be familiar with normal ranges of RV size and function.[5,6] TTE showing right heart structure and function abnormalities increases suspicion of PH.[7] It also allows detection of left heart (systolic and diastolic dysfunction, valvular heart disease) and congenital heart disease as potential causes of PH.[8] RV function surrogates such as RV fractional area change, right atrial size, pericardial effusion, tricuspid annular plane systolic excursion (TAPSE), systolic pulmonary artery pressure (SPAP)/TAPSE ratio, and eccentricity index are recommended in follow-up and assessment of therapy response.[9] However, it is important to note that these surrogates should be interpreted in the context of other clinical and imaging parameters, as they are not standalone diagnostic tools. Doppler can be used to estimate the possibility of PH by measuring tricuspid regurgitant jet velocity (TR) and calculating SPAP using the modified Bernoulli equation. When no TR is present or the signal is inadequate, pulmonary acceleration time can be used to calculate mPAP obtained from pulse wave Doppler signal of pulmonary flow. Pulmonary artery diastolic pressure can be estimated if pulmonary regurgitation is present. The velocity at end-diastole is converted into a pressure gradient, adding the estimated right atrial pressure to the resulting value. Finally, both left ventricle and RV output can be calculated.[9] In clinical practice, differentiating acute, chronic, and chronic acute PH can be challenging (Table 1).

The following recent advances in echocardiography have improved our understanding and ability to better characterize RV dysfunction in PH:

1. Three-dimensional echocardiography (3DE) can provide detailed information on the size and function of the RV. It has been demonstrated that 3DE is more accurate than 2-dimensional echocardiography in assessing RV function in PH.
2. Speckle tracking echocardiography (STE) can be used to quantify RV free-wall strain, which is a measure of how much the RV is able to contract and relax. RV strain has demonstrated to be both a sensitive marker of RV dysfunction and a predictor of clinical outcomes and death in patients with PH.
3. Real-time 3DE makes it possible to acquire rapid information on RV volumes, RV stroke, and RV ejection fraction, as well as RV strain and strain rate. It is especially useful in assessing RV function in dynamic tests, such as exercise.
4. Contrast-enhanced echocardiography (CEE) improves the visualization of the cardiac chambers. CEE can be used to detect the presence of a clot, a mass, or other abnormalities.

Keywords

Pulmonary Hypertension; Diagnosis; Risk Factors

Mailing Address: Pedro Gutiérrez-Fajardo •
Cardiotest, Laboratorio de Ecocardiografia, Hospital de Especialidades San Francisco de Asís. Av. Americas, 1946, Postal code: 44630. Guadalajara, Jalisco - Mexico
E-mail: drpedrogutierrez@yahoo.com
Manuscript received April 20, 2023; revised manuscript April 27, 2023; accepted April 27, 2023.
Editor responsible for the review: Daniela do Carmo Rassi Frota

DOI: https://doi.org/10.36660/abcimg.20230041i

Table 1 – Differentiating acute, chronic, and chronic acute pulmonary hypertension

Echocardiographic parameter	Acute	Chronic	Chronic acute
Dilated right ventricle	Yes	Yes	Yes +++
Hypertrophied right ventricle	Absent	Present	Present
Tricuspid regurgitation	Present	Present	Present
Pulmonary regurgitation	+ to ++	+++ to ++++	+++ to ++++
Pulmonary pressure	MPAP < 40 mmhg	Supra-systemic SPAP	Supra-systemic SPAP
Right ventricle hypokinesis	Severe	Late finding	Severe to very severe
Paradoxical septal motion	Present	Present (marked)	Present (severe)
Dilated pulmonary artery	Not common	Frequent	Very frequent

MPAP: mean pulmonary artery pressure; SPAP: systolic pulmonary artery pressure.

Cardiac magnetic resonance imaging

CMRI easily provides complete information about RV structure and function in patients with suspected or confirmed PH with high sensitivity and specificity in measuring RV mass index, RV diameters, RV thickness, RV free-wall motion, end-diastolic volume, end-systolic volume, stroke volume, and RV ejection fraction. CMRI can also provide information on the size and structure of pulmonary arteries and the blood flow through the lungs. It is more accurate than TTE in the assessment and follow-up of patients with PH, but it is a more time-consuming, higher cost, and less available technique. CMRI does not expose the patient to radiation; however, it can be difficult to perform in claustrophobic patients, and renal function should be checked before the test. Outside of PH centers, it is not widely used in diagnostic approach.[4] Both TTE and CMRI play important roles in disease assessment, risk stratification, and evaluation of therapeutic intervention.

Computed tomography

CT provides detailed information about the pulmonary vasculature, lung parenchyma, and cardiac structure. Thus, information on the size and structure of the pulmonary arteries (PA) and the blood flow through the lungs can be obtained, identifying the presence of blood clots or other abnormalities. Accordingly, it is useful in the diagnosis of chronic thromboembolic pulmonary hypertension (CTEPH) and can also identify distal obstructions, narrowing of the PA and their branches and distal stenosis. Additionally, it identifies pouch-like defects, intimal irregularities, PA webs or bands, and enlargement of bronchial arteries due to collateral blood supply, which is of prognostic significance, as these patients have better postsurgical evolution. CT can also detect underlying lung disease, such as interstitial lung disease or emphysema, which also contributes to PH.[10] Currently, CT is a readily available technique, but patients are exposed to ionizing radiation and in some cases requires the administration of contrast dye.

Ventilation perfusion scan

Finally, V/Q scan evaluates the probability of blood clots in pulmonary vasculature. It involves the injection of a radioactive tracer and the inhalation of a radioactive gas in order to investigate if there is a V/Q mismatch, indicating the presence of a blood clot in wedge-shaped perfusion defects with normal ventilation. Due to its high sensitivity, V/Q scan is the test of choice when screening patients with suspected CTEPH. A normal V/Q scan practically excludes the probability of CTEPH. Importantly, complete absence of perfusion in one lung should raise the possibility of other conditions different to CTEPH, such as vasculitis, malignancy and fibrosing mediastinitis. One of the drawbacks of V/Q scan is the high number of non-diagnostic or indeterminate tests, as well as underestimation of central vascular obstruction and its incapacity to differentiate pulmonary veno-occlusive disease and fibrosing mediastinitis.[4] In clinical practice, V/Q scan seems to be underutilized, even though it is part of the current recommendations for suspicion of PH due to its high sensitivity and specificity.

In summary, advances in echocardiography have improved our ability to consider pulmonary pressure probability and to characterize RV dysfunction. TTE RV function surrogates are practical parameters, especially in follow-up. STE, 3DE, real-time 3DE, and CCE are all useful modern modalities that can provide more detailed information on RV function or dysfunction in PH. CMRI, CT, and V/Q scanning are useful imaging modalities in the diagnosis and risk stratification of PH. These techniques can help to guide treatment decisions and to improve clinical outcomes in this patient population. Every imaging modality has advantages and disadvantages (Table 2). Technique selection will be based on the clinical scenario and individual patient needs. According to findings, it is important to consider consultation with a health care professional who specializes in PH, avoiding unnecessary delays that could impact patient´s health. Artificial intelligence will be available in the near future and will allow faster, reliable assessment of both RV and left ventricular volume, ejection fraction, mass, and global and segmental function. These advances will certainly be of major significance in patients with PH.

Editorial

Table 2 – Imaging modalities in pulmonary hypertension: advantages and disadvantages

Imaging modality	Advantages	Disadvantages
Echocardiography	First choice, widely available Easily repeatable - monitoring Heart rhythm independent Pulmonary pressure calculation 2D, 3D, RT3D, ST, CEE Low cost No radiation	Operator dependent Acoustic window dependent Pulmonary pressure underestimation Pulmonary pressure overestimation
Cardiac magnetic resonance imaging	Acoustic window independent Complete RV structure and function Pulmonary circulation evaluation Myocardial tissue characterization Low intra-interobserver variability High quality images	Not widely available Technically limited in arrhythmias Contraindicated in renal failure Secondary renal damage in few cases Caution in claustrophobic patients High cost
Computed tomography	Acoustic window independent RV quantification Lung parenchyma assessment Mediastinum assessment Useful in CTEPH	Radiation exposure Contrast use Not for monitoring High cost
V/Q lung scan	Pulmonary vascular assessment Good for CTEPH screening High sensitivity and specificity	Non-specific findings High number of non-diagnostic tests Not for monitoring Radiotracer use High cost

2D: two-dimensional echocardiography; 3D: three-dimensional echocardiography; CEE: contrast-enhancement echocardiography; CTEPH: chronic thromboembolic pulmonary hypertension; RT3D: real-time three-dimensional echocardiography; RV: right ventricle; ST: speckle tracking echocardiography; V/Q: ventilation perfusion.

References

1. Humbert M, Kovacs G, Hoeper MM, Badagliacca R, Berger RMF, Brida M, et al. 2022 ESC/ERS Guidelines for the Diagnosis and Treatment of Pulmonary Hypertension. Eur Heart J. 2022;43(38):3618-3731. doi: 10.1093/eurheartj/ehac237.

2. Zarate JS, Jerjes-Sanchez C, Ramirez-Rivera A, Zamudio TP, Gutierrez-Fajardo P, Gonzalez JE, et al. Mexican Registry of Pulmonary Hypertension: REMEHIP. Arch Cardiol Mex. 2017;87(1):13-7. doi: 10.1016/j.acmx.2016.11.006.

3. Huang WC, Hsieh SC, Wu YW, Hsieh TY, Wu YJ, Li KJ, et al. 2023 Taiwan Society of Cardiology (TSOC) and Taiwan College of Rheumatology (TCR) Joint Consensus on Connective Tissue Disease-Associated Pulmonary Arterial Hypertension. Acta Cardiol Sin. 2023;39(2):213-41. doi: 10.6515/ACS.202303_39(2).20230117A.

4. Kligerman S, Horowitz M, Hsiao A, Hahn L, Weihe E. Multimodality Imaging in Pulmonary Hypertension. Advances in Pulmonary Hypertension. 2019;18:115-25. doi: 10.21693/1933-088X-18.4.115.

5. Addetia K, Miyoshi T, Citro R, Daimon M, Gutierrez Fajardo P, et al. Two-Dimensional Echocardiographic Right Ventricular Size and Systolic Function Measurements Stratified by Sex, Age, and Ethnicity: Results of the World Alliance of Societies of Echocardiography Study. J Am Soc Echocardiogr. 2021;34(11):1148-57.e1. doi: 10.1016/j.echo.2021.06.013.

6. Lang RM, Badano LP, Mor-Avi V, Afilalo J, Armstrong A, Ernande L, et al. Recommendations for Cardiac Chamber Quantification by Echocardiography in Adults: An Update from the American Society of Echocardiography and the European Association of Cardiovascular Imaging. Eur Heart J Cardiovasc Imaging. 2015;16(3):233-70. doi: 10.1093/ehjci/jev014.

7. Zaidi A, Knight DS, Augustine DX, Harkness A, Oxborough D, Pearce K, et al. Echocardiographic Assessment of the Right Heart in Adults: A Practical Guideline from the British Society of Echocardiography. Echo Res Pract. 2020;7(1):G19-G41. doi: 10.1530/ERP-19-0051.

8. Vedage NA, Vaidya A. What Echocardiography Can Reliably Tell Us About Our Pulmonary Hypertension Patients. Advances in Pulmonary Hypertension. 2019;18:110-14. doi: 10.21693/1933-088X-18.4.110.

9. Topyła-Putowska W, Tomaszewski M, Wysoki□ski A, Tomaszewski A. Echocardiography in Pulmonary Arterial Hypertension: Comprehensive Evaluation and Technical Considerations. J Clin Med. 2021;10(15):3229. doi: 10.3390/jcm10153229.

10. Remy-Jardin M, Ryerson CJ, Schiebler ML, Leung ANC, Wild JM, Hoeper MM, et al. Imaging of Pulmonary Hypertension in Adults: A Position Paper from the Fleischner Society. Eur Respir J. 2021;57(1):2004455. doi: 10.1183/13993003.04455-2020.

Right Ventricle Diastolic Function: Correlation with Age

Arthur Nascimento de Moura,[1] Ana Cristina Camarozano,[1] Cintia Rocha Fortes de Sá,[1] Daniela de Castro Carmo,[1] Jerônimo Antonio Fortunato,[1] Rubens Zenóbio Darwich,[1] Liz Andréa Villela Baroncini[1]

Hospital da Cruz Vermelha, Cruz Vermelha Brasileira,[1] Curitiba, PR – Brazil

Abstract

Introduction: **Right ventricle (RV) elasticity tends to decrease with aging and may alter its diastolic function.**

Objective: **To evaluate the correlation between echocardiographic changes in RV diastolic function and advancing age in individuals with normal biventricular systolic function.**

Methods: **This retrospective observational cohort study included 110 patients: 66 (60%) women (62 [SD, 13.7] years) and 44 (40%) men (60.6 [SD, 10.8] years). The transthoracic echocardiography data included: spectral Doppler of tricuspid inflow E wave, A wave, E/A ratio, and E wave deceleration time; tissue Doppler of lateral tricuspid annulus e' wave, a' wave, and E/e' ratio. Correlations were calculated using Pearson's and Spearman's correlation coefficients.**

Results: **Only 35.2% of the sample had RV diastolic dysfunction. Of the evaluated echocardiographic variables, the E wave was negatively correlated with age in both women (r 0.473; p < 0.001) and men (r -0.37, p = 0.015). The E/A ratio was negatively correlated with age only in women (r -0.32; p = 0.001), and E wave deceleration time was positively correlated with age only in women (r 0.31; p = 0.014). The other variables were not significantly correlated with age in men or women.**

Conclusions: **We found a significant correlation between age and echocardiographic parameters for RV diastolic dysfunction, which was more evident in women.**

Keywords: **Heart Ventricles; Heart Failure, Diastolic; Echocardiography.**

Introduction

In the last 10 years, interest in the right ventricle (RV) and its effect on clinical outcomes has increased, largely due to advancements in pharmacological treatment for pulmonary arterial hypertension.[1] However, like the left ventricle (LV), the RV is affected by numerous physiological changes inherent to age that must be distinguished from those resulting from heart disease.[2-3] Thus, more accurate assessment of both systolic and diastolic function in the RV is needed in clinical practice. The lack of studies on this chamber is likely due to its relative structural and functional complexity.[4] Unlike the LV, which has a conical shape, the RV has a hemiellipsoid shape that adheres to the LV. In clinical practice, indices of systolic performance, such as ejection fraction, reflect LV contractility as an intrinsic property of the myocardium. For the RV, systolic performance is based on analysis of ejection fraction, fractional area change, and tricuspid valve annular plane systolic excursion. These parameters are more associated with atrioventricular coupling related to elasticity, which shows the importance of RV compliance in both systolic and diastolic function.[5] In patients over 70 years of age, studies on the RV, in addition to being fewer, are incomplete, eg, the prognostic relationship between RV dysfunction and heart failure mortality is still unknown.[6] Thus, the objective of the present study was to evaluate the correlation between echocardiographic parameters of RV diastolic function with advancing age in patients with preserved biventricular function.

Mailing Address: Arthur Nascimento de Moura •
Departamento de Ensino e Pesquisa. Av. Vicente Machado, 1310, Batel.
Postal Code: 80420-011. Curitiba, PR – Brazil
E-mail: drarthurnmoura@gmail.com
Manuscript received August 11, 2022; revised manuscript September 18, 2022; accepted March 3, 2023.
Editor responsible for the review: Daniela do Carmo Rassi Frota

DOI: https://doi.org/10.36660/abcimg.2023333i

Methods

Study population

This observational retrospective cohort study was based on data from the electronic medical records of 110 patients over 18 years of age of both sexes who underwent transthoracic echocardiography at the Curitiba Red Cross Hospital (Curitiba, PR, Brazil) for any clinical indication between June 2020 and August 2020.

The patient sample was chosen by convenience, rather than any statistical criteria, according to necessary echocardiographic data in the electronic medical records. For each patient, clinical and echocardiographic parameters were collected. The analyzed clinical data included: age, sex, body mass index, systemic arterial hypertension, diabetes mellitus, diabetes duration (in treatment), coronary artery disease, stroke, cerebral palsy, and smoking (current or former), in addition to regularly used medications.

The exclusion criteria were: a) medical records and reports lacking the echocardiographic values analyzed in this study, b) significant valve disease (moderate or severe), c) valve prostheses, d) segmental changes in LV contraction due to ischemic heart disease or other cardiomyopathies, e) pulmonary emphysema or overt chronic obstructive pulmonary disease, f) moderate-to-severe pulmonary arterial hypertension (pulmonary artery systolic pressure > 50 mmHg), g) left ventricular contractile dysfunction (ejection fraction < 52% for men or < 54% for women), h) infiltrative diseases or pericardiomyopathy; i) congenital heart disease with increased pulmonary flow (with or without surgical correction), and j) pacemakers.

Transthoracic echocardiography was performed with a Phillips IE 33, Phillips HD 11, Phillips Envisor (Koninklijke Philips N.V., Amsterdam, Netherlands), or GE Vivid IQ Premium (General Electric, Boston, MA, USA) ultrasound machine. To be included in the analysis, the echocardiographic reports had to contain all standard acoustic windows (with all echocardiographic measurements) and a complete assessment of RV diastolic function.

All ultrasound measurements were performed by experienced echocardiographers qualified in echocardiography by Brazilian Society of Cardiology's Department of Cardiovascular Imaging. This study was approved by the institutional research ethics committee.

Main echocardiographic parameters analyzed in this study

- Spectral Doppler of the tricuspid inflow: E and A waves, E/A ratio and E wave deceleration time
- Tissue Doppler of the free wall of the tricuspid annulus: waves e' and a'
- E/e' ratio
- Cavity diameters in the two-dimensional echocardiography of the right chambers
- RV systolic function through analysis of fractional area change, tricuspid valve annular plane systolic excursion
- S' wave in lateral tissue Doppler of the tricuspid annulus.

These parameters were not used in the final data analysis. Patients with any signs of RV contractile dysfunction, such as fractional area change < 35%, tricuspid valve annular plane systolic excursion < 17 mm, or S' wave < 10 cm/s, were excluded from the study.

RV diastolic dysfunction was classified according to the following criteria: a tricuspid E/A ratio < 0.8 suggests relaxation (Grade I), a tricuspid E/A ratio of 0.8-2.1 with predominant diastolic flow in hepatic veins suggests a "pseudonormal" (Grade II) filling pattern, and a tricuspid E/A ratio > 2.1 with an E wave deceleration time < 120 ms suggests a restrictive filling pattern (Grade III).[7-11]

All quantifications and values used in the present study were based on American Society of Echocardiography and European Society of Cardiovascular Imaging guidelines.[7-11]

Statistical analysis

The analysis was performed separately for women and men. The results were described as means, medians, minimum and maximum values, and SD for quantitative variables or as frequencies and percentages for categorical variables. Pearson's or Spearman's correlation coefficients were estimated for age and echocardiographic variables. The normality of continuous variables was assesses with the Kolmogorov-Smirnov test. P-values < 0.05 were considered statistically significant. The data were analyzed in IBM SPSS Statistics 20.0 (IBM, Armonk, NY, USA).

Results

The analysis included data from 110 patients, 66 (60%) women with a mean age of 62.6 (SD, 13.70] years (median 64 [18-90] years), and 44 (40%) men with a mean age of 60.6 (SD, 10.8) years (median 62.5 [37-85] years). The sample's clinical characteristics are shown in Table 1. Baseline echocardiographic parameters (Table 2) were in agreement with literature.[7]

Regarding RV diastolic dysfunction (Table 3): 70 patients (64.8%) were normal, 18 (16.7%) had grade I dysfunction, 19 (17.6%) had grade II dysfunction, and only 1 patient (male) had grade III dysfunction.

In the correlation analysis (Table 4), the E wave was negatively correlated with age in both women (r -0.473, p < 0.001) and men (r -0.37, p = 0.015). The E/A ratio was negatively correlated with age only in women (r -0.36; p = 0.004), and E wave deceleration was only positively correlated with age only in women (r 0.31, p = 0.014) (Figures 1 and 2). The other variables were not significantly correlated with age in men or women.

Discussion

Most individuals in the sample (mean age 62 years) had normal RV diastolic function. We also found that the echocardiographic parameters, such as E wave, E/A ratio, and E wave deceleration of the tricuspid valve change more with advancing age in women than men in the same age group. In a similar population, Lasari Melo et al.[12] also found a significant decrease in RV E wave and E/A ratio with age, but no significant sex differences. One reason that age-related RV diastolic dysfunction was more prevalent in women could be the significant drop in estrogen levels after menopause. It is known that estrogen receptors in female hearts can act protectively against heart failure with preserved ejection fraction, which is more common in women. Estrogen causes reduced angiotensin-converting enzyme activity, a reduction in angiotensin-II, and increased production of angiotensin-I, which has an antioxidant and anti-inflammatory effect, among other benefits.[13]

The sample of Lasari Melo et al.[12] had normal diastolic function. Despite having similar populations, approximately 35% of our sample had diastolic dysfunction (Table 3). Nevertheless, we consider this a very low degree of diastolic dysfunction, which raises the question of whether this low level of diastolic dysfunction was related to the fact that we used LV diastolic dysfunction criteria to assess the RV.

Table 1 – Descriptive statistical analysis of comorbidities, stratified by sex

Variable	Grade	Sex		General
		Female	Male	
ECG	Sinus	28 (96.6%)	25 (96.2%)	53 (96.4%)
	Non-sinus	1 (3.5%)	1 (3.9%)	2 (3.6%)
SAH	No	30 (45.5%)	12 (27.3%)	42 (38.2%)
	Yes	36 (54.6%)	32 (72.7%)	68 (61.8%)
DM	No	46 (69.7%)	28 (63.6%)	74 (67.3%)
	Yes	20 (30.3%)	16 (36.4%)	36 (32.7%)
Dyslipidemia	No	45 (68.2%)	16 (36.4%)	61 (55.5%)
	Yes	21 (31.8%)	28 (63.6%)	49 (44.5%)
Previous AMI	No	63 (95.5%)	33 (75.0%)	96 (87.3%)
	Yes	3 (4.6%)	11 (25.0%)	14 (12.7%)
Previous CAD	No	58 (87.9%)	29 (65.9%)	87 (79.1%)
	Yes	8 (12.1%)	15 (34.1%)	23 (20.9%)
History of smoking	No	53 (81.5%)	32 (72.7%)	85 (78.0%)
	Yes	12 (18.5%)	12 (27.3%)	24 (22.0%)
HF	No	65 (98.5%)	40 (90.9%)	105 (95.5%)
	Yes	1 (1.5%)	4 (9.1%)	5 (4.5%)
Valve disease	No	66 (100.0%)	43 (97.7%)	109 (99.1%)
	Yes	0 (0.0%)	1 (2.3%)	1 (0.9%)
COPD	No	63 (95.5%)	42 (95.5%)	105 (95.5%)
	Yes	3 (4.6%)	2 (4.6%)	5 (4.5%)
Chronic kidney disease	No	64 (97.0%)	44 (100.0%)	108 (98.2%)
	Yes	2 (3.0%)	0 (0.0%)	2 (1.8%)
Arrhythmias	No	63 (95.5%)	40 (90.9%)	103 (93.6%)
	Yes	3 (4.6%)	4 (9.1%)	7 (6.4%)

ECG: electrocardiogram; SAH: systolic arterial hypertension; DM: diabetes mellitus; AMI: acute myocardial infarction; CAD: coronary artery disease; HF: heart failure; COPD: chronic obstructive pulmonary disease.

Table 2 – Descriptive statistical analysis of echocardiographic variables

Variable	N	Mean (SD)	Median (min-max)
RV – E wave (m/s)	110	0.49±0.13	0.5 (0.1-0.8)
RV – A wave (m/s)	108	0.42±0.13	0.4 (0.18-0.8)
RV – E/A ratio	108	1.22±0.44	1.2 (0.5-2.7)
RV – e' lateral (m/s)	110	0.14±0.17	0.1 (0.02-0.9)
RV – A´ (m/s)	108	0.18±0.16	0.14 (0.03-0.9)
RV – E/e´	110	4.95±2.24	4.9 (0.5-11)
RV – E deceleration (ms)	109	204.71±75.96	194.0 (84-690)

RV: right ventricle; SD: standard deviation.

Table 3 – Descriptive statistical analysis of right ventricular diastolic dysfunction

Variable	Grade	Sex		General
		Female	Male	
RV diastolic dysfunction	0	41 (63.1%)	29 (67.4%)	70 (64.8%)
	1	15 (23.1%)	3 (7.0%)	18 (16.7%)
	2	9 (13.8%)	10 (23.3%)	19 (17.6%)
	3	0 (0.0%)	1 (2.3%)	1 (0.9%)

RV: right ventricle.

The shortening and lengthening of the RV are greater longitudinally than radially, unlike the LV, in which radial torsion is greater. Thus, pulsed tissue Doppler can be considered an ideal technique for assessing changes in age-related RV function.[9] Changes that occur in the myocardium with aging include increased deposition of extracellular matrix, cardiomyocyte loss and, consequently, hypertrophy of the remaining cells, leading to myocardial stiffness.[13] Homeostasis between extracellular matrix synthesis and degradation is the key factor in maintaining cardiac structure and function.[14] However, especially in women, there is an excessive increase in the synthesis of type I and III collagen with aging, which leads to increased myocardial thickness and rigidity, causing heart failure with preserved LV ejection fraction.[15-16] In our data, tissue Doppler of the tricuspid annulus did not change significantly with age. Corroborating these findings, Lindqvist et al.[17] (255 healthy patients) and Alam et al.[18] found that systolic myocardial velocities were preserved with aging. In Lindqvist et al.,[17] the E/A ratio decreased over time, similar to our findings in the present study.

Inneli et al.[19] divided a sample of 298 healthy individuals into 7 decade-based age groups, finding a significant positive correlation between the E/e′ ratio and aging and a negative correlation between e′ wave and age. However, this appears to be the only study to date that has found such correlations.

Our findings reinforce the hypothesis that E wave velocity and RV E/A ratio (indicators of diastolic function change) decrease with age, and this decrease was more pronounced in women.

Our study's main limitation was its small sample size and the fact that it was conducted retrospectively by analyzing medical records. Another relevant factor was the exclusion of patients with significant pulmonary arterial hypertension, making it impossible to assess diastolic dysfunction in this condition.[20] However, our main objective was to assess RV diastolic function in isolation according to age.

Conclusions

The present study demonstrated that age influenced the progression of RV diastolic dysfunction, which was more evident in women. However, more studies are needed to confirm these findings.

Table 4 – Descriptive statistical analysis of the association between age and echocardiographic variables

Variable	General			Women			Men		
	n	r	p	n	r	p	n	r	p
Age (years) x RV – E wave (m/s)	107	-0.43	< 0.001	64	-0.47	< 0.001	43	-0.37	0.015
Age (years) x RV – E/A Ratio	107	-0.32	0.001	64	-0.36	0.004	43	-0.23	0.145
Age (years) x RV – E/e'	107	-0.01	0.925	64	-0.13	0.315	43	0.19	0.234
Age (years) x RV – E deceleration (ms)	107	0.14	0.139	64	0.31	0.014	43	-0.03	0.841
Age (years) x RV – A wave (m/s)	108	0.00	0.964	65	0.01	0.924	43	-0.07	0.651
Age (years) x RV – e' lateral (m/s)	110	-0.14	0.135	66	-0.16	0.212	44	-0.19	0.209
Age (years) x RV – H' (m/s)	108	0.18	0.057	65	0.13	0.306	43	0.18	0.237

**r: Pearson's or Spearman's correlation coefficient, p < 0.05. RV: right ventricle*

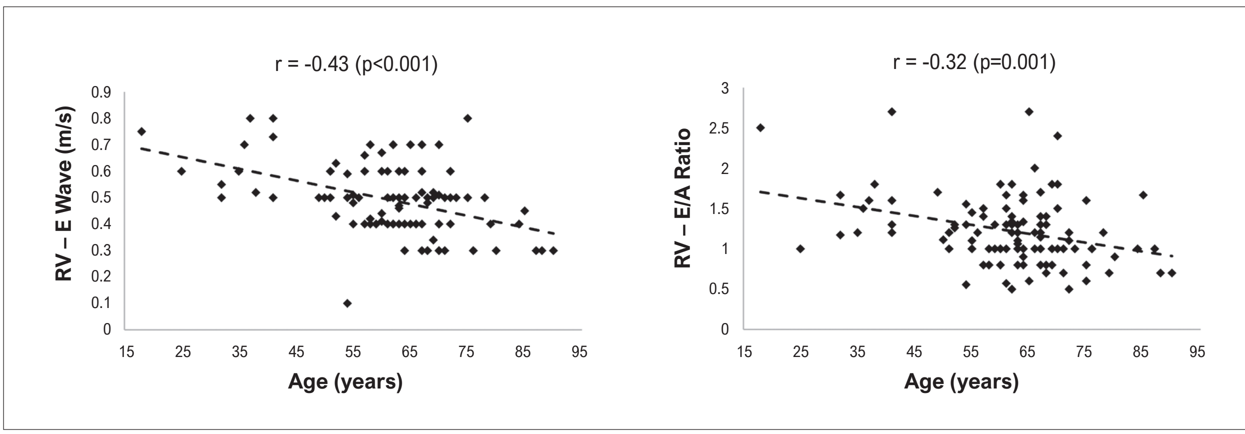

Figure 1 – *Correlation between age, E wave, and E/A ratio among men. RV: right ventricle; r: Pearson's or Spearman's correlation coefficient.*

Author Contributions

Conception and design of the research, writing of the manuscript and critical revision of the manuscript for intellectual content: Moura AN, Camarozona AC, Fortunato JA, Baroncini LAV; acquisition of data, analysis and interpretation of the data and statistical analysis: Moura AN, Camarozona AC, Sá CRF, Carmo DC, Fortunato JA, Darwich RZ, Baroncini LAV.

Potential Conflict of Interest

No potential conflict of interest relevant to this article was reported.

Sources of Funding

There were no external funding sources for this study.

Study Association

This article is part of Arthur Nascimento de Moura's completion of the specialization course in transthoracic echocardiography by Hospital da Cruz Vermelha, Paraná, and Instituto Saber e Aprendir.

Ethics Approval and Consent to Participate

This study was approved by the Ethics Committee of the Universidade Positivo under the protocol number 5.582.981. All the procedures in this study were in accordance with the 1975 Helsinki Declaration, updated in 2013. Informed consent was obtained from all participants included in the study.

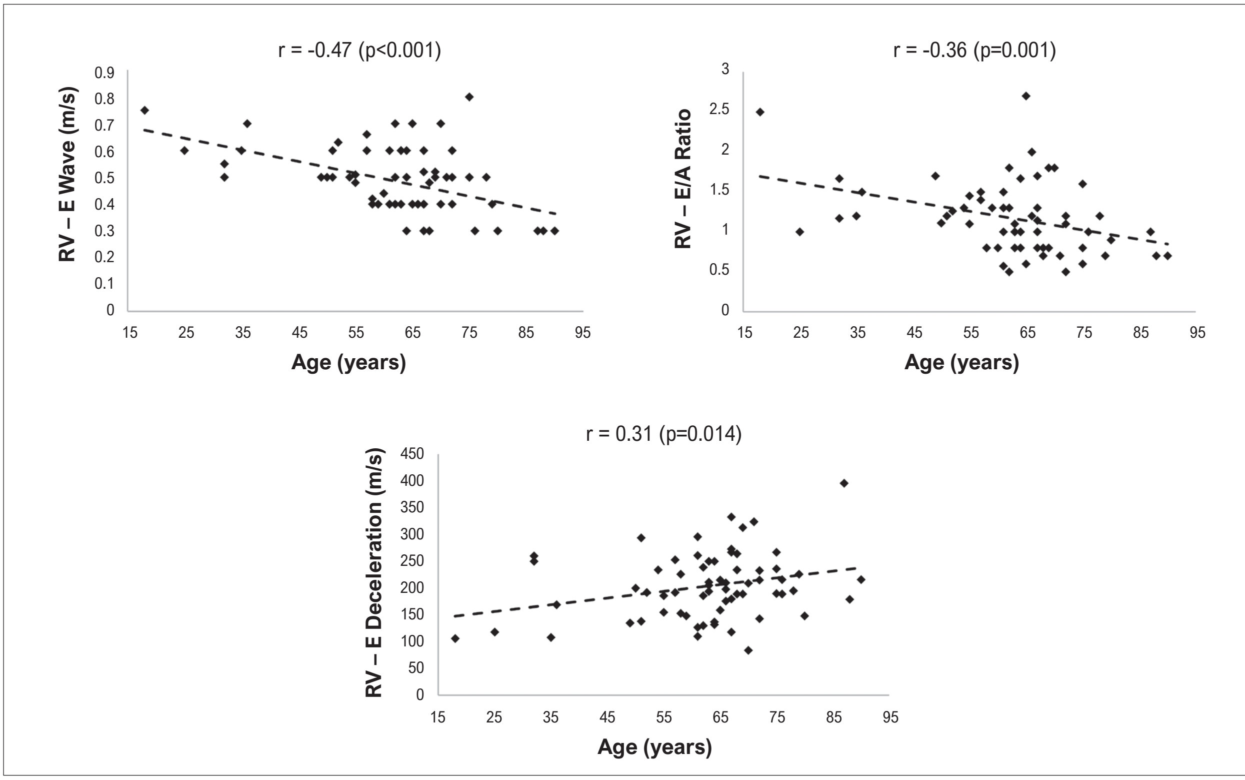

Figure 2 – *Correlation between age and E wave, E/A ratio, and E wave deceleration among women. RV: right ventricle; r: Pearson's or Spearman's correlation coefficient.*

References

1. Amsallem M, Mercier O, Kobayashi Y, Moneghetti K, Haddad F. Forgotten No More: A Focused Update on the Right Ventricle in Cardiovascular Disease. JACC Heart Fail. 2018;6(11):891-903. doi: 10.1016/j.jchf.2018.05.022.

2. López-Candales A, Rajagopalan N, Saxena N, Gulyasy B, Edelman K, Bazaz R. Right Ventricular Systolic Function is Not the Sole Determinant of Tricuspid Annular Motion. Am J Cardiol. 2006;98(7):973-7. doi: 10.1016/j.amjcard.2006.04.041.

3. Gavazzi A, Berzuini C, Campana C, Inserra C, Ponzetta M, Sebastiani R, et al. Value of Right Ventricular Ejection Fraction in Predicting Short-Term Prognosis of Patients with Severe Chronic Heart Failure. J Heart Lung Transplant. 1997;16(7):774-85.

4. Levine RA, Gibson TC, Aretz T, Gillam LD, Guyer DE, King ME, et al. Echocardiographic Measurement of Right Ventricular Volume. Circulation. 1984;69(3):497-505. doi: 10.1161/01.cir.69.3.497.

5. Dell'Italia LJ, Walsh RA. Application of a Time Varying Elastance Model to Right Ventricular Performance in Man. Cardiovasc Res. 1988;22(12):864-74. doi: 10.1093/cvr/22.12.864.

6. Groote P, Millaire A, Foucher-Hossein C, Nugue O, Marchandise X, Ducloux G, et al. Right Ventricular Ejection Fraction is an Independent Predictor of Survival in Patients with Moderate Heart Failure. J Am Coll Cardiol. 1998;32(4):948-54. doi: 10.1016/s0735-1097(98)00337-4.

7. Lang RM, Badano LP, Mor-Avi V, Afilalo J, Armstrong A, Ernande L, et al. Recommendations for Cardiac Chamber Quantification by Echocardiography in Adults: An Update from the American Society of Echocardiography and the European Association of Cardiovascular Imaging. J Am Soc Echocardiogr. 2015;28(1):1-39.e14. doi: 10.1016/j.echo.2014.10.003.

8. Grünig E, Biskupek J, D'Andrea A, Ehlken N, Egenlauf B, Weidenhammer J, et al. Reference Ranges for and Determinants of Right Ventricular Area in Healthy Adults by Two-Dimensional Echocardiography. Respiration. 2015;89(4):284-93. doi: 10.1159/000371472.

9. Voelkel NF, Quaife RA, Leinwand LA, Barst RJ, McGoon MD, Meldrum DR, et al. Right Ventricular Function and Failure: Report of a National Heart, Lung, and Blood Institute Working Group on Cellular and Molecular Mechanisms of Right Heart Failure. Circulation. 2006;114(17):1883-91. doi: 10.1161/CIRCULATIONAHA.106.632208.

10. Levine RA, Gibson TC, Aretz T, Gillam LD, Guyer DE, King ME, et al. Echocardiographic Measurement of Right Ventricular Volume. Circulation. 1984;69(3):497-505. doi: 10.1161/01.cir.69.3.497.

11. Rudski LG, Lai WW, Afilalo J, Hua L, Handschumacher MD, Chandrasekaran K, et al. Guidelines for the Echocardiographic Assessment of the Right Heart in Adults: A Report from the American Society of Echocardiography Endorsed by the European Association of Echocardiography, a Registered Branch of the European Society of Cardiology, and the Canadian Society of Echocardiography. J Am Soc Echocardiogr. 2010;23(7):685-713. doi: 10.1016/j.echo.2010.05.010.

12. Melo LL, Camarozano AC, Carmo DC, Fortunato JA, Darwich RZ, Sá CRF, et al. Echocardiographic Correlation between Right Ventricular Diastolic Function and Age and Gender in Subjects with Preserved Left and Right Systolic Function. Arq Bras Cardiol Imagem Cardiovasc. 2021;34(2):1-8. 10.47593/2675-312X/20213402eabc126.

13. Sabbatini AR, Kararigas G. Menopause-Related Estrogen Decrease and the Pathogenesis of HFpEF: JACC Review Topic of the Week. J Am Coll Cardiol. 2020;75(9):1074-82. doi: 10.1016/j.jacc.2019.12.049.

14. Dworatzek E, Baczko I, Kararigas G. Effects of Aging on Cardiac Extracellular Matrix in Men and Women. Proteomics Clin Appl. 2016;10(1):84-91. doi: 10.1002/prca.201500031.

15. Mendes AB, Ferro M, Rodrigues B, Souza MR, Araujo RC, Souza RR. Quantification of Left Ventricular Myocardial Collagen System in Children, Young Adults, and the Elderly. Medicina. 2012;72(3):216-20.

16. Frangogiannis NG. Matricellular Proteins in Cardiac Adaptation and Disease. Physiol Rev. 2012;92(2):635-88. doi: 10.1152/physrev.00008.2011.

17. Lindqvist P, Waldenström A, Henein M, Mörner S, Kazzam E. Regional and Global Right Ventricular Function in Healthy Individuals Aged 20-90 Years: A Pulsed Doppler Tissue Imaging Study: Umeå General Population Heart Study. Echocardiography. 2005;22(4):305-14. doi: 10.1111/j.1540-8175.2005.04023.x.

18. Alam M, Wardell J, Andersson E, Samad BA, Nordlander R. Characteristics of Mitral and Tricuspid Annular Velocities Determined by Pulsed Wave Doppler Tissue Imaging in Healthy Subjects. J Am Soc Echocardiogr. 1999;12(8):618-28. doi: 10.1053/je.1999.v12.a99246.

19. Innelli P, Esposito R, Olibet M, Nistri S, Galderisi M. The Impact of Ageing on Right Ventricular Longitudinal Function in Healthy Subjects: A Pulsed Tissue Doppler Study. Eur J Echocardiogr. 2009;10(4):491-8. doi: 10.1093/ejechocard/jen313.

20. Kittipovanonth M, Bellavia D, Chandrasekaran K, Villarraga HR, Abraham TP, Pellikka PA. Doppler Myocardial Imaging for Early Detection of Right Ventricular Dysfunction in Patients with Pulmonary Hypertension. J Am Soc Echocardiogr. 2008;21(9):1035-41. doi: 10.1016/j.echo.2008.07.002.

Pulmonary Congestion in Heart Failure With Reduced Ejection Fraction: Comparison Between Lung Ultrasound and Remote Dielectric Sensing

Maria Estefânia Bosco Otto,[2] Vanessa Andreoli Esmanhoto,[1] Edileide de Barros Correia,[1] Ana Cristina de Souza Murta,[1] Larissa Ventura Ribeiro Bruscky,[1] Andrea de Andrade Vilela,[1] Antonio Tito Paladino Filho,[1] Jorge Eduardo Assef[1]

Instituto Dante Pazzanese de Cardiologia,[1] São Paulo, SP – Brazil

Instituto de Cardiologia e Transplante do Distrito Federal,[2] Brasília, DF – Brazil

Abstract

Backgound: Outpatient assessment of pulmonary congestion in patients with heart failure with reduced ejection fraction (HFREF) can minimize hospitalizations due to decompensation and optimize the use of diuretics.

Objective: To compare the remote dielectric sensor (REDS), a validated device for detecting pulmonary extravascular fluid, with clinical parameters, transthoracic echocardiogram (TTE) and lung ultrasound (ULSP).

Methods: We included 38 patients from heart failure clinic (63±12 years; 21 men). All were submitted within 24 hours to clinical evaluation with description of paroxysmal nocturnal dyspnea, leg edema (LE), presence of dizziness; laboratory evaluation of NT-ProBNP; evaluation by REDS and TTE with analysis of parameters of systemic congestion by the inferior vena cava evaluation, function of the right ventricle and of pulmonary congestion, such as evaluation of filling pressures by average of E/e' and indexed left atrial volume. The ULSP was performed using the 8 points anterior quadrants protocol, counting B lines in one respiratory cycle.

Results: 22 patients had REDS ≥ 35% (indicative of pulmonary congestion) and 16 patients REDS<35%. Clinical and echocardiographic parameters were compared with REDS ≥ 35%. In the multivariate analysis, the variables body surface area, B lines and LE were associated with REDS ≥ 35%. NT-ProBNP was similar and elevated in both groups.

Conclusions: Outpatient monitoring of HFREF for volume control can be sensitized by the presence of B lines on the ULSP with good correlation to REDS ≥ 35%. NT pro BNP was not able to differentiate patients with congestion detected by REDS.

Keywords: Ultrasonography; Lung; Heart Failure.

Introduction

Outpatient evaluation of the blood volume status of patients with heart failure with reduced ejection fraction (HFrEF), regardless of etiology, is complex and requires the integration of clinical and laboratory signs.[1,2] Early detection of higher blood volume by invasive methods was able to improve the optimization of pharmacological treatment, as well as avoid hospitalizations and complications, such as renal failure and inappropriate increase of diuretics.[3] However, the outpatient management of patients with HFrEF cannot use invasive methods, needing the analysis of clinical parameters associated with imaging methods, such as echocardiography[4-6] and lung ultrasound (LUS).[7-9]

Mailing Address: Maria Estefânia Bosco Otto •
Instituto de Cardiologia do Distrito Federal (ICDF): Ecocardiograma. SQSW 301. Bloco F. Ap 508. Postal Code: 70673-106. Brasília, DF – Brazil
E-mail: mariaestefaniaotto@gmail.com
Manuscript received March 10,2023; revised March 16, 2023; accepted March 16, 2023
Editor responsável pela revisão: Daniela do Carmo Rassi Frota

DOI: https://doi.org/10.36660/abcimg. 20230027i

Recently, a new volume assessment technology,[10] called ReDS (Remote Dielectric Sensing: Sensible Medical Innovations, Ltd, Klar Neter, Israel), has shown promising results in monitoring extravascular lung fluid, including validation by tomography.[11] Nevertheless, LUS has not been compared with ReDS performed in outpatient clinics to monitor patients with HFrEF and difficult therapeutic management. The advantage of using LUS associated with physical examination and laboratory analysis is its low cost, easy training, and good reproducibility.[8,9,12,13]

Thus, this study aimed to compare LUS with ReDS as the gold standard for extravascular lung fluid analysis in the diagnosis of pulmonary congestion among outpatients with HFrEF and difficult therapeutic management. Moreover, clinical, echocardiographic, and laboratory parameters were added to this analysis to provide sensitivity to the detection of systemic blood volume balance in this patient group.

Methods

In this prospective cohort pilot study, conducted from December 2021 to February 2022, we included patients over 18 years selected from the cardiomyopathy outpatient clinic of the Instituto Dante Pazzanese de Cardiologia (IDPC) who receive serial follow-up at the volume outpatient clinic because they have HFrEF with difficult volume control. Informed consent was obtained from each patient, and the study protocol complies with the ethical guidelines of the 1975 Helsinki Declaration. The IDPC Research Committee approved the protocol under the Certificate of Presentation for Ethical Consideration number 53224821.0.0000.5462.

Cases and study design

Patients with HFrEF and difficult volume control are evaluated in a specific IDPC outpatient clinic to reduce complications that may occur by the use of high doses of diuretics and earlier returns. In this scenario, the inclusion of patients could be concentrated on these days so that ReDS could be available for IDPC once a week, with echocardiography — focused on the analysis of parameters related to volume — and LUS — for the evaluation of B-lines — performed on the same day or in the next morning. The researchers responsible for ultrasound evaluations were not aware of the volume result obtained by ReDS.

We included 38 consecutive patients with HFrEF of various etiologies. Inclusion was based on the availability of ReDS and the possibility of timely performing the echocardiography and LUS.

Clinical evaluation

The selected patients were evaluated in routine outpatient visits. The following clinical data were chosen for comparison with the volume state: weight, body surface area (BSA), body mass index (BMI), lower extremity edema (LEE), and functional class by *the New York Heart Association*.[1] An experienced clinical cardiologist supervised and checked all clinical examinations.

Laboratory evaluation

Following the clinical evaluation, NT-proBNP was collected. The collection and analysis of blood tests were performed by IDPC's clinical laboratory. Collection standardization, methods, and analysis equipment are in accordance with the service routine.

Use of ReDS

After the collection of laboratory tests, the volunteers underwent a ReDS (Sensible Medical Innovations, Ltd, Klar Neter, Israel) evaluation. The ReDS technology consists of a miniature radar that transmits low-power electromagnetic signals to the body.[11,14] It can be used to evaluate the patient with a chest vest (Figure 1). Two sensors integrated into the vest are attached to the body: one in the anterior chest, on the right side, and the other in the posterior back. Each sensor can transmit and receive the beam of electromagnetic waves passing through the lung. The reflected signal is analyzed, translating the dielectric properties of the lung tissue between the sensors. Because water has a very high dielectric coefficient, tissue dielectric

Figure 1 – *ReDS. Image provided by the ReDS manufacturer (Remote Dielectric Sensing: Sensible Medical Innovations, Ltd, Klar Neter, Israel).*

coefficients are predominantly determined by their fluid content.[15] A healthy human lung (for an average person with 70 kg) has 450 to 500 mL of blood. The extravascular compartment usually has another 250 to 700 mL of fluid. As the normal total lung air volume is 1.8 to 2.2 L, considering a tidal volume of 500 mL, the normal intrathoracic fluid content can be estimated to vary between 20 and 34% of the total volume.[16] This range was confirmed by density measurements performed by different quantitative imaging technologies.[11,14]

ReDS measurements were taken by professionals trained to use the device. These patients remained seated at rest with the ReDS for 45 seconds, after which the device automatically provided the percentage of thoracic fluid. The normal value is defined as up to 34%, possible hypervolemia as 35–50%, significant hypervolemia as above 50%, and hypovolemia as below 20% (manufacturer data).

LUS

LUS was performed on GE Vivid E95 equipment (GE Health Care, Norway), using the eight-point anterior segment protocol with a 2-5 MHz sector transducer and the echocardiography device adjusted for "abdominal" mode. Images were acquired in 6 seconds, allowing the evaluation of a respiratory cycle. This protocol is called BLUE (Bedside Lung Ultrasound in Emergency),[12,17-19] with the patient at a 45-degree chest inclination in the bed. The protocol aims to evaluate the presence of B-lines — artifacts formed in the LUS due to the increase in parenchymal fluid — and count them in each segment during a respiratory cycle (Figure 2).[19] The finding of more than three B-lines in 2 quadrants of each hemithorax means congestion in patients with HFrEF. We chose to count the total of B-lines in both hemithorax.[9,19] This evaluation was performed by a trained examiner, who had no knowledge of the patient's clinical condition or of the results of laboratory tests and the estimated blood volume in the ReDS. Images were recorded and saved on specific media so that another professional involved in the study could analyze the B-line count variability.

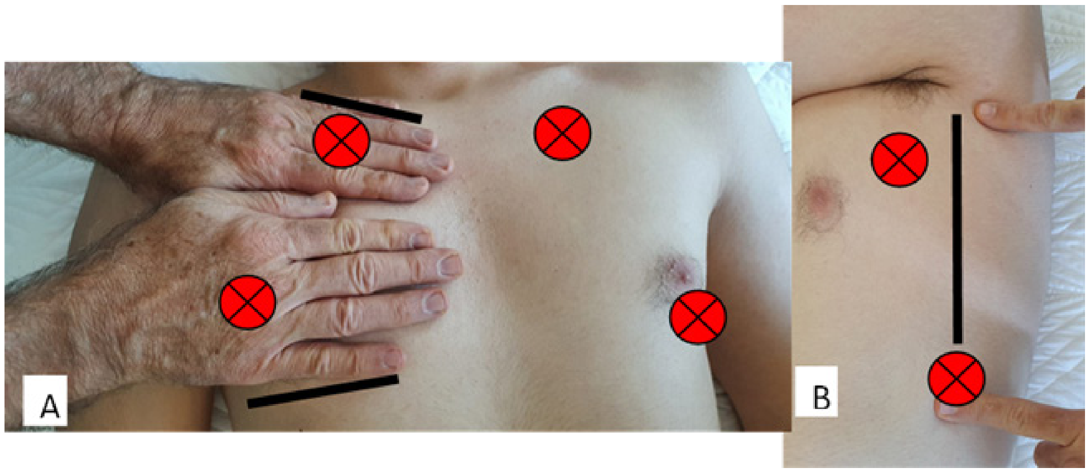

Figure 2 – *Schematic representation of the Bedside LUS in Emergency (BLUE) protocol. A) Analysis of the anterior thorax; B) Analysis of the lateral area using the posterior axillary line as a reference.*
Location model of points to be assessed in LUS using the BLUE protocol. A) Both hands are placed in the patient's hemithorax with the upper little finger right below the clavicle (black line above the little finger); excluding the thumbs, the lower part of the other hand is placed at the level of the diaphragm line (black line). The point called "upper BLUE" (red dot) is in the middle of the upper hand. The "lower BLUE point" is in the middle of the lower palm. These four points roughly follow the lung anatomy and avoid the heart area. B) The point of the costophrenic recess area (red dot) is built from the horizontal line continuing from the lower BLUE point and the vertical line continuing the posterior axillary line (black line). Lastly, an upper point can be added between the posterior and anterior axillary lines in the upper thorax. That way, we would have 4 points in each hemithorax. Image created by Maria Estefânia Bosco Otto, MD.[19]

Echocardiography

The echocardiography with assessment measurements for the biventricular function and specific parameters related to blood volume was performed concomitantly with LUS, on the same equipment, and by the same professional, who only changed the image analysis mode to "adult echocardiography". We evaluated the following left ventricle (LV) parameters: systolic diameter, diastolic diameter, and ejection fraction (EF) by Simpson's biplane method; LV outflow tract velocity time integral (LVOT VTI); integrated measures of diastolic function, such as mitral E-wave velocity, mitral A-wave velocity, E/A ratio, tissue Doppler of the septal and lateral mitral annulus to evaluate the e' wave velocity, mean E/e' ratio, left atrial volume (LAV), and pulmonary artery systolic pressure by continuous Doppler of tricuspid regurgitation; semi-quantitative assessment of right ventricular function with tricuspid annular plane systolic excursion (TAPSE) analysis, tricuspid lateral annular systolic velocity, and subjective evaluation; right atrial pressure (RAP) assessment with analysis of the inferior vena cava (IVC) according to guidelines of the American Society of Echocardiography.[20,21]

Echocardiographic images were recorded and saved in specific media.

Statistical analysis

We compared imaging and clinical parameters among patients with ReDS <35% and ≥35% using Student's *t* test or the non-parametric Mann-Whitney test for quantitative variables and the chi-square test or exact chi-square test for qualitative variables.

Evaluation of independent indicators of pulmonary congestion consisted of comparing heart and clinical parameters and adjustment of Poisson regression models with robust variance for the ReDS ≥35% result associated with epidemiological, vital signs, and anthropometric variables, LV mass, volume, and function, diastolic function, right ventricle (RV), IVC, and clinical variables, adopting prevalence ratio and their respective confidence intervals as the effect measure. The analysis had two stages: univariate and multivariate. In both, we calculated prevalence ratios and their respective 95% confidence intervals.

The univariate analysis revealed an association between each independent variable and ReDS≥35%; those with p<0.25 were included in the multivariate analysis. In the multivariate analysis, the models were constructed by the consecutive exclusion of a variable with the highest p-value in the Wald test from each complete model, as described by Hosmer and Lemeshow, followed by the readjustment and verification of the model stability after the removal of each variable, in order to obtain a more parsimonious model, with a better fit to the data. Once the final model was obtained, the variables that had been excluded after the univariate analysis were added one by one, repeating the Poisson regression analysis to identify the variables that could contribute to the model.

We also evaluated the multicollinearity between independent variables. The multicollinearity threshold was defined as a tolerance indicator with values less than 0.40.

In addition, p<0.05 was considered significant. The analyses were performed in the SAS 9.4 application.

Results

Among the 38 patients, 22 (58%) had pulmonary congestion with ReDS ≥ 35%, and 16 did not have congestion (patients with ReDS < 35%). Tables 1 (qualitative variables) and 2 (quantitative variables) describe the characteristics of the patient sample. Table 3 compares the groups with ReDS ≥ 35% and < 35% as to systemic and pulmonary congestion parameters. REDs>35% group was older than REDs < 35%, ≥ 35% group (pulmonary congestion). Although the mean number of B-lines was higher in the ReDS ≥35% group than in the ReDS < 35% group, no statistical significance was found. The remaining parameters showed no differences.

Clinical data — such as BSA, gender, dizziness, paroxysmal nocturnal dyspnea, and LEE —, NT-proBNP, and TTE measurements — such as LAV, LVOT VTI, mean E/e′ ratio, RV peak lateral tricuspid annular systolic velocity (RV S′), TAPSE, IVC analysis, and B-line count — were compared with Poisson models with robust variance adjusted for ReDS ≥35%. In the multivariate analysis, these were the variables associated with ReDS≥35% and their adjusted prevalence ratio (aPR): BSA: 8.7 (2.7; 27.8), p = 0.003; RV S′: 1.12 (1.00; 1.04), p = 0.03; B-lines: 1.02 (1.00; 1.04), p = 0.04; and LEE: 1.56 (1.00; 2.57), p = 0.04 (Table 4).

NT-proBNP was similar and high in both groups, with no correlation with ReDS (4311 ± 3289 mg/dL for ReDS <35% and 4267 ± 4136 mg/dL for ReDS ≥35%, p = 0.97) (Table 4).

The B-line count variability among observers was assessed based on stored images from 20 patients, with a 97% correlation coefficient.

Table 1 – Categorical variables (n = 38)

Variables	Frequency (n)	Percentage (%)
ReDS		
<35%	16	42%
≥35%	22	58%
Gender		
Female	17	45
Male	21	55
Mitral regurgitation		
None	2	5.3
Mild	7	18.4
Moderate	12	31.6
Severe	17	44.7
Tricuspid regurgitation		
None	4	10.5
Mild	18	47.4
Moderate	8	21.1
Severe	8	21.1
Etiology of cardiomyopathy		
Idiopathic	26	68.4
Chagas	9	23.6
Ischemic	3	7.8

ReDS: Remote Dielectric Sensing.

Table 2 – Continuous variables

Parameters	Mean	SD	Minimum	Maximum
Age (years)	63.2	12.4	26	81
Systolic blood pressure (mmHg)	112.8	21.4	70	160
Diastolic blood pressure (mmHg)	72.5	14.4	50	100
BSA (m^2)	1.8	0.2	1.41	2.3
BMI (kg/m^2)	29.5	8.1	16.5	55.7
LV diastolic diameter (mm)	66.5	7.9	55	84
Simpson's LV EF (%)	23.9	6.7	15	40
LV mass index (g/m^2)	126.5	39.4	69	246
LA volume index (mL/m^2)	65.1	23.4	31	158
RA volume index (mL/m^2)	48.9	32.9	14	172
RV basal diameter (mm)	40.9	9.3	20	61
RV lateral annular tissue velocity	8.2	2.6	4	16
TAPSE (mmHg)	14.5	4.6	4	26

SD: standard deviation; LV: left ventricle; RV: right ventricle; LA: left atrium; RA: right atrium; TAPSE: tricuspid annular plane systolic excursion; BSA: body surface area; BMI: body mass index; EF: ejection fraction.

Discussion

The main finding of this pilot study of patients with HFrEF and difficult therapeutic volume management was the significant correlation between LUS B-lines and a high-accuracy device for the detection of pulmonary congestion (ReDS). Thus, LUS can be adopted in the outpatient management of pulmonary congestion, reducing the costs of frequent hospitalizations and optimizing the use of diuretics.

ReDS has an excellent correlation with chest computed tomography for the detection of pulmonary congestion, using software that analyzes the pulmonary density of patients with decompensated HFrEF and normal volunteers,[11] as well as those with pulmonary capillary pressure by an invasive method.[14] However, no studies have compared the number of B-lines in outpatient LUS among patients with HFrEF and ReDS as the gold standard.

The use of LUS to evaluate pulmonary congestion is well established. A multicenter study conducted by the Study and Research Center of the Italian Society of Emergency Medicine (*Società Italiana di Medicina di Emergenza Urgenza* — SIMEU) found that clinical evaluation associated with the detection of B-lines in LUS had a 97% accuracy in detecting pulmonary congestion, a number that exceeded even that of NT-proBNP, which presented only 62% accuracy.[9] These findings agree with those of our study, with B-lines correlated with ReDS≥35%, and NT-proBNP, although high in both groups, showing no correlation with ReDS.

Table 3 – Comparison between REDs ≥35% and REDs <35% groups

Parameters	ReDS		p-value
	< 35%	≥ 35%	
Age (years)	59±14.5	67±8.3	0.03
LVOT VTI	12.5 ± 4.8	12.8 ± 4.1	0.82
Mean E/e'	16.1 ± 7.2	17.1 ± 7.1	0.69
IVC (mm)	17.4 ± 7.3	17.95 ± 4.6	0.76
Vena cava collapse (%)	42.5 ± 41.5	33.36 ± 25.4	0.89
RA estimated blood pressure (mmHg)	6.6 ± 5.3	7.23 ± 4.41	0.44
NT-proBNP (pcg/mL)	4311.4 ± 3289.7	4267.7 ± 4136.9	0.97
B-lines (units)	7.19 ± 4.43	9.82 ± 7.43	0.18
Dizziness			0.97
No	11 (42.31)	15 (57.69)	
Yes	5 (41.67)	7 (58.33)	
Paroxysmal nocturnal dyspnea			0.19
No	12 (50.00)	12 (50.00)	
Yes	4 (28.57)	10 (71.43)	
Jugular vein distention			0.11
No	4 (26.67)	11 (73.33)	
Yes	12 (52.17)	11 (47.83)	
LEE			0.08
No	11 (50.00)	9 (45.00)	
Yes	5 (27.78)	13 (72.22)	
Hepatomegaly			0.57
No	8 (38.10)	13 (61.90)	
Yes	8 (47.06)	9 (52.94)	
Troponin			0.24
Abnormal (≥0.04 ng/mL)	11 (50.00)	11 (50.00)	
Normal (<0.04 ng/mL)	5 (31.25)	11 (68.75)	
Creatinine			0.66
Normal (<1.4 mg/dL)	8 (42.11)	11 (57.89)	
Mild abnormality (1.4–2.0 mg/dL).	5 (35.71)	9 (64.29)	
Moderate abnormality (>2.1 mg/dL)	3 (60.00)	2 (40.00)	
NYHA FC HF			0.82
I	0 (0.00)	2 (100.00)	
II	8 (47.06)	9 (52.94)	
III	7 (41.18)	10 (58.82)	
IV	1 (50.00)	1 (50.00	

ReDS: Remote Dielectric Sensing; LVOT VTI: left ventricular outflow tract velocity time integral; E/e': ratio between the mitral inflow E velocity and the mean lateral and medial annular tissue Doppler; RA: right atrium; NT-proBNP: N-terminal pro-B-type natriuretic peptide; LEE: lower extremity edema; IVC: inferior vena cava; NYHA FC HF: New York Heart Association Functional Class of Heart Failure.

Table 4 – Multivariate analysis with adjusted variance for ReDS≥35%

Variables	Crude PR		Adjusted PR*	
	PR (95%CI)	p-value	PR (95%CI)	p-value
Gender		0.0862	-	-
Female	1	-	-	-
Male	1.73 (0.92; 3.25)	0.09	-	-
Systolic blood pressure	1.01 (1.00; 1.03)	0.05	-	-
Diastolic blood pressure	1.01 (0.99; 1.03)	0.16	-	-
BSA	5.41 (2.2; 13.6)	0.0003	8.67 (2.71; 27.82)	0.0003
BMI	1.02 (0.99; 1.06)	0.25	-	-
End-diastolic diameter	1.02 (0.99; 1.05)	0.23	-	-
LA volume index	1.00 (1.00; 1.01)	0.34	-	-
RV S'	1.07 (0.99; 1.20)	0.06	1.12 (1.01; 1.24)	0.0262
TAPSE	1.03 (0.97; 1.09)	0.36	-	-
LVOT VTI	1.01 (0.94; 1.07)	0.82	-	-
Mean E/e'	1.01 (0.97; 1.05)	0.68	-	-
IVC	1.01 (0.96; 1.06)	0.78	-	-
Vena cava collapse	1.00 (0.99; 1.01)	0.43	-	-
RA estimated blood pressure	1.01 (0.95; 1.07)	0.70	-	-
NT-proBNP	1.00 (1.00; 1.00)	0.97	-	-
B-lines	1.03 (0.99; 1.06)	0.09	1.02 (1.00; 1.04)	0.0403
Dizziness/BP drop		0.97	-	-
No	1	-	-	-
Yes	1.01 (0.57; 1.81)	0.97	-	-
Paroxysmal nocturnal dyspnea		0.17	-	-
No	1	-	-	-
Yes	1.43 (0.85; 2.40)	0.18	-	-
LEE		0.09		0.0479
No	1	-	1	-
Yes	1.60 (0.91; 2.82)	0.09	1.56 (1.00; 2.57)	0.0479

ReDS: Remote Dielectric Sensing; PR: prevalence ratio; 95%CI: 95% confidence interval; LA: left atrium; RV S': right ventricle tricuspid annular systolic velocity by tissue Doppler imaging; TAPSE: tricuspid annular plane systolic excursion; LVOT VTI: left ventricular outflow tract velocity time integral; E/e': ratio between the mitral inflow E velocity and the mean lateral and medial annular tissue Doppler; RA: right atrium; NT-proBNP: N-terminal pro-B-type natriuretic peptide; BP: blood pressure; LEE: lower extremity edema; BSA: body surface area; BMI: body mass index; IVC: inferior vena cava.

The increase in B-lines identified in LUS, in addition to improve diagnose the cause of dyspnea in the emergency department,[22] is associated with a higher number of hospitalizations[23] and worse prognosis in post-myocardial infarction patients.[24] Miglioranza et al.[8] revealed that the finding of 15 B-lines in LUS indicated the possibility of imminent decompensation among patients in outpatient follow-up, but did not compare the congestion results from LUS with any gold standard. Our study found that, compared to a gold standard (ReDS), B-lines were correlated with increased pulmonary congestion in outpatients with HFrEF and difficult volume control.

Regarding systemic congestion parameters, we detected a correlation with ReDS≥35% only in the evaluation of the longitudinal function of RV S′ by tissue Doppler imaging and in the finding of LEE on physical examination. ReDS was not expected to correlate with systemic congestion parameters, since it measures the amount of extravascular lung fluid. Nonetheless, patients with greater pulmonary congestion and RV dysfunction might present higher systemic congestion and, consequently, LEE.[1,2]

BSA had a good correlation with ReDS, as the calculation used by the device depends on the patient's weight and height.[11]

Potential limitations and strengths of the study

The main study limitation is the small number of patients, all recruited from a single center. Another possible limitation was the lack of invasive measures that could directly detect filling pressures for comparison with the number of B-lines and ReDS.

Given the significant correlation of B-lines with ReDS≥35%, despite the reduced number of individuals included in the study, this result is the main strength of the research, due to the high sensitivity of B-line detection by LUS among patients with difficult volume control.

Conclusions

In this pilot study, LUS presented a good correlation with pulmonary congestion measured by a high-accuracy device (ReDS) and can be a particularly useful tool in the outpatient management of patients with HFrEF, reducing hospitalizations and improving blood volume control among these individuals.

Regarding systemic congestion parameters, only RV S' was significant, indicating that patients with greater RV dysfunction have concomitant pulmonary congestion and systemic congestion.

Acknowledgments

The authors thank Professor Eduardo Freitas da Silva for the outstanding work in correcting and guiding the statistical analysis.

Author Contributions

Conception and design of the research: Otto MEB, Vilela AA, Paladino Filho AT, Assef JE; acquisition of data: Otto MEB, Esmanhoto VA, Vilela AA, Paladino Filho AT; analysis and interpretation of the data and critical revision of the manuscript for intellectual content: Otto MEB, Esmanhoto VA, Vilela AA, Paladino Filho AT, Assef JE; statistical analysis: Otto MEB; writing of the manuscript: Otto MEB, Esmanhoto VA, Assef JE.

Potential Conflict of Interest

No potential conflict of interest relevant to this article was reported.

Sources of Funding

There were no external funding sources for this study.

Study Association

This study is not associated with any thesis or dissertation work.

Ethics Approval and Consent to Participate

This study was approved by the Ethics Committee of the Instituto Dante Pazzanese under the protocol number 532248210.0000.5462. All the procedures in this study were in accordance with the 1975 Helsinki Declaration, updated in 2013. Informed consent was obtained from all participants included in the study.

References

1. Sano H, Tanaka H, Motoji Y, Fukuda Y, Mochizuki Y, Hatani Y, et al. Right Ventricular Relative Wall Thickness as a Predictor of Outcomes and of Right Ventricular Reverse Remodeling for Patients with Pulmonary Hypertension. Int J Cardiovasc Imaging. 2017;33(3):313-21. doi: 10.1007/s10554-016-1004-z.
2. McDonald K. Monitoring Fluid Status at the Outpatient Level: The Need for More Precision. Congest Heart Fail. 2010;16 Suppl 1:S52-5. doi: 10.1111/j.1751-7133.2010.00171.x.
3. Abraham WT, Adamson PB, Bourge RC, Aaron MF, Costanzo MR, Stevenson LW, et al. Wireless Pulmonary Artery Haemodynamic Monitoring in Chronic Heart Failure: A Randomised Controlled Trial. Lancet. 2011;377(9766):658-66. doi: 10.1016/S0140-6736(11)60101-3.
4. Androne AS, Hryniewicz K, Hudaihed A, Mancini D, Lamanca J, Katz SD. Relation of Unrecognized Hypervolemia in Chronic Heart Failure to Clinical Status, Hemodynamics, and Patient Outcomes. Am J Cardiol. 2004;93(10):1254-9. doi: 10.1016/j.amjcard.2004.01.070.
5. Chouihed T, Rossignol P, Bassand A, Duarte K, Kobayashi M, Jaeger D, et al. Diagnostic and Prognostic Value of Plasma Volume Status at Emergency Department Admission in Dyspneic Patients: Results from the PARADISE Cohort. Clin Res Cardiol. 2019;108(5):563-73. doi: 10.1007/s00392-018-1388-y.
6. Massari F, Scicchitano P, Iacoviello M, Passantino A, Guida P, Sanasi M, et al. Multiparametric Approach to Congestion for Predicting Long-Term Survival in Heart Failure. J Cardiol. 2020;75(1):47-52. doi: 10.1016/j.jjcc.2019.05.017.
7. Girerd N, Seronde MF, Coiro S, Chouihed T, Bilbault P, Braun F, et al. Integrative Assessment of Congestion in Heart Failure Throughout the Patient Journey. JACC Heart Fail. 2018;6(4):273-85. doi: 10.1016/j.jchf.2017.09.023.
8. Miglioranza MH, Gargani L, Sant'Anna RT, Rover MM, Martins VM, Mantovani A, et al. Lung Ultrasound for the Evaluation of Pulmonary Congestion in Outpatients: A Comparison with Clinical Assessment, Natriuretic Peptides, and Echocardiography. JACC Cardiovasc Imaging. 2013;6(11):1141-51. doi: 10.1016/j.jcmg.2013.08.004.
9. Pivetta E, Goffi A, Lupia E, Tizzani M, Porrino G, Ferreri E, et al. Lung Ultrasound-Implemented Diagnosis of Acute Decompensated Heart Failure in the ED: A SIMEU Multicenter Study. Chest. 2015;148(1):202-10. doi: 10.1378/chest.14-2608.
10. Yancy CW, Jessup M, Bozkurt B, Butler J, Casey DE Jr, Colvin MM, et al. 2017 ACC/AHA/HFSA Focused Update of the 2013 ACCF/AHA Guideline for the Management of Heart Failure: A Report of the American College of Cardiology/American Heart Association Task Force on Clinical Practice Guidelines and the Heart Failure Society of America. Circulation. 2017;136(6):e137-e161. doi: 10.1161/CIR.0000000000000509.
11. Amir O, Azzam ZS, Gaspar T, Faranesh-Abboud S, Andria N, Burkhoff D, et al. Validation of Remote Dielectric Sensing (ReDS™) Technology for Quantification of Lung Fluid Status: Comparison to High Resolution Chest Computed Tomography in Patients with and without Acute Heart Failure. Int J Cardiol. 2016;221:841-6. doi: 10.1016/j.ijcard.2016.06.323.
12. Picano E, Pellikka PA. Ultrasound of Extravascular Lung Water: A New Standard for Pulmonary Congestion. Eur Heart J. 2016;37(27):2097-104. doi: 10.1093/eurheartj/ehw164.
13. Zisis G, Yang Y, Huynh Q, Whitmore K, Lay M, Wright L, et al. Nurse-Provided Lung and Inferior Vena Cava Assessment in Patients with Heart Failure. J Am Coll Cardiol. 2022;80(5):513-23. doi: 10.1016/j.jacc.2022.04.064.

14. Uriel N, Sayer G, Imamura T, Rodgers D, Kim G, Raikhelkar J, et al. Relationship between Noninvasive Assessment of Lung Fluid Volume and Invasively Measured Cardiac Hemodynamics. J Am Heart Assoc. 2018;7(22):e009175. doi: 10.1161/JAHA.118.009175.

15. Gabriel C, Gabriel S, Corthout E. The Dielectric Properties of Biological Tissues: I. Literature Survey. Phys Med Biol. 1996;41(11):2231-49. doi: 10.1088/0031-9155/41/11/001.

16. Wallin CJ, Leksell LG. Estimation of Extravascular Lung Water in Humans with Use of 2H2O: Effect of Blood Flow and Central Blood Volume. J Appl Physiol. 1994;76(5):1868-75. doi: 10.1152/jappl.1994.76.5.1868.

17. Gargani L, Volpicelli G. How I do It: Lung Ultrasound. Cardiovasc Ultrasound. 2014;12:25. doi: 10.1186/1476-7120-12-25.

18. Lichtenstein DA. BLUE-Protocol and FALLS-Protocol: Two Applications of Lung Ultrasound in the Critically Ill. Chest. 2015;147(6):1659-70. doi: 10.1378/chest.14-1313.

19. Otto MEB, Esmanhoto VA. My Approach to Lung Ultrasound to Evaluate Extravascular Lung Water. Arq Bras Cardiol: Imagem Cardiovasc. 2022;35(3):1-4. doi: 10.47593/2675-312X/20223503ecom22.

20. Lang RM, Badano LP, Mor-Avi V, Afilalo J, Armstrong A, Ernande L, et al. Recommendations for Cardiac Chamber Quantification by Echocardiography in Adults: An Update from the American Society of Echocardiography and the European Association of Cardiovascular Imaging. J Am Soc Echocardiogr. 2015;28(1):1-39.e14. doi: 10.1016/j.echo.2014.10.003.

21. Nagueh SF, Smiseth OA, Appleton CP, Byrd BF 3rd, Dokainish H, Edvardsen T, et al. Recommendations for the Evaluation of Left Ventricular Diastolic Function by Echocardiography: An Update from the American Society of Echocardiography and the European Association of Cardiovascular Imaging. J Am Soc Echocardiogr. 2016;29(4):277-314. doi: 10.1016/j.echo.2016.01.011.

22. Zanobetti M, Scorpiniti M, Gigli C, Nazerian P, Vanni S, Innocenti F, et al. Point-of-Care Ultrasonography for Evaluation of Acute Dyspnea in the ED. Chest. 2017;151(6):1295-301. doi: 10.1016/j.chest.2017.02.003.

23. Platz E, Campbell RT, Claggett B, Lewis EF, Groarke JD, Docherty KF, et al. Lung Ultrasound in Acute Heart Failure: Prevalence of Pulmonary Congestion and Short- and Long-Term Outcomes. JACC Heart Fail. 2019;7(10):849-58. doi: 10.1016/j.jchf.2019.07.008.

24. Araujo GN, Silveira AD, Scolari FL, Custodio JL, Marques FP, Beltrame R, et al. Admission Bedside Lung Ultrasound Reclassifies Mortality Prediction in Patients With ST-Segment-Elevation Myocardial Infarction. Circ Cardiovasc Imaging. 2020;13(6):e010269. doi: 10.1161/CIRCIMAGING.119.010269.

Lung Ultrasound in Outpatients with Heart Failure

Marco Stephan Lofrano-Alves[1]

Universidade Federal do Paraná,[1] *Curitiba, PR – Brazil*

Short Editorial related to the article: Pulmonary Congestion in Heart Failure With Reduced Ejection Fraction: Comparison Between Lung Ultrasound and Remote Dielectric Sensing

Over the last decade, we have witnessed the widespread use of lung ultrasound (LU) in the assessment of pulmonary congestion. In addition to the well-known technique of auscultation of adventitious lung sounds, LU makes an important contribution by sharpening our vision to the diagnosis of pulmonary interstitial edema by quantification of B-lines. LU has emerged as a relevant and updated method, since it is a safe, low-cost, rapid and available at bedside, being an alternative to imaging methods associated with ionizing radiation, such as chest tomography and X-ray.[1]

LU is a standardized tool in diagnosis and treatment monitoring today, and has been studied in different clinical scenarios of pulmonary congestion of cardiogenic origin.[2-5] In outpatients with heart failure and reduced ejection fraction (HFrEF), B-line counting by LU showed an 89% accuracy with a cutoff ≥ 15 B-lines.[6] In another study with patients hospitalized for HFrEF, the risk of an adverse in-hospital event increased with the rising number of B-lines at admission, and the risk of HF hospitalization and all-cause death was greater in patients with a higher number of B-lines at discharge.[2]

In the current issue of ABC *Imagem Cardiovascular*, Otto *et al.* present an interesting correlation of LU with ambulatory monitoring of pulmonary congestion using a remote dielectric sensing (ReDS) technology in 38 HFrEF patients and inappropriate control of blood volume. ReDS technology uses low-power electromagnetic signals that are emitted to the thorax to estimate lung fluid volume, which is expressed as percentage of total lung volume.[7] By using the ReDS method and adopting a cutoff ≥35% of net volume, the authors found that pulmonary congestion was present in 58% of HFrEF patients, mostly in older patients. Among the variables studied, the presence of B-lines on LU, the lateral tricuspid annulus peak velocity on tissue Doppler, and the presence of lower limb edema were associated with pulmonary congestion on ReDS. In contrast, neither serum NT-proBNP levels nor the E/E' ratio was correlated with pulmonary congestion.

To the new generation of physicians, the diagnosis of pulmonary congestion depends much more on "seeing" than "hearing". However, caution is needed in interpreting the B-lines and their association with cardiogenic edema. B-lines can be found in pulmonary diseases including interstitial pneumonia, atelectasis, and severe acute respiratory syndrome, and are a sensitive, although nonspecific sign of cardiogenic pulmonary edema. The distinguishing of B-lines for excess interstitial fluid from fibrotic B-lines, for example, may be difficult by LU. Studies comparing LU with other methods of assessing pulmonary fluid content are scarce but needed for its validation. Therefore, the study by Otto *et al.* is very welcome.

Author Contributions

Conception and design of the research and writing of the manuscript: Lofrano-Alves M

Potential Conflict of Interest

No potential conflict of interest relevant to this article was reported.

Sources of Funding

There were no external funding sources for this study.

Study Association

This study is not associated with any thesis or dissertation work.

Ethics Approval and Consent to Participate

This article does not contain any studies with human participants or animals performed by any of the authors.

Keywords

Ultrasonics; Lung; Heart Failure

Mailing Address: Marco Stephan Lofrano-Alves •
Universidade Federal do Paraná, Clínica Médica. Rua General Carneiro, 181.
Postal Code: 82060-900. Alto da Glória, Curitiba, PR – Brazil
E-mail: mslalves@hotmail.com
Editor responsible for the review: Daniela do Carmo Rassi Frota

DOI: https://doi.org/10.36660/abcimg.20230049i

References

1. Picano E, Pellikka PA. Ultrasound of Extravascular Lung Water: A New Standard for Pulmonary Congestion. Eur Heart J. 2016;37(27):2097-104. doi: 10.1093/eurheartj/ehw164.

2. Platz E, Campbell RT, Claggett B, Lewis EF, Groarke JD, Docherty KF, et al. Lung Ultrasound in Acute Heart Failure: Prevalence of Pulmonary Congestion and Short- and Long-Term Outcomes. JACC Heart Fail. 2019;7(10):849-58. doi: 10.1016/j.jchf.2019.07.008.

3. Araujo GN, Silveira AD, Scolari FL, Custodio JL, Marques FP, Beltrame R, et al. Admission Bedside Lung Ultrasound Reclassifies Mortality Prediction in Patients With ST-Segment-Elevation Myocardial Infarction. Circ Cardiovasc Imaging. 2020;13(6):e010269. doi: 10.1161/CIRCIMAGING.119.010269.

4. Scali MC, Zagatina A, Ciampi Q, Cortigiani L, D'Andrea A, Daros CB, et al. Lung Ultrasound and Pulmonary Congestion During Stress Echocardiography. JACC Cardiovasc Imaging. 2020;13(10):2085-95. doi: 10.1016/j.jcmg.2020.04.020.

5. Wiley BM, Luoma CE, Kucuk HO, Padang R, Kane GC, Pellikka PA. Lung Ultrasound During Stress Echocardiography Aids the Evaluation of Valvular Heart Disease Severity. JACC Cardiovasc Imaging. 2020;13(3):866-72. doi: 10.1016/j.jcmg.2019.06.026.

6. Miglioranza MH, Gargani L, Sant'Anna RT, Rover MM, Martins VM, Mantovani A, et al. Lung Ultrasound for the Evaluation of Pulmonary Congestion in Outpatients: A Comparison with Clinical Assessment, Natriuretic Peptides, and Echocardiography. JACC Cardiovasc Imaging. 2013;6(11):1141-51. doi: 10.1016/j.jcmg.2013.08.004.

7. Imamura T, Hori M, Ueno Y, Narang N, Onoda H, Tanaka S, et al. Association between Lung Fluid Levels Estimated by Remote Dielectric Sensing Values and Invasive Hemodynamic Measurements. J Clin Med. 2022;11(5):1208. doi: 10.3390/jcm11051208.

Original Article

Long-Term Evolution of Patients with Important Pulmonary Hypertension due to Schistosomiasis

José Maria Del Castillo,[1,2] Katarina Barros de Oliveira,[1] Rafael Ricardo de Oliveira Travassos,[1] Ângela Maria Pontes Bandeira,[3] Carlos Antônio da Mota Silveira,[3] Djair Brindeiro Filho[1]

Escola de Ecografia de Pernambuco (ECOPE),[1] Recife, PE – Brazil

Universidade Católica de Pernambuco (UNICAP),[2] Recife, PE – Brazil

Pronto Socorro Cardiológico de Pernambuco (PROCAPE), UPE,[3] Recife, PE – Brazil

Abstract

Introduction: **Hepatosplenic schistosomiasis mansoni, associated with pulmonary arterial hypertension (PAH), causes cardiac chamber remodeling. Little is known about its long-term evolution.**

Objective: **To evaluate the alterations caused by PAH in patients with schistosomiasis and analyze the clinical and echocardiographic evolution over a period of 10 years.**

Methods: **The study included 60 patients with PAH due to schistosomiasis and 50 healthy control patients. Clinical and echocardiographic data were evaluated, including dimensions, parietal thickness, function of the right and left chambers, and parameters of myocardial strain. Patients in the group with PAH due to schistosomiasis were followed for 10 years. Data were compared using Student's t test for unpaired samples with significance level of < 5%.**

Results: **Patients with PAH had smaller left ventricular dimension without alteration in the ejection fraction, but with decreased left ventricular global longitudinal strain and left atrial reservoir strain. The right ventricular dimensions and parietal thickness were increased, and the parameters of systolic function (tricuspid annular plane systolic excursion, fractional area change, tricuspid s' wave, and the right ventricular global longitudinal strain) were significantly reduced. During the follow-up period, 18 patients (32%) died, and death was associated with higher functional class, decreased right ventricular longitudinal strain, larger right ventricular size, decreased fractional area change, and decreased tricuspid annular s' wave velocity.**

Conclusion: **PAH related to schistosomiasis causes remodeling of the right chambers, with decreased parameters of systolic function and myocardial strain. The long-term evolution, with elevated mortality, presents with larger right ventricular dimensions, lower fractional area change, lower tricuspid annular systolic velocity, lower right ventricular global longitudinal strain, and more advanced functional class.**

Keywords: **Pulmonary Hypertension; Schistosomiasis; Echocardiography.**

Introduction

Schistosomiasis is considered a neglected tropical disease[1] originally from North Africa, caused by trematodes of the genus *schistosoma*, comprising several species. *Schistosoma mansoni* is the only one that exists in South and Central America, and it was likely introduced during the era of slavery. [2] It is widespread throughout almost all of Brazilian territory, especially in the Northeast Region, and it presents several clinical forms. The main ones are the initial phase, predominantly characterized by allergic manifestations due to the entry of cercariae transmitted into the water by snails of the *biomphalaria* species, and the late phase. During the late phase, the most frequent forms are hepatointestinal and hepatic, generally with few symptoms, and the hepatosplenic form, which may be compensated, decompensated, or complicated, and may progress to portal hypertension, splenomegaly, esophageal varices, and ascites. [2]

Approximately 10% of patients with the hepatosplenic form have the vasculopulmonary form, with pre-capillary pulmonary hypertension, caused by obstruction of pulmonary arterioles by eggs, dead worms, and/or pulmonary vasculitis due to immune complexes. In more severe cases, there may be cyanosis due to the presence of fistulas between the portal system and the pulmonary veins. It causes major dilation of the right chambers and the pulmonary artery, and little is known about its long-term evolution, even with treatment with pulmonary vasodilators. Other rarer complications are renal, neurological, pseudoneoplastic, and lymphoproliferative. The diagnosis can be direct (visualization of *S. mansoni* eggs

Mailing Address: José Maria Del Castillo •
Rua Jorge de Lima, 245, apto 303. Salute. Postal code: 51160-070. Imbiribeira, Recife, PE – Brazil
E-mail: castillojmd@gmail.com
Manuscript received January 1, 2023; revised manuscript January 11, 2023; accepted March 19, 2023.
Editor responsible for the review: Daniela do Carmo Rassi Frota

DOI: https://doi.org/10.36660/abcimg.2023373i

in feces or tissues) or indirect (based on immunological tests such as ELISA, periovular reaction, and intradermal reaction). Abdominal ultrasonography is particularly useful in the hepatosplenic form, because, in severe cases, it provides evidence of Symmers' hepatic fibrosis with greater sensitivity than percutaneous biopsy.[3]

The method of choice to assess pulmonary hypertension and its cardiac repercussions is Doppler echocardiography, allowing estimation of pulmonary pressures, dimensions, parietal thickness, and systolic function of the right ventricle (RV). Based on this fact, the objective of this study was to evaluate, through clinical and echocardiographic data, the long-term evolution of patients with hepatosplenic schistosomiasis and pulmonary hypertension.

Material and methods

This prospective longitudinal study studied 60 patients diagnosed with hepatosplenic schistosomiasis with pulmonary hypertension (PAH group) for a period of 10 years (between January 2012 and June 2022). For comparison, 50 healthy individuals in the same age group (control group) were studied.

All patients were clinically stratified according to New York Heart Association functional class (FC).

The exclusion criteria for the PAH group were the absence of direct or laboratory diagnosis of schistosomiasis; the occurrence of previous pulmonary disease, with or without pulmonary hypertension; any type of congenital heart disease; and patients who did not complete clinical follow-up.

Echocardiographic analysis

Using conventional echocardiography, the following data were evaluated: dimensions and function of the left chambers; mean left atrial (LA) pressure using the ratio between the mitral E wave and the mean e' wave of the mitral annulus by tissue Doppler (E/e'); dimensions and function of the right chambers by tricuspid annular plane systolic excursion (TAPSE), RV fractional area change, and tricuspid annular s' wave; RV systolic pressure by tricuspid regurgitation gradient; pulmonary vascular resistance in Wood units; and the relative RV thickness, by the quotient between the basal RV diameter and the thickness of the RV lateral wall. All measurements were taken according to American Society of Echocardiography recommendations.[4]

The following formula was used to assess RV systolic pressure:

$$RVSP = TRV^2 \times 4$$

RVSP: right ventricular systolic pressure; TRV: maximal tricuspid regurgitation velocity.

The following formula was used to assess pulmonary vascular resistance:[5]

$$PVR = (TRV \times TVI_{RVOT}) \times 10 + 0.16$$

PVR: pulmonary vascular resistance; TRV: tricuspid regurgitation velocity; TVI_{RVOT}: right ventricular outflow tract time-velocity integral.

Using the speckle tracking method, the longitudinal strain of the ventricular and atrial chambers was evaluated. To obtain the global longitudinal strain of the left ventricle (LV), the apical 4-, 2- and 3-chamber views were used.[6] To obtain the global longitudinal strain of the RV, the apical 4-chamber view focused on this cavity was used.[7] The apical 4-chamber view aligned with the atrial cavities was used to obtain the longitudinal strain of the reservoir of the LA [8] and right atrium (RA). [9]

In a prospective analysis, the outcome and evolution of the patients was determined by studying the clinical records and the echocardiographic examinations performed during the study period.

Echocardiographic examinations were performed using CX50 and Affiniti 70 equipment (Philips, Andover, MA) by a single examiner. Qlab 15 (Koninklijke Philips Electronics N.V. 2020) software was used for the analysis of strain data stored in DICOM format.

Statistical analysis

Study sample size was defined by convenience. The data, between the first examination of patients in the PAH group, expressed as mean and standard deviation of the mean, were compared with those of individuals in the control group using Student's t test for unpaired samples, with a statistical significance level of < 5 %. To verify the homoscedasticity between numerical data, analysis of variances was performed (Z test). For all statistical measurements, the Bioestat 5.0 program was used.

Results

The mean age at the time of the first examination was 48 ± 12 years, with 38 female patients and 22 male patients. The control group included 50 healthy individuals in the same age group (49 ± 17 years, 30 females and 20 males).

The demographic data of the control and PAH groups are displayed in Table 1, where LV diastolic diameter and LV mass index were reduced in the PAH group.

Table 2 displays data on diastolic function, RV parameters, and RV systolic pressure in the control and PAH groups, showing a decrease in the mitral E wave and the e' wave by tissue Doppler in the PAH group, with normal E/e' ratio, decreased tricuspid annular s' wave velocity, and increased RV systolic pressure.

Table 3 displays the dimensions and function of the RV and the indexed RA volume in the control and PAH groups, with increased diameters, increased RV thickness, increased RA volume, decreased RV function parameters, and increased pulmonary resistance in the PAH group.

Table 4 shows the parameters of myocardial strain of the ventricles and atria, with a decrease in strain observed in all cavities in the PAH group.

Graph 1 shows that, from January 2012 to June 2022, 18 patients died (32%). In this group there were no patients in FC I. There were 3 patients in FC II, 9 in FC III, and 6 in FC IV. Among the 42 surviving patients who remained under treatment with pulmonary vasodilators, there were 7 patients in FC I, 29 in FC II, 6 in FC III, and no patients in FC IV. Patients

Table 1 – Demographic data and dimensions of the left chambers, n (%) or mean ± standard deviation

Group	Sex	Age (years)	BSA (m²)	LVDD (mm)	LVMI (g/m²)	LVEF (%)	LAVi (mL/m²)
Control	M 20(41%) F 30(59%)	48.95 (±17.45)	1.75 (±0.19)	49.41 (±3.84)	83.48 (±24.36)	58.68 (±5.07)	24.09 (±4.39)
PAH	M 22(37%) F 38 (63%)	48.49 (±12.01)	1.67 (±0.20)	44.57 (±6.20)	72.71 (±19.33)	59.65 (±6.59)	21.10 (±14.05)
P value		0.44	0.06	<0.0001	0.05	0.29	0.07

BSA: body surface area; F: female sex; LAVi: indexed left atrial volume; LVDD: left ventricular diastolic diameter; LVEF: left ventricular ejection fraction; LVMI: left ventricular mass index; M: male sex; PAH: pulmonary arterial hypertension.

Table 2 – Data obtained with flow Doppler and tissue Doppler echocardiography, mean ± standard deviation

Group	Mitral E wave (cm/s)	TD e' wave (cm/s)	E/e' ratio	PCP (mmHg)	TV s' wave (cm/s)	TRV (m/s)	RVSP (mmHg)
Control	84.78 (±13.48)	15.38 (±3.14)	5.82 (±1.81)	7.1 (±1.9)	15.00 (±1.31)	2.63 (±0.15)	32.55 (±2.94)
PAH	63.66 (±18.15)	11.40 (±3.45)	5.89 (±1.84)	8.5 (±2.1)	9.80 (±2.40)	4.23 (±0.78)	89.52 (±21.92)
P value	<0.0001	<0.0001	0.44	0.74	<0.0001	<0.0001	<0.0001

PAH: pulmonary arterial hypertension; PCP: pulmonary capillary pressure; RVSP: right ventricular systolic pressure; TD: tissue Doppler; TRV: tricuspid regurgitation velocity; TV: tricuspid valve.

Table 3 – Dimensions and functional parameters of the right chambers, mean ± standard deviation

Group	RV basal diameter (mm)	RV thickness (mm)	RV FAC (%)	TAPSE (cm)	RRVT	PVR (Wood units)	RAVi mL/m²
Control	32.52 (±4.40)	5.06 (±0.62)	46.58 (±4.63)	2.25 (±0.38)	0.16 (±0.02)	1.25 (±0.61)	24.465 (±4.22)
PAH	43.80 (5.68)	8.93 (±2.04)	28.21 (±10.71)	1.9 (±0.46)	0.24 (±0.11)	3.51 (±1.42)	55.67 (±35.74)
P value	<0.0001	<0.0001	<0.0001	0.0011	<0.0001	<0.0001	<0.0001

FAC: fractional area change; PAH: pulmonary arterial hypertension; PVR: pulmonary vascular resistance; RAVi: indexed right atrial volume; RV: right ventricle; RRVT: relative right ventricular thickness; TAPSE: tricuspid annular plane systolic excursion.

Table 4 – Strain data of right and left chambers, mean ± standard deviation

Group	LV GLS (%)	LA LS (%)	RV GLS (%)	RA LS (%)
Control	-19.96 (±1.0)	37.74 (±10.84)	-28.80 (±8.56)	40.18 (±13.01)
PAH	-17.27 (±4.65)	30.84 (±15.8)	-12.9 (±7.9)	20.9 (±8.5)
P value	<0.0001	<0.0001	<0.0001	<0.0001

LA LS: left atrial reservoir longitudinal strain; LV GLS: left ventricular global longitudinal strain; PAH: pulmonary arterial hypertension; RA LS: right atrial reservoir longitudinal strain; RV GLS: right ventricular global longitudinal strain.

who died had a significantly lower mean age (45.7 ± 13.1 years versus 51.1 ± 10.8 years, $p < 0.0001$).

Regarding the echocardiographic parameters, as shown in Graph 2, the patients who died had larger RV diameter (44.9 ± 9 mm versus 40.8 ± 5 mm, $p < 0.0001$), lower RV fractional area change (25.7% ± 9.2% versus 29.5% ± 10.2%, $p < 0.0001$), lower tricuspid annular s' wave (9.7 ± 2.1 cm/s versus 11.6 ± 2.6 cm/s, $p < 0.0001$), lower absolute RV global longitudinal strain (−12.4 ± 5.3% versus −17.3 ± 4.5%, $p < 0.0001$), and lower absolute LV global longitudinal strain (−14.2% ± 3.9% versus −16.7% ± 3.4%, $p < 0.0001$). TAPSE, relative thickness of the RV

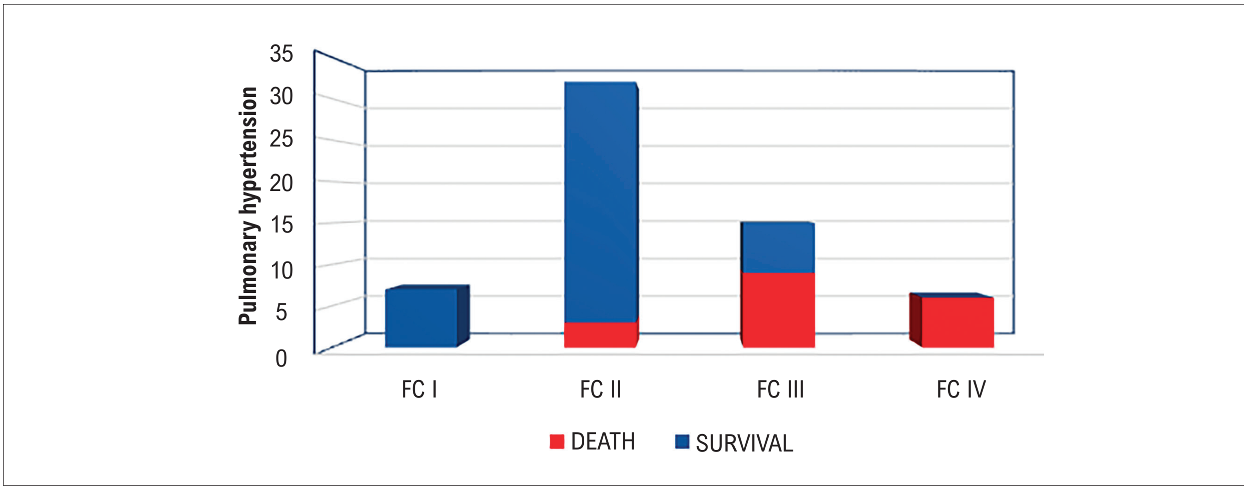

Graph 1 – *Pulmonary hypertension outcome. FC: functional class.*

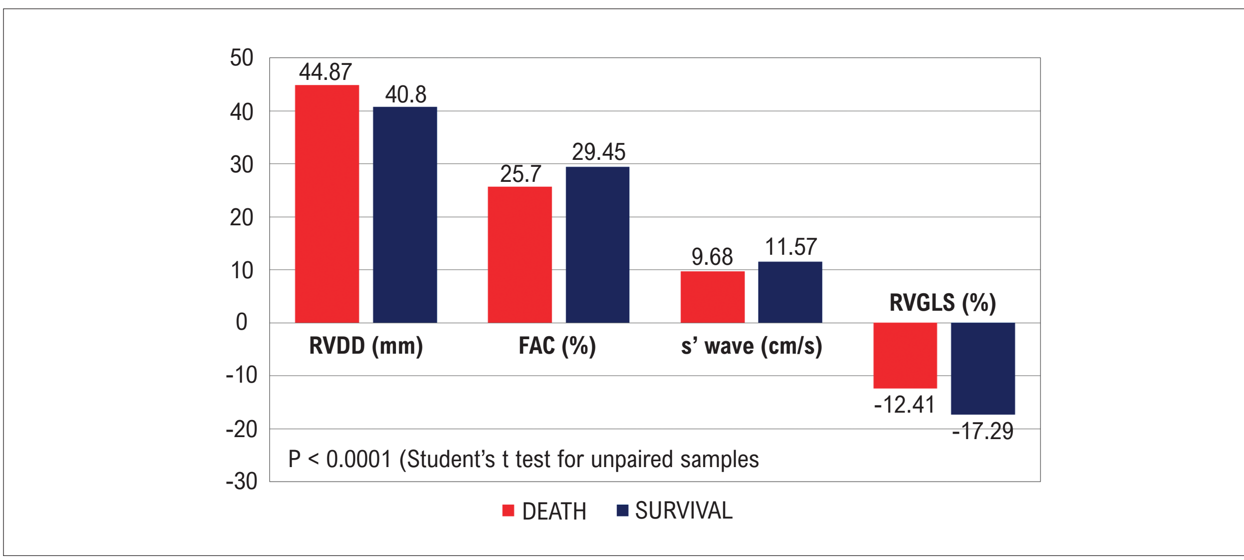

Graph 2 – *Pulmonary hypertension Echocardiographic parameters of the right ventricle. DdVD: diâmetro diastólico do ventrículo direito; FAC: mudança da área fracional;FAC: fractional area change; RVDD: right ventricular diastolic diameter; RVGLS: right ventricular global longitudinal strain.*

walls, and tricuspid regurgitation velocity did not show significant differences.

Discussion

When comparing patients with pulmonary hypertension due to schistosomiasis with healthy individuals, we observed a decrease in LV size and mass index, probably due to RV dilation that pushes the interventricular septum. The ejection fraction did not change, but LV longitudinal strain was significantly reduced, suggesting that there is also subclinical systolic dysfunction in this cavity.[10] This condition has been observed in other studies, indicating that myocardial involvement is not restricted to the right cavities.[11, 12] With regard to diastolic function, there was a significant decrease in the velocity of the mitral E wave and mean e′ wave by tissue Doppler in patients with PAH; however, the E/e′ ratio was normal, allowing estimation of mean LA pressure within the normal values, which characterizes pre-capillary pulmonary hypertension. Tricuspid regurgitation velocity and, consequently, RV systolic pressure were significantly increased, characterizing pulmonary hypertension. We did not use correction with diameter and expansion of the inferior vena cava due to the great variability of this measurement, which makes it unreliable.[13]

When we evaluated the right cavities, the differences were more evident, with important dilation of the cavity, increased lateral wall thickness, and decreased functional parameters (RV fractional area change, tricuspid annular s′ wave velocity, and TAPSE), RA dilation, and significantly increased pulmonary resistance.

Relative RV thickness, determined by the quotient between the basal RV diameter and the diastolic thickness of the lateral wall, obtained from the subcostal position, was significantly increased, as a response to the remodeling of the cavity caused by the pressure overload, translating the relationship between the diameter of the cavity and wall thickness. The RV has the particularity of remodeling by simultaneously increasing cavity size and wall thickness, in both pressure and volume overload.[10] Under physiological conditions, relative RV thickness is low, adapted to the low pressure of the right cavities. Under pressure overload, the relationship between cavity dilation and wall thickness reflects the degree of concentric or eccentric remodeling that occurs in response to increased pressure.[14] One study used relative thickness of the RV, analogously to that of the LV, to determine the type of remodeling in this cavity.[15] The greater the predominance of hypertrophy at the expense of cavity dilation (concentric remodeling), the more favorable the evolution of patients. The cutoff value used to detect better survival was ≥ 0.21. In the present study, we were unable to verify this condition, because there was no significant difference between survivors (whose relative RV thickness was 0.22 ± 0.05) and patients who died (whose relative RV thickness was 0.21 ± 0.05).

All myocardial strain parameters were reduced. In addition to LV longitudinal strain, LA reservoir longitudinal strain was decreased, although still within normal limits. The global longitudinal strain of the RV and RA were markedly reduced, indicating systolic dysfunction of the right cavities observed on the echocardiogram. The longitudinal strain values of the RV lateral wall were not used because, in this study, there were no relevant differences in relation to the global longitudinal strain of this chamber.

When we compare the results of the patients who died with those who survived, in addition to FC, where all patients in FC IV died, while no patient in FC I had this outcome (Graph 1), RV dimensions, RV fractional area change, tricuspid annular s' wave velocity, RV global longitudinal strain, and LV global longitudinal strain showed a significant relation with death (Graph 2). The decrease in LV longitudinal strain may be related to the greater severity of pulmonary hypertension which, by affecting the RV musculature, also decreases LV systolic function.[11, 12]

Conclusion

Pulmonary hypertension related to the hepatosplenic form of schistosomiasis causes remodeling of the right chambers, with decreased parameters of RV systolic function and myocardial strain. Patients who died during the 10-year follow-up showed larger RV dimensions, lower fractional area change, lower tricuspid annular systolic velocity, lower RV global longitudinal strain, and more advanced functional class.

Author Contributions

Conception and design of the research: Del Castillo JM, De Oliveira KB, Bandeira AMP, Brindeiro Filho D; Acquisition of data: Del Castillo JM, De Oliveira KB, Bandeira AMP, Brindeiro Filho D; Analysis and interpretation of the data: Del Castillo JM, De Oliveira KB; Statistical analysis and Writing of the manuscript: Del Castillo JM; Critical revision of the manuscript for intellectual content: De Oliveira KB, Travassos RRO, Bandeira AMP, Silveira CAM, Brindeiro Filho D.

Potential Conflict of Interest

No potential conflict of interest relevant to this article was reported.

Sources of Funding

There were no external funding sources for this study.

Study Association

This study is not associated with any thesis or dissertation work.

Ethics Approval and Consent to Participate

This article does not contain any studies with human participants or animals performed by any of the authors.

References

1. Posada-Martínez EL, Gonzalez-Barrera LG, Liblik K, Gomez-Mesa JE, Saldarriaga C, Farina JM, et al. Schistosomiasis & Heart - On Behalf of the Neglected Tropical Diseases and Other Infectious Diseases affecting the Heart (the NET-Heart Project). Arq Bras Cardiol. 2022;118(5):885-93. doi: 10.36660/abc.20201384.
2. Brasil. Ministério da Saúde. Vigilância da Esquistossomose Mansoni. Diretrizes Técnicas. Brasília: Ministério da Saúde; 2014.
3. Carbonell C, Rodríguez-Alonso B, López-Bernús A, Almeida H, Galindo-Pérez I, Velasco-Tirado V, et al. Clinical Spectrum of Schistosomiasis: An Update. J Clin Med. 2021;10(23):5521. doi: 10.3390/jcm10235521.
4. Mitchell C, Rahko PS, Blauwet LA, Canaday B, Finstuen JA, Foster MC, et al. Guidelines for Performing a Comprehensive Transthoracic Echocardiographic Examination in Adults: Recommendations from the American Society of Echocardiography. J Am Soc Echocardiogr. 2019;32(1):1-64. doi: 10.1016/j.echo.2018.06.004.
5. Abbas AE, Franey LM, Marwick T, Maeder MT, Kaye DM, Vlahos AP, et al. Noninvasive Assessment of Pulmonary Vascular Resistance by Doppler echocardiography. J Am Soc Echocardiogr. 2013;26(10):1170-7. doi: 10.1016/j.echo.2013.06.003.
6. Kocabay G, Muraru D, Peluso D, Cucchini U, Mihaila S, Padayattil-Jose S, et al. Normal Left Ventricular Mechanics by Two-Dimensional Speckle-Tracking Echocardiography. Reference Values in Healthy Adults. Rev Esp Cardiol. 2014;67(8):651-8. doi: 10.1016/j.rec.2013.12.009.
7. Wang TKM, Grimm RA, Rodriguez LL, Collier P, Griffin BP, Popović ZB. Defining the Reference Range for Right Ventricular Systolic Strain by Echocardiography in Healthy Subjects: A Meta-Analysis. PLoS One. 2021;16(8):e0256547. doi: 10.1371/journal.pone.0256547.
8. Pathan F, D'Elia N, Nolan MT, Marwick TH, Negishi K. Normal Ranges of Left Atrial Strain by Speckle-Tracking Echocardiography: A Systematic Review and Meta-Analysis. J Am Soc Echocardiogr. 2017;30(1):59-70.e8. doi: 10.1016/j.echo.2016.09.007.

9. Hosseinsabet A, Mahmoudian R, Jalali A, Mohseni-Badalabadi R, Davarpasand T. Normal Ranges of Right Atrial Strain and Strain Rate by Two-Dimensional Speckle-Tracking Echocardiography: A Systematic Review and Meta-Analysis. Front Cardiovasc Med. 2021;8:771647. doi: 10.3389/fcvm.2021.771647.

10. Del Castillo JM, Albuquerque ES, Silveira CAM, Lamprea DP, Bandeira AP, Mendes AA, et al. Right Ventricle: Echocardiographic Evaluation of Pressure and Volume Overload. Rev Fed Argent Cardiol. 2016; 84(6):511-3. doi: 10.7775/rac.v84.i6.9467.

11. Rosenkranz S, Gibbs JS, Wachter R, De Marco T, Vonk-Noordegraaf A, Vachiéry JL. Left Ventricular Heart Failure and Pulmonary Hypertension. Eur Heart J. 2016;37(12):942-54. doi: 10.1093/eurheartj/ehv512.

12. Hardegree EL, Sachdev A, Fenstad ER, Villarraga HR, Frantz RP, McGoon MD, et al. Impaired Left Ventricular Mechanics in Pulmonary Arterial Hypertension: Identification of a Cohort at High Risk. Circ Heart Fail. 2013;6(4):748-55. doi: 10.1161/CIRCHEARTFAILURE.112.000098.

13. Patel AR, Alsheikh-Ali AA, Mukherjee J, Evangelista A, Quraini D, Ordway LJ, et al. 3D Echocardiography to Evaluate Right Atrial Pressure in Acutely Decompensated Heart Failure Correlation with Invasive Hemodynamics. JACC Cardiovasc Imaging. 2011;4(9):938-45. doi: 10.1016/j.jcmg.2011.05.006.

14. Franco V. Right Ventricular Remodeling in Pulmonary Hypertension. Heart Fail Clin. 2012;8(3):403-12. doi: 10.1016/j.hfc.2012.04.005.

15. Sano H, Tanaka H, Motoji Y, Fukuda Y, Mochizuki Y, Hatani Y, et al. Right Ventricular Relative Wall Thickness as a Predictor of Outcomes and of Right Ventricular Reverse Remodeling for Patients with Pulmonary Hypertension. Int J Cardiovasc Imaging. 2017;33(3):313-21. doi: 10.1007/s10554-016-1004-z.

The Use of Echocardiography in Schistosomiasis

Daniela do Carmo Rassi[1]
Faculdade de Medicina da Universidade de Goiás,[1] Goiânia, GO – Brazil
Short Editorial related to the article: Long-Term Evolution of Patients with Important Pulmonary Hypertension due to Schistosomiasis

Schistosomiasis, a neglected tropical disease, affects 240 million people worldwide, with more than 90% of cases reported in Africa, according to the World Health Organization. The disease is endemic to South America, the Caribbean, Southeast Asia, and Africa, in areas with little infrastructure, especially lack of drinking water and basic sanitation. The infection is caused by helminths of the genus *Schistosoma*. Contamination occurs through contact with water where host snails are present. After penetrating human skin, the worms can migrate and produce eggs in the liver, lungs, and intestines.

During the acute phase, patients may be asymptomatic or develop myocarditis and pericarditis related to an allergic reaction to the schistosomes, in which eosinophils play an important role. Myocardial ischemia may rarely occur, and the exact mechanism remains unknown.

The most important complication of schistosomiasis is pulmonary arterial hypertension (PAH), and schistosomiasis is considered the main cause of PAH in some endemic countries.[1] Of the approximately 23 million people worldwide with hepatosplenic schistosomiasis, up to 5% develop PAH.[2]

Several mechanisms have been suggested for PAH in schistosomiasis, including obstruction of the pulmonary circulation by eggs, endothelial dysfunction due to inflammation, and portal hypertension leading to pulmonary overflow and endothelial cell dysfunction, similar to portopulmonary hypertension.

Schistosomiasis-induced PAH can be asymptomatic in early stages, but most patients will develop right heart failure in later stages of the disease.[3]

Echocardiography is the initial imaging method of choice for suspected cardiac involvement in patients with schistosomiasis. In the acute phase, it allows assessment of left ventricular systolic function and pericardial effusion in patients with suspected myopericarditis. In the chronic phase, when there are signs and symptoms of right ventricular failure or pulmonary hypertension, echocardiography may reveal an enlarged right ventricle, hypertrophy of the right ventricular free wall, deviation of the interventricular septum to the left, tricuspid insufficiency, and increased right ventricular systolic pressure.

Castillo et al. evaluated 60 patients with PAH due to schistosomiasis and compared them with 50 healthy control subjects. Clinical and echocardiographic data were analyzed, and the group with PAH due to schistosomiasis was followed up for 10 years. The group with schistosomiasis-related PAH showed involvement of the right chambers with decreased parameters of systolic function and myocardial deformation, as well as lower values of left ventricular global longitudinal strain. The long-term evolution of patients with schistosomiasis showed elevated mortality, with larger dimensions of the right ventricle, lower fractional area change, lower tricuspid annular systolic velocity, and lower right ventricular global longitudinal strain.[4]

A systematic review has shown that patients with schistosomiasis-associated PAH have more favorable hemodynamic profile and survival rate than those with idiopathic PAH.[5]

Although there are reports of cardiac complications of this infection, they have not yet been validated by robust population data. This can be attributed to these patients' limited access to health care. Therefore, the true impact of this disease on the cardiovascular system may be underestimated, due to underdiagnosis and underreporting bias

Likewise, the cardiovascular manifestations of this disease require attention, because they are rarely identified or are identified late, with devastating consequences.[1] Adequate recognition and treatment can improve these patients' survival and reduce the use of resources that are scarce in their regions.

Keywords

Schistosomiasis; Echocardiography; Cardiovascular Diseases

Mailing Address: Daniela do Carmo Rassi •
Hospital São Francisco de Assis, Ecocardiografia. Rua 9A. Postal code: 74075-250. Goiânia, GO – Brazil.
E-mail: dani.rassi@hotmail.com
Manuscript received April 6, 2023; revised manuscript April 6, 2023; accepted April 20, 2023.

DOI: https://doi.org/10.36660/abcimg.20230037i

References

1. Posada-Martínez EL, Gonzalez-Barrera LG, Liblik K, Gomez-Mesa JE, Saldarriaga C, Farina JM, et al. Schistosomiasis & Heart - On Behalf of the Neglected Tropical Diseases and other Infectious Diseases affecting the Heart (the NET-Heart Project). Arq Bras Cardiol. 2022;118(5):885-893. doi: 10.36660/abc.20201384.

2. Farina JM, Liblik K, Iomini P, Miranda-Arboleda AF, Saldarriaga C, Mendoza I, et al. Infections and Cardiovascular Disease: JACC Focus Seminar 1/4. J Am Coll Cardiol. 2023;81(1):71-80. doi: 10.1016/j.jacc.2022.08.813.

3. Gavilanes F, Fernandes CJ, Souza R. Pulmonary Arterial Hypertension in Schistosomiasis. Curr Opin Pulm Med. 2016;22(5):408-14. doi: 10.1097/MCP.0000000000000300.

4. Del Castillo JM, Oliveira KB, Travassos RRO, Bandeira AMP, Silveira CAM, Brindeiro D Filho. Long-Term Evolution of Patients with Important Pulmonary Hypertension due to Schistosomiasis. Arq Bras Cardiol: Imagem Cardiovasc. 2023;36(2): e2023373. doi: 10.36660/abcimg.2023373.

5. Knafl D, Gerges C, King CH, Humbert M, Bustinduy AL. Schistosomiasis-Associated Pulmonary Arterial Hypertension: A Systematic Review. Eur Respir Rev. 2020;29(155):190089. doi: 10.1183/16000617.0089-2019.

Review Article

My Approach to Three-Dimensional Echocardiography for Pathophysiological Classification of Tricuspid Regurgitation

Alex dos Santos Felix,[1,2] Monica Luiza de Alcantara,[3] Konstantinos Papadopoulos[4]
Instituto Nacional de Cardiologia,[1] Rio de Janeiro, RJ – Brazil
DASA,[2] Rio de Janeiro, RJ – Brazil
Instituto D'Or de Pesquisa e Ensino,[3] Rio de Janeiro, RJ – Brazil
European Interbalkan Medical Center,[4] Athens – Greece

Introduction

Although it was known as the "forgotten valve" in the past, there has been increasing interest in studying the tricuspid valve (TV) during the last two decades. Tricuspid regurgitation (TR) has been identified as a prognostic marker not only when associated with other cardiac diseases, like heart failure, mitral regurgitation, or aortic stenosis,[1-3] but also as an isolated entity.[4] Understanding the pathophysiological mechanisms of this disease is of paramount importance, since new options of transcatheter devices and techniques are emerging, offering invasive treatment for high-risk patients unsuitable for surgical intervention.[5]

The TV is difficult to image in transesophageal echocardiography (TEE) for the following reasons: 1) the leaflets are much thinner compared to mitral leaflets, with greater anatomic variability; 2) it is an anterior structure, far away from the esophagus, with acoustic shadowing from the fibrous heart skeleton; and 3) it cannot be aligned to the esophageal probe in order to acquire en face views and requires use of lateral resolution. These restrictions may limit the ability of traditional TEE to evaluate the TV, making it necessary to complement the evaluation with special windows from the lower esophagus and transgastric views. Different from other cardiac valves, images of the TV obtained from transthoracic echocardiography (TTE) usually have better resolution than images obtained by TEE. Even though all protocols start with two-dimensional (2D) assessment of the TV, three-dimensional echocardiography (3DE) plays an important role in the evaluation of TV diseases, due not only to its ability to precisely depict the anatomy of the valve and the subvalvular apparatus, but also to its accuracy in quantitation of right ventricular (RV) and right atrial volumes and function and functional analysis of valvular dysfunction, especially for grading TR and evaluating dynamics of the tricuspid annulus (TA) through dedicated software. All of this information is of unparalleled importance for patient management and pre-procedural planning in surgical and transcatheter approaches.

Keywords

Tricuspid Valve; Tricuspid Valve Insufficiency; Echocardiography, Three-Dimensional

Mailing Address: Alex dos Santos Félix •
National Institute of Cardiology. Rua das Laranjeiras, 374. Postal Code: 20521-290. Rio de Janeiro, RJ – Brazil
E-mail: alexsfelix@gmail.com
Manuscript received June 2, 2023; revised manuscript June 13, 2023; accepted June 13, 2023
Editor responsible for the review: Daniela do Carmo Rassi Frota

DOI: https://doi.org/10.36660/abcimg.20230055i

TV anatomy

The TV complex is a functional unity composed of leaflets, subvalvular apparatus, papillary muscles (PM), and TA (Figure 1), which interact during the cardiac cycle in a dynamic fashion in order to maintain valvular function. Although it is called traditionally "tricuspid", this valve has a great anatomical variability. As a matter of fact, up to 46% of them can have two, four or even more cusps[6] (Figure 2). TV leaflets are asymmetric; the anterior leaflet is typically the largest in radial diameter and area. The septal leaflet has the least mobility and is the shortest in radial diameter, while the posterior is the shortest circumferentially and often has multiple scallops. The attachment of the TV is more apically positioned than the mitral valve (normal distance ≤ 10 mm in relation to the anterior mitral leaflet).

The TV subvalvular apparatus is normally composed of two well differentiated PM: anterior and posterior, with a variable presence of a septal PM. The anterior PM is the most prominent and lends chordal support to anterior and posterior leaflets. It blends with the right end of the septal marginal trabeculae (moderator band) below the antero-posterior commissure. The posterior PM, which can be bifid or trifid, lends chordal support to the posterior and septal leaflets. The septal PM, when present, may be small or multiple, and is often indistinguishable from the ventricular wall. There are usually some small chords that emerge directly from the ventricular septum and attach to anterior and septal leaflets.[6] Accessory chords may be directly attached to the RV free wall or to the moderator band (Figure 3). In the RV, the subvalvular chords are less distensible than those seen in the mitral valve, with dense collagen bundles, helping to explain why there is more extensive tethering when there is ventricular remodeling, with displacement of either the RV septal or lateral wall positions, affecting leaflet coaptation.

One of the most important structures for maintaining adequate TV function is the TA. It is a very dynamic structure, with varying size and geometry during the cardiac cycle, usually oval and saddle-shaped. It becomes more spherical and planar when dilated, extending towards the anterolateral and posterior RV walls, regions where there is no fibrous tissue around the valve, making it less resistant to remodelling.[7] Based on current guidelines,[8,9] a significant dilatation of the TA is present when there is a linear medial-lateral measurement > 40 mm or > 21 mm/m²

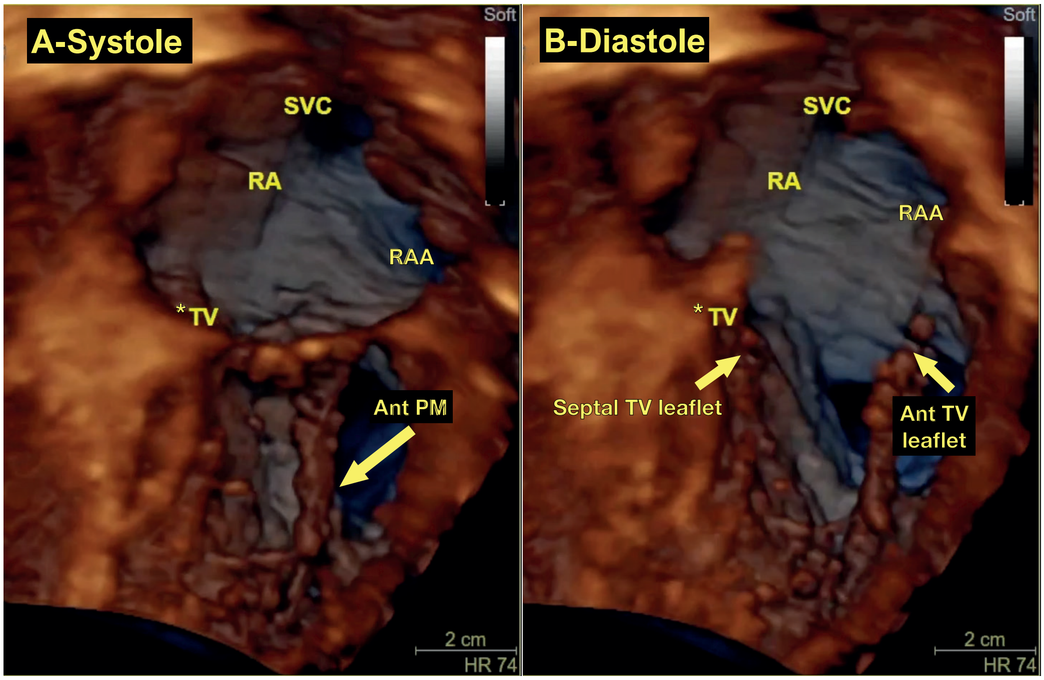

Figure 1 – *TV complex anatomy viewed by 3DE. A functional unity composed of leaflets, subvalvular apparatus, PM, and TA. Ant PM: anterior papillary muscle; Ant TV leaflet: anterior tricuspid valve leaflet; RA: right atrium; RAA: right atrial appendage; SVC: superior vena cava; *TV: tricuspid valve annulus.*

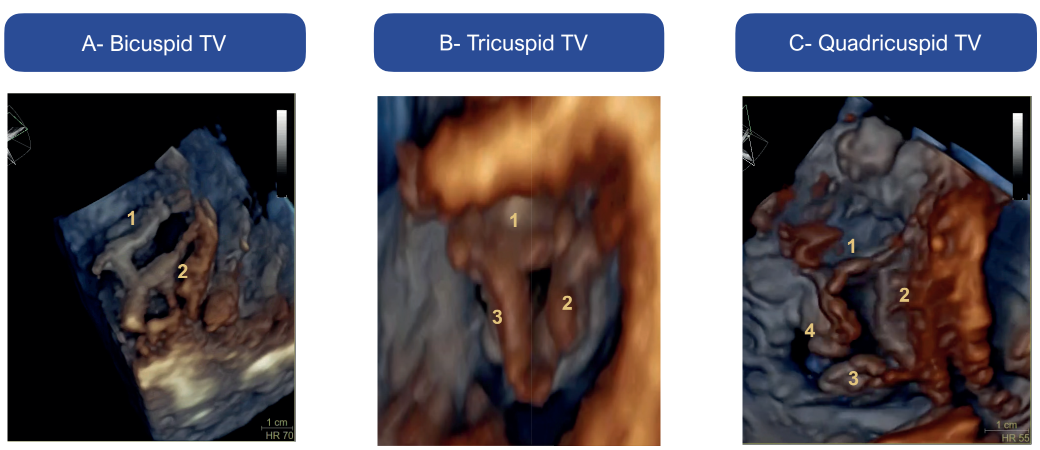

Figure 2 – *Anatomical variations of TVs viewed by 3DE (ventricular perspective). In A we can see a bicuspid TV; in B a tricuspid TV; and in C a quadricuspid TV. TV: tricuspid valve*

acquired by 2D echocardiography in apical 4-chamber view (during diastole). 3DE identifies numerous different linear dimensions for every TA in a cross section (Figure 4), as expected for an oval structure, and it is important to mention that 2D apical 4-chamber view almost always fails to demonstrate the largest TV diameter. Using 3DE, we can measure the largest dimensions and area of the TA with great accuracy with multiplanar reconstruction tools. At the end of ventricular diastole, the normal value for the largest diameter of the TA is 40 ± 5 mm on 3DE (23 ± 3 mm/m^2),[10] always bearing in mind that this is a highly dynamic structure, whose area undergoes significant variations during the cardiac cycle (approximately 35%), being larger in the end of diastole and smaller in the middle and end of ventricular systole.[11]

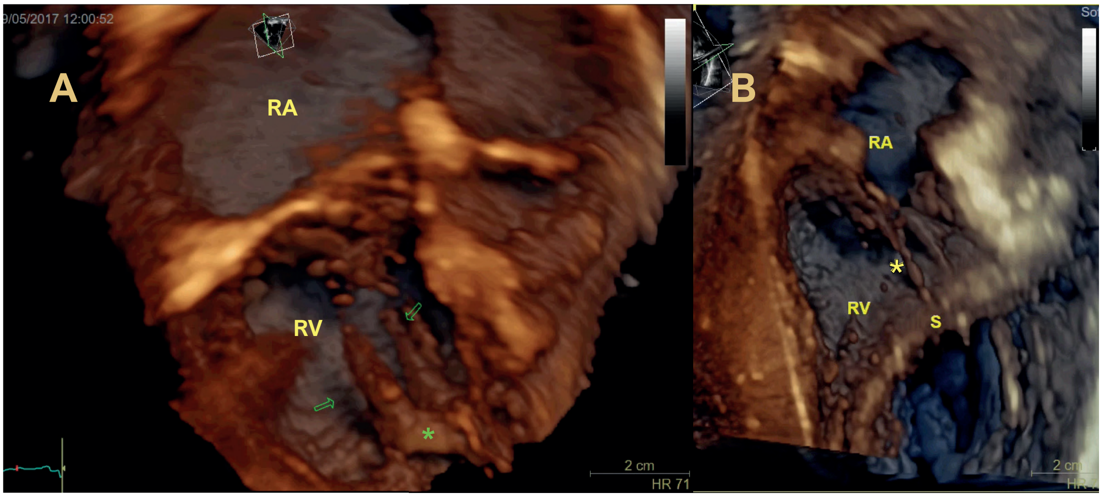

Figure 3 – *Anatomical detail of a TV complex viewed by transthoracic 3DE. A) 3D rendered coronal view showing anterior papillary muscle (green arrow) rising from the septomarginal trabeculeae (green asterisk) at the anterolateral wall. B) Oblique view, where we can see direct chordal attachment (yellow asterisk) to the interventricular septum. RA: right atrium; RV: right ventricle.*

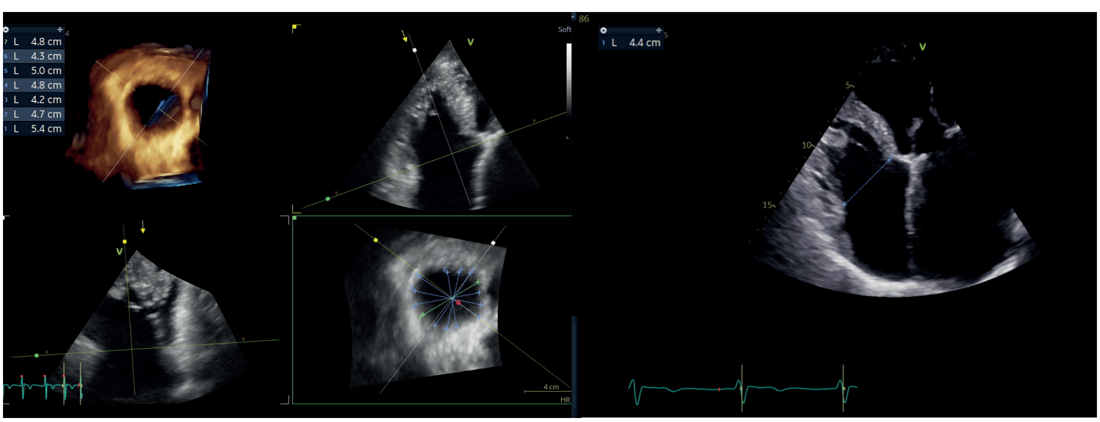

Figure 4 – *Most TV annuli are oval-shaped, and 3DE is able to identify numerous different linear dimensions in a cross section with multiplanar reconstruction (A), and it is important to mention that 2D apical 4-chamber view almost always fails to demonstrate the largest TV diameter.*

Pathophysiological classification of TR

It is of great importance to understand the pathophysiological mechanisms responsible for the development of TR, not only to define the best treatment modality and intervention timing for each specific patient, but also to prevent TR progression in some conditions, for example, in patients with atrial fibrillation that is amenable to cardioversion.

Traditionally, TR is stratified by the presence of leaflet tissue involvement into two broad categories: primary TR (organic) and secondary TR (functional). However, given the great complexity and superposition of different mechanisms in TR development, a new classification was made necessary to provide a better understanding, integrating more information, not only focusing on the tricuspid leaflet tethering, but also considering right atrial, TA, and RV dilatation, as well as RV dysfunction. In this new approach, functional or secondary TR is divided into two categories: atrial functional TR (AFTR) and ventricular functional TR (VFTR). Furthermore, cardiac implantable electronic device (CIED)-related TR is also included as a new separate category.[12] Based on this new concept we propose a practical framework to differentiate between these pathophysiological phenotypes (Figure 5). This new classification provides further information to understand the great diversity of phenotypes of TR, assisting therapeutic and interventional planning.

Primary TR (organic)

TR may be the result of organic valvular disease (primary TR), when tissue damage or degeneration is the main reason for valvular incompetence. Primary TR is far less common than secondary TR, with reported prevalence in literature of less than 10%, and generally more difficult to repair, demanding surgical TV replacement. In the new integrated classification of TR, the main pathophysiologic mechanisms for primary TR are leaflet changes leading to restricted or excessive leaflet mobility or leaflet perforation. Specific conditions have also been included in the Carpentier classification with type I including congenital heart diseases and endocarditis (both vegetations and perforation), type II referring to myxomatous valve disease with prolapse, traumatic TR (e.g., chest trauma) and TR after biopsy, and type IIIA including carcinoid, rheumatic dysfunction, radiotherapy, and tumors (Figure 6). Imaging plays a major role in the identification of these subgroups of valvopathies, because the echocardiographic criteria are definitive for diagnosis and easily detectable.

Ventricular secondary TR

Secondary TR is the most prevalent form. It is frequently the result of inappropriate leaflet coaptation as a secondary mechanism, in response to volume or pressure overload, due to RV remodeling, annular dilatations, displacement of the PM, and leaflet tethering (Figure 7). Left-sided heart diseases are the leading cause of secondary TR, either as a consequence of elevated pulmonary pressures due to left-sided valvular heart diseases or secondary to non-valvular heart failure, with high diastolic filling pressures, both in reduced or preserved ejection fraction. Secondary TR may also be frequently present in advanced isolated RV diseases, such as pulmonary hypertension (cor pulmonale), congenital heart diseases, or primary RV myocardial diseases (arrhythmogenic cardiomyopathy, RV myocardial infarction). For each patient with secondary TR, it is very important to have a full understanding of the mechanisms involved, to evaluate the possibility and best technical approach for a surgical management (when submitted to left-sided heart valve surgery), or in patients with high surgical risk, to explore transcatheter therapeutic options. Optimization of pharmacologic therapy for heart failure may change the degree of secondary TR, which is very sensitive to preload (volume) and afterload (elevated left ventricular filling pressures transmitted retrograde as elevation of capillary pressures and pulmonary artery systolic pressures), and, according to ACC and ESC guidelines, secondary TR should be treated percutaneously in patients under optimal medical treatment only.

Atrial secondary TR

What was previously known as “idiopathic” TR, today is recognized as AFTR, or “atriogenic” TR, a distinct pathophysiological phenotype, where TA dilatation and dysfunction is the main substrate of valvular incompetence. It is primarily caused by right atrial remodeling, as we often notice in patients with persistent atrial fibrillation,[13] where right atrial volume is the key factor to determine alterations in the TV/TA complex[14-16] (Figure 8). Differently from the classic form of functional TR (“ventricular” TR), patients with AFTR have normal-sized or only mildly dilated (conical-shaped) RV, usually without RV dysfunction.[17,18]

For the diagnosis of AFTR, we have to exclude other conditions which may justify the development of TR, such as all causes of primary TR, the presence of left-sided valvular heart disease, left ventricular systolic dysfunction, pulmonary hypertension, or the presence of pacemaker wires. Distinguishing atrial from ventricular forms of secondary TR is very important, not only because they carry different prognostic implications (atrial TR develops more rapidly than ventricular TR, which is usually seen only in advanced stages of disease), but also to help guide specific interventions such as rhythm control or cardioversion in patients with persistent atrial fibrillation.

CIED-related TR

CIED-related TR is a multifactorial disease, comprising different possible types of pathophysiology, and it can share features of primary or secondary TR, depending on its etiological features. Primary CIED-related TR may be caused by lead impingement or adherence to TV leaflets (Figure 9), interference with subvalvular apparatus, leaflet perforation, laceration, or in some dramatic cases even leaflet avulsion (caused by lead extraction).

Approximately 25% to 29% of patients with permanent pacemaker have TR, which is more than double the frequency of TR compared to control groups.[19] Defining the underlying mechanism is very important to explore the therapeutic options or even the need for lead extraction in some cases.[12] CIED-related TR is associated with poor outcomes[20] and must be avoided at any cost. By using 3DE it is feasible to guide lead positioning intraoperatively, avoiding complications and leaflet impingement, or evaluate the interference of the wire with the TV in the early postoperative period, when there is still the option to intervene and reposition the wire.

The pathophysiological link between the existence of device leads and the development of a significant TR or worsening of a pre-existent regurgitation is not always related to mechanical interference of the device with leaflet mobility or the subvalvular apparatus (primary TR); it can also be due to secondary mechanisms, for example, in cases where pacing causes chamber dilatation and/or heart failure, or when it causes significant RV dyssynchrony. In fact, secondary mechanisms may be responsible for more than 60% of cases of CIED-related TR,[21] and even when primary TR is the initial mechanism, long-lasting volumetric overload may lead to RV dilatation and remodeling, generating a model of coexistent primary and secondary TR.

When considering lead extraction in an attempt to reduce TR, we must perform a detailed evaluation of the TV complex to determine if there is a significant secondary component (isolated or mixed); specifically looking for annular dilation, RV remodeling, RV dysfunction, and leaflet tethering, which can be determinants of worse treatment response.

Analysis of TV anatomy and mechanisms of TR with 3DE

3DE is a promising technique for accurate qualitative and quantitative analysis of the TV, obtaining important

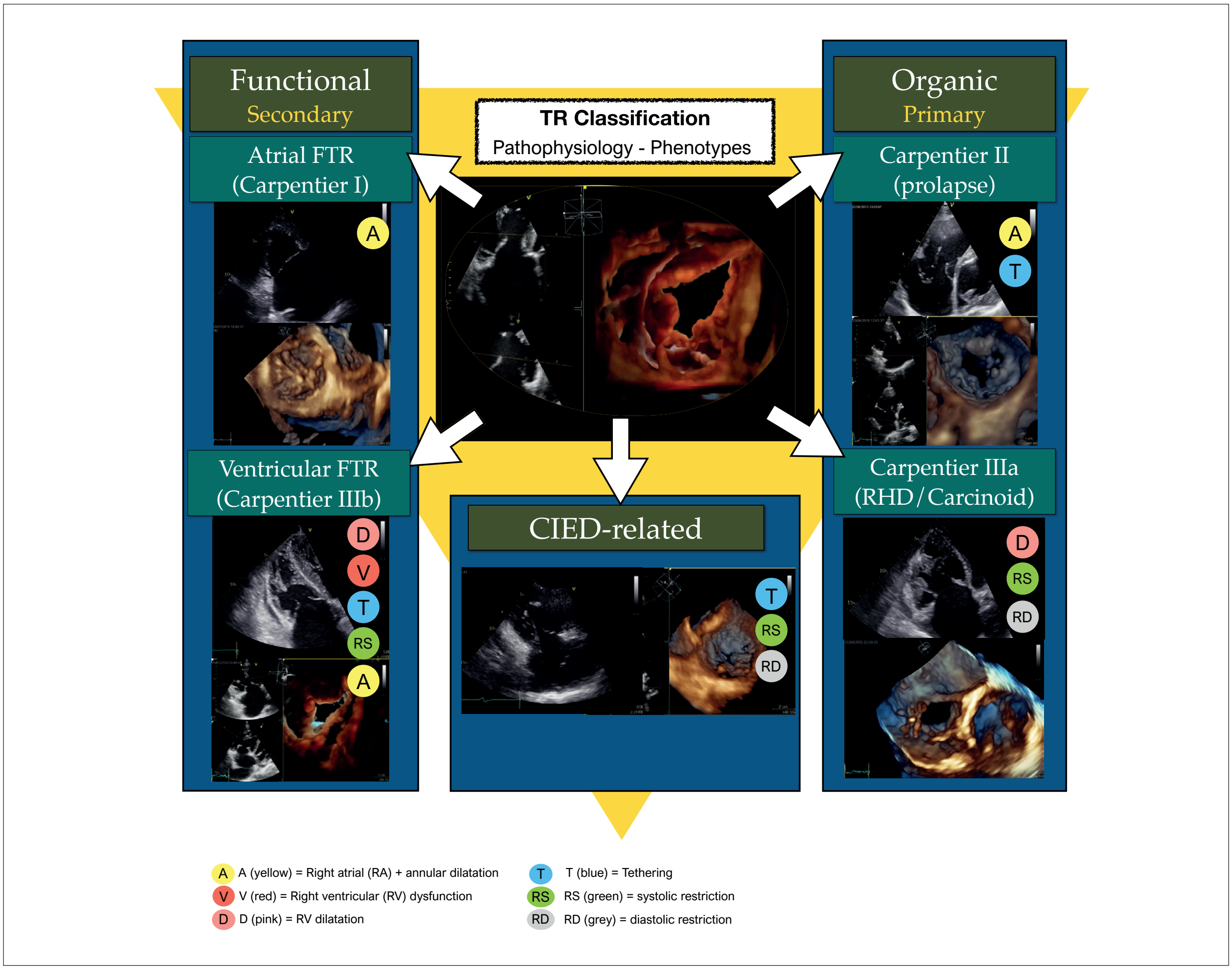

Figure 5 – *Integrative classification of TR according to pathophysiology and predominant phenotypes. CIED: cardiac implantable electronic device; FTR: functional tricuspid regurgitation; RHD: rheumatic heart disease; TR: tricuspid regurgitation.*

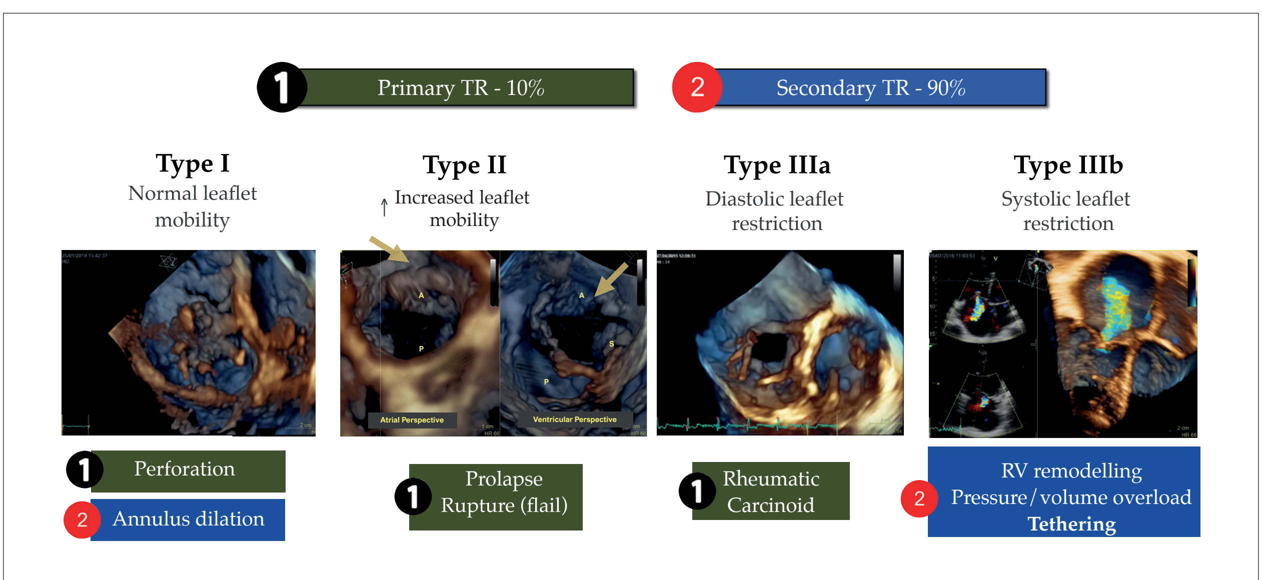

Figure 6 – *TR mechanisms, adapted from classical Carpentier classification (Carpentier A., et al. J Thorac Cardiovasc Surg 1983). RV: right ventricle.*

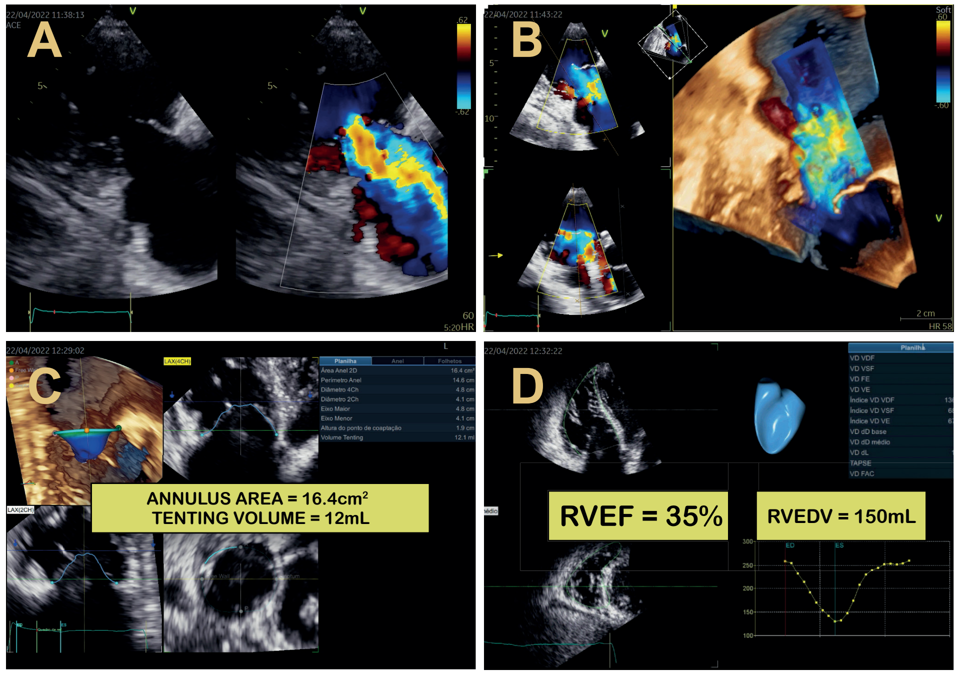

Figure 7 – *Example of ventricular secondary TR. Young patient with chronic renal failure, high output A-V fistula with congestive heart failure. A) Simultaneous 2D images with and without color Doppler showing severe tenting of leaflets and torrential TR. B) Color 3D rendered image, from a sagittal perspective, of the huge coaptation gap and the large TR color jet. C) Using dedicated software for analysis of TV, we can see also a dilated annulus (16.4 cm²) pointing to already mixed mechanism and a tenting volume of 12 mL. D) Volumetric analysis of right ventricular volumes and function by 3DE, showing a dilated right ventricle with dysfunction (RVEF = 35%). RVEDV: right ventricular end-diastolic volume; RVEF: right ventricular ejection fraction.*

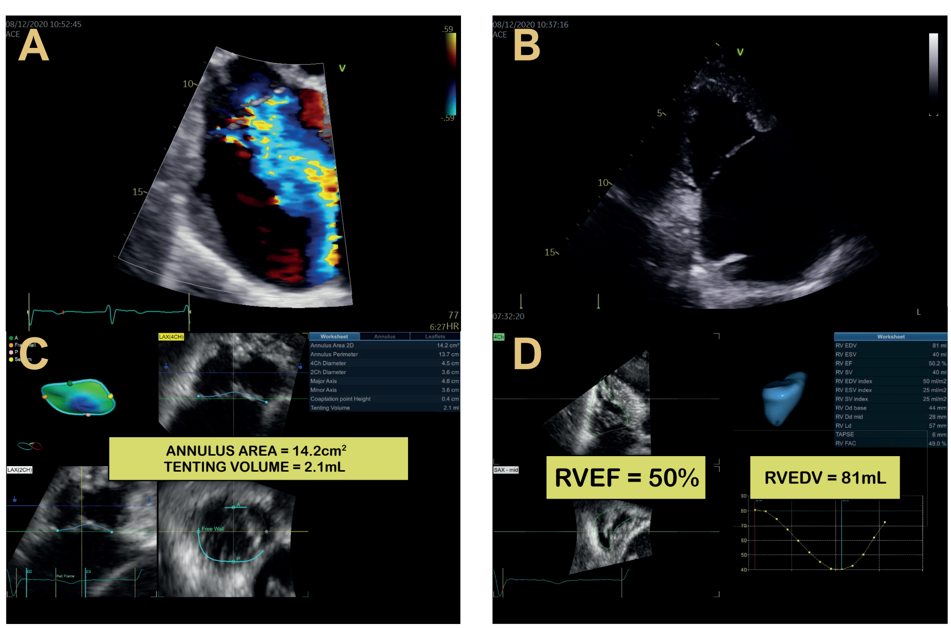

Figure 8 – *Example of secondary atriogenic TR. An elderly patient with persistent atrial fibrillation. A) Torrential TR with eccentric jet in a hugely dilated right atrium. There is no significant tenting of leaflets on 2D parasternal right ventricular inflow view (B), and a dilated annulus showed on quantitative analysis (16.4 cm²). This patient has no right ventricular pathology, with normal volumes and ejection fraction in 3D volumetric analysis (D). RVEDV: right ventricular end-diastolic volume; RVEF: right ventricular ejection fraction.*

parameters which can guide the best therapeutic option for each patient. 3DE is more accurate than 2D in severity assessment with vena contracta area and anatomic evaluation of the valve. With 3DE, it is possible to study any of the components of the TV complex in a dynamic way, with good temporal and spatial resolution.

Step by Step approach for acquisiton and analysis of an optimized TV 3DE Dataset:

- The main key to a reliable 3DE analysis is to obtain a good echocardiographic dataset. Specifically, focusing on the RV is important, along with good patient positioning at left lateral decubitus, preferentially with a proper examination

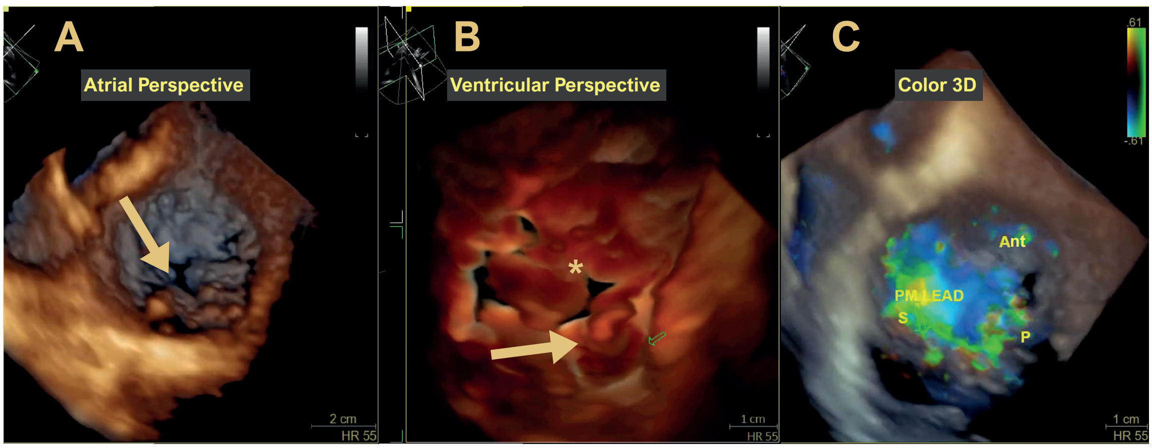

Figure 9 – *CIED-related TR caused by pacemaker lead impingement (arrows). Transthoracic acquisition, with 3D rendered views of the TV from atrial perspective (A), ventricular perspective showing lack of coaptation of leaflets (asterisk) caused by septal leaflet impingement (B). In C, 3D color image from atrial perspective showing torrential TR. Ant: anterior leaflet; P: posterior leaflet; PM: pacemaker; S: septal leaflet.*

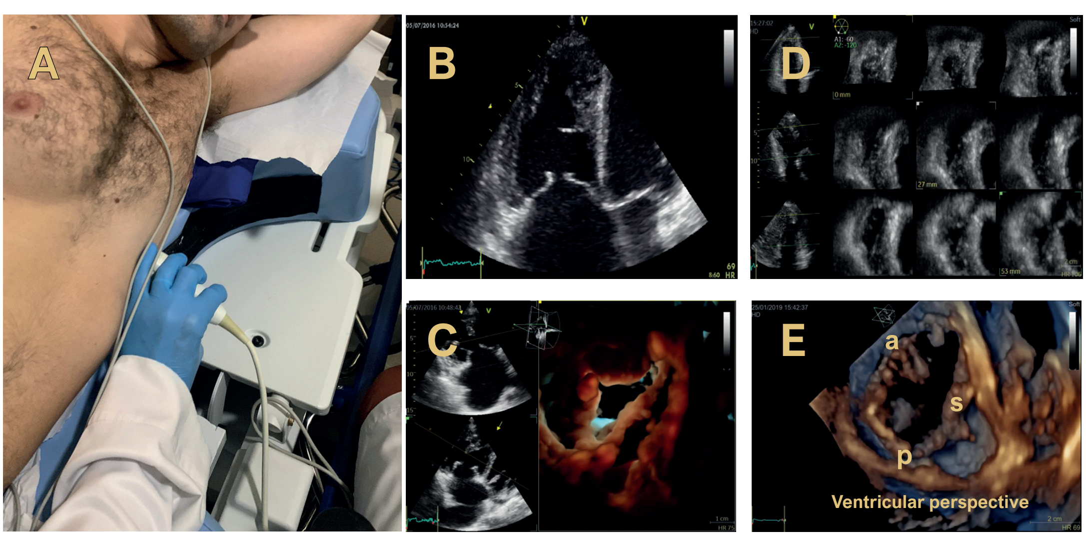

Figure 10 – *Acquiring an optimized TV 3DE dataset. A) Acquiring a good apical right ventricular focused view is very important. Ensure good patient positioning at left lateral decubitus, preferentially with a proper examination bed, with a removable lateral part to properly expose the chest to the transducer. B) To obtain good 2D images, it is essential to have a good 3D image, including all the TV in the dataset, in the most central position possible, with some surrounding structures, such as the interventricular septum and aorta for spatial orientation (C). Before storing the acquired dataset, we should always check the quality of the images obtained, verifying whether all right ventricular walls are included and looking for artifacts. We can do this on rendered images or with a multislice tool (D). The suggested anatomic view of the TV is acquired from the ventricular side, by placing the septum on our right side (3 o'clock) and the aortic valve on top of it (1 o'clock). Thus, the septal leaflet (s) is shown on the right side, next to the septum, the anterior leaflet (a) on top, next to the aortic valve, and the posterior leaflet (p) on the bottom side opposite the aortic valve (E).*

bed, with a removable lateral part to properly expose the chest to the transducer (Figure 10A).

• The first important rule in 3DE is that optimal 2D images are necessary in order to achieve adequate analysis of 3DE views. In case of poor acoustic window, the acquisition of 3DE will be difficult and data obtained may not be interpretable or reliable (Figure 10B).

• Asking for breath-hold from the patient, if possible, to enable a multi-beat acquisition without significant artifacts (stitching), can help us achieve decent temporal and spatial resolution at the same time. This requires a patient on sinus rhythm or at least not on a significant arrhythmia with great R-R variation between the cardiac cycles. Even with atrial fibrillation, it may be possible to acquire multi-beat images, but never for example with a bigeminy rhythm.

• In order to achieve a good temporal resolution, ensuring a satisfactory volume rate, we have to use the maximum number of beats possible for each patient (difficult when the patient cannot or is not cooperative or in the setting of rhythm disturbances), while limiting lateral and elevation widths and focusing on the TV and subvalvular apparatus only. Surrounding structures such as the interventricular septum and the aortic valve should also be included and serve as markers during 3D analysis (Figure 10C).

• Before storing the acquired dataset, we should always check the quality of the images obtained, looking for artifacts (significant stitching) and confirm if the entire structure of interest was adequately included. This can be done either in volume rendering mode or in the 2D multi-slice/multiplanar mode (Figure 10D).

• For post-processing we can navigate freely into the dataset looking for anatomic abnormalities and the relation to surrounding structures. The suggested anatomic view of the TV is acquired from the ventricular side, by placing the septum on our right side (3 o'clock) and the aortic valve on top of it (1 o'clock). That way the septal leaflet is demonstrated on the right side, next to the septum, the anterior leaflet on the top, next to the aortic valve, and the posterior on the bottom side opposite to the aortic valve (Figure 10E). Easy cropping features are also available, embedded in most machines, and they are an important tool to understand the etiology and pathophysiology of TR.

• It is possible to analyze dimensions of the TV annulus using multiplanar slicing or multiplanar reconstruction tools. Both modalities enable the alignment of planes to obtain accurate annular dimensions and area (Figure 11).

• To analyze tenting volume, coaptation height, annulus area, and other quantitative parameters, we can adapt the mitral valve software (available from many vendors), or use a specific software dedicated to the TV developed by GE Healthcare (AutoTVQ) (Figure 12). These applications are easy to use and have a good correlation of measurements, when compared to cardiac computed tomography.

Conclusion

Echocardiography is the most important noninvasive diagnostic method for evaluation of TV diseases, and 3DE has been proven to have additional value, not only for evaluation of valve anatomy and quantitation of TR, but also for a complete understanding of its pathophysiological mechanisms, playing a decisive role in planning the best therapeutic strategy. Quantitative data obtained from 3D TV analysis by specific software can provide valuable information to tailor the best surgical or percutaneous technique for each patient and to help develop new treatment strategies for valve intervention in the near future.

Author Contributions

Conception and design of the research and writing of the manuscript: Félix AS, Alcantara ML, Papadopoulos K; critical revision of the manuscript for intellectual content: Félix AS.

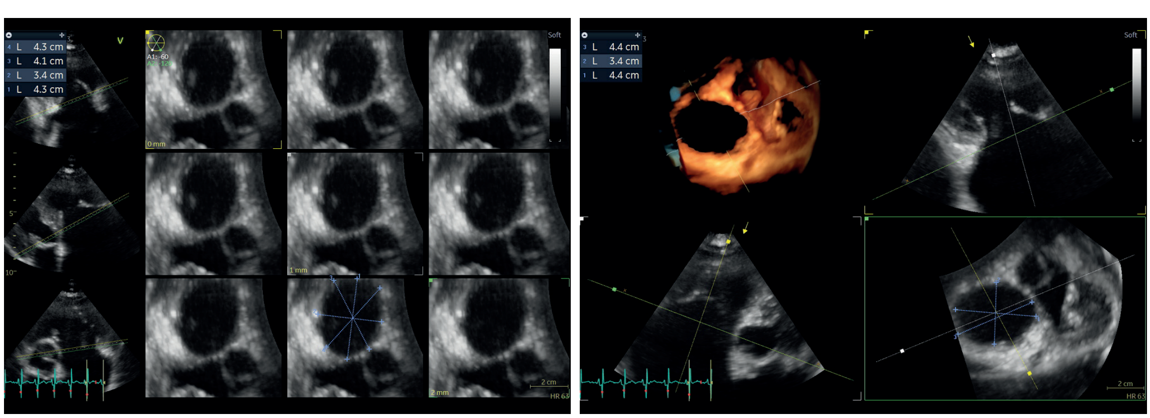

Figure 11 – *Tricuspid annular dimensions and area analysis by 3DE post-processing. A) multi-slice tool with appropriate alignment for TV annulus (hinge point of leaflets) in 3 different projections (2D on the left image) showing an oval annulus with different dimensions depending on the axis chosen. B) The same aspect is showed by multiplanar reconstruction.*

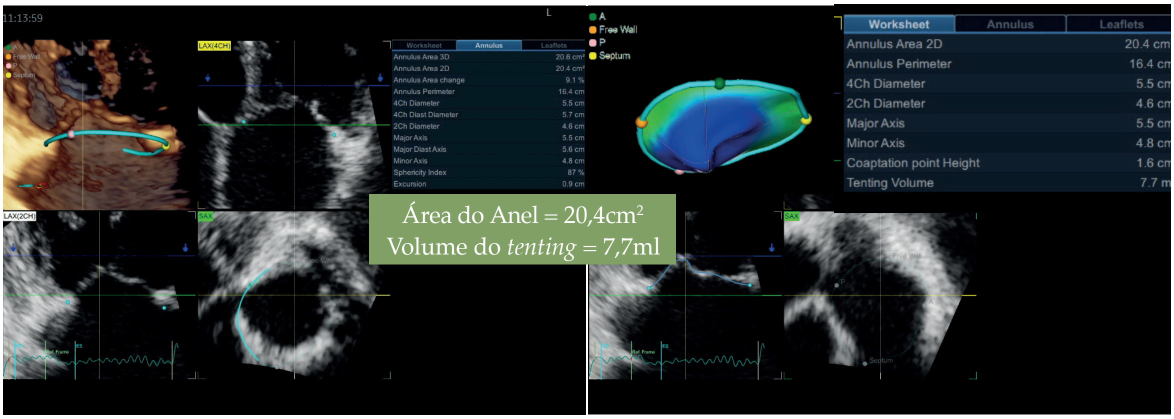

Figure 12 – *TV analysis using dedicated software (GE healthcare) in a patient with pulmonary arterial hypertension. In this case, we can see not only an important ventricular mechanism of secondary TR, with large tenting volume of 7.7 mL (normal volume = 1.1 ± 0.6 [Sukmawan, R, JASE 2007]), but also annular dilatation = 20.4 cm² (normal = 8.6 ± 2.0 cm² [Addetia et al., JACC 2017]), secondary to a chronic associated volumetric overload due to torrential TR.*

Potential Conflict of Interest

No potential conflict of interest relevant to this article was reported.

Sources of Funding

There were no external funding sources for this study.

Study Association

This study is not associated with any thesis or dissertation work.

Ethics Approval and Consent to Participate

This article does not contain any studies with human participants or animals performed by any of the authors.

References

1. Neuhold S, Huelsmann M, Pernicka E, Graf A, Bonderman D, Adlbrecht C, et al. Impact of Tricuspid Regurgitation on Survival in Patients with Chronic Heart Failure: Unexpected Findings of a Long-Term Observational Study. Eur Heart J. 2013;34(11):844-52. doi: 10.1093/eurheartj/ehs465.
2. Calafiore AM, Gallina S, Iacò AL, Contini M, Bivona A, Gagliardi M, et al. Mitral Valve Surgery for Functional Mitral Regurgitation: Should Moderate-or-More Tricuspid Regurgitation Be Treated? A Propensity Score Analysis. Ann Thorac Surg. 2009;87(3):698-703. doi: 10.1016/j.athoracsur.2008.11.028.
3. Dahou A, Magne J, Clavel MA, Capoulade R, Bartko PE, Bergler-Klein J, et al. Tricuspid Regurgitation Is Associated with Increased Risk of Mortality in Patients with Low-Flow Low-Gradient Aortic Stenosis and Reduced Ejection Fraction: Results of the Multicenter TOPAS Study (True or Pseudo-Severe Aortic Stenosis). JACC Cardiovasc Interv. 2015;8(4):588-96. doi: 10.1016/j.jcin.2014.08.019.
4. Topilsky Y, Nkomo VT, Vatury O, Michelena HI, Letourneau T, Suri RM, et al. Clinical Outcome of Isolated Tricuspid Regurgitation. JACC Cardiovasc Imaging. 2014;7(12):1185-94. doi: 10.1016/j.jcmg.2014.07.018.
5. Taramasso M, Benfari G, van der Bijl P, Alessandrini H, Attinger-Toller A, Biasco L, et al. Transcatheter versus Medical Treatment of Patients with Symptomatic Severe Tricuspid Regurgitation. J Am Coll Cardiol. 2019;74(24):2998-3008. doi: 10.1016/j.jacc.2019.09.028.
6. Dahou A, Levin D, Reisman M, Hahn RT. Anatomy and Physiology of the Tricuspid Valve. JACC Cardiovasc Imaging. 2019;12(3):458-68. doi: 10.1016/j.jcmg.2018.07.032.
7. Mahmood F, Kim H, Chaudary B, Bergman R, Matyal R, Gerstle J, et al. Tricuspid Annular Geometry: A Three-Dimensional Transesophageal Echocardiographic Study. J Cardiothorac Vasc Anesth. 2013;27(4):639-46. doi: 10.1053/j.jvca.2012.12.014.
8. Otto CM, Nishimura RA, Bonow RO, Carabello BA, Erwin JP 3rd, Gentile F, et al. 2020 ACC/AHA Guideline for the Management of Patients with Valvular Heart Disease: Executive Summary: A Report of the American College of Cardiology/American Heart Association Joint Committee on Clinical Practice Guidelines. Circulation. 2021;143(5):e35-e71. doi: 10.1161/CIR.0000000000000932.
9. Vahanian A, Beyersdorf F, Praz F, Milojevic M, Baldus S, Bauersachs J, et al. 2021 ESC/EACTS Guidelines for the Management of Valvular Heart Disease. Eur Heart J. 2022 Feb;43(7):561-632. doi: 10.1093/eurheartj/ehab395.
10. Addetia K, Muraru D, Veronesi F, Jenei C, Cavalli G, Besser SA, et al. 3-Dimensional Echocardiographic Analysis of the Tricuspid Annulus Provides New Insights Into Tricuspid Valve Geometry and Dynamics. JACC Cardiovasc Imaging. 2019;12(3):401-12. doi: 10.1016/j.jcmg.2017.08.022.
11. Miglioranza MH, Mihăilă S, Muraru D, Cucchini U, Iliceto S, Badano LP. Dynamic Changes in Tricuspid Annular Diameter Measurement in Relation to the Echocardiographic View and Timing During the Cardiac Cycle. J Am Soc Echocardiogr. 2015;28(2):226-35. doi: 10.1016/j.echo.2014.09.017.
12. Hahn RT, Badano LP, Bartko PE, Muraru D, Maisano F, Zamorano JL, et al. Tricuspid Regurgitation: Recent Advances in Understanding Pathophysiology, Severity Grading and Outcome. Eur Heart J Cardiovasc Imaging. 2022;23(7):913-29. doi: 10.1093/ehjci/jeac009.
13. Prihadi EA, Delgado V, Leon MB, Enriquez-Sarano M, Topilsky Y, Bax JJ. Morphologic Types of Tricuspid Regurgitation: Characteristics and Prognostic Implications. JACC Cardiovasc Imaging. 2019;12(3):491-99. doi: 10.1016/j.jcmg.2018.09.027.

14. Utsunomiya H, Harada Y, Susawa H, Ueda Y, Izumi K, Itakura K, et al. Tricuspid Valve Geometry and Right Heart Remodelling: Insights Into the Mechanism of Atrial Functional Tricuspid Regurgitation. Eur Heart J Cardiovasc Imaging. 2020;21(10):1068-78. doi: 10.1093/ehjci/jeaa194.

15. Muraru D. 22nd Annual Feigenbaum Lecture: Right Heart, Right Now: The Role of Three-Dimensional Echocardiography. J Am Soc Echocardiogr. 2022;35(9):893-909. doi: 10.1016/j.echo.2022.05.011.

16. Florescu DR, Muraru D, Florescu C, Volpato V, Caravita S, Perger E, et al. Right Heart Chambers Geometry and Function in Patients with the Atrial and the Ventricular Phenotypes of Functional Tricuspid Regurgitation. Eur Heart J Cardiovasc Imaging. 2022;23(7):930-40. doi: 10.1093/ehjci/jeab211.

17. Guta AC, Badano LP, Tomaselli M, Mihalcea D, Bartos D, Parati G, et al. The Pathophysiological Link between Right Atrial Remodeling and Functional Tricuspid Regurgitation in Patients with Atrial Fibrillation: A Three-Dimensional Echocardiography Study. J Am Soc Echocardiogr. 2021;34(6):585-594.e1. doi: 10.1016/j.echo.2021.01.004.

18. Muraru D, Badano LP. Shedding New Light on the Fascinating Right Heart. Eur Heart J Cardiovasc Imaging. 2022;23(7):863-6. doi: 10.1093/ehjci/jeac085.

19. Al-Bawardy R, Krishnaswamy A, Bhargava M, Dunn J, Wazni O, Tuzcu EM, et al. Tricuspid Regurgitation in Patients with Pacemakers and Implantable Cardiac Defibrillators: A Comprehensive Review. Clin Cardiol. 2013;36(5):249-54. doi: 10.1002/clc.22104.

20. Höke U, Auger D, Thijssen J, Wolterbeek R, van der Velde ET, Holman ER, et al. Significant Lead-Induced Tricuspid Regurgitation is Associated with poor Prognosis at Long-Term Follow-Up. Heart. 2014;100(12):960-8. doi: 10.1136/heartjnl-2013-304673.

21. Seo J, Kim DY, Cho I, Hong GR, Ha JW, Shim CY. Prevalence, Predictors, and Prognosis of Tricuspid Regurgitation Following Permanent Pacemaker Implantation. PLoS One. 2020;15(6):e0235230. doi: 10.1371/journal.pone.0235230.

My Approach to Echocardiographic Evaluation after Pediatric Heart Transplantation to Control Rejection and/or Graft Vascular Disease

Adailson Wagner da Silva Siqueira,[1] *Mirela Frederico de Almeida*[2]
Universidade de São Paulo, Instituto do Coração,[1] *São Paulo, SP – Brazil*
Universidade Federal da Bahia,[2] *Salvador, BA – Brazil*

Abstract

Pediatric heart transplantation is the definitive therapeutic option for patients with heart failure refractory to optimized clinical treatment, due either to cardiomyopathies or congenital heart disease. Morbidity and mortality remain concerning factors during evolution, and primary dysfunction, rejection, and graft vascular disease (GVD) are the main causes of death in the first 5 years after transplantation. As a surveillance method, transthoracic echocardiography has significant benefits in assisting diagnosis when there is clinical suspicion of rejection or GVD. The objective of this article is to present, in a clear and objective manner, which echocardiographic data assist pediatric cardiologists in follow-up of transplanted patients. The use of echocardiography, either through conventional tools or advanced methods, carefully focusing on different early and late post-cardiac transplantation phases, with information from current and comparative examination of evolution, mainly regarding tissue Doppler and longitudinal strain, can assist pediatric cardiologists in the decision to anticipate endomyocardial biopsy and coronary angiography (gold standard) for early diagnosis and immediate intervention, allowing greater graft durability.

Introduction

Pediatric heart transplantation is the definitive therapeutic option for patients with heart failure refractory to optimized clinical treatment, due either to cardiomyopathies or congenital heart disease.[1,2] Since the first pediatric heart transplant by Dr. Adrian Kantrowitz in 1967 to the present day, when approximately 700 transplants per year are performed, there has been substantial progress in the study of the immune response to grafts, the use of medications, surgical techniques, and lifestyle changes. Therefore, survival after pediatric transplantation has progressively improved in recent years, with a median survival of 18 years for all age groups; for transplants performed in patients younger than 1 year of age, the median survival is greater than 24 years.[3]

Morbidity and mortality remain concerning factors during evolution, and primary dysfunction, rejection, and graft vascular disease (GVD) are the main causes of death in the first 5 years after transplantation.[3] Other complications are associated with the use of immunosuppressive drugs, such as infections, lymphoproliferative disorders, diabetes, and target organ damage, such as kidney failure.[4]

For evaluation of graft integrity, the gold standard is the presence of direct cardiomyocyte damage on microscopy obtained through endomyocardial biopsy and the study of the coronary arteries by catheterization. However, it is an invasive procedure with risks of complications (perforation, tamponade, thrombi, arrhythmias, tricuspid valve injury) and, in the pediatric age range, the need for sedation/anesthesia. As a surveillance method, transthoracic echocardiography has significant benefits in assisting diagnosis when there is clinical suspicion of rejection or GVD. The new methods associated with myocardial deformation have shown promising results in anticipating outcomes and long-term patient survival, as untreated episodes of subclinical rejection can progress to GVD and progressive deterioration of the organ.[5] After diagnosis of GVD, survival drops significantly to 58% at 5 years and to only 40% at 10 years. These complications can lead to graft failure, and retransplantation is indicated, occurring in approximately 25% to 30% of pediatric heart transplants in the past decade.[1]

The objective of this article is to present, in a clear and objective manner, which echocardiographic data assist pediatric cardiologists in follow-up of transplanted patients, focusing on alterations that may, as early as possible, suggest graft anomalies before hemodynamic worsening, given that ventricular dysfunction due to reduced ejection fraction calculated by traditional methods is usually a late finding.[4]

Transplant timing: early versus late

Cardiac grafts present some peculiarities during the first postoperative months, requiring careful evaluation and interpretation of the data obtained by echocardiography in order to correlate and differentiate evolution suggestive of graft rejection in adaptation to the new hemodynamic state. Initially, during the period prior to implantation, the following factors may influence immediate organ function: ischemia time, donor age, presence of donor comorbidities, care in hemodynamic maintenance, and adequate preservation of the organ. After implantation, the graft may present temporary alterations due to reperfusion

Keywords

Echocardiography; Heart Transplantation; Heart Defects, Congenital; Coronary Disease.

Mailing Address: Adailson Wagner da Silva Siqueira •
Universidade de São Paulo, Instituto do Coração. Rua Doutor Enéas de Carvalho Aguiar, 44. Postal code: 05403-000. São Paulo, SP – Brazil
E-mail: adailson.siqueira@gmail.com
Manuscript received April 25, 2023; revised manuscript April 28, 2023; accepted April 28, 2023
Editor responsible for the review: Karen Saori Shiraishi Sawamura

DOI: https://doi.org/10.36660/abcimg.20230045i

injury, adaptation of the right ventricle to elevated pulmonary artery pressure, and the presence of circulating inflammatory mediators.[2,3] The use of immunosuppressants, mainly cyclosporine,[6] increased circulating catecholamines, systemic arterial hypertension, and worsening lymphatic drainage lead to a progressive increase in ventricular mass, which peaks around the third postoperative month and progressively reduces until normalization in the first year after transplantation[5] (Figure 1).

Non-invasive detection of acute rejection is particularly challenging in the early post-transplant period as systolic and diastolic function (relaxation disorder and restrictive physiology) undergo changes during the first few months. The denervated heart has a particular physiology, with an impact on the validation and reliability of non-invasive methods; therefore, echocardiographic evaluation must take this graft modification/adaptation into consideration during the initial months. The follow-up protocols of most large transplant centers include mandatory hemodynamic study and endomyocardial biopsy at pre-established periods during the first months, regardless of good clinical evolution[5] (Figure 2).

Conventional echocardiography measurements

Tissue Doppler imaging

Myocardial inflammation caused by graft rejection alters tissue characteristics even before the onset of systolic or diastolic dysfunction. Tissue Doppler imaging (TDI) quantifies the velocity of movement in a myocardial region in relation to the transducer. TDI is, thus, a tool that characterizes myocardial mechanics and a non-invasive imaging instrument that can monitor acute cellular rejection in adults and children.[7]

TDI values are normally lower in pediatric transplant patients without rejection in relation to the values found in healthy controls.[8] Thus, variations in TDI measurement values are more predictive for evaluation of rejection than when considered alone. The longitudinal evaluation of patients makes it possible to detect changes in graft systolic and diastolic function.

Derek et al. studied 53 transplanted children, and 8 of them evolved to terminal graft failure (death or retransplantation). The authors detected a reduction in the S′ velocity of the tricuspid valve approximately 6 months before the terminal failure. A reduction in mitral valve S′ velocity occurred only 3 months before the event, demonstrating left ventricular failure after right ventricular failure.[9]

Lunze et al. demonstrated that a reduction of up to 15% in S′ velocity and up to 5% in A′ velocity of the left ventricle was able to predict absence of rejection in pediatric transplant patients with an accuracy greater than 99%.[10]

The E/E′ ratio of the mitral and tricuspid valves is also a useful parameter in suspected humoral graft rejection, as demonstrated by Behera et al.,[11] who studied 148 pediatric heart transplant patients. Echocardiography was performed on the same day as endomyocardial biopsy. The mitral and tricuspid E/E′ ratio was significantly lower in patients with rejection compared to patients without alterations on biopsy.

The myocardial performance index (MPI) derived from TDI is a useful parameter in suspected graft rejection in transplant patients. The MPI can increase by an average of 98% during the period of rejection compared to the baseline value and return to pretreatment index levels after resolution of myocardial inflammation.[6]

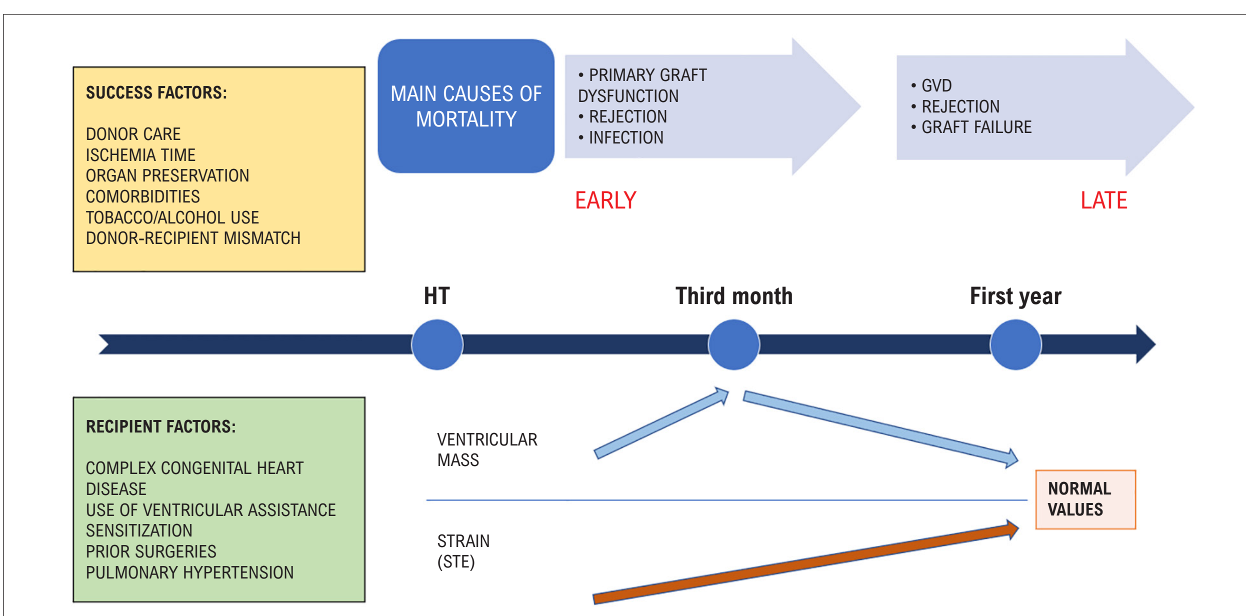

Figure 1 – *Main factors associated with success in early and late transplantation that influence graft function and echocardiographic findings, showing the evolution of ventricular mass and ventricular strain (STE). HT: heart transplantation; STE: speckle-tracking echocardiography; GVD: graft vascular disease.*

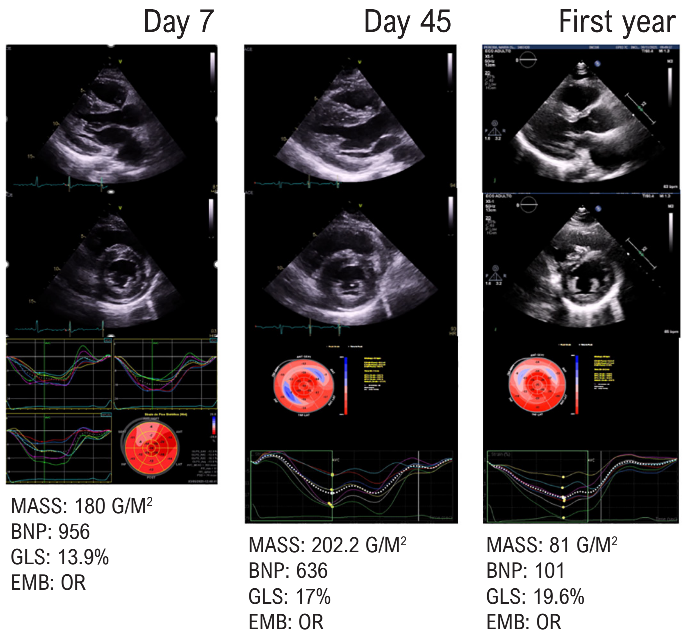

Figure 2 – *Temporal follow-up of evolution after cardiac transplantation in parasternal longitudinal and short-axis echocardiographic views, showing 2-dimensional imaging, global longitudinal strain, ventricular mass, biomarkers, and paired endomyocardial biopsy results. BNP: B-type natriuretic peptide; EMB: endomyocardial biopsy; GLS: global longitudinal strain.*

Flanagan et al. studied 40 children with heart transplant (60 days after the procedure) with endomyocardial biopsy-proven acute cellular rejection and compared them with 40 children with transplantation, but without rejection. The authors identified a significant increase in left ventricular MPI during the rejection period in relation to the same patient's baseline value (0.59 +/− 017 versus 0.41 +/− 0.11; $p < 0.001$) and similar values of left ventricular MPI after resolution of inflammation compared to the baseline value without rejection (0.41 +/− 0.11 versus 0.42 +/− 0.11; $p = 0.65$). Thus, the authors concluded that an increase of ≥ 0.47 in the baseline value of left ventricular MPI had a sensitivity of 82.5% and specificity of 85% in the detection of acute cellular rejection and that an increase of ≥ 20.4% in left ventricular MPI in relation to the patient's baseline value has a sensitivity of 90% and specificity of 100% in the detection of acute cellular rejection. Their study illustrates the importance of longitudinal evaluation of left ventricular MPI in patients with heart transplantation.[12]

Tricuspid annular plane systolic excursion (TAPSE)

Echocardiographic markers are essential for diagnosis and monitoring of the graft in cases of rejection. Initially, this evaluation focused mainly on the left ventricle. More recently, parameters for evaluating right ventricular function have been studied in this scenario.

TAPSE is a measure that evaluates right ventricular longitudinal function. Using the M mode, with the cursor positioned on the lateral wall of the tricuspid annulus, it is possible to measure the displacement distance of this annulus, a parameter that evaluates right ventricular longitudinal function. Heart transplantation alters the geometry of the heart and thus modifies the longitudinal movement of the right ventricle. Changes in TAPSE soon after heart transplantation may correspond to changes in the mechanism of right ventricular contractility rather than solely systolic dysfunction in this chamber.[12] Hence, longitudinal follow-up of patients is important in order to detect variations in graft performance.

Brian et al. studied 127 stable pediatric heart transplant patients and compared them with 380 age-matched healthy children. The authors demonstrated a reduction in TAPSE values in transplant patients compared to healthy controls (mean Z score: −3.38).[13] Michalski et al. retrospectively studied 52 patients (pediatric and adult) with heart transplantation and observed a reduction in TAPSE immediately after transplantation, with progressive improvement over time. They also demonstrated an association between a reduction in TAPSE and an increase in mean pulmonary artery pressure calculated by cardiac catheterization 10 years after transplantation.[14]

Pediatric patients show a decrease in TAPSE during an episode of rejection, and the values improve after resolution of the condition, as demonstrated in a retrospective study carried out by Arthur et al., which evaluated 44 pediatric heart transplant patients.[15]

Mitral annular plane systolic excursion (MAPSE)

MAPSE is a parameter for evaluating left ventricular systolic function, measured using the M mode of the lateral portion of the mitral annulus in 4-chamber view. This index may also be reduced in pediatric patients who have undergone heart transplantation.

Chinalli et al. studied 60 children who underwent heart transplantation and compared them with 60 healthy controls.

All patients had normal ejection fraction by Simpson's method. The transplanted patients had lower MAPSE values than patients in the control group (13 mm +/− 2.6 versus 18 mm +/− 2.3; $p < 0.0001$).[16]

New technologies: applications in the pediatric range?

Echocardiography is commonly the primary non-invasive technique for surveillance of the transplanted heart; however, the traditionally used parameters are affected by heart rate, pre- and after-load conditions, and paradoxical movement of the graft septum, leading to calculations of ventricular function with low sensitivity and specificity to detect asymptomatic episodes of rejection.[17,18] The greatest advantage in cardiac graft evaluation is the method's ability to distinguish between passive and active myocardial movement.

The use of speckle tracking in 2-dimensional echocardiography is relatively new, non-invasive, and reliable, with adequate sensitivity, and it is not angle-dependent for measuring ventricular systolic and diastolic function.[17,19] Two-dimensional strain and strain rate analyze myocardial deformity by tracking natural acoustic markers (speckles) during the cardiac cycle.[20]

The ability of myocardial strain to detect subclinical abnormalities, including subtle changes in regional mobilities, has led to its being explored as an early predictor of rejection. Longitudinal peak systolic strain has been shown to be more sensitive in the evaluation of lesions and reliable in relation to myocardial maturity in the pediatric population.[17]

A gradual increase occurs in longitudinal peak systolic strain values during the first 2 years after heart transplantation, and many patients continue with values below the normality of control groups, even in the absence of rejection or GVD, constituting the "new normal" for stable transplant patients, with absolute values between 16% and 18%.[16,19]

Chanana et al., simultaneously comparing data obtained by catheterization and echocardiography, obtained a cut-off value of 14% for longitudinal strain as a predictor of acute rejection in pediatric recipients, reaching sensitivity greater than 85% and specificity greater than 80%.[17]

Engelhardt et al., using global longitudinal strain comparatively during stable phase and episodes of rejection in transplanted children, observed that a 33% reduction in values from the baseline result was associated with the presence of rejection.[21]

Regardless of the presence or absence of focal coronary stenosis, GVD may be associated with low global longitudinal strain and strain rate values. The use of the method for evaluating left ventricular synchrony and synergy allows the detection of regional differences in the left ventricle and may even indicate the relationship with coronary perfusion and the area it encompasses (Figure 3).

GVD typically manifests loss of the distal coronary vasculature by proliferation of the intima and media layer, and it occurs diffusely, affecting the entire microvasculature, resulting in diastolic dysfunction and graft loss. Zoller et al. have described a reduction in left ventricular global longitudinal strain in patients with coronary vasculopathy, preceding diagnosis via cardiac catheterization by approximately 2 years.[17]

It is important to remember that it is very difficult to establish cut-off values in the pediatric age group, as the samples are numerically small for generalization, and the available data are from single-center studies; consequently, other echocardiographic measurements such as circumferential strain, radial strain, and twist present conflicting data. Due to the already mentioned aspects of the transplanted heart, stress echocardiography, whether induced by exercise or by the infusion of dobutamine, has limitations in the pediatric range. The use of the 3-dimensional method and right atrial and left atrial strain, with numerous studies carried out in adults, still require better validation in the pediatric range.

How can these data help?

The main objective of a multidisciplinary team is to provide quality of life to patients with heart transplant, limiting damage to the graft, by means of strict monitoring for early diagnosis of rejection and GVD, which are associated with significant morbidity and mortality. The use of echocardiography, either through conventional tools or advanced methods, carefully focusing on different early and late post-cardiac transplantation phases, with information from current and comparative examination of evolution, mainly regarding TDI and longitudinal strain, can assist pediatric cardiologists in the decision to anticipate endomyocardial biopsy and coronary angiography (gold standard) for early diagnosis and immediate intervention, allowing greater graft durability. In recent decades, the progressive increase in the survival of children who undergo heart transplantation has shown evidence of this continuous effort to adapt technological innovations without losing the human relationship (Figure 4).

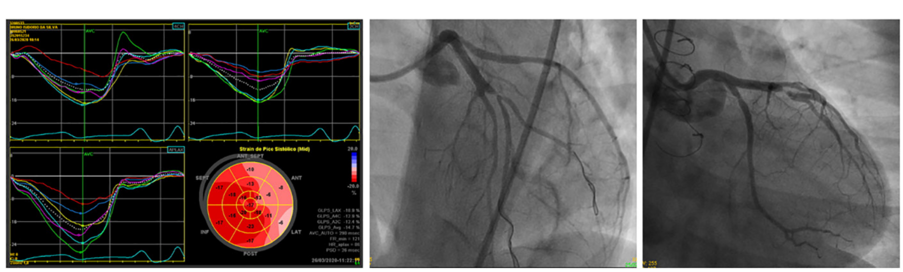

Figure 3 – *Regional alterations demonstrated by segments in global longitudinal strain correlated with diffuse focal lesions in the left coronary artery visualized in coronary angiography.*

Author Contributions

Conception and design of the research and critical revision of the manuscript for intellectual content: Siqueira AWS; acquisition of data and writing of the manuscript: Siqueira AWS, Almeida MF.

Potential Conflict of Interest

No potential conflict of interest relevant to this article was reported.

Sources of Funding

There were no external funding sources for this study.

Study Association

This study is not associated with any thesis or dissertation work.

Ethics Approval and Consent to Participate

This article does not contain any studies with human participants or animals performed by any of the authors.

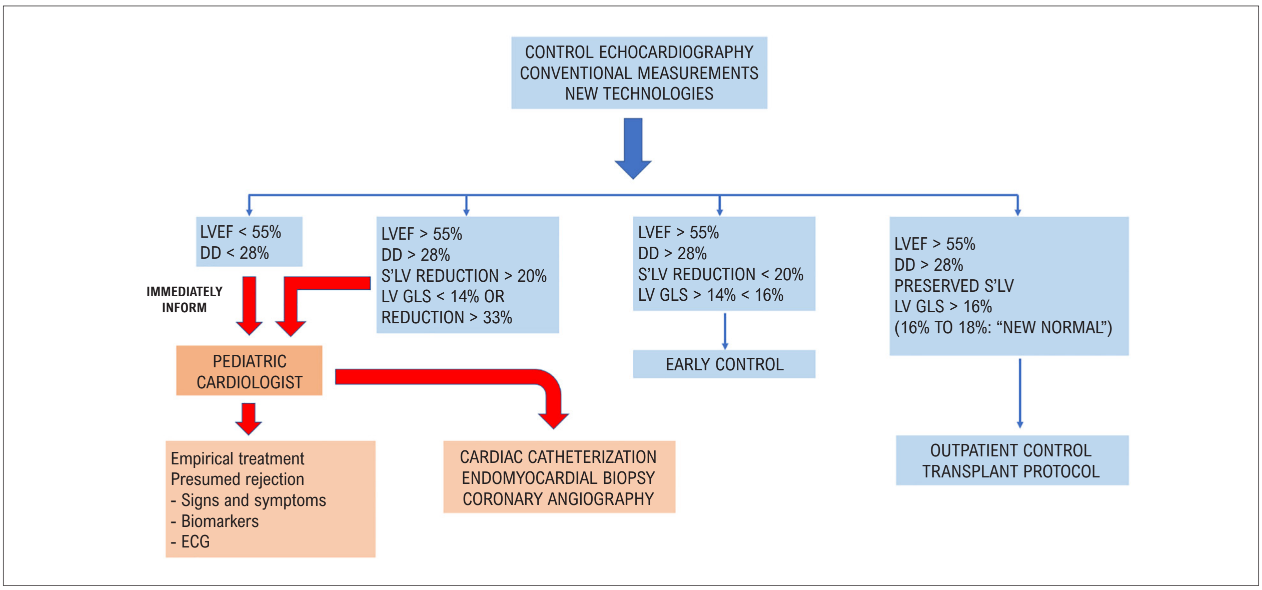

Figure 4 – *Diagram of echocardiography findings directly associated with suspected alteration of the cardiac graft, highlighting the main data for pediatric cardiologists to intervene. DD: delta D or shortening fraction; ECG: electrocardiogram; GLS: global longitudinal strain; LVEF: left ventricular ejection fraction; s'LV: s' of the left ventricular lateral wall.*

References

1. Thrush PT, Hoffman TM. Pediatric Heart Transplantation-Indications and Outcomes in the Current Era. J Thorac Dis. 2014;6(8):1080-96. doi: 10.3978/j.issn.2072-1439.2014.06.16.

2. Kim YH. Pediatric Heart Transplantation: How to Manage Problems Affecting Long-Term Outcomes? Clin Exp Pediatr. 2021;64(2):49-59. doi: 10.3345/cep.2019.01417.

3. Dipchand AI. Current State of Pediatric Cardiac Transplantation. Ann Cardiothorac Surg. 2018;7(1):31-55. doi: 10.21037/acs.2018.01.07.

4. Dandel M, Hetzer R. Post-Transplant Surveillance for Acute Rejection and Allograft Vasculopathy by Echocardiography: Usefulness of Myocardial Velocity and Deformation Imaging. J Heart Lung Transplant. 2017;36(2):117-31. doi: 10.1016/j.healun.2016.09.016.

5. Olymbios M, Kwiecinski J, Berman DS, Kobashigawa JA. Imaging in Heart Transplant Patients. JACC Cardiovasc Imaging. 2018;11(10):1514-30. doi: 10.1016/j.jcmg.2018.06.019.

6. Vivekananthan K, Kalapura T, Mehra M, Lavie C, Milani R, Scott R, et al. Usefulness of the Combined Index of Systolic and Diastolic Myocardial Performance to Identify Cardiac Allograft Rejection. Am J Cardiol. 2002;90(5):517-20. doi: 10.1016/s0002-9149(02)02525-0.

7. Kindel SJ, Hsu HH, Hussain T, Johnson JN, McMahon CJ, Kutty S. Multimodality Noninvasive Imaging in the Monitoring of Pediatric Heart Transplantation. J Am Soc Echocardiogr. 2017;30(9):859-70. doi: 10.1016/j.echo.2017.06.003.

8. Strigl S, Hardy R, Glickstein JS, Hsu DT, Addonizio LJ, Lamour JM, et al. Tissue Doppler-Derived Diastolic Myocardial Velocities are Abnormal in Pediatric Cardiac Transplant Recipients in the Absence of Endomyocardial Rejection. Pediatr Cardiol. 2008;29(4):749-54. doi: 10.1007/s00246-007-9188-6.

9. Fyfe DA, Ketchum D, Lewis R, Sabatier J, Kanter K, Mahle W, et al. Tissue Doppler imaging Detects Severely Abnormal Myocardial Velocities that Identify Children with Pre-Terminal Cardiac Graft Failure after Heart Transplantation. J Heart Lung Transplant. 2006;25(5):510-7. doi: 10.1016/j.healun.2005.11.453.

10. Lunze FI, Colan SD, Gauvreau K, Perez-Atayde AR, Smith RN, Blume ED, et al. Tissue Doppler Imaging for Rejection Surveillance in Pediatric Heart Transplant Recipients. J Heart Lung Transplant. 2013;32(10):1027-33. doi: 10.1016/j.healun.2013.06.016.

11. Behera SK, Trang J, Feeley BT, Levi DS, Alejos JC, Drant S. The use of Doppler Tissue Imaging to Predict Cellular and Antibody-Mediated Rejection In Pediatric Heart Transplant Recipients. Pediatr Transplant. 2008;12(2):207-14. doi: 10.1111/j.1399-3046.2007.00812.x.

12. Flanagan R, Cain N, Tatum GH, Debrunner MG, Drant S, Feingold B. Left Ventricular Myocardial Performance Index Change for Detection of Acute Cellular Rejection in Pediatric Heart Transplantation. Pediatr Transplant. 2013;17(8):782-6. doi: 10.1111/petr.12153.

13. White BR, Katcoff H, Faerber JA, Lin KY, Rossano JW, Mercer-Rosa L, et al. Echocardiographic Assessment of Right Ventricular Function in Clinically Well Pediatric Heart Transplantation Patients and Comparison with Normal Control Subjects. J Am Soc Echocardiogr. 2019;32(4):537-544.e3. doi: 10.1016/j.echo.2019.01.015.

14. Michalski M, Haas N, Dalla Pozza R, Michel S, Fischer M, Lehner A, et al. Tricuspid Annular Plane Systolic Excursion (TAPSE) Correlates with Mean Pulmonary Artery Pressure Especially 10 Years after Pediatric Heart Transplantation. Clin Transplant. 2023;37(3):e14710. doi: 10.1111/ctr.14710.

15. Arthur L, Knecht K, Ferry J, Grigsby D, Spencer H, Zakaria D. Serial Assessment of Right Ventricular Function Can Detect Acute Cellular Rejection in Children with Heart Transplantation. Pediatr Transplant. 2022;26(4):e14231. doi: 10.1111/petr.14231.

16. Chinali M, Esposito C, Grutter G, Iacobelli R, Toscano A, D'Asaro MG, et al. Cardiac Dysfunction in Children and Young Adults with Heart Transplantation: A Comprehensive Echocardiography Study. J Heart Lung Transplant. 2017;36(5):559-66. doi: 10.1016/j.healun.2016.11.007.

17. Sehgal S, Blake JM, Sommerfield J, Aggarwal S. Strain and Strain Rate Imaging Using Speckle Tracking in Acute Allograft Rejection in Children with Heart Transplantation. Pediatr Transplant. 2015;19(2):188-95. doi: 10.1111/petr.12415.

18. Sahewalla R, Sehgal S, Blake J, Aggarwal S. Left Ventricular Adaptation Following Orthotopic Heart Transplantation in Children: A Speckle Tracking Echocardiographic Imaging Study. Clin Transplant. 2019;33(8):e13632. doi: 10.1111/ctr.13632.

19. Chanana N, van Dorn CS, Everitt MD, Weng HY, Miller DV, Menon SC. Alteration of Cardiac Deformation in Acute Rejection in Pediatric Heart Transplant Recipients. Pediatr Cardiol. 2017;38(4):691-9. doi: 10.1007/s00246-016-1567-4.

20. Buddhe S, Richmond ME, Gilbreth J, Lai WW. Longitudinal Strain by Speckle Tracking Echocardiography in Pediatric Heart Transplant Recipients. Congenit Heart Dis. 2015;10(4):362-70. doi: 10.1111/chd.12263.

21. Engelhardt K, Das B, Sorensen M, Malik S, Zellers T, Lemler M. Two-Dimensional Systolic Speckle Tracking Echocardiography Provides a Noninvasive Aid in the Identification of Acute Pediatric Heart Transplant Rejection. Echocardiography. 2019;36(10):1876-83. doi: 10.1111/echo.14481.

My Approach to Echocardiographic Assessment of the Premature Newborn

Karen Saori Shiraishi Sawamura,[1,2,3] Márcio Miranda Brito[4,5]
Hospital das Clínicas, Faculdade de Medicina, Universidade de São Paulo,[1] São Paulo, SP – Brazil
Hospital Israelita Albert Einstein,[2] São Paulo, SP – Brazil
Hospital do Coração,[3] São Paulo, SP – Brazil
Universidade Federal do Norte do Tocantins,[4] Araguaína, TO – Brazil
Hospital Municipal de Araguaína,[5] Araguaína, TO – Brazil

Abstract

Echocardiographic assessment of preterm infants, why do it?

The incidence of premature births has been increasing worldwide and already affects about 10% of live births. Extremely preterm newborns (PTNB) are at increased risk of developing pulmonary immaturity, leading to pulmonary hypertension (PH), in addition to cardiovascular immaturity and patent ductus arteriosus (PDA).

Hemodynamic monitoring of this population is challenging and differs from critically ill pediatric patients due to hemodynamic lability. Thus, minimal manipulation is essential to avoid complications. In this context, non-invasive monitoring methods such as transthoracic echocardiography (TTE) gain importance for hemodynamic assessment. It is a low-cost, radiation-free test that offers good anatomical and functional visualization in pediatric patients, making it a useful tool in the clinical management of severe preterm newborns.

What you will find in this article:

We will take an objective, didactic, and at times humorous approach to the use of echocardiography in premature newborns in the neonatal intensive care unit (NICU), and we will discuss the echocardiographic particularities of premature infants, especially regarding equipment adjustments, PH, and persistence of the ductus arteriosus (DA).

Introduction

The incidence of premature births has increased significantly in recent decades and already affects about 10% of live births worldwide.[1] The advent of surfactants, corticosteroids and better understanding of respiratory and hemodynamic management resulted in a reduction in morbidity and mortality in these patients, although these advances are not yet widely accessible across the country.

Extremely preterm newborns (PTNB) are at greater risk of presenting pulmonary immaturity with consequent alterations in alveolar development, affecting the pulmonary vasculature, in addition to patent ductus arteriosus (PDA). It is also known that prematurity alone is an independent risk factor for cardiac remodeling, which, associated with increased pulmonary vascular resistance, results in overload of the cardiovascular system.[2]

It is also worth noting that the hemodynamic monitoring of this population differs from that of severe adult and pediatric patients, due to several factors such as low weight (many patients weighing less than 1 kilogram), hemodynamic lability, reduced blood volume and immaturity of all systems, especially the respiratory system. In this context, minimal manipulation of the PTNB is essential. Many of the invasive monitoring devices used in other groups of critically ill patients cannot be used here, increasing the importance of non-invasive monitoring methods. Transthoracic echocardiography (TTE) is a low-cost exam, without radiation, with good anatomical and dynamic functional visualization in pediatric patients, which therefore comes to add a lot to the clinical management of severe PTNB.

In this article, a didactic and objective approach was taken to the echocardiogram in premature infants in the neonatal intensive care unit (NICU); there was no pretension to discuss all the parameters contained in the neonatal echocardiogram, but rather the particularities inherent to premature babies.

Echocardiogram in patients weighing less than 1Kg, now what?

Given the scenario of minimal manipulation of the PTNB in the NICU, before starting TTE itself, one should observe an overview of the conditions found and try to obtain as much information as possible so that the examination is brief and brings as much information as possible to the handling of the case.

- Is the patient using invasive ventilation? If non-invasive, is there positive airway pressure in this ventilation mode?
- Is there use of vasoactive drugs?
- Are catheters used? What position?
- Age in days?

Keywords

Premature Infant; Echocardiography; Neonatology; Pulmonary Hypertension; Ductus Arteriosus

Mailing Address: Karen Saori Shiraishi Sawamura •
Hospital das Clínicas, Faculdade de Medicina Universidade de São Paulo, Diagnóstico e Imagem. Av. Dr. Enéas Carvalho de Aguiar, 647.
Postal Code: 05403-000. São Paulo, SP – Brazil
E-mail: kasaori@gmail.com
Manuscript received April 4, 2023; revised manuscript April 3, 2023; accepted April 5, 2023
Editor responsible for the review: Daniela do Carmo Rassi Frota

DOI: https://doi.org/10.36660/abcimg.20230035i

It seems obvious, but it is worth noting that these patients have a tenuous hemodynamic balance, so an increase in pressure on the inferior vena cava (IVC) when evaluating the subcostal plane with the transducer, for example, may be enough to collapse it, preventing return venous system and reducing ventricular preload. Thus, attention should be paid to the amount of force applied to the transducer on the abdomen and chest. PTNB are also more susceptible to hypothermia; therefore, it is essential to open as few incubator doors as possible and not forget to close them at the end of TTE.[3]

How to adjust the equipment for preterm echocardiography?

New echocardiogram software have made great advances in recent years, favoring better image quality in very low weight patients. Many devices come with specific presets for the neonatal or even premature population, however, some specific tips can help to improve the exam:

- Use transducer with the higher frequency as possible, therefore, the higher the frequency, the higher the frame rate. There are, ideally, 12 Mhz transducers (Figure 1), however, if this type of transducer is not available, try to use one with a minimum frequency of 8 Mhz;
- Turn off the ultrasound harmonics (small structures very close to the transducer evaluated with high frequency transducers do not need this feature);
- You can use the device's "penetration/resolution" adjustment feature; in this case, reduce penetration and increase resolution (frequency); and
- PTNB smaller than 1Kg commonly have a limited parasternal window (especially when ventilated with positive pressure); therefore, the use of the subcostal window with alternative planes is very useful.

What is special about the echocardiogram of the preterm newborn?

Considering the importance of "looking at the whole", mentioned earlier, it is possible to make an analogy with a hunting eagle: it is important to fly free and look at the general panorama (patient conditions and acquisition of general parameters of the echocardiogram), however, when it spots its prey, it focuses on calculations of speed of descent and precision of attack. Like an eagle hunting, the TTE of PTNB should focus on the peculiarities inherent to prematurity. Therefore, this article will not detail parameters such as evaluation of left ventricular systolic function, evaluation of pericardial effusion repercussions, evaluation of intracardiac masses or complex congenital heart diseases. These themes are better addressed in other references, we will focus on the peculiarities of PTNB.

Lung immaturity plays a crucial role in this pathophysiology. The lung undergoes pre- and postnatal injuries, altering the growth of the pulmonary vasculature, which in turn leads to increased afterload imposed on the right ventricle (RV), leading to pulmonary hypertension (PH). In extreme cases, there is overload of the cardiovascular system with right heart failure and consequent worsening of the left cardiac output.[4] Thus, a cautious assessment of the entire right heart system, starting with the systemic venous return, RV dimensions, and systolic function, the estimation of pulmonary vascular resistance and the interrelationship with the left ventricle (LV) is necessary.

Figure 1 – *High frequency transducer used to assess nearby structures (4-6cm) to the sternum, useful for evaluating low weight patients.*

Another relevant point is the evaluation of the PDA. Its prevalence in premature newborns is inversely proportional to gestational age, occurring in 20% of patients with gestational age greater than 32 weeks and in 80-90% of premature infants with extremely low birth weight (less than 1,000g) and gestational age of less than 26 weeks.[5]

How to assess PH in preterm infants?

First, the presence of congenital heart diseases must be excluded, except for patent foramen ovale (PFO), atrial septal defect (ASD) and PDA. Once this is done, the assessment of PH in preterm infants can begin. Here, it is possible to think of it as a system of closed connections and to segment the reasoning as follows:

- The increase in pulmonary pressure is directly proportional to the increase in pulmonary vascular resistance (either secondary to the immaturity of the pulmonary vascular bed, or due to persistence of the fetal pattern or other injuries) while the pulmonary cardiac output is maintained;
- There is RV pressure overload, which evolves with dilation and systolic dysfunction;
- RV dilation (when important) added to suprasystemic pulmonary pressure physically makes the RV insinuate against the LV, disturbing the systemic cardiac output

by reducing the LV filling volume, in addition to the lower return preload of the pulmonary veins;

- This whole process leads to an increase in RV end-diastolic pressure (RV DP_2) which means enlargement of the right atrium (RA), leading to venous congestion; and
- Evaluation of flow pattern across communications.

1.Quantifying is good! Is it always possible?

1.1 Pulmonary artery systolic pressure (PASP)

PASP measurement can be performed using tricuspid regurgitation (TR) Doppler. PASP can be estimated using the modified Bernoulli formula[6] (Equation 1):

$$\mathbf{PASP = 4xVTR^2 + RAP} \quad (1)$$

Where:

PASP: pulmonary artery systolic pressure (mmHg);

VTR: maximum velocity of tricuspid regurgitation (m/s); and

RAP: RA pressure (mmHg).

RAP is often not measured and can be considered as 3-5mmHg[3], except in cases of invasive mechanical ventilation with high pressure parameters or IVC dilation and reduced collapsibility, considering 7-10 mmHg.

However, it is not always possible to estimate the PASP, recommending aligning the cursor with the TR orifice, usually in the apical 4-chamber plane (Figure 2). One should pay attention to the quality of the Doppler curve, since the PASP is proportional to the maximum velocity squared. Thus, if there is an error in the measurement, its dimension will be exponentially underestimated.

If the neonate has PDA, PASP can be estimated by Doppler alignment of the DA through Equation 2:

$$\mathbf{PASP = SBP - 4xVAoTP^2} \quad (2)$$

Where

PASP: pulmonary artery systolic pressure (mmHg);

SBP: systolic blood pressure (mmHg); and

VAoPT: maximum flow velocity from the aorta (Ao) to the pulmonary trunk (PT) (m/s).

It is essential to compare the pulmonary pressure obtained with the patient's systemic systolic pressure and not just the absolute value. It is worth reporting if the pulmonary pressure obtained is less than 50% of the systemic pressure, greater than 50% of the systemic pressure, or greater than the systemic pressure (important PH).

1.2 Mean pulmonary artery pressure (MPAP)

The MPAP can be estimated using the pulmonary artery reflux (PR) curve, using Equation 3:[6,7]

$$\mathbf{MPAP = 4x\ VRP^2 + PD2VD} \quad (3)$$

Where

MPAP: mean pulmonary artery pressure (mmHg);

PRV: maximum pulmonary reflux velocity (m/s); and

RV DP_2: right ventricular end-diastolic pressure (mmHg).

1.3 Pulmonary vascular resistance: The pulmonary Doppler pattern

The Doppler pattern of the RV outflow tract can provide relevant information on the estimation of RV afterload. It is known that a shortening of the systolic acceleration time correlates with an increase in pulmonary pressure. Thus, a "symmetrical" flow pattern is expected during systole for normal pressures, a shortening of the systolic acceleration time as pulmonary pressure increases and, finally, a mid-systolic notch when there is suprasystemic PH[8] (Figure 3). Analogously, the integral velocity over time (IVT) decreases proportionally with the increase in pulmonary vascular resistance.[6]

2. Brute force versus complacency: Dilation and dysfunction

2.1 The evaluation of the dimensions of the RV

The RV is a compliant cardiac chamber that evolves with hypertrophy and dilation in response to increased afterload. That said, one should actively look for signs of ventricular dilation in all planes. It is known that access to RV morphology is complex through the assessment of two-dimensional TTE,

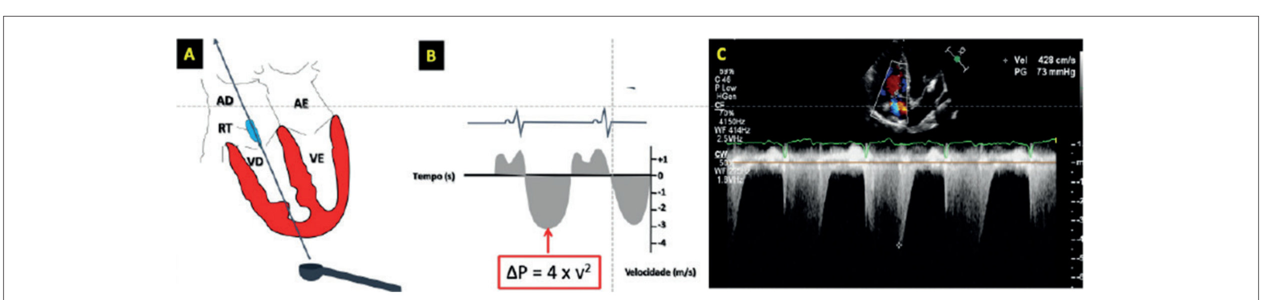

Figure 2 – *A: Image showing how to align the cursor with the tricuspid regurgitation jet (TR) in the apical 4-chamber plane. B: TR Doppler. C: Tricuspid continuous Doppler flow pattern. RA: right atrium; LA: left atrium; RV: right ventricle; LV: left ventricle; TR: Tricuspid regurgitation; P: pressure (mmHg); v: flow velocity (m/s).*

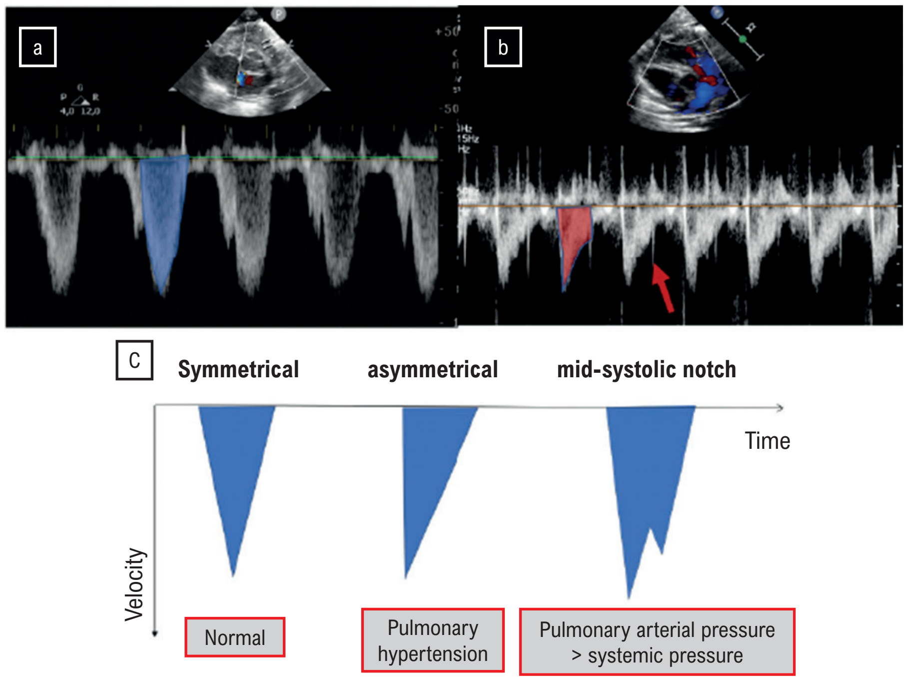

Figure 3 – *Pulmonary artery Doppler pattern. In the first image (a) the symmetrical Doppler pattern of the pulmonary artery can be seen in the patient with normal pulmonary vascular resistance, in blue, the area under the curve proportional to the pulmonary VTI. In the second image (b), the mid-systolic notch (arrow) and the representation of the VTI (red area) of the patient with increased pulmonary vascular resistance can be seen. Image below shows representation of Doppler patterns.*

as can be seen in Figure 4-A of the three-dimensional echocardiogram of the RV, reinforcing the importance of imaging assessment in different echocardiographic planes. The RV and LV commonly have similar dimensions in the apical 4-chamber view during the neonatal period, but the RV should not be larger than the LV (Figure 4-B and 4-C). The parasternal short axis plane complements the RV assessment and can be indexed by body surface area and age.[9]

2.2 Assessment of right ventricular systolic function:

2.2.1 Tricuspid Annular Plane Systolic Excursion (TAPSE)

TAPSE is the measure of the distance traveled by the tricuspid valve annulus toward the cardiac apex during systole. It is acquired in the apical four-chamber plane, usually positioning the M-mode cursor on the lateral portion of the valve annulus

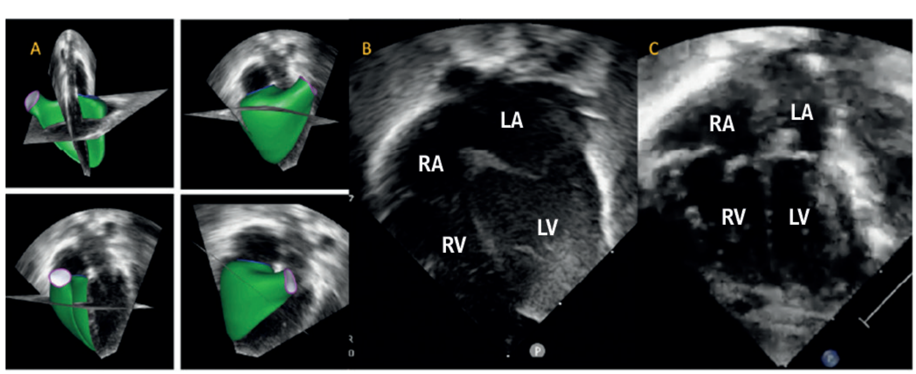

Figure 4 – *Three-dimensional echocardiogram of the right ventricle, seen from different angles, showing the complexity of its morphology (A). Two-dimensional echocardiogram showing the apical 4-chamber view in a normal PTNB without pulmonary hypertension with normal proportions of LV and RV dimensions (B) and PTNB with pulmonary hypertension showing dilation of the right chambers (C). RA: Right atrium; LA: Left atrium; RV: Right ventricle; LV: left ventricle; PTNB: Preterm newborn*

(Figure 5). The TAPSE value is negatively correlated with pulmonary vascular resistance and pulmonary pressure values.[10] Normality values for TAPSE in neonates are indexed by body surface area and vary over the days of life. Jain et al. found a mean TAPSE of 0.92 cm on the first day of life.[9]

2.2.2 Fractional area change (FAC)

The FAC is the variation of the RV area in systole compared to diastole. It incorporates the global RV systolic function and can be obtained with a two-dimensional image of the apical four-chamber view modified for the RV, in which the endocardial walls should be traced in diastole (end diastolic area) and in systole (end systolic area), as shown in Figure 5. The normal value of FAC in adults is greater than 35%; in neonates it can also vary with the days of life and with the body surface.[9] It can be obtained by the following equation:

$$\text{FAC} = \frac{\text{end diastolic area} - \text{end systolic area} \times 100}{\text{end diastolic area}}$$

There are other ways of assessing RV systolic function that will not be approached in this article.[6,7] The ones mentioned above are the most used in practice.

3. High pressure: Two bodies do not occupy the same space. Straightening of the interventricular septum (IVS)

RV pressure overload leads to rectification of the IVS at the end of ventricular systole, resulting in a change in LV configuration that goes from an "O" shape (normal) to a "crescent" shape (in severe PH) passing through the "D" shape, when visualized in the short axis parasternal view. The assessment of IVS offers indirect evidence of increased pressure in the right chambers and is especially important when it is impossible to obtain an objective estimate of pulmonary pressure (Figure 6). It is even possible to infer the relationship between pulmonary and systemic pressure according to the curvature of the IVS,[6] as seen in Table 1.

3.1. Eccentricity Index (EI)

The EI is derived from the ratio between the anteroposterior and septolateral diameters of the LV obtained in the parasternal short axis view at the level of the papillary muscle at the end of ventricular systole (Figure 7). EI > 1.3 is related to pulmonary pressure greater than half the systemic pressure, with good specificity.[11]

4. Pipes and connections: Impaired systemic venous return

It has been observed so far that PTNB with PH show an increase in RV DP_2, with a consequent increase in RA pressure and often show IVC dilation and reduced collapsibility. In this population, the evaluation of the dimensions of the IVC is done subjectively and collapsibility can be calculated using Equation 4:

Observou-se até aqui que o RNPT com HP apresenta aumento da PD_2 do VD, com consequente aumento da pressão do AD e frequentemente apresenta dilatação e redução de colapsabilidade da VCI. Nessa população, a avaliação das dimensões da VCI é feita de forma subjetiva e a colapsabilidade pode ser calculada pela Equação 4:

$$D_{max} - D_{min}/D_{max} \quad (4)$$

Where D_{max} is the maximum diameter of the IVC and D_{min} is the minimum diameter measured, as in Figure 1. This measurement is expressed as a percentage.[7] Another subjective indicator of increased pulmonary pressure that can be observed in the systemic venous return is the evident reverse flow in the hepatic veins (Figure 8). It is worth emphasizing that the increase in RA pressure can be due to several causes in addition to PH (hypervolemia, important tricuspid insufficiency, RV systolic or diastolic dysfunction, etc.), which highlights the importance of correlation with clinical data.

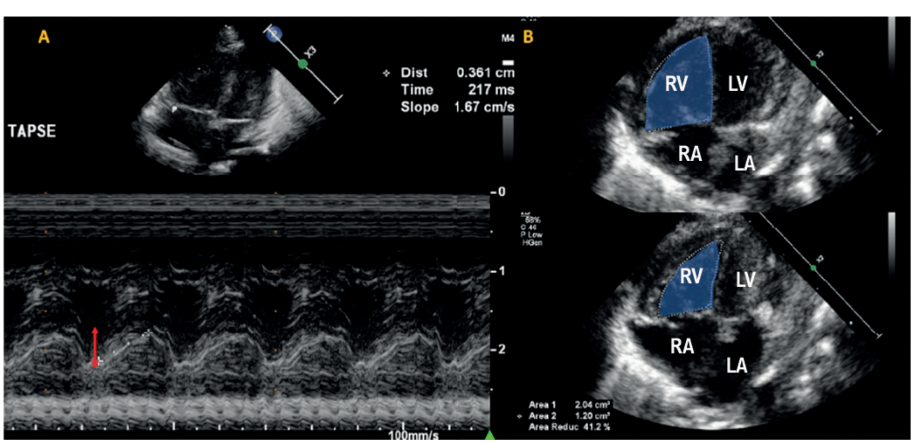

Figure 5 – *A: Apical 4-chamber view showing the M-mode of the RV free wall, the red arrow shows the tricuspid annular plane systolic excursion (TAPSE). B: RV fractional area change (FAC). RV: Right ventricle; LV: left ventricle; AD: Right atrium; LA: Left atrium.*

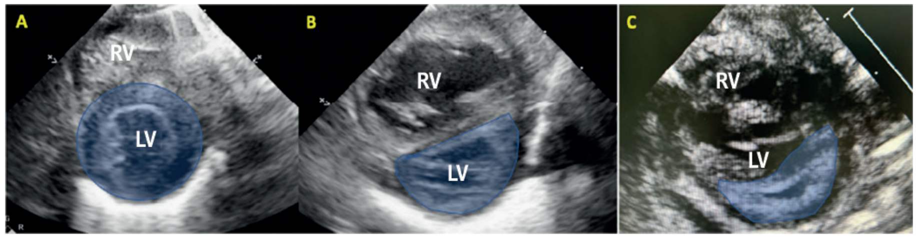

Figure 6 – *Echocardiogram on the short axis, showing the shape of the LV. A: "O" shape, estimate of RVP <50% of LVP; B: NB with pulmonary hypertension, "D" shape, estimate of RVP 50-100% of LVP; C: NB with diaphragmatic hernia and significant PH, "crescent" shape, estimated RVP > 100% of LVP. LV: left ventricle; RVP: Right ventricular pressure; LVP: Left ventricular pressure; NB: newborn; PH: Pulmonary hypertension.*

Table 1 – RVP estimate based on LV configuration

LV configuration	RVP estimate
"O" shape	<50% of LVP
"D" shape	50-100% of LVP
"crescent" shape	>100% of LVP

Modified from WP from Boode et al., 2018. RVP: Right ventricular pressure; LV: left ventricle; LVP: Left ventricular pressure.

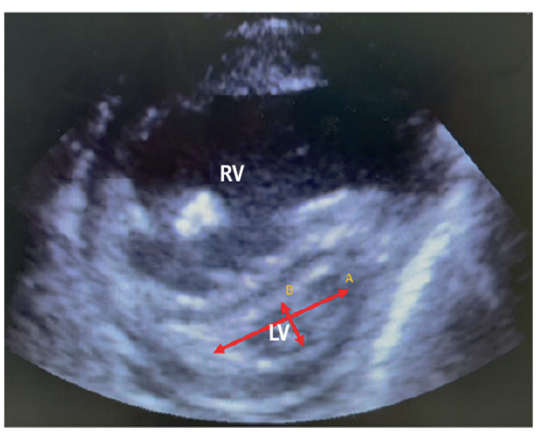

Figure 7 – *Echocardiogram in the parasternal short axis view at the level of the papillary muscle at the end of ventricular systole. EI= A/B. EI: Eccentricity index.*

5. Communications between the systemic and pulmonary bed: A problem or a relief?

In situations of normal pulmonary pressure, shunts such as the ASD and the PDA present flow directed from the left to the right chambers. Increased pressure in the right chambers causes flow from the AD to the left atrium (LA) through the ASD. The inversion of flow in the ductus arteriosus (DA) translates into important PH since the pulmonary pressure exceeds the systemic one. Pulmonary pressure can be estimated as discussed above. In cases of severe PH, the LV preload from the pulmonary venous return may be greatly reduced, the flow coming from the right side through the communications can help complement this preload and increase the systemic cardiac output.

Importance of assessing the DA in preterm infants

PDA is a common problem in the NICU and can have deleterious effects on both the severely ill full-term newborn and the PTNB.

A failure to close the DA associated with a drop in postpartum pulmonary vascular resistance results in a left-to-right shunt. Consequences may include pulmonary hyperflow and/or systemic hypoperfusion, both of which are associated with increased morbidity. Clinical impact depends on the magnitude of the flow, existing comorbidities and the ability of the neonate to initiate compensatory mechanisms. The increase in pulmonary flow and the accumulation of interstitial fluid secondary to the large patent ductus contribute to a decrease in lung compliance and an increase in LV DP_2, which can be more pronounced in preterm infants, since ventricular compliance is lower.

In PTNB, a hemodynamically significant channel is associated with an increased risk of pulmonary edema, pulmonary hemorrhage, bronchopulmonary dysplasia, and increased duration of pulmonary ventilation. Although the presence of a wide duct supports increased cardiac output, post-ductal blood flow is reduced due to the left-to-right shunt, resulting in reduced oxygen delivery and perfusion to vital organs, thus contributing to an increased risk of intra- and periventricular hemorrhage, necrotizing enterocolitis, renal injury, and hypotension.[12]

Clinical findings may develop earlier in those patients treated with surfactant because the reduction in pulmonary vascular resistance associated with improved lung function results in increased left-to-right shunting.

Surgical or pharmacological closure should be postponed in patients with severe PH due to the risk of right heart failure. The assessment of ventricular function should be performed using qualitative and quantitative methods in these cases, always comparing to previous exams, if available.

The quantification of the size of the left cardiac chambers reflects the chronic effect of the left ventricular volume

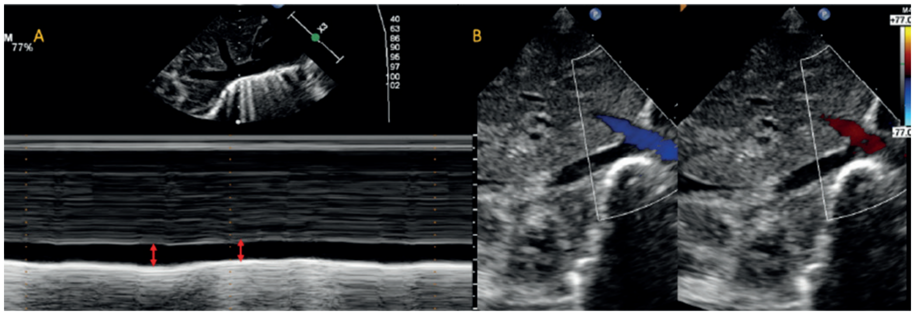

Figure 8 – *IVC M-mode, the red arrows show the respiratory variation of the IVC diameter; B: Color flow mapping of the hepatic vein showing forward (blue) and reverse (red) flow. IVC: Inferior vena cava.*

overload due to the left-right shunt through the duct and, therefore, is not an early parameter of hemodynamic repercussions.[13]

1. Anatomical assessment of the DA

The first echocardiographic assessment should always be comprehensive to exclude congenital heart defects. The following plans are used in DA assessment:

- On the parasternal short axis, the channel can be seen lateral to the left pulmonary branch and connecting to the descending thoracic aorta at the opposite end. With a slight inclination, it is possible to elongate the aorta and obtain a better image of the canal;
- In the high left parasternal short axis, also called the canal cut, it is possible to evaluate the entire path of the DA. This cut is obtained by placing the transducer in the left infraclavicular area, between the sternal notch and the conventional parasternal plane. This plane allows a more precise measurement of the size of the defect, normally acquired at its narrowest point, close to the left pulmonary artery (LPA). Prefer this measurement to the two-dimensional one, since the color Doppler tends to overestimate the DA size (Figure 9); and
- Suprasternal long-axis view angled toward the LPA allows a wide view of the DA.

The echocardiographer must provide information regarding the morphology, measurements of the diameters of the pulmonary and aortic extremities, total length and site of greatest canal narrowing, especially in cases that are candidates for percutaneous closure. An assertive determination of the diameter is extremely important in the sense of a probable hemodynamic impact, and a diameter ≤1.5 mm is associated with a risk of slight clinical repercussions, a diameter between 1.5 and 3.0 mm with moderate hemodynamic repercussions, and above 3.0 mm with significant repercussions.[14]

Krichenko et al.[15] described isolated PDA as seen by angiography in five main groups, using the site of canal narrowing as a reference:

- Group A or conical ductus: narrow pulmonary end and hourglass at the aortic end;
- Group B or window-type ductus: short and narrow channel in the aortic region, wide in the pulmonary region;
- Group C: comprises the tubular ductus without constriction at the aortic and pulmonary end;
- Group D or saccular: the ductus has a wide central region with aortic and pulmonary constriction;
- Group E: channel is elongated, with constriction at the lung end; and
- Group F (fetal): in premature neonates who do not fit any of the morphologies previously described, generally with wide and tortuous canals, without significant stenoses (Figure 10).

2. Doppler assessment of the canal: new paradigms

Color flow mapping improves visualization of the DA, especially small caliber ones (<1mm), and allows visualization of the site of greatest flow acceleration,

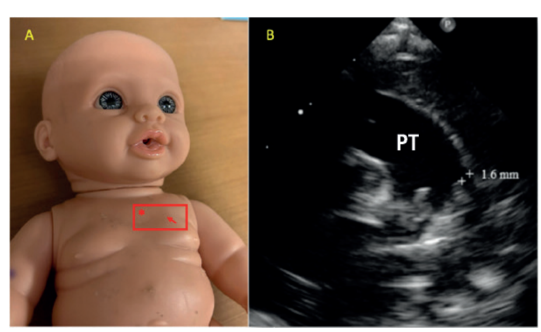

Figure 9 – *High left parasternal view. A: Representation on the dummy of the site of the upper left parasternal cut ("canal cut"). B: Echocardiogram in the upper left parasternal plane demonstrating the location of the ductus arteriosus measurement, as well as its relationship with the left pulmonary artery, pulmonary trunk, and aorta. PT: pulmonary trunk; PDA: patent ductus arteriosus; Ao: descending aorta.*

improving the positioning and alignment of the Doppler sample. Flow direction can be left-right, bidirectional or right-left, as seen in severe PH with suprasystemic pulmonary pressure and in heart diseases with DA-dependent systemic flow (Figure 11). Flow velocities below 1m/s should be recorded with pulsed Doppler. Continuous Doppler with the sample in the DA allows quantifying the pulmonary artery pressure using the modified Bernoulli equation. This measurement correlates with the instantaneous peak gradient between the aorta and the pulmonary artery by cardiac catheterization. Thus, by measuring the patient's systemic systolic pressure using conventional methods during the echocardiogram and subtracting it by the peak gradient obtained by continuous Doppler, it is possible to estimate the PASP. In the case of right-left flow, the pulmonary systolic pressure is estimated by adding the pressure gradient obtained by the Bernoulli equation to the systemic systolic pressure measured at the time of the test. If the Doppler flow pattern is bidirectional, with right-left flow occupying less than 30% of the cardiac cycle, the pulmonary pressure is probably lower than the systemic one. This bidirectional flow time measurement can also be obtained using the color M-mode in doubtful cases. Additional care must be taken with continuous Doppler flow contamination of structures adjacent to the canal, such as the LPA, aorta, and pulmonary systemic collaterals.

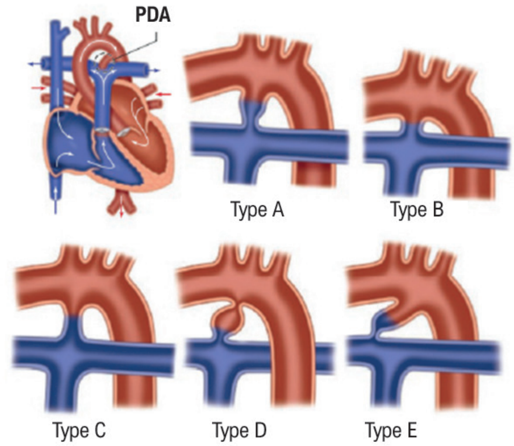

Figura 10 – *Classificação de Krichenco para canal arterial isolado Adaptado de: DeFaria Yeh, Doreen; Bhatt, Ami (2018). [*In Clinical Practice*]* Adult Congenital Heart Disease in Clinical Practice || Patent Ductus Arteriosus. *, (*Chapter 7*), 91–105. doi:10.1007/978-3-319-67420-9_7*

The appearance and speed of the Doppler curve also already give us important signals about the degree of flow restriction. In a small, restrictive DA without hemodynamic repercussions, the Doppler curve shows a high continuous flow velocity, both in systole and diastole, with a maximum

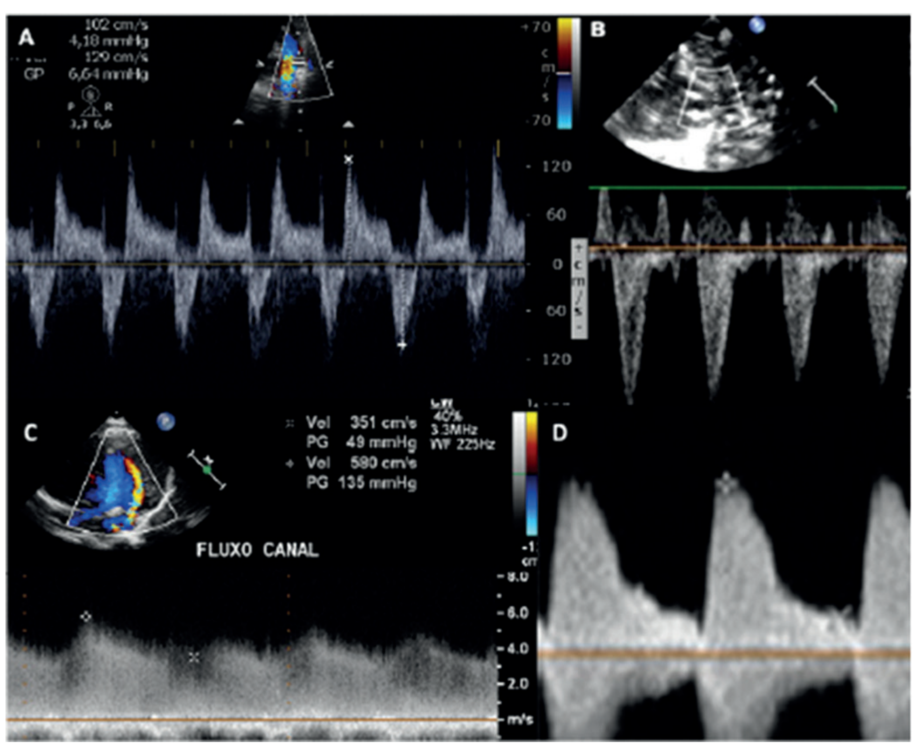

Figure 11 – *Doppler pattern of the ductus arteriosus. A: Bidirectional pulsatile flow through the ductus arteriosus. B: right-left pulsatile flow through the ductus arteriosus. C: Flow curve with a continuous left-right pattern with diastolic velocity greater than 50% of the systolic velocity, suggestive of a restrictive canal. D: Flow curve tending to pulsatile, with diastolic velocity < 50% of the systolic velocity.*

diastolic velocity greater than 2.0 m/s. Wide channels, without flow restriction, with important hemodynamic repercussions, present a flow curve tending more toward pulsatile flow, with a diastolic component with a velocity lower than 1.0 m/s and a wide difference in systolic and diastolic velocity. Channels with moderate hemodynamic repercussions have a pulsatile, non-restrictive flow model and maximum diastolic velocity lower than 2.0 m/s (Figure 11).

When analyzing the maximum velocity of the canal at the end of systole, it is possible to classify as a small canal those with velocity above 2.5m/s, moderate between 1.5 and 2.5m/s, and large with velocity below 1.5m /s.

It is important to differentiate the Doppler patterns of the pulmonary artery from the DA with a right-to-left shunt. The spectral Doppler of the pulmonary artery begins at the beginning of systole and reaches maximum amplitude quickly, while the flow from the DA with a right-to-left shunt begins at a later stage of systole and reaches maximum amplitude between mid- and late-systole.

In some cases, a characteristic serration on the pulsed Doppler curve of the pulmonary valve may be observed, raising the suspicion of a small DA not visualized previously on the exam (Figure 12).

The diastolic anterograde flow of the LPA has been considered a marker of pulmonary hyperflow in neonates. This measurement is obtained with the marker in the proximal third of the LPA. Some authors have demonstrated that a mean LPA velocity of 0.42m/s and/or an end-diastolic velocity of 0.2m/s are predictive of a Q_p/Q_s above 2, with high sensitivity and specificity (Figure 12-B).[16]

Evaluation of the E/A ratio on pulsed Doppler of the mitral valve may show signs of increased left heart filling pressure, with an E/A ratio greater than 1.5 in large ducts and an E/A ratio of 1 to 1.5 in moderate channels (Figure 13).

3. And does the Q_p/Q_s measurement really matter in preterm newborns?

In congenital heart diseases with increased pulmonary blood flow, it is common to use measures to compare pulmonary cardiac output with systemic output (Q_p/Q_s) to estimate the degree of the shunt. Echocardiography can estimate this relationship with good correlation with the data obtained during the hemodynamic study. In the DA, the calculation of Q_p/Q_s is performed differently from other congenital heart diseases such as ASD and ventricular septal defect. The flow through the pulmonary valve corresponds

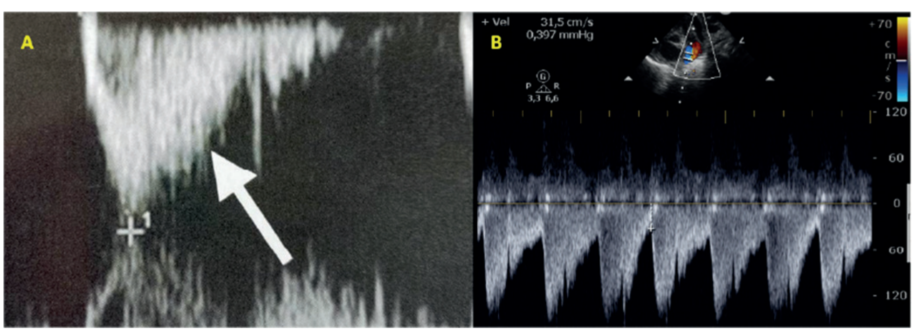

Figura 12 – *A: Pulsed Doppler of the pulmonary valve demonstrating a serration in the ascending part of the curve as shown by the arrow, suggestive of contamination of flow from the ductus arteriosus. B: Doppler flow pattern in the left pulmonary artery demonstrating an end-diastolic component with high velocity predictive of increased pulmonary hyperflow.*

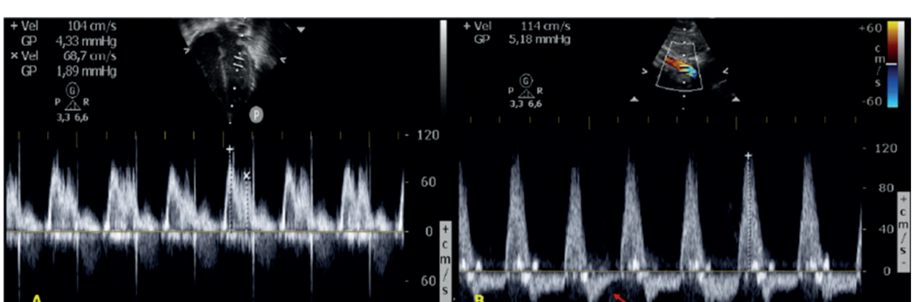

Figura 13 – *A: Doppler pattern of the mitral valve in the apical 4-chamber view demonstrating alteration in the E/A wave ratio in preterm newborns with wide ductus arteriosus. B: Doppler pattern of the descending abdominal aorta, arrow shows the presence of holodiastolic reverse flow.*

to the systemic flow (Q_s) and the flow through the aortic valve represents the effective pulmonary flow (sum of Q_s with the flow from the DA, causing overload of the left heart chambers). The presence of a PFO in the neonate, ASDs greater than 3mm, as well as alterations in the flow from the vena cava, can alter the estimation of the right ventricular output and, consequently, the systemic flow.[17]

4. Are signs of systemic flow steal easily assessed?

A large AC with significant left-to-right flow shunt will result in significant retrograde flow from the thoracic and abdominal aorta. The amount of retrograde diastolic flow can be >50% of the total aortic flow in neonates with a large AC, contributing to decreased systemic perfusion (renal, intestinal, and even coronary). Various indices based on pulmonary, aortic, and peripheral arterial flow velocity patterns have been proposed as objective methods for assessing the magnitude of ductal steal. The qualitative evaluation of the pulsed Doppler tracing of the descending aorta allows identifying the presence of reverse holodiastolic flow in the abdominal aorta and superior mesenteric artery, both evaluated in the subcostal or sagittal abdominal plane (Figure 13-B). The presence of holodiastolic reverse flow suggests moderate flow steal, which is associated with a Q_p/Q_s greater than 1.6, being one of the most specific signs of hemodynamic repercussion. Reverse flow in the abdominal aorta can occur in other congenital heart diseases that must be exhaustively investigated and ruled out.

5. DA assessment proposal based on a scorecard

A recent study by a group from Iowa[18] proposes a useful echocardiographic score to assess the hemodynamic repercussions of DA through signs of pulmonary hyperflow and systemic hypoflow. The score is obtained with the sum of the points of the variables listed in the table below, added to the canal diameter divided by the weight (Table 2). Treatment has been considered when score ≥ 6.

Soon after DA ligation, some PTNB become hemodynamically unstable due to acute changes in pre- and afterload, with oxygenation failure and systemic hypoperfusion, particularly in the first 8 to 12 hours after DA ligation. Thus, an early echocardiographic evaluation is necessary to optimize the treatment of these patients.

6. Does percutaneous treatment have its role?

More recently, several studies have reported experiences with the percutaneous closure technique, using various devices for closing the canal in PTNB. Comparison with surgical ligation revealed a positive impact on post-procedure pulmonary outcome. Currently, percutaneous closure of the DA in extremely low-weight premature patients weighing more than 700 grams is a safe procedure, with high efficacy, low complication rates, and is proven to be associated with improved prognosis in well-selected patients. TTE is the exam of choice both for selecting favorable cases and for guiding the procedure, thus reducing the amount of contrast used. Canals with a diameter < 4.0mm and length > 3.0mm are the most appropriate for the devices currently used.[19]

Table 2 – IOWA Score: echocardiographic evaluation of PDA severity

PDA IOWA SCORE	0	1	2
Mitral E velocity (cm/s)	< 45	45 - 80	> 80
IVRT (ms)	> 50	30 - 50	< 30
VD PV velocity	< 0.3	0.3 - 0.5	> 0.5
LA/Ao	< 1.3	1.3 - 2.2	> 2.2
LVEF:RVEF	≤ 1	1 - 1.7	> 1.7
Aorta/peripheral flow	Anterograde		Reverse

PDA: patent ductus arteriosus; IVRT: isovolumetric relaxation time; PV: pulmonary vein; LA: left atrium; Ao: aorta; LVEF: left ventricular ejection fraction; RVEF: right ventricular ejection fraction. Adapted from John M. Dagle, Matthew A. Rysavy, Stephen K. Hunter, Tarah T. Colaizy, Timothy G. Elgin, Regan E. Giesinger, Steve J. McElroy, Heidi M. Harmon, Jonathan M. Klein, Patrick J. McNamara, Cardiorespiratory management of infants born at 22 weeks' gestation: The Iowa approach, Seminars in Perinatology, Volume 46, Issue 1, 2022

New perspectives in assessing DA and PH in preterm newborns

More recent methods for assessing myocardial contractility were incorporated into the echocardiogram with the aim of assessing LV and RV function regardless of their geometry or ventricular filling.[20] One of these methods, speckle tracking (ST) by TTE, assesses myocardial fiber deformation during the cardiac cycle, allowing earlier diagnosis of myocardial dysfunction, before a drop in ejection fraction occurs. Levy et al.[21] demonstrated in a prospective study that it is possible to perform global longitudinal strain (GLS) of the RV using the ST method in PTNB patients with reliable reproducibility of right ventricular function and hemodynamic variations. Almeida et al.[22] confirmed that the analysis of myocardial deformation through the ST technique by TTE is feasible and reproducible in PTNB ≤ 34 weeks of gestational age. It was also shown that radial and circumferential strain and GLS measurements are significantly higher in PTNB with DA with hemodynamic repercussions, possibly as a means of compensating for the left ventricular volume overload imposed by the large duct.

Acknowledgments

To dear Dr. Adriana Mello and Dr. Gabriela Leal, who contributed by sharing experience and bibliography.

Author Contributions

Conception and design of the research: Sawamura KSS; acquisition of data, analysis and interpretation of the data, writing of the manuscript and critical revision of the manuscript for intellectual content: Sawamura KSS, Brito MM.

Potential Conflict of Interest

No potential conflict of interest relevant to this article was reported.

Review Article

Sources of Funding

There were no external funding sources for this study.

Study Association

This study is not associated with any thesis or dissertation work.

Ethics Approval and Consent to Participate

This article does not contain any studies with human participants or animals performed by any of the authors.

References

1. Chawanpaiboon S, Vogel JP, Moller AB, Lumbiganon P, Petzold M, Hogan D, et al. Global, Regional, and National Estimates of Levels of Preterm Birth in 2014: A Systematic Review and Modelling Analysis. Lancet Glob Health. 2019;7(1):e37-e46. doi: 10.1016/S2214-109X(18)30451-0.
2. Youssef L, Castellani R, Valenzuela-Alcaraz B, Sepulveda-Martinez Á, Crovetto F, Crispi F. Cardiac Remodeling from the Fetus to Adulthood. J Clin Ultrasound. 2023;51(2):249-64. doi: 10.1002/jcu.23336.
3. Mertens L, Seri I, Marek J, Arlettaz R, Barker P, McNamara P, et al. Targeted Neonatal Echocardiography in the Neonatal Intensive Care Unit: Practice Guidelines and Recommendations for Training: Eur J Echocardiogr. 2011;12(10):715-36. doi: 10.1093/ejechocard/jer181.
4. Alvira CM, Morty RE. Can We Understand the Pathobiology of Bronchopulmonary Dysplasia? J Pediatr. 2017;190:27-37. doi: 10.1016/j.jpeds.2017.08.041.
5. Heuchan AM, Clyman RI. Managing the Patent Ductus Arteriosus: Current Treatment Options. Arch Dis Child Fetal Neonatal Ed. 2014;99(5):F431-6. doi: 10.1136/archdischild-2014-306176.
6. Boode WP, Singh Y, Molnar Z, Schubert U, Savoia M, Sehgal A, et al. Application of Neonatologist Performed Echocardiography in the Assessment and Management of Persistent Pulmonary Hypertension of the Newborn. Pediatr Res. 2018;84(Suppl 1):68-77. doi: 10.1038/s41390-018-0082-0.
7. Sawamura KSS, Lianza AC, Leal GN, Morhy SS. Echocardiographic Evaluation of Pulmonary Hypertension in Children. Arq Bras Cardiol - Imagem Cardiovasc. 2019;32(4). doi:10.5935/2318-8219.20190049.
8. Koestenberger M, Grangl G, Avian A, Gamillscheg A, Grillitsch M, Cvirn G, et al. Normal Reference Values and z Scores of the Pulmonary Artery Acceleration Time in Children and Its Importance for the Assessment of Pulmonary Hypertension. Circ Cardiovasc Imaging. 2017;10(1):e005336. doi: 10.1161/CIRCIMAGING.116.005336.
9. Jain A, Mohamed A, El-Khuffash A, Connelly KA, Dallaire F, Jankov RP, et al. A Comprehensive Echocardiographic Protocol for Assessing Neonatal Right Ventricular Dimensions and Function in the Transitional Period: Normative Data And Z Scores. J Am Soc Echocardiogr. 2014;27(12):1293-304. doi: 10.1016/j.echo.2014.08.018.
10. Sato T, Tsujino I, Ohira H, Oyama-Manabe N, Yamada A, Ito YM, et al. Validation Study on the Accuracy of Echocardiographic Measurements of Right Ventricular Systolic Function in Pulmonary Hypertension. J Am Soc Echocardiogr. 2012;25(3):280-6. doi: 10.1016/j.echo.2011.12.012.
11. Abraham S, Weismann CG. Left Ventricular End-Systolic Eccentricity Index for Assessment of Pulmonary Hypertension in Infants. Echocardiography. 2016;33(6):910-5. doi: 10.1111/echo.13171.
12. Santos AMR, Meira ZMA, Pereira MCN. Echocardiography Role in Assessing Cardiovascular Changes in Very Low Birth Weight Babies, with Emphasis on the Presence of the Ductus Arteriosus. Arq Bras Cardiol - Imagem Cardiovasc. 2016;29(2):47-57. doi: 10.5935/2318-8219.20160014.
13. Stefano JL, Abbasi S, Pearlman SA, Spear ML, Esterly KL, Bhutani VK. Closure of the Ductus Arteriosus with Indomethacin in Ventilated Neonates with Respiratory Distress Syndrome. Effects of Pulmonary Compliance and Ventilation. Am Rev Respir Dis. 1991;143(2):236-9. doi: 10.1164/ajrccm/143.2.236.
14. El-Khuffash AF, McNamara PJ, Noori S. Diagnosis, Evaluation, and Monitoring of Patent Ductus Arteriosus in the Very Preterm Infant. In: Seri I, editor. Hemodynamics and Cardiology: Neonatology Questions and Controversies. New York: Elsevier; 2019. p. 387-410.
15. Krichenko A, Benson LN, Burrows P, Möes CA, McLaughlin P, Freedom RM. Angiographic Classification of the Isolated, Persistently Patent Ductus Arteriosus and Implications for Percutaneous Catheter Occlusion. Am J Cardiol. 1989;63(12):877-80. doi: 10.1016/0002-9149(89)90064-7.
16. El Hajjar M, Vaksmann G, Rakza T, Kongolo G, Storme L. Severity of the Ductal Shunt: A Comparison of Different Markers. Arch Dis Child Fetal Neonatal Ed. 2005;90(5):F419-22. doi: 10.1136/adc.2003.027698.
17. Sanders SP, Yeager S, Williams RG. Measurement of Systemic and Pulmonary Blood Flow and QP/QS Ratio Using Doppler and Two-Dimensional Echocardiography. Am J Cardiol. 1983;51(6):952-6. doi: 10.1016/s0002-9149(83)80172-6.
18. Dagle JM, Rysavy MA, Hunter SK, Colaizy TT, Elgin TG, Giesinger RE, et al. Cardiorespiratory Management of Infants Born at 22 Weeks' Gestation: The Iowa Approach. Semin Perinatol. 2022;46(1):151545. doi: 10.1016/j.semperi.2021.151545.
19. Manica JLL, Neves JR, Arrieta R, Abujamra P, Rossi RI Filho, Giuliano LC, et al. Percutaneous Closure of Ductus Arteriosus in Preterm Babies: The Initial Brazilian Experience. Arq Bras Cardiol. 2022;119(3):460-7. doi: 10.36660/abc.20210818.
20. Di Maria MV, Younoszai AK, Sontag MK, Miller JI, Poindexter BB, Ingram DA, et al. Maturational Changes in Diastolic Longitudinal Myocardial Velocity in Preterm Infants. J Am Soc Echocardiogr. 2015;28(9):1045-52. doi: 10.1016/j.echo.2015.04.016.
21. Levy PT, Dioneda B, Holland MR, Sekarski TJ, Lee CK, Mathur A, et al. Right Ventricular Function in Preterm and Term Neonates: Reference Values for Right Ventricle Areas and Fractional Area of Change. J Am Soc Echocardiogr. 2015;28(5):559-69. doi: 10.1016/j.echo.2015.01.024.
22. Almeida KFS, Leal GN, Morhy SS, Rodrigues ACT, Cerri GG, Doria-Filho U, et al. Influence of Patent Ductus Arteriosus on Left Ventricular Myocardial Deformation in Preterm Neonates in the Early Neonatal Period. Early Hum Dev. 2020;147:105093. doi: 10.1016/j.earlhumdev.2020.105093.

Review Article

My Approach To Nuclear Medicine in the Evaluation of Prosthetic Valve and Cardiac Implantable Electronic Device Endocarditis

Claudio Tinoco Mesquita,[1,2,3,4] Maria Fernanda Rezende,[3] Davi Shunji Yahiro,[1] Isabella Caterina Palazzo[3,4]
Universidade Federal Fluminense,[1] Niterói, RJ – Brazil
Academia de Medicina do Estado do Rio de Janeiro (ACAMERJ),[2] Niterói, RJ – Brazil
Hospital Vitória da Barra da Tijuca,[3] Rio de Janeiro, RJ – Brazil
Hospital Pró-Cardíaco,[4] Rio de Janeiro, RJ – Brazil

Summary

Nuclear medicine has played an increasing role in the evaluation of patients with a suspected or confirmed diagnosis of infective endocarditis. Scintigraphy with marked leukocytes (ML) is a method widely used in clinical practice to detect sites of infection, being especially indicated in patients with suspected infective endocarditis (IE) in prosthetic valves or implantable cardiac devices (ICD) when other conventional imaging methods studies are not conclusive. The technique involves labeling the patient's own leukocytes with a radiotracer, such as 99m Tc-HMPAO, maintaining its biological properties. Upon injection into the bloodstream, leukocytes actively mark sites of active inflammation, allowing detection of infection.

Blood collection for ML scintigraphy requires a sufficient amount of leukocytes, which can be a major limiting factor in patients with neutropenia. Another point of limitation is that the leukocyte labeling process and the start of obtaining scintigraphic images can take about 2 hours. The images are acquired at different times, and the presence of capture in the 4-hour and 24-hour images is important to confirm the presence of active infection.

ML scintigraphy has been recommended as part of the diagnostic algorithm for IE in patients with prosthetic valves or implantable cardiac devices such as pacemakers who suspect the disease, being considered a major modified Duke criterion when positive. It is indicated when the echocardiogram is inconclusive or doubtful, and may change the categorization of IE from possible to defined in up to 25% of patients. In addition, it can also be used in the investigation of embolic events in extracardiac sites, such as the lung, spleen and bone/joint tissue.

Positron Emission Tomography coupled with Computed Tomography (PET-CT) is a molecular imaging technique that has shown great importance in the management of IE. PET-CT uses a radiopharmaceutical labeled with a short-lived radioactive substance, such as 18F-fluordeoxyglucose (18F-FDG), which is captured by cells with high metabolism, such as inflammatory cells present in areas of active infection. This allows for accurate, non-invasive detection of areas of inflammation, including the lesions, vegetations and abscesses associated with IE.

The use of PET-CT in IE has shown promise in the early detection of infection, providing important information for diagnosis and treatment planning. Additionally, PET-CT can help differentiate between active infection and post-surgical complications, as well as identify areas of infection in extracardiac sites, which can be useful in evaluating more complex cases. The high sensitivity and specificity of PET-CT in detecting active inflammation make it a valuable tool in the clinical management of IE, especially in cases of moderate clinical suspicion or when conventional imaging methods are inconclusive. However, it is important to consider the limitations of PET-CT, such as its availability in some health centers, cost and exposure to ionizing radiation, and to use PET-CT findings in conjunction with other clinical and laboratory data for an proper diagnosis and management of IE.

Keywords

Endocarditis; Valve Prostheses and Implantable Electronic Heart Devices; PET-CT; Scintigraphy; Echocardiography

Mailing Address: Claudio Tinoco Mesquita •
Hospital Universitário Antônio Pedro, Rua Marques do Paraná, 303. Postal Code 324330-900. Centro, Niterói, RJ – Brazil
E-mail: claudiotinocomesquita@gmail.com
Manuscript received February 23, 2023; revised manuscript March 2, 2023; accepted March 2, 2023
Editor responsible for the review: Daniela do Carmo Rassi Frota

DOI: https://doi.org/10.36660/abcimg.20230018i

Introduction

The incidence of infective endocarditis (IE) has been increasing. It is estimated to be 3-15 cases per 100,000 inhabitants per year and associated with elevated morbidity and mortality. The most common cause of IE is Staphylococcus aureus infection, affecting mostly male and older individuals. In the United States and Europe, 16-30% of all cases of IC are prosthetic valve (PV) endocarditis, and 25-35% of native valve endocarditis are acquired in the hospital. In Brazil, rheumatic valve disease is still an important predisposing factor for infection, in contrast with developed countries where rheumatic disease has become rare.[1]

Difficulty in raising clinical suspicion and confirming the diagnosis of IE are among the greatest challenges faced by cardiologists in their clinical practice. Although the use of clinical rules such as the Duke criteria increases the success of IE diagnosis and its clinical management, the presence of infection by atypical organisms, PVs or cardiac implantable electronic devices (CIEDs) can make the diagnosis of IE difficult.[1,2]

Risk factors for IE

The major risk factors for IE are congenital heart disease (CHD), previous episode of IE, and the presence of PV or

CIED.[1] Regarding CHDs, the incidence of post-surgical IE varies from 1.3 to 13.3%, in addition to the high risk of mortality for CHDs, estimated at 6-14%.[3] Recurrence or reinfection occurs in 2.6-8.8% of patients who survived IE, with high rates of complications and mortality.[1]

Epidemiology of IE in patients with PVs

Patients with PVs are at higher risk of IE in the first year after valve replacement, and the risk gradually decreases to a low and stable risk. Bioprosthetic valves are associated with a higher risk of IE as compared with mechanical valves. Besides, the risk of transcatheter aortic valve implantation (TAVI) for IE seems not to differ from that found in conventional surgery, with an incidence of 1.4-2.8 per 100 patient-years in the first year and 0.8 in each of the four following years.[2-4]

CIED-related IE corresponds to nearly 10% of the IE episodes.[1] In these cases, in-hospital mortality varies from six to 14%, with an overall mortality of approximately 20% a year.[5] PV endocarditis is a severe, life-threatening condition, accounting for 10-30% of all cases of IE, with an incidence of 0.3-1.2% per patient-year. Patients with PVs are considered to be at high risk for IE, with higher morbidity and mortality, often requiring surgical interventions, with associated risks.

Challenges in the management of IE in PVs and CIEDs

Echocardiography and laboratory tests are still the basis of diagnostic investigation of IE. However, conventional imaging techniques still yield inconclusive results in up to 40% of patients with PVs or CIEDs.[6] Transesophageal echocardiography (TEE) should be considered in all suspected cases of PV endocarditis for assessment of valve hemodynamics, and detection of vegetations, abscesses or fistulas. Detection of vegetation may be extremely difficult due to artifacts related to the material used in the PVs. Sensitivity of TEE in detecting IE in PVs varies from 82% to 96%, in contrast to transthoracic echocardiogram that has a sensitivity of 17-36%.[6] In case of suspicion of CIED endocarditis, echocardiography is the first test to be considered for detection of vegetations in the electrodes and cardiac valves, with TEE being superior to transthoracic echocardiography. Both techniques, however, have similar limitations for the detection of IE, be it for the size and location of vegetations, be it for the presence of foreign material to the body limits the visibility of echocardiogram. It is important to highlight that a normal echocardiogram does not rule out the diagnosis of IE in patients with CIEDs and clinical suspicion of IE.[7]

In light of the increasing number of cases of IE, its high morbidity and mortality, and diagnostic limitations of conventional techniques, studies investigating the usefulness of nuclear imaging techniques, including the 18F-fluorodeoxyglucose positron emission tomography/computed tomography (18F-FDG PET-CT) for in diagnosis of IE have been conducted. These techniques showed good cost-effectiveness relationship, preventing prolonged hospitalizations and unnecessary studies, and improving patient clinical outcomes. The set of studies in the literature, including meta-analysis and systematic reviews have demonstrated the clinical impact of 18F-FDG PET/CT, supporting its inclusion in the European guidelines on the investigation of PV endocarditis since 2015[1] and in the North American guidelines since 2020.[8] In addition to PET-CT, another useful alternative is labeled leukocyte scintigraphy (LLS), currently the gold-standard method in the investigation of infections of prosthetic orthopedic implants. The method is also specific for IE, and useful in confirming the diagnosis in case of possible false-positive PET-CT results, as in the first months after surgery.[1,9-11]

How to use PET-CT in IE

The main use of PET-CT in the management of IE is in patients with suspicion of PV or CIED endocarditis, whose results from transthoracic or transesophageal echocardiogram were inconclusive or negative. In 18F-FDG PET/CT, FDG uptake occurs in areas of increased metabolic activity, since 18-fluorine is intensively captured by inflammatory cells. Thus, accumulation of the marker around the PV or in perivalvular cardiac tissues is a powerful indicator of active infection. Besides, whole-body 18F-FDG PET-CT allows the detection of infectious complications of endocarditis, such as splenic embolization, embolism to the lower extremities, spondylodiscitis, or even the portal entry in case of infection of soft tissues or the oral cavity.

The study supporting the inclusion of PET-CT in the European Society of Cardiology guidelines was the study by Saby et al.[12] The authors prospectively studied 72 consecutive patients with PV endocarditis, who were subjected to clinical, microbiological, and echocardiographic evaluation. Thirty-six patients (50%) exhibited abnormal FDG uptake around the site of the PV. The sensitivity, specificity, positive predictive value, negative predictive value, and global accuracy were as follows (95% confidence interval): 73% (54% to 87%), 80% (56% to 93%), 85% (64% to 95%), 67% (45% to 84%), and 76% (63% to 86%), respectively. Adding abnormal FDG uptake around the PV significantly increased the sensitivity of the modified Duke criteria at admission (70% [52% to 83%] vs. 97% [83% to 99%] and became a new major criterion for IE diagnosis. This study was crucial in demonstrating the usefulness of 18F-FDG PET-CT in diagnosing IE in patients with PV.[12] In 2015, the ESC included the 18F-FDG PET-CT in the algorithm for the detection of VP endocarditis as a major diagnostic criterion (Figure 1). PET CT should be carried out in patients whose modified Duke criteria are inconclusive (possible or rejected IE, in the presence of high clinical suspicion), two months after cardiac surgery, due to the risk of false-positive results related to scarring inflammatory process. At this point, the exam of choice is 18F-FDG PET-CT with labeled leukocytes.[1] In Figure 2, we illustrate the use of 18F-FDG PET-CT in a patient with suspected IE and persistently negative echocardiography despite positive blood cultures. PET-CT clearly demonstrated abnormal glycolytic metabolism in the aortic prosthesis that was subcutaneously implanted on a valve-tube graft (valve-in-valve), compatible with IE.

It is worth noting that PET CT has also been indicated for patients with suspected IE in native valves and even for patients with confirmed IE, for localization of both local (e.g. cardiac abscesses) and distal (e.g. septic embolism) complications. This has been compiled in the literature by systematic

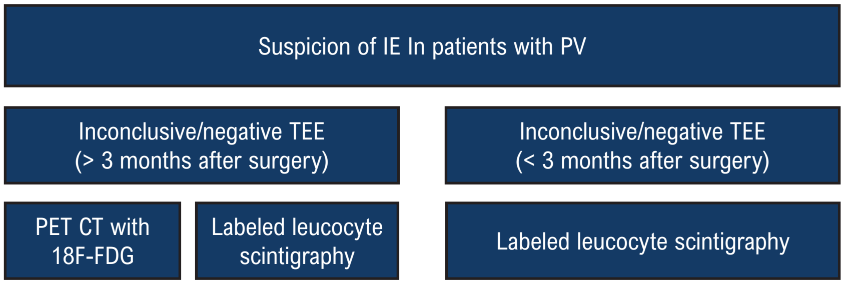

Figure 1 – *Patients with suspected PV endocarditis benefit from the use of nuclear medicine after echocardiographic investigation, particularly TEE (adapted from Habib et al.1). IE: infective endocarditis; TEE: transesophageal echocardiography, 18F-FDG PET-CT: 18F-fluorodeoxyglucose positron emission tomography/computed tomography; PV: prosthetic valve*

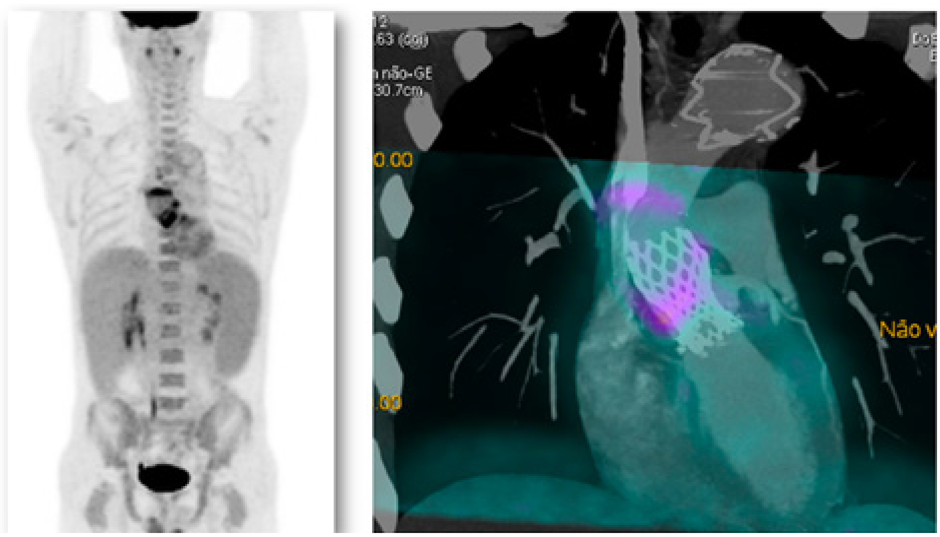

Figura 2 - *PET CT with 18F-FDG showing tracer uptake around valve endoprosthesis (valve-in-valve transcatheter aortic valve replacement) in a patient with positive blood cultures for streptococcus and persistently negative transesophageal echocardiograph; positive PET CT scan for IE*

reviews and meta-analyses, and been recommended by guidelines, including the updated Brazilian guideline on nuclear cardiology, updated in 2020.[13] The use of PET-CT in the assessment of cardiac inflammation is one of the branches of nuclear medicine in precision medicine, not only in IE but also in the evaluation of myocarditis, particularly cardiac sarcoidosis, and pericardial inflammation.[14]

When to use LLS in the management of IE in PVs and CIEDs

LLS has been widely used to detect infection sites and applied in clinical practice for decades. Today, its use is recommended in patients with suspected IE, particularly in those with PVs or CIEDs, with negative results from conventional imaging methods but still with moderate/high suspicion of IE. In LLS, patient blood is aseptically prepared for labeling of leukocytes with a radiotracer, such as the ^{99m}Tc-hexamethylpropyleneamine oxime (HMPAO). The leukocytes are then radiolabeled, without losing their biological properties of chemotaxis and diapedesis, *i.e.*, they can actively accumulate in active inflammation sites after being injected into the circulation.

In this method, a sufficient number of leukocytes is required; 50mL of blood is collected from the patient, and for neutropenic individuals ($<2x10^3$ neutrophils/mm^3), an additional sample of blood may be required. Thus, the presence of neutropenia may be a limitation for the test. Also, LLS takes longer than 18F-FDG PET/CT, due to the whole process of labeling of leukocytes, and plasma and leukocyte isolation, which may take approximately two hours. For IE investigation, scintigraphic images are acquired at four and 24 hours after injection. This is important, since the scintigraphic criteria for detecting active infection is the presence of radiolabeled leukocyte uptake at four hours and an increase of the uptake at 24 hours. If radiolabeled leukocyte uptake is detected at four hours but not at 24 hours, the scans are classified as negative.[2] The type of scintigraphic imaging is also important. In addition to the conventional whole-body and static images of the region of interest (*i.e.*, the chest), single photon emission computerized tomography (SPECT) images are also indispensable in the investigation of endocarditis. Hybrid CT/scintigraphy devices allow acquisition of SPECT-CT images, which are more sensitive and specific than conventional scintigraphy and important in the diagnosis of IE (Figure 3).

99mTc-HMPAO-labeled leukocytes has several indications, including in IE investigation. In 2015, the method was formally included in the ESC guidelines in the diagnostic algorithm of IE in patients with PV or CIED and suspected IE, as a major modified Duke criterion.[1] According to the guidelines, ^{99m}Tc-HMPAO-labeled leukocytes is indicated for patients with suspected IE, when echocardiographic findings are inconclusive or doubtful, as it can change patient classification from possible IE (by the Duke criteria) to definite IE in up to 25% of cases. The method is also indicated for detection of embolic events in extracardiac sites. Scintigraphic findings of embolic disease/metastatic infection in the lungs, spleen, bone and articular tissue.[6] For the investigation of PV endocarditis, scintigraphy combined with ^{99}mTc-HMPAO-labeled leukocyte SPECT-CT has a sensitivity of 86% and specificity of 97%.[15] Sensitivity of this method can reach 100% with the presence of perivalvular abscess.[5] For CIED-associated IE, scintigraphy with ^{99}mTc-HMPAO-labeled leukocyte SPECT-CT had 94% sensitivity, 100% specificity, 100% positive predictive value and 94% negative predictive value.[16] Besides, in these cases, the method helps to describe the extension of the infection, and whether it was specific to the generator or if the cables were involved. Patients with positive scintigraphy have higher risk of in-hospital mortality and complications.[8] The literature recommends 18F-FDG PET-CT as the first line imaging modality due to its higher sensitivity compared with scintigraphy. Scintigraphy has higher specificity and is particularly useful for patients with a history of recent surgery (within the last two months) due to higher chance of false-positive 18F-FDG PET-CT.[17]

One of the greatest advantages of LLS is its high specificity for IE related to PV or devices, especially when compared with 18F-FDG PET-CT, and the earlier screening for IE in patients with recent surgery compared with PET-CT. Also, as compared with 18F-FDG PET-CT, there is no need for a special diet or fasting. Another advantage is the test is covered by the Brazilian national agency for supplementary health, which is not true for PET-CT.

Limitations for LLS in clinical practice include manipulation of patient's blood, the minimum volume of blood required for labeling, equipment (laminar flow cabinet and centrifuge) for leukocyte labeling). While in LLS, images should be obtained at two time points (four and 24 hours), in 18F-FDG PET-CT, 60- minute image acquisition was performed. Other clinical situations that may limit the use of LLS and its sensitivity are neutropenia, use of antibiotics or steroids, type of pathogens (higher sensitivity for neutrophil-mediated infections) and small vegetations (<6mm).[6]

Finally, similar to PET-CT, LLS uses ionizing radiation, which, *per se*, is contraindicated in pregnancy. Lactating women should be instructed to discontinue breastfeeding for 24 hours mainly due to exposure of the infants to radiation while on their laps.

Comparison of 18F-FDG PET CT *versus* LLS

How to choose a nuclear imaging technique when both 18F-FDG PET CT and LLS are available? Referral centers for patients with suspected IE should have both techniques available; the methods are complementary, especially in highly complex cases and recent surgeries. The decision on which method to use should be individualized for each patient. Factors like technical characteristics, costs and availability of the methods, expertise of the group, and patient severity should be considered. In general, 18F-FDG PET CT is the method of choice in the literature, considering its wide availability in first-world countries, where the factor "cost" is less relevant in light of such a lethal disease as IE.[18] What makes FDG PET CT scintigraphy the method of choice is its operational characteristics. Rouzet et al.[19] compared the performance of 18F-FDG PET and LLS in patients with PVs and showed that the former offers high sensitivity for the detection of active infection in patients with suspected

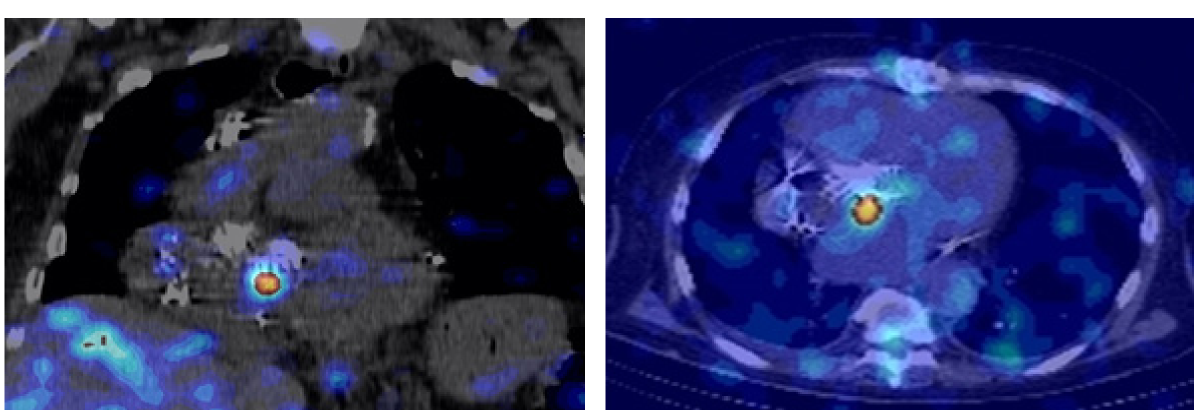

Figure 3 – *99mTc- HMPAO-labeled leukocyte scintigraphy with SPECT/CT in coronal (a) and axial (B) planes, with focal uptake in percutaneously inserted aortic valve prosthesis*

PV endocarditis and inconclusive echocardiography.[19] However, LLS offered a higher specificity than for diagnosis of IE and should, mainly in the first two months after cardiac surgery. A direct comparison of nuclear imaging techniques in patients with CIEDs was conducted by Calais et al.,[20] who compared 18F-FDG PET CT with LLS. Forty-eight patients underwent both 18F-FDG PET CT and LLS. The diagnostic sensitivity, specificity, positive predictive value, and negative predictive value were respectively 80%, 91%, 80%, and 91% for 18F-FDG PET CT and 60%, 100%, 100%, and 85% for LLS. Although PET-CT was more sensitive than LLS, the latter showed higher specificity.[20]

Conclusions

Nuclear medicine has become part of the diagnostic investigation of IE in patients with PVs or CIEDs. 18F-FDG PET CT has high sensitivity for detecting active infection when echocardiographic findings are inconclusive or negative. LLS is more specific than18F-FDG PET CT for the diagnosis of IE and should be considered in cases of doubtful or suspected false-positive 18F-FDG PET CT or in the first two months after cardiac surgery.

Author Contributions

Conception and design of the research: Mesquita CT, Rezende MF; writing of the manuscript and critical revision of the manuscript for intellectual content: Mesquita CT, Rezende MF, Yahir DS, Palazzo IC.

Potential Conflict of Interest

No potential conflict of interest relevant to this article was reported.

Sources of Funding

This study was funded by CNPq.

Study Association

This study is not associated with any thesis or dissertation work.

Ethics Approval and Consent to Participate

This article does not contain any studies with human participants or animals performed by any of the authors.

References

1. Habib G, Lancellotti P, Antunes MJ, Bongiorni MG, Casalta JP, Del Zotti F, et al. 2015 ESC Guidelines for the Management of Infective Endocarditis: The Task Force for the Management of Infective Endocarditis of the European Society of Cardiology (ESC). Endorsed by: European Association for Cardio-Thoracic Surgery (EACTS), the European Association of Nuclear Medicine (EANM). Eur Heart J. 2015;36(44):3075-128. doi: 10.1093/eurheartj/ehv319.
2. Sousa C, Pinto FJ. Infective Endocarditis: Still More Challenges Than Convictions. Arq Bras Cardiol. 2022;118(5):976-88. doi: 10.36660/abc.20200798.
3. Moore B, Cao J, Kotchetkova I, Celermajer DS. Incidence, Predictors and Outcomes of Infective Endocarditis in a Contemporary Adult Congenital Heart Disease Population. Int J Cardiol. 2017;249:161-5. doi: 10.1016/j.ijcard.2017.08.035.
4. Ando T, Ashraf S, Villablanca PA, Telila TA, Takagi H, Grines CL, et al. Meta-Analysis Comparing the Incidence of Infective Endocarditis Following Transcatheter Aortic Valve Implantation Versus Surgical Aortic Valve Replacement. Am J Cardiol. 2019;123(5):827-32. doi: 10.1016/j.amjcard.2018.11.031.
5. Maciel AS, Silva RMFLD. Clinical Profile and Outcome of Patients with Cardiac Implantable Electronic Device-Related Infection. Arq Bras Cardiol. 2021;116(6):1080-8. doi: 10.36660/abc.20190546.
6. Ivanovic B, Trifunovic D, Matic S, Petrovic J, Sacic D, Tadic M. Prosthetic Valve Endocarditis - A Trouble or a Challenge? J Cardiol. 2019;73(2):126-33. doi: 10.1016/j.jjcc.2018.08.007.
7. Blomström-Lundqvist C, Traykov V, Erba PA, Burri H, Nielsen JC, Bongiorni MG, et al. European Heart Rhythm Association (EHRA) International Consensus Document on How to Prevent, Diagnose, and Treat Cardiac Implantable Electronic Device Infections-Endorsed by the Heart Rhythm Society (HRS), the Asia Pacific Heart Rhythm Society (APHRS), the Latin American Heart Rhythm Society (LAHRS), International Society for Cardiovascular Infectious Diseases (ISCVID), and the European Society of Clinical Microbiology and Infectious Diseases (ESCMID) in collaboration with the European Association for Cardio-Thoracic Surgery (EACTS). Eur Heart J. 2020;41(21):2012-32. doi: 10.1093/eurheartj/ehaa010.
8. Otto CM, Nishimura RA, Bonow RO, Carabello BA, Erwin JP 3rd, Gentile F, et al. 2020 ACC/AHA Guideline for the Management of Patients with Valvular Heart Disease: A Report of the American College of Cardiology/American Heart Association Joint Committee on Clinical Practice Guidelines. J Thorac Cardiovasc Surg. 2021;162(2):e183-e353. doi: 10.1016/j.jtcvs.2021.04.002.
9. Vries EF, Roca M, Jamar F, Israel O, Signore A. Guidelines for the Labelling of Leucocytes with (99m)Tc-HMPAO. Inflammation/Infection Taskgroup of the European Association of Nuclear Medicine. Eur J Nucl Med Mol Imaging. 2010;37(4):842-8. doi: 10.1007/s00259-010-1394-4.
10. Kooshki N, Grambow-Velilla J, Mahida B, Benali K, Nguyen C, Cimadevilla C, et al. Diagnostic Performance of White Blood Cell SPECT Imaging Against Intra-Operative Findings in Patients with a Suspicion of Prosthetic Valve Endocarditis. J Nucl Cardiol. 2022;29(2):528-34. doi: 10.1007/s12350-021-02674-y.
11. Erba PA, Sollini M, Conti U, Bandera F, Tascini C, De Tommasi SM, et al. Radiolabeled WBC Scintigraphy in the Diagnostic Workup of Patients with Suspected Device-Related Infections. JACC Cardiovasc Imaging. 2013;6(10):1075-86. doi: 10.1016/j.jcmg.2013.08.001.
12. Saby L, Laas O, Habib G, Cammilleri S, Mancini J, Tessonnier L, et al. Positron Emission Tomography/Computed Tomography for Diagnosis of Prosthetic Valve Endocarditis: Increased Valvular 18f-Fluorodeoxyglucose Uptake as a Novel Major Criterion. J Am Coll Cardiol. 2013;61(23):2374-82. doi: 10.1016/j.jacc.2013.01.092.
13. Mastrocola LE, Amorim BJ, Vitola JV, Brandão SCS, Grossman GB, Lima RSL, et al. Update of the Brazilian Guideline on Nuclear Cardiology - 2020. Arq Bras Cardiol. 2020;114(2):325-429. doi: 10.36660/abc.20200087.
14. Mesquita CT, Ker WDS, Azevedo JC. Nuclear Cardiology in 2020 - Perspectives of the New SBC Guideline. Arq Bras Cardiol. 2020;114(2):196-8. doi: 10.36660/abc.20190874.
15. Kooshki N, Grambow-Velilla J, Mahida B, Benali K, Nguyen C, Cimadevilla C, et al. Diagnostic Performance of White Blood Cell SPECT Imaging Against Intra-Operative Findings in Patients with a Suspicion of Prosthetic Valve Endocarditis. J Nucl Cardiol. 2022;29(2):528-34. doi: 10.1007/s12350-021-02674-y.

16. Erba PA, Conti U, Lazzeri E, Sollini M, Doria R, De Tommasi SM, et al. Added Value of 99mTc-HMPAO-labeled Leukocyte SPECT/CT in the Characterization and Management of Patients with Infectious Endocarditis. J Nucl Med. 2012;53(8):1235-43. doi: 10.2967/jnumed.111.099424.

17. Holcman K, Szot W, Rubiś P, Leśniak-Sobelga A, Hlawaty M, Wiśniowska-Śmiałek S, et al. 99mTc-HMPAO-labeled Leukocyte SPECT/CT and Transthoracic Echocardiography Diagnostic Value in Infective Endocarditis. Int J Cardiovasc Imaging. 2019;35(4):749-58. doi: 10.1007/s10554-018-1487-x.

18. Holcman K, Rubiś P, Ząbek A, Ćmiel B, Szot W, Boczar K, et al. The Prognostic Value of ^{99m}Tc-HMPAO-Labeled Leucocyte SPECT/CT in Cardiac Device-Related Infective Endocarditis. JACC Cardiovasc Imaging. 2020;13(8):1739-51. doi: 10.1016/j.jcmg.2020.01.025.

19. Rouzet F, Chequer R, Benali K, Lepage L, Ghodbane W, Duval X, et al. Respective Performance of 18F-FDG PET and Radiolabeled Leukocyte Scintigraphy for the Diagnosis of Prosthetic Valve Endocarditis. J Nucl Med. 2014;55(12):1980-5. doi: 10.2967/jnumed.114.141895.

20. Calais J, Touati A, Grall N, Laouénan C, Benali K, Mahida B, et al. Diagnostic Impact of ^{18}F-Fluorodeoxyglucose Positron Emission Tomography/Computed Tomography and White Blood Cell SPECT/Computed Tomography in Patients with Suspected Cardiac Implantable Electronic Device Chronic Infection. Circ Cardiovasc Imaging. 2019;12(7):e007188. doi: 10.1161/CIRCIMAGING.117.007188.

My Approach to Imaging Cardiac Amyloidosis: Role of Bone-Seeking Tracers Scintigraphy

Adriana Pereira Glavam,[1,2,3] *Rafael Willain Lopes,*[4] *Simone Cristina Soares Brandão*[5,6,7]
Instituto Nacional de Cardiologia,[1] *Rio de Janeiro, RJ – Brazil*
Hospital Copa Star,[2] *Rio de Janeiro, RJ – Brazil*
Clínica de Diagnóstico por Imagem CDPI/DASA,[3] *Rio de Janeiro, RJ – Brazil*
Hospital do Coração (Hcor),[4] *São Paulo, SP – Brazil*
Universidade Federal de Pernambuco,[5] *Recife, PE – Brazil*
DIA Medicina Nuclear,[6] *Recife, PE – Brazil*
Diagson, João Pessoa,[7] *PB – Brazil*

Abstract

Amyloidosis is a systemic infiltrative disease characterized by the extracellular deposition of amyloid fibrils. Heart involvement is common and associated with a poor prognosis. The most predominant types of cardiac amyloidosis (CA) are amyloid immunoglobulin light chain (AL) and amyloid transthyretin (ATTR). Diagnosis of CA and differentiation between the types are important for prognosis, therapy, and genetic counseling. ATTR-CA is an under-diagnosed cause of heart failure. However, great accomplishments in non-invasive imaging methods, as well as the possibility of effective clinical treatment, have shifted ATTR-CA from a rare and untreatable disease to a condition that clinicians should consider on a daily basis. The advent of scintigraphy imaging with bone-seeking tracers has allowed the early diagnosis of ATTR-CA with high accuracy once monoclonal gammopathies have been excluded. Interpretation of cardiac scintigraphy with bone-seeking tracers requires expertise, and we propose a step-by-step guide to performing this exam in clinical practice according to the most recent guidelines. Moreover, we reviewed some crucial points that we believe are of paramount importance in clinical practice and patient outcomes.

Introduction

Amyloidosis is a systemic infiltrative disease characterized by the extracellular deposition of misfolded proteins which aggregate as amyloid fibrils. Heart involvement is common and, unfortunately, associated with a poor prognosis for those patients. The most predominant types of cardiac amyloidosis (CA) are amyloid immunoglobulin light chain (AL) and amyloid transthyretin (ATTR). The latter is further subtyped into hereditary (ATTRv), which results from protein mutations, and wild type (ATTRw), formerly known as senile type, which is not associated with DNA mutations.[1]

ATTR-CA has been considered a rare disease, but recent data have shown an exponential increase in incidence over the past 10 years, especially for ATTR-CA wild type.[2] Until very recently, only endomyocardial biopsy (EMB) could diagnose CA, and no specific treatment was available. Great accomplishments in non-invasive imaging methods, as well as the possibility of effective clinical treatment, have shifted ATTR-CA from a rare and untreatable disease to a condition that clinicians should consider on a daily basis.[3] Bone-seeking tracers scintigraphy has assumed a central role in diagnosis since it is currently the only non-invasive imaging method capable of accurately diagnosing ATTR-CA.[4]

In order to guide good practice, consensus,[5,6] practice points,[7] and guidelines[1,8] have been proposed by highly valued international societies. In this context, the authors decided to devise this guide based on their own experiences in the real world and call attention to some crucial points that we believe are of paramount importance in clinical practice and patient outcomes.

Keywords

Scintigraphy; Amyloidosis; Pre-Albumin; Diphosphates; Cardiac insufficiency

Mailing Address: Simone Cristina Soares Brandão •
Universidade Federal de Pernambuco. Av. Prof Moraes Rego, SN.
CEP: 50670-901. Cidade Universitária, Recife, PE – Brazil
E-mail: sbrandaonuclearufpe@gmail.com
Manuscript received February 5, 2023; revised February 11, 2023; accepted March 6, 2023
Editor responsible for the review: Marco Stephan Lofrano Alves

DOI: https://doi.org/10.36660/abcimg.20230012i

Bone-seeking tracers scintigraphy

Bone-seeking tracers

Amyloid deposits are the most direct targets to diagnose and type CA. They consist of insoluble b-pleated sheets of fibrils formed from misfolded precursor proteins, as well as non-fibrillar components of serum amyloid P (SAP), glycosaminoglycans, and calcium.[9] Nuclear medicine methods act on a molecular level and can identify amyloid deposits even before structural and functional changes can be observed on echocardiography or cardiac magnetic resonance (CMR), leading to an early diagnosis that directly impacts prognosis.[6]

In the past, bone-seeking tracers were used to detect myocardial necrosis, and their potential use to diagnose CA has been recently described.[10] The phosphate domains in those tracers are supposed to bind to calcium in transthyretin fibrils. Pepys et al.[11] suggest that the P-component could bind to amyloid fibrils via a calcium-mediated mechanism, and Stats et al.[12] showed microcalcifications in EMB samples. The precise molecular mechanism behind differential uptake in ATTR and AL-CA is not well known, but it has been postulated that it might be related to a higher calcium content, i.e., microcalcifications in TTR amyloid fibrils.[10] Even so, in a few cases of AL-CA, the amount of microcalcifications is comparable to ATTR-CA, explaining why bone-seeking tracers are not specific for ATTR-CA.[4]

Perugini et al.[13] first described that 3,3-diphosphono-1,2-propanodicarboxylic acid linked to technetium-99m (^{99m}Tc-DPD) scintigraphy is highly sensitive and specific in differentiating ATTR-CA from AL-CA in patients with documented CA. Subsequently, other authors have confirmed scintigraphy as an accurate diagnostic method, even when other types of bone-seeking tracers were used.[14]

Gillmore et al.[4] have revolutionized clinical practice by proposing that ATTR-CA could be non-invasively diagnosed using bone scintigraphy. In a multicenter study involving 1217 patients with suspected CA, grades 2 or 3 of myocardial radiotracer uptake, in the absence of monoclonal gammopathies in serum or urine, had a specificity and positive predictive value of 100% to detect ATTR-CA. The results were similar among the most available bone-seeking tracers, as well as for patients with hereditary and wild-type ATTR-CA. Therefore, in this context, EMB is not needed, and specific treatment can be safely initiated.

As expected, after the publication of Gilmore et al.'s results,[4] an increase in the number of patients referred to scintigraphy was observed. However, it is worth mentioning that the study had included patients with a high pretest probability of CA, i.e., symptoms of heart failure and echocardiogram or CMR consistent with CA, and the scans were carried out in reference centers following the best practices.

Nowadays, three types of ^{99m}Tc-labeled myocardial bone-avid radiotracer have been used for the diagnosis of ATTR-CA: 99mTc-pyrophosphate (^{99m}Tc-PYP), ^{99m}Tc-DPD, and 99mTc-hydroxymethylene diphosphonate (^{99m}Tc-HMPD), and all have shown high accuracy for imaging cardiac TTR amyloid.[5]

^{99m}Tc-PYP is the most used radiotracer in the United States and Brazil. ^{99m}Tc-DPD and ^{99m}Tc-HMPD are currently the most used in Europe and other countries. It is worth noting that, because of the ^{99m}Tc-PYP shortage, some centers in the United States have been using ^{99m}Tc-methylene diphosphonate (^{99m}Tc-MPD) as well. It is important to highlight that ^{99m}Tc-MDP is currently used for bone scintigraphy, but it is not recommended for ATTR-CA diagnosis because of its low sensitivity compared to the other bone-seeking tracers.[13]

Imaging protocols and interpretation

Since ^{99m}Tc-PYP is the only radiotracer used for ATTR-CA diagnosis in Brazil, it will be the focus of this document.

^{99m}Tc-PYP scintigraphy is a simple, inexpensive procedure available in major centers in Brazil. No absolute contraindications are described, and modern scans have allowed the use of lower doses of radiation. Furthermore, no preparation is required.[5,15]

An activity dose of 10 to 20 mCi (370 to 740 MBq) of ^{99m}Tc-PYP is administered intravenously. Subsequently, 2 to 3 hours after the injection, anterior and left lateral chest planar images are acquired, followed by a cardiac single photon emission computed tomography (SPECT) imaging. Whenever possible, a hybrid acquisition using SPECT associated to computed tomography (SPECT/CT) is advisable.[5,15]

Former consensus[5] and practice points[15] recommended that planar and SPECT images should be obtained 1 hour after radiotracer injection. If a blood pool was present, a 3-hour image should be performed. Most recent data[16] suggest that the 1-hour imaging is optional. Hutt et al.[17] have demonstrated that myocardial and bone uptake over time is distinct. As the peak myocardial counts on planar images occur 1 hour after injection of ^{99m}Tc-DPD followed by a progressive decline over time, bone counts increase gradually and peak after 2 to 3 hours. Therefore, 1-hour imaging is more sensitive, and 3-hour imaging is more specific for ATTR-CA diagnosis. Similar kinetics is observed with the other radiotracers. It is important to emphasize that a 1-hour imaging protocol is equivalent to a 3-hour protocol since SPECT images are incorporated, which positively impacts patient comfort and laboratory output.[18]

The first step in scan interpretation is to proceed to a visual or semi-quantitative analysis using planar imaging. Radiotracer uptake into the bones (ribs) is compared to heart uptake and rated as previously described by Perugini et al.:[13] grade 0 (no heart uptake and normal rib uptake), grade 1 (heart uptake less than rib uptake), grade 2 (heart uptake equal to rib uptake) and grade 3 (greater than rib uptake with mild/absent rib uptake), as illustrated in Figure 1. Heart uptake must be confirmed in SPECT or SPECT/CT images. Scans showing visual scores greater than or equal to 2, i.e., 2 or 3 on planar and SPECT images, are classified as positive and suggestive of ATTR-CA (Figure 2). Analysis of planar images alone is no longer accepted, irrespective of the time between injection and scans, showing the importance of directly visualizing and confirming myocardial uptake. Then, we must always perform SPECT imaging.[16]

The second step is quantitative analysis. Bokhari et al.[14] defined a simple technique based on drawing a circular region of interest (ROI) over the heart on the anterior chest planar imaging and mirroring this ROI over the contralateral chest to adjust for background and ribs. Heart-to-contralateral lung uptake ratio (H/CL) is calculated as a ratio of heart ROI mean counts to contralateral chest ROI mean counts. $H/CL > 1.5$ at 1 hour-imaging and $H/CL > 1.3$ at 3-hour imaging are highly accurate to diagnose ATTR-CA (Figure 3). Hence, some caution is required when drawing the ROI, for example, size adjustment to maximize coverage of the heart without including the adjacent lung and avoiding sternal, ribs, and right ventricle areas to obtain reliable ratios.

Planar imaging alone is limited in spatial resolution when compared to SPECT or SPECT/CT. Myocardial uptake cannot be differentiated from blood pool uptake; overlying rib uptake may add counts to the region of the heart, and attenuation correction is not feasible. SPECT overcomes these limitations and should always be performed.[19] Indeed, Régis et al.[20] showed that visual analysis on SPECT imaging has led to fewer scans interpreted as equivocal when compared to quantitative analysis (H/CL ratio).

Review Article

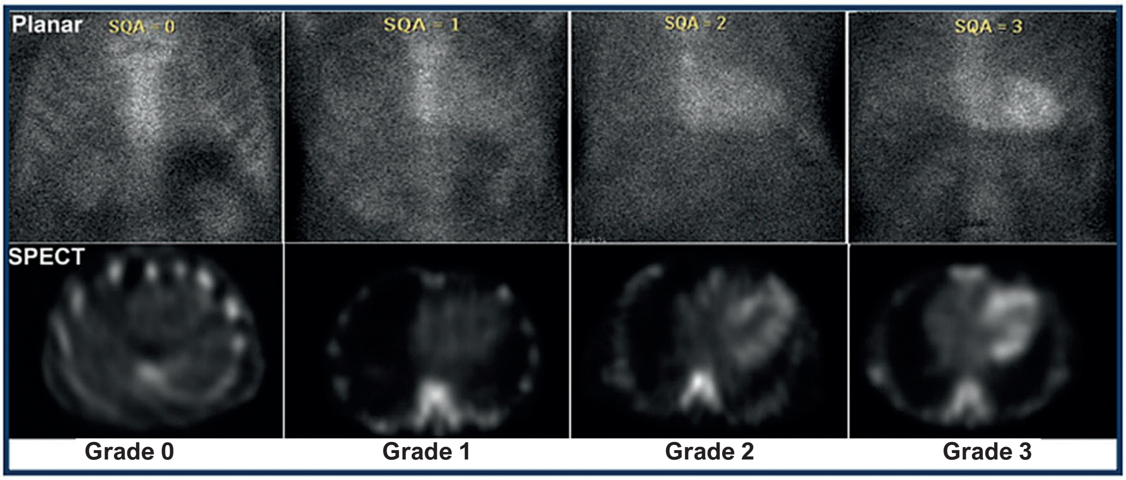

Figure 1 – *Grading ^{99m}Tc-PYP uptake on planar and SPECT images. This figure illustrates visual semi-quantitative analysis of cardiac ^{99m}Tc-PYP uptake using planar (upper) and SPECT (lower) imaging. Radiotracer uptake into the rib is compared to heart uptake and rated: grade 0 (no heart uptake and normal rib uptake), grade 1 (heart uptake less than rib uptake), grade 2 (heart uptake equal to rib uptake) and grade 3 (greater than rib uptake with mild/absent rib uptake). From "99mTechnetium-pyrophosphate Imaging for Transthyretin Cardiac Amyloidosis" by Dorbala et al., 2019, ASNC Cardiac Amyloidosis Practice Points. Copyright 2019 by American Society of Nuclear Cardiology. Reprinted with permission.[15] ^{99m}Tc-PYP: ^{99m}Tc-pyrophosphate; SPECT: single photon emission computed tomography; SQA: semiquantitative score.*

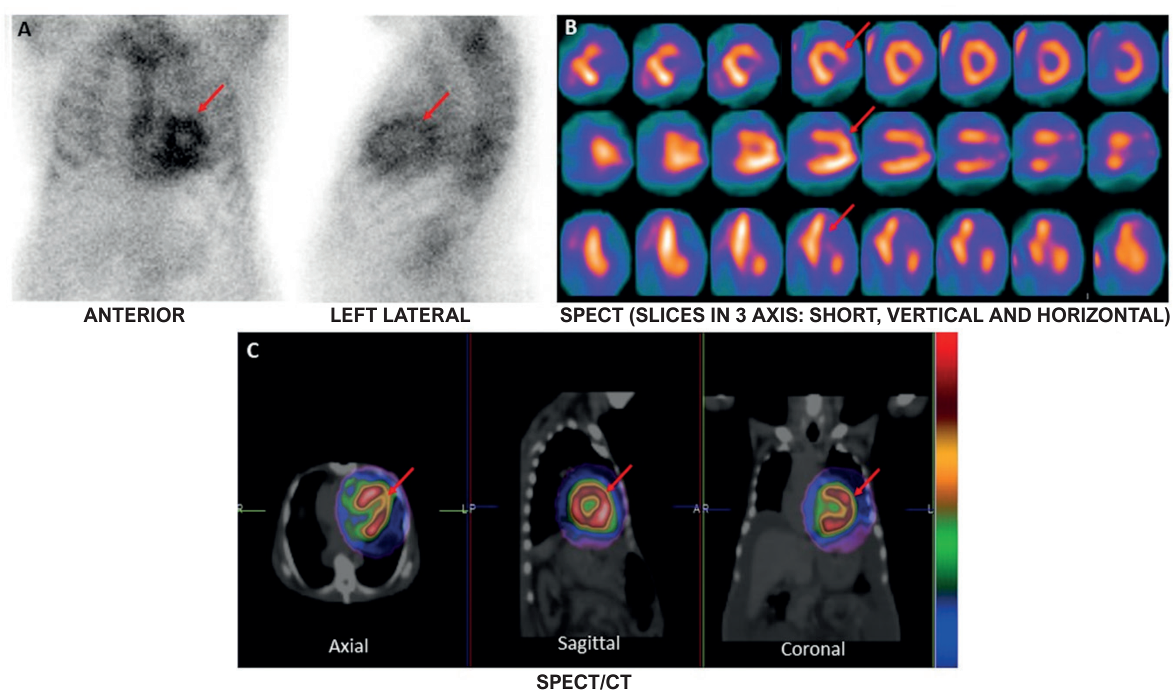

Figure 2 – *Positive cardiac ^{99m}Tc-PYP scintigraphy. Planar images (A) demonstrate abnormally increased radiotracer activity in the heart (arrows) and greater than the ribs (Perugini grade 3), and SPECT (B) and SPECT/CT (C) images confirm radiotracer uptake throughout the left ventricle (arrows). Those findings are highly suggestive of ATTR-CA. The advantage of SPECT/CT imaging is to better identify myocardial ^{99m}Tc-PYP uptake. Source: the authors. ATTR-CA: amyloid transthyretin cardiac amyloidosis; ^{99m}Tc-PYP: ^{99m}Tc-pyrophosphate; SPECT: single photon emission computed tomography; SPECT/CT: single photon emission computed tomography associated to computed tomography.*

Another important change in diagnostic criteria is the role of the H/CL ratio. In a former consensus,[6] H/CL ratio > 1.5 was considered as strongly suggestive of ATTR-CA. Currently, a scan is strongly suggestive of ATTR-CA if diffuse myocardial uptake grade 2 or 3 is observed in SPECT imaging, even if the H/CL ratio is < 1.5. Nevertheless, the H/CL ratio can still be useful to reclassify equivocal exams as positive or negative.[16]

False-positive and false-negative results

As previously stated, scintigraphy with bone-seeking tracers is a highly accurate method to diagnose ATTR-CA. However, some peculiar scenarios should always be considered, given that false-positive and false-negative results may occur, as described in Table 1.[6,8,21]

Regarding possible false negatives of scintigraphy for detecting ATTR-CA, the most common causes are an early-stage disease where myocardial infiltration can be minimal or mild and not yet detectable, as well as some pathogenic TTR mutations such as Phe64Leu, Val30Met, Thr59Lys, Se77Tyr, and Glu61Ala;[22] VaL122Ile has more recently been described in some subjects as well.[23] It is well known that the sensitivity of bone avid tracer scintigraphy in hereditary ATTR-CA might be lower in some cases.[5,21]

Scintigraphy with bone-seeking tracers has led to fewer cases where EMB is required, but EMB is still considered the gold standard for the diagnosis of CA. EMB should always be considered in the following cases: 1) ^{99m}Tc-PYP scan is negative or equivocal, but clinical suspicion is high, i.e., echocardiogram or CMR show typical findings in patients with suggestive symptoms; 2) ^{99m}Tc-PYP scan is positive, but free light chains are elevated, or monoclonal gammopathy is present. It has been described in the literature that, in elderly patients, AL-CA and ATTR-CA might coexist; 3) Bone-seeking tracer scintigraphy is unavailable.[21]

It is worth mentioning that fat-pad biopsy is not highly sensitive to exclude ATTR amyloidosis and should not be routinely ordered.[21]

How to properly exclude gammopathies

Clinicians must not rely solely on imaging to confirm or exclude ATTR-CA. Gilmore et al.[4] have shown that any grade of radiotracer uptake was associated with 99% sensitivity and 68% specificity to diagnose ATTR-CA. The poorer specificity was due to false positives related to AL-CA. Indeed, 40% of patients with AL-CA might show any grade of radiotracer uptake on scintigraphy. Therefore, only uptake grade 2 or 3 after the exclusion of AL- CA was associated with 100% specificity and positive predictive value for the non-invasive diagnosis of ATTR-CA.

Serum-free light chain concentration and serum and urine immunofixation electrophoresis is > 99% sensitive to detect AL amyloidosis. However, serum plasma and urine plasma electrophoresis are much less sensitive and should be avoided.[8] It is important to point out that up to 40% of patients with ATTR-CA may have a condition called monoclonal gammopathy of unknown significance (MGUS), and EMB is necessary to confirm ATTR-CA. Also, in some cases, MGUS may progress to AL amyloidosis or multiple myeloma, and those patients must be closely followed by a hematologist.[24]

Algorithms to diagnose CA

The Brazilian Society of Cardiology has proposed a very practical algorithm to guide CA diagnosis based on two main routes: Hematological and Cardiological (Figure 4).[25]

Perspectives for the near future

Studies have demonstrated that cardiac absolute quantification of ^{99m}Tc-PYP uptake is feasible with cadmium-zinc-telluride gamma cameras (SPECT/CT), and that different quantification parameters correlated strongly with extracellular volume obtained by CMR. Larger studies are necessary to definitively establish the value of quantification in ATTR-CA and move to the next frontier in the non-invasive diagnostic evaluation of CA.[26]

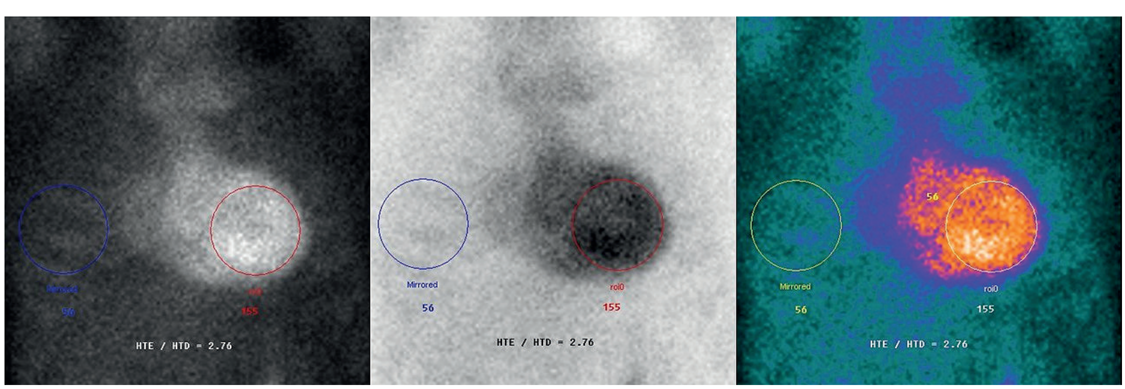

Figure 3 – *Quantitation of cardiac ^{99m}Tc-PYP using heart-to-contralateral (H/CL) lung uptake ratio over the heart on the anterior chest planar imaging. This image (shown in 3 different colors) was acquired 3 hours after the radiotracer injection. The H/CL was 1.76, which is highly accurate to diagnose ATTR-CA. Source: the authors. ATTR-CA: amyloid transthyretin cardiac amyloidosis; ^{99m}Tc-PYP: ^{99m}Tc-pyrophosphate*

Table 1 – Possible causes of false-positive scans for detecting transthyretin CA.

AL-CA: AL-CA is the most common and important cause of misdiagnosis. Most clinicians are not familiar with the fact that nearly 20% of scans can be positive in patients with AL-CA; therefore, **always properly rule out AL-CA.**
Blood pool uptake in planar images: Although they are not recommended, some labs still use solely planar images to diagnose CA, and a blood pool can be interpreted as a positive scan. Cardiac uptake must always be confirmed in SPECT images. **Always perform SPECT.**
Rib fractures, valvular and annular calcifications, and breast implants: These structures may overlay the heart, thereby affecting H/CL results. Currently, H/CL alone is not recommended to diagnose CA. **Always perform SPECT.**
Acute or subacute myocardial infarction (< 4 months): Focal uptake may be present, and scintigraphy should not be used to diagnose CA in this early phase.
Hydroxychloroquine cardiotoxicity (histological confirmation).
Rare forms of CA for example, apolipoprotein A1).

AL-CA: amyloid immunoglobulin light chain cardiac amyloidosis; CA: cardiac amyloidosis; H/CL: heart-to-contralateral lung uptake ratio; SPECT: single photon emission computed tomography.

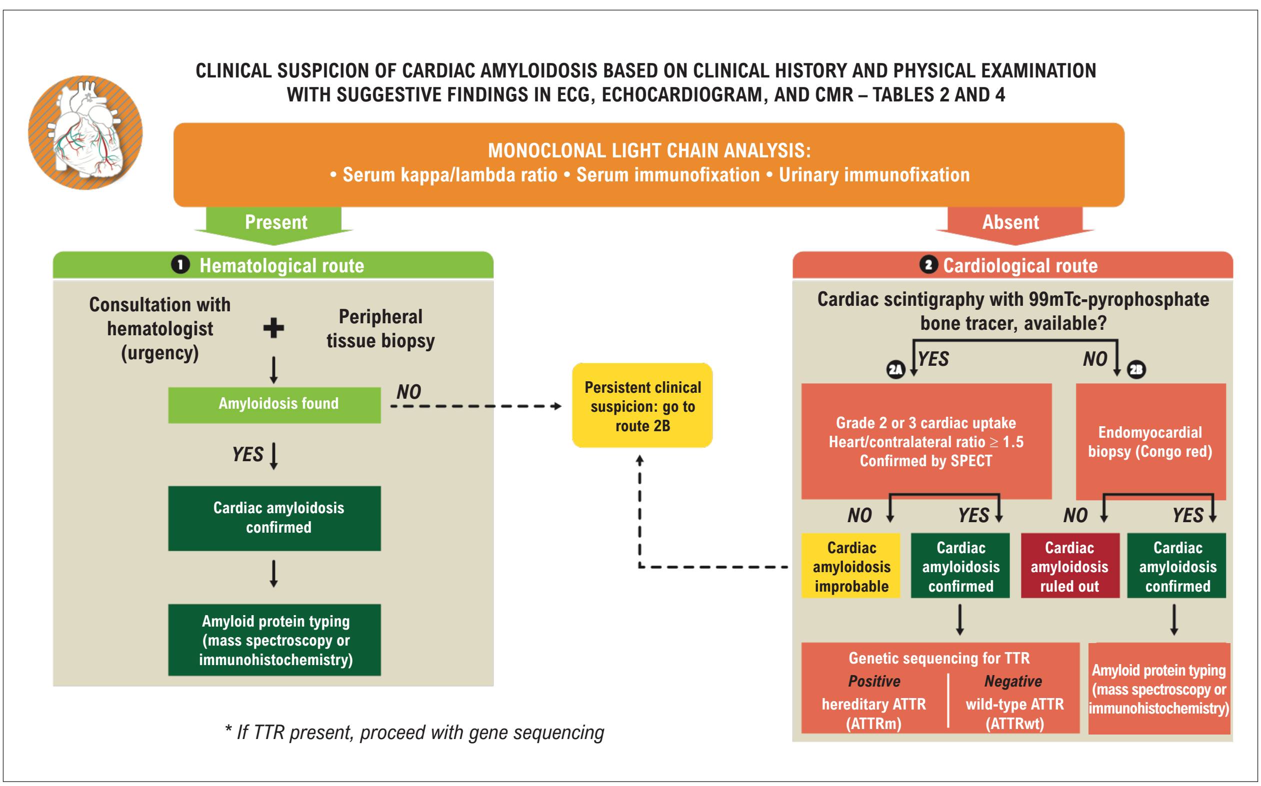

Figure 4 – *Flowchart for diagnosing cardiac amyloidosis. Brazilian Society of Cardiology practical algorithm to diagnose CA based on two main routes: Hematological and Cardiological. Adapted from Position Statement on Diagnosis and Treatment of CA – 2021.[25] CMR: cardiac magnetic resonance; ECG: eletrocardiogram; ATTR: amyloid transthyretin; TTR: transthyretin; SPECT: single photon emission computed tomography*

The advent of specific positron emission tomography (PET) amyloid-binding radiotracers has the potential to change currently employed diagnostic algorithms for imaging CA. These PET tracers have promising potential for the early detection of a particular type of CA, pursuing relevant medical intervention, assessing amyloid burden, monitoring treatment response, and determining overall prognosis.[27]

Final considerations

The advent of scintigraphy imaging with bone-seeking tracers has allowed the diagnosis of ATTR-CA with high accuracy once monoclonal gammopathies have been excluded. Interpretation of cardiac ^{99m}Tc-PYP images requires expertise, and we have proposed a step-by-step guide to performing this exam in clinical practice according to the most recent guidelines. We would like to highlight the importance of always performing SPECT imaging to truly ensure a positive test result and emphasize that false negatives can also occur, mostly in some inherited forms of ATTR-CA; in this scenario, an EMB might be necessary.

Author Contributions

Conception and design of the research, acquisition of data, analysis and interpretation of the data, writing of the manuscript and critical revision of the manuscript for intellectual content: Glavam AP, Lopes RW, Brandão SCS.

Potential Conflict of Interest

No potential conflict of interest relevant to this article was reported.

Sources of Funding

There were no external funding sources for this study.

Study Association

This study is not associated with any thesis or dissertation work.

Ethics Approval and Consent to Participate

This article does not contain any studies with human participants or animals performed by any of the authors.

References

1. Garcia-Pavia P, Rapezzi C, Adler Y, Arad M, Basso C, Brucato A, et al. A Position Statement of the European Society of Cardiology Working Group on Myocardial and Pericardial Diseases. Eur J Heart Fail. 2021;23(4):512-26. doi: 10.1002/ejhf.2140.
2. Ruberg FL, Grogan M, Hanna M, Kelly JW, Maurer MS. Transthyretin Amyloid Cardiomyopathy: JACC State-of-the-Art Review. J Am Coll Cardiol. 2019;73(22):2872-91. doi: 10.1016/j.jacc.2019.04.003.
3. Witteles RM, Bokhari S, Damy T, Elliott PM, Falk RH, Fine NM, et al. Screening for Transthyretin Amyloid Cardiomyopathy in Everyday Practice. JACC Heart Fail. 2019;7(8):709-16. doi: 10.1016/j.jchf.2019.04.010.
4. Gillmore JD, Maurer MS, Falk RH, Merlini G, Damy T, Dispenzieri A, et al. Nonbiopsy Diagnosis of Cardiac Transthyretin Amyloidosis. Circulation. 2016;133(24):2404-12. doi: 10.1161/CIRCULATIONAHA.116.021612.
5. Dorbala S, Ando Y, Bokhari S, Dispenzieri A, Falk RH, Ferrari VA, et al. ASNC/AHA/ASE/EANM/HFSA/ISA/SCMR/SNMMI Expert Consensus Recommendations for Multimodality Imaging in Cardiac Amyloidosis: Part 1 of 2-Evidence Base and Standardized Methods of Imaging. J Nucl Cardiol. 2019;26(6):2065-123. doi: 10.1007/s12350-019-01760-6.
6. Maurer MS, Bokhari S, Damy T, Dorbala S, Drachman BM, Fontana M, et al. Expert Consensus Recommendations for the Suspicion and Diagnosis of Transthyretin Cardiac Amyloidosis. Circ Heart Fail. 2019;12(9):e006075. doi: 10.1161/CIRCHEARTFAILURE.119.006075.
7. Singh B, Bateman TM, Case JA, Heller G. Attenuation Artifact, Attenuation Correction, and the Future of Myocardial Perfusion SPECT. J Nucl Cardiol. 2007;14(2):153-64. doi: 10.1016/j.nuclcard.2007.01.037.
8. Kittleson MM, Maurer MS, Ambardekar AV, Bullock-Palmer RP, Chang PP, Eisen HJ, et al. Cardiac Amyloidosis: Evolving Diagnosis and Management: A Scientific Statement From the American Heart Association. Circulation. 2020;142(1):e7-e22. doi: 10.1161/CIR.0000000000000792.
9. Dorbala S, Cuddy S, Falk RH. How to Image Cardiac Amyloidosis: A Practical Approach. JACC Cardiovasc Imaging. 2020;13(6):1368-83. doi: 10.1016/j.jcmg.2019.07.015.
10. Singh V, Falk R, Di Carli MF, Kijewski M, Rapezzi C, Dorbala S. State-of-the-art Radionuclide Imaging in Cardiac Transthyretin Amyloidosis. J Nucl Cardiol. 2019;26(1):158-73. doi: 10.1007/s12350-018-01552-4.
11. Pepys MB, Dyck RF, Beer FC, Skinner M, Cohen AS. Binding of Serum Amyloid P-Component (SAP) by Amyloid Fibrils. Clin Exp Immunol. 1979;38(2):284-93.
12. Stats MA, Stone JR. Varying Levels of Small Microcalcifications and Macrophages in ATTR and AL Cardiac Amyloidosis: Implications for Utilizing Nuclear Medicine Studies to Subtype Amyloidosis. Cardiovasc Pathol. 2016;25(5):413-7. doi: 10.1016/j.carpath.2016.07.001.
13. Perugini E, Guidalotti PL, Salvi F, Cooke RM, Pettinato C, Riva L, et al. Noninvasive Etiologic Diagnosis of Cardiac Amyloidosis Using 99mTc-3,3-Diphosphono-1,2-Propanodicarboxylic Acid Scintigraphy. J Am Coll Cardiol. 2005;46(6):1076-84. doi: 10.1016/j.jacc.2005.05.073.
14. Bokhari S, Castaño A, Pozniakoff T, Deslisle S, Latif F, Maurer MS. (99m)Tc-Pyrophosphate Scintigraphy for Differentiating Light-Chain Cardiac Amyloidosis from the Transthyretin-Related Familial and Senile Cardiac Amyloidoses. Circ Cardiovasc Imaging. 2013;6(2):195-201. doi: 10.1161/CIRCIMAGING.112.000132.
15. Dorbala S, Bokhari, Miller E, Bullock-Palmer R, Soman P, Thompson R. 99mTechnetium-Pyrophosphate Imaging for Transthyretin Cardiac Amyloidosis. Fairfax: American Society of Nuclear Cardiology; 2019.
16. Dorbala S, Ando Y, Bokhari S, Dispenzieri A, Falk RH, Ferrari VA, et al. Addendum to ASNC/AHA/ASE/EANM/HFSA/ISA/SCMR/SNMMI Expert Consensus Recommendations for Multimodality Imaging in Cardiac Amyloidosis: Part 1 of 2-Evidence Base and Standardized Methods of Imaging. J Card Fail. 2022;28(7):e1-e4. doi: 10.1016/j.cardfail.2021.06.012.
17. Hutt DF, Quigley AM, Page J, Hall ML, Burniston M, Gopaul D, et al. Utility and Limitations of 3,3-Diphosphono-1,2-Propanodicarboxylic Acid Scintigraphy in Systemic Amyloidosis. Eur Heart J Cardiovasc Imaging. 2014;15(11):1289-98. doi: 10.1093/ehjci/jeu107.
18. Sperry BW, Burgett E, Bybee KA, McGhie AI, O'Keefe JH, Saeed IM, et al. Technetium Pyrophosphate Nuclear Scintigraphy for Cardiac Amyloidosis: Imaging at 1 vs 3 Hours and Planar vs SPECT/CT. J Nucl Cardiol. 2020;27(5):1802-7. doi: 10.1007/s12350-020-02139-8.

19. Asif T, Gomez J, Singh V, Doukky R, Nedeltcheva A, Malhotra S. Comparison of Planar with Tomographic Pyrophosphate Scintigraphy for Transthyretin Cardiac Amyloidosis: Perils and Pitfalls. J Nucl Cardiol. 2021;28(1):104-11. doi: 10.1007/s12350-020-02328-5.

20. Régis C, Harel F, Martineau P, Grégoire J, Abikhzer G, Juneau D, et al. Tc-99m-Pyrophosphate Scintigraphy for the Diagnosis of ATTR Cardiac Amyloidosis: Comparison of Quantitative and Semi-Quantitative Approaches. J Nucl Cardiol. 2020;27(5):1808-15. doi: 10.1007/s12350-020-02205-1.

21. Hanna M, Ruberg FL, Maurer MS, Dispenzieri A, Dorbala S, Falk RH, et al. Cardiac Scintigraphy with Technetium-99m-Labeled Bone-Seeking Tracers for Suspected Amyloidosis: JACC Review Topic of the Week. J Am Coll Cardiol. 2020;75(22):2851-62. doi: 10.1016/j.jacc.2020.04.022.

22. Pilebro B, Suhr OB, Näslund U, Westermark P, Lindqvist P, Sundström T. (99m)Tc-DPD Uptake Reflects Amyloid Fibril Composition in Hereditary Transthyretin Amyloidosis. Ups J Med Sci. 2016;121(1):17-24. doi: 10.3109/03009734.2015.1122687.

23. Yadalam A, Ceballos A, Bigham T, Rim A, Yalamanchili S, Brown MT, et al. False Negative Cardiac Scintigraphy in Patients with Val122Ile Transthyretin Cardiac Amyloidosis. J Am Coll Cardiol. 2022;79(9):427. doi: 10.1016/S0735-1097(22)01418-8.

24. Phull P, Sanchorawala V, Connors LH, Doros G, Ruberg FL, Berk JL, et al. Monoclonal Gammopathy of Undetermined Significance in Systemic Transthyretin Amyloidosis (ATTR). Amyloid. 2018;25(1):62-67. doi: 10.1080/13506129.2018.1436048.

25. Simões MV, Fernandes F, Marcondes-Braga FG, Scheinberg P, Correia EB, Rohde LEP, et al. Position Statement on Diagnosis and Treatment of Cardiac Amyloidosis - 2021. Arq Bras Cardiol. 2021;117(3):561-98. doi: 10.36660/abc.20210718.

26. Grossman GB. Quantitation in ATTR Cardiac Amyloidosis: The Next Step is Almost There! J Nucl Cardiol. 2023;30(1):140-3. doi: 10.1007/s12350-022-03044-y.

27. Saeed S, Saad JM, Ahmed AI, Han Y, Al-Mallah MH. The Utility of Positron Emission Tomography in Cardiac Amyloidosis. Heart Fail Rev. 2022;27(5):1531-41. doi: 10.1007/s10741-021-10183-w.

Dual Mechanism of Mitral Valve Injury: Additional Value of Three-Dimensional Transesophageal Echocardiography

Larissa Neto Espíndola,[1] Angele Azevedo Alves Mattoso,[2] Geórgia dos Santos Couto,[3] Pompílio Sampaio Britto[2]

Hospital Municipal de Salvador,[1] Salvador, BA – Brazil

Hospital Santa Izabel,[2] Salvador, BA – Brazil

Escola de Ecocardiografia da Bahia da Santa Casa de Misericórida de Feira de Santana,[3] Feira de Santana, BA – Brazil

Abstract

Infective endocarditis (IE) is a life-threatening condition and during its course several complications may occur, including embolic events, perivalvular extension and valvular destruction. Echocardiography is fundamental across all stages of the disease, from the diagnosis until the follow-up after completion of the definitive therapy. Three-dimensional transesophageal echocardiography (TEE) can demonstrate a better anatomical definition and it is especially useful in the assessment of perivalvular extension of the infection, prosthetic valve dehiscence and valve perforation. In this article we report a case of double damage in the same mitral valve: leaflet perforation and rupture of chords in a patient with IE.

Introduction

Echocardiography has a known important role in the diagnosis of IE, the prediction of embolic risk, the prognostic assessment of the patients, as well as for their follow-up under therapy, helping the physician in decision-making, mainly when a surgical intervention is considered. In this rare case, we demonstrate the additional value of the 3D TEE in the assessment of double lesion in the same mitral valve (perforation and ruptured chords) in the presence of IE with a realistic, single and peculiar *en face* view of the mitral valve.

Case Presentation

A 55-year-old male patient with *Acquired Immunodeficiency Syndrome (AIDS)* and chronic kidney disease, undergoing dialysis, was admitted to a hospital complaining of progressive dyspnea for 3 months, lower-limb edema and sporadic episodes of fever. He had multiple reports of previous hospitalizations due to dialysis catheter infection and currently with multiple dental abscesses.

Keywords

Endocarditis; Echocardiography, Three-Dimensional; Mitral Valve.

Mailing Address: Larissa Neto Espíndola •
Praça Conselheiro Almeida Couto, 500. Centro Médico Celso Figueiroa, Sala 209. Nazaré. Postal code: 40.050-410. Salvador, BA – Brazil.
E-mail: lara.moc@gmail.com
Manuscript received July 5, 2022; revised manuscript October 6, 2022; accepted March 6, 2023
Editor responsible for the review: Daniela do Carmo Rassi Frota

DOI: https://doi.org/10.36660/abcimg.2023322i

Antibiotic therapy was introduced, and the patient was submitted to cardiac evaluation.

A transthoracic echocardiography (TTE) showed diffuse left ventricular hypokinesia with an ejection fraction estimated at 45% (Simpson's method). The valve was diffusely thickened with multiple, small, movable thread-like strands structures carpeting the entire atrial surface of both leaflets. It was also observed that the mitral valve had a suggestive image of perforation in the anterior leaflet, which was responsible for generating a significant regurgitation jet at the Color Doppler flow mapping. Furthermore, the presence of a second regurgitation jet was demonstrated from the posterior leaflet (Figure 1; Video 1). Two-dimensional TEE (2D TEE) showed a characteristic anterior leaflet perforation image with significant regurgitation (Figure 2A, 2B; Videos 2 and 4). Additionally, a chordal rupture image was observed in the apical two-chamber view, related to the medial scallop of the posterior leaflet (P3) with a second and eccentric valve regurgitation jet (Figure 2C, 2D). The 3D TEE in the *en face* view of the mitral valve realistically demonstrated the two valve dysfunction mechanisms (Video 3). In a single and peculiar image, the presence of an evident perforation and its precise location were observed in the attachment basis of the anterior mitral leaflet at the aortic-mitral curtain associated with the presence of ruptured chords in the P3 scallop of the posterior leaflet (Figure 3A).

After a period of antibiotic therapy, the patient underwent cardiac surgery. The intraoperative findings related to the double damage in the same valve - rupture of the posterior leaflet chordal and perforation of the anterior leaflet of the mitral valve - were confirmed (Figure 3B, 3C). Mitral valve replacement was performed with implantation of a biological prosthesis, without complications.

Discussion

IE may be responsible for acute mitral regurgitation through several mechanisms, including leaflet perforation, mitral valve annulus alteration secondary to abscess formation, or chordae tendineae rupture.[1]

Native valve perforations develop in 10% to 30% of patients with IE.[2] An accurate differentiation between true vegetations and other IE-related changes, such as ruptured chordae, is frequently difficult to establish.[3]

Even with 2D TEE, which is much more sensitive than TTE (90% vs 45%), perforations can be difficult to visualize using 2D imaging alone. 3D TEE imaging can significantly enhance detection of valvular perforations complicating IE.[4]

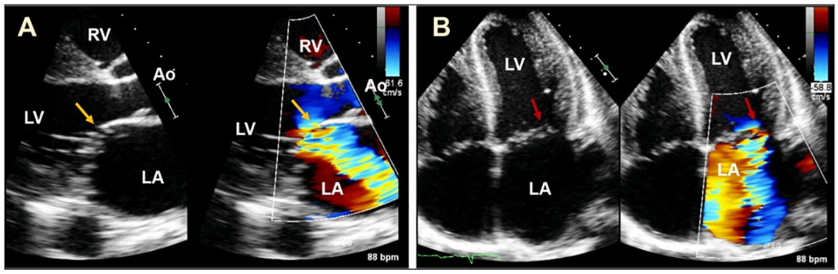

Figure 1 – TTE. A) Parasternal long-axis view showing a thickened mitral valve with characteristic image of perforation (orange arrow) in the anterior leaflet (left) and significant severe mitral regurgitation jet at the color Doppler flow mapping (right) originating from the perforation orifice; B) Apical four-chamber view showing the thickened aspect of the entire valve (left) with a second jet of severe eccentric mitral regurgitation related to the posterior leaflet. RV: right ventricle; LV: left ventricle; LA: left atrium; Ao: aorta.

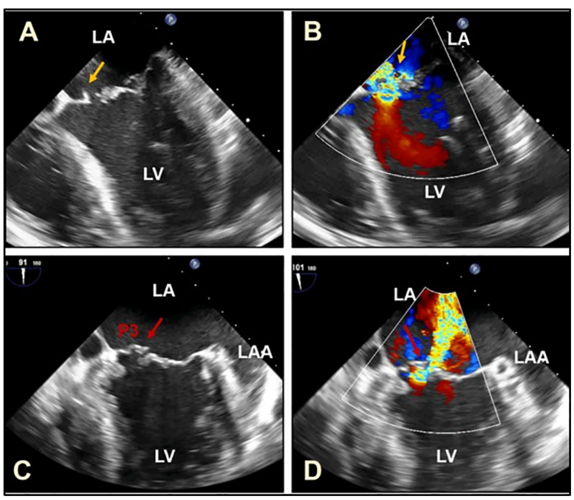

Figure 2 – A) Four-chamber view showing the characteristic perforation image in the anterior mitral leaflet (orange arrow); B) Color Doppler flow mapping showing the regurgitation jet (orange arrow) originating from the orifice; C) Two-chamber view showing ruptured chord associated with P3 scallop of the posterior leaflet of the mitral valve; D) Significant jet of severe mitral regurgitation related to the rupture of the P3 scallop chords. RV: right ventricle; LV: left ventricle; LA: left atrium; LAA: left atrial appendage.

Real-time 3D TEE is particularly useful in the assessment of perivalvular extension of the infection, prosthetic valve dehiscence and valve perforation.[5] We present a rare case of two dysfunction mechanisms present in the same valve.

But that is the question: Is the chordae rupture of primary etiology (since we have a diffusely thickened valve, even without a previous diagnosis of mitral valve prolapse - MVP) or secondary to the infection itself?

It is known that there are multiple causes of chordae tendineae rupture. IE was considered the main etiology in the remote past. However, currently, after some studies of case series, it appears that the main etiology is primary, with mitral valve prolapse being the leading cause.[6]

It is worth remembering that mitral valve prolapse is considered a predisposing condition for both chordae tendineae rupture and IE, since it makes the valve anatomically abnormal and, therefore, a substrate for the occurrence of vegetations.

Once an infection is installed, it is not a simple task to identify the cause of the rupture: primary etiology or endocarditis.

In a study conducted by Shirley Portuguese et al.,[6] 66% of patients diagnosed with endocarditis were previously aware of the presence of MVP, while only 9% of the primary etiology group knew that they had the pathology.

This allows us to affirm that it is not safe, in this case, to state that the chordae rupture is due to IE. It is possible that this is a patient with rupture secondary to MVP, which was a predisposing condition for the occurrence of endocarditis.

Still regarding this case, although the 2D TEE established the diagnosis, the 3D TEE, through the singular *en face* view, was able to demonstrate additional information, such as extension and actual location of the valve perforation and the ruptured chords with a realistic and peculiar view of the mitral valve.

Especially in the context of IE, providing valuable data such the mechanisms intrinsically responsible for valve regurgitation, the exact location of the perforation is of great importance and have not only diagnostic but also prognostic value. The three-dimensional echocardiographic imaging is ideal for interrogating the anatomy of each individual components of the mitral apparatus.[7-10] So it is a better approach to plan the surgical procedure, since it is possible to define the valve dysfunction mechanism, as well as the precise lesion location.

Conclusion

The 3D TEE is important for the accurate characterization of the complexity of mitral valve lesions through a better anatomical definition of the valve. This accurate characterization of valve disease is fundamental for the determination and planning of the surgical procedure.

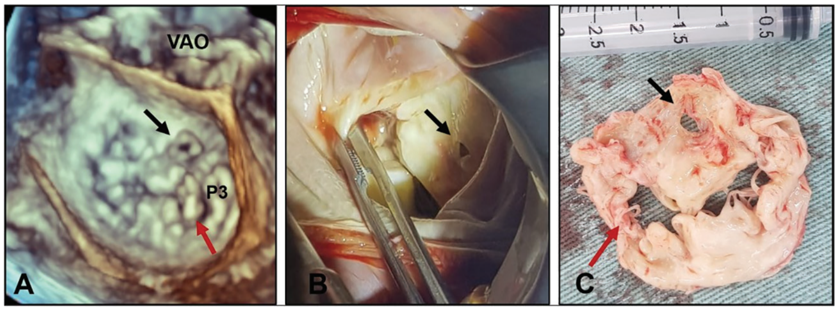

Figure 3 – A) Zoomed three-dimensional TEE imaging through en face view of the mitral valve, as seen from the left atrium showing the evident perforation orifice (black arrow) in the attachment basis of the anterior mitral leaflet - scallop A2 - and ruptured chords (red arrow) in the P3 scallop of the posterior leaflet; B) Surgical view of the mitral valve after opening the left atrium showing perforation in the anterior leaflet (black arrow); C) Surgically removed mitral valve seen on its left ventricular face corroborating the echocardiographic image, showing perforation (black arrow) in the anterior leaflet and the P3 scallop (red arrow) of the posterior leaflet, where the presence of ruptured chords (red arrow) can be observed.

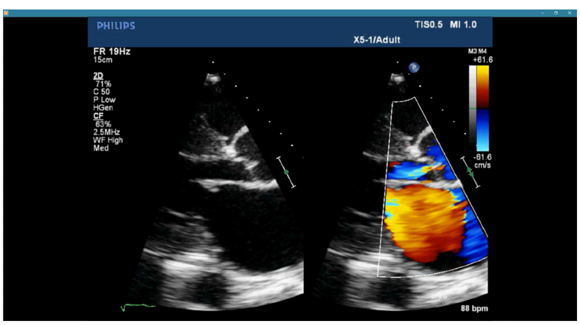

Video 1 – *TTE showing a thickened mitral valve with image of perforation and a significant regurgitation mitral jet origination from the orifice. Link: http://abcimaging.org/supplementary-material/2023/3602/abc-322-video-1.mp4*

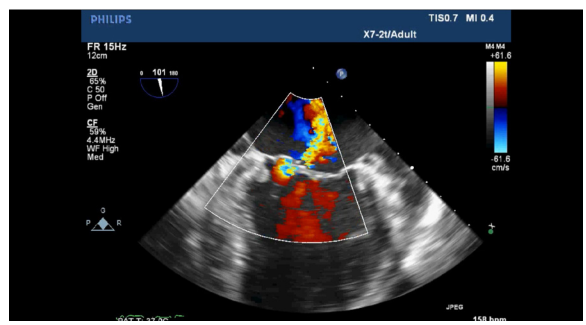

Video 2 – *2D TEE showing a significant jet of mitral regurgitation related to the rupture of P3 scallop chords. Link: http://abcimaging.org/supplementary-material/2023/3602/abc-322-video-2.mp4*

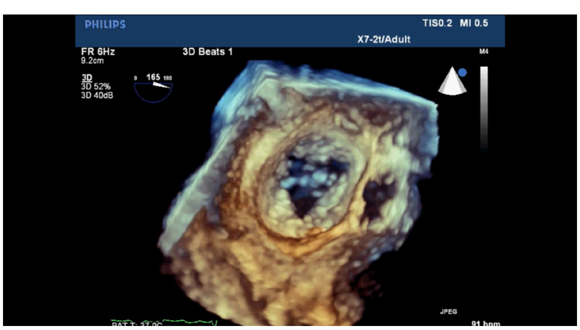

Video 3 – *3D TEE mitral en face view showing the double damage: perforation and ruptured chords. Link: http://abcimaging.org/supplementary-material/2023/3602/abc-322-video-3.mp4*

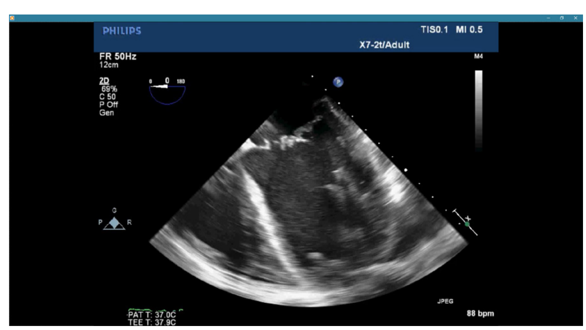

Video 4 – *2D TEE 4 chamber view showing the perforation image in the anterior mitral leaflet. Link: http://abcimaging.org/supplementary-material/2023/3602/abc-322-video-4.mp4*

Author Contributions

Conception and design of the research and critical revision of the manuscript for intellectual content: Mattoso AAA; acquisition of data Mattoso AAA, Couto GS, Espíndola LN, Britto PS; analysis and interpretation of the data: Mattoso AAA, Couto GS, Espíndola LN; writing of the manuscript: Espíndola LN, Mattoso, AAA;

Potential Conflict of Interest

No potential conflict of interest relevant to this article was reported.

Sources of Funding

There were no external funding sources for this study.

Study Association

This study is not associated with any thesis or dissertation work.

Ethics Approval and Consent to Participate

This article does not contain any studies with human participants or animals performed by any of the authors.

References

1. Austin WJ, Ambrose J, Greenberg BH. Acute Presentations of Valvular Heart Disease. Cardiac Intensive Care. 2010;339-354. doi: 10.1016/b978-1-4160-3773-6.10027-8.
2. Tribouilloy C, Rusinaru D, Sorel C, Thuny F, Casalta JP, Riberi A, et al. Clinical Characteristics and Outcome of Infective Endocarditis in Adults with Bicuspid Aortic Valves: A Multicentre Observational Study. Heart. 2010;96(21):1723-9. doi: 10.1136/hrt.2009.189050.
3. Bayer AS, Bolger AF, Taubert KA, Wilson W, Steckelberg J, Karchmer AW, et al. Diagnosis and Management of Infective Endocarditis and Its Complications. Circulation. 1998;98(25):2936-48. doi: 10.1161/01.cir.98.25.2936.
4. Hansalia S, Biswas M, Dutta R, Hage FG, Hsiung MC, Nanda NC, et al. The Value of Live/Real Time Three-Dimensional Transesophageal Echocardiography in the Assessment of Valvular Vegetations. Echocardiography. 2009;26(10):1264-73. doi: 10.1111/j.1540-8175.2009.01042.x.
5. Liu YW, Tsai WC, Lin CC, Hsu CH, Li WT, Lin LJ, et al. Usefulness of Real-Time Three-Dimensional Echocardiography for Diagnosis of Infective Endocarditis. Scand Cardiovasc J. 2009;43(5):318-23. doi: 10.1080/14017430902737940.
6. Portugese S, Amital H, Tenenbaum A, Bar-Dayan Y, Levy Y, Afek A, et al. Clinical Characteristics of Ruptured Chordae Tendineae in Hospitalized Patients: Primary Tear versus Infective Endocarditis. Clin Cardiol. 1998;21(11):813-6. doi: 10.1002/clc.4960211106.
7. Lancellotti P, Moura L, Pierard LA, Agricola E, Popescu BA, Tribouilloy C, et al. European Association of Echocardiography recommendations for the Assessment of Valvular Regurgitation. Part 2: Mitral and Tricuspid Regurgitation (Native Valve Disease). Eur J Echocardiogr. 2010;11(4):307-32. doi: 10.1093/ejechocard/jeq031.
8. Baddour LM, Wilson WR, Bayer AS, Fowler VG Jr, Tleyjeh IM, Rybak MJ, et al. Infective Endocarditis in Adults: Diagnosis, Antimicrobial Therapy, and Management of Complications: A Scientific Statement for Healthcare Professionals From the American Heart Association. Circulation. 2015;132(15):1435-86. doi: 10.1161/CIR.0000000000000296.
9. Lang RM, Badano LP, Tsang W, Adams DH, Agricola E, Buck T, et al. EAE/ASE Recommendations for Image Acquisition and Display Using Three-Dimensional Echocardiography. J Am Soc Echocardiogr. 2012;25(1):3-46. doi: 10.1016/j.echo.2011.11.010.
10. Schwalm SA, Sugeng L, Raman J, Jeevanandum V, Lang RM. Assessment of Mitral Valve Leaflet Perforation as a Result of Infective Endocarditis by 3-Dimensional Real-Time Echocardiography. J Am Soc Echocardiogr. 2004;17(8):919-22. doi: 10.1016/j.echo.2004.04.013.

Case Report

Comparative Analysis of Myocardial Work After Decongestion Therapy in a Patient With Acutely Decompensated HFrEF

Alexandre Costa Souza,[1,2] *Stephanie de Azevedo Drubi,*[1,2] *Bruna de Mattos Ivo Junqueira,*[1,2] *Ricardo André Sales Pereira Guedes,*[1,2] *Adriano Chaves de Almeida Filho,*[1,2] *Carolina Thé Macêdo*[1,2]

Hospital São Rafael, Rede D'Or São Luiz,[1] *Salvador, BA – Brazil*

Instituto D'Or de Ensino e Pesquisa (IDOR),[2] *Salvador, BA – Brazil*

Introduction

Acutely decompensated reduced ejection fraction heart failure (HFrEF) is one of the leading causes of hospitalization in our setting, with a 90-day readmission rate of 50%.[1] The use of additional tools in the assessment of the left ventricular function, such as the measurement of myocardial deformation through the Global Longitudinal Strain of the left ventricle (GLS) has greater prognostic value than the evaluation of the left ventricular ejection fraction (LVEF) by the Simpson method.[2] Despite the analysis of the myocardial deformity through the GLS being considered an independent predictor of mortality in patients with HFrEF, it is a parameter that experiences changes in pre- and after-load and, therefore, has limitations regarding the assessment of ventricular performance.[2-4] Myocardial work (MW) has stood out in recent years as a complementary tool to access parameters of myocardial function from the GLS-derived analysis, with the benefit of incorporating afterload information through the interpretation of the dynamic curve of deformity due to non-invasive left ventricular (LV) filling pressure.[5] Hence, the analysis of MW has been encouraging in patients with HFrHF, and, when analyzed in combination with classic hemodynamic parameters, it can add information with greater accuracy and prognostic value in the cardiac decompensation scenario.[3-5]

Clinical Case

Male patient, 52 years old, hypertensive, dyslipidemic, former smoker, admitted to the emergency unit for progressive Dyspnea Functional Class IV (NYHA) approximately one month ago. He presented worsening of the clinical condition in the last few days associated with orthopnea, lower limb (LL) edema and reduced urinary volume. The patient was admitted to the intensive care unit (ICU), using low-flow oxygen through a nasal catheter, for investigation and standard treatment of decompensated heart failure, including decongestion therapy with intravenous diuretics and vasodilators. Electrocardiogram in sinus rhythm on admission, with first-degree atrioventricular (AV) block, signs of left chamber overload with LV strain pattern and QRS duration of 100ms. Transthoracic echocardiogram (TTE) showed significant LV systolic dysfunction (LVEF: 25%) and right ventricle with borderline diameters (basal segment: 42mm and medial segment: 34mm); RV S': 09 cm/s; TAPSE: 15mm; FAC: 30%; mild tricuspid valve reflux with estimated pulmonary artery systolic pressure (PASP) through tricuspid reflux of 75mmHg, considering right atrial pressure of 15mmHg (inferior vena cava measurement of 21mm with inspiratory collapse < 50%); in addition to mitral valve reflux of an important degree of functional etiology. During the examination, blood pressure was 140 x 80 mmHg. The GLS analysis resulted in a value of -04%, global MW index of 385 mmHg%, constructive MW of 678 mmHg%, wasted MW of 359 mmHg% and efficiency of MW of 65%.

From the laboratory point of view, the patient had plateau troponin I (TnI) (0.135 > 0.133μg/L), increased NT pro-BNP and creatinine (6670 pg/m and 1.5 mg/dl, respectively), with no signs of associated infection. Cardiac catheterization was indicated to investigate coronary disease, without evidence of obstructive lesions.

The patient evolved with progressive clinical and hemodynamic improvement, being discharged from the ICU within 48 hours and responding well to the therapy instituted, without the use of supplemental oxygen and maintaining a negative fluid balance. He remained stable after converting the diuretic to oral administration, showing improvement in objective laboratory parameters (TnI: 0.135> 0.133> 0.09 μg/L; NT pro-BNP: 6670> 5594> 3818 pg/m), function stability (Cr: 1.5> 1.4> 1.5 mg/dl), in addition to improvement in dyspnea (CF II NYHA) and LL edema, with good deambulation tolerance and estimated weight loss of 3.6 kg since admission and negative cumulative fluid balance of 4,000ml.

TTE was performed at the time of hospital discharge, 72 hours after admission, with evidence of maintenance of the LVEF (26%), however, it showed indirect signs of reduced venous pressure in the right chambers (measurement of the inferior vena cava of 16mm with inspiratory collapse > 50% and minimal tricuspid valve regurgitation with Doppler curve limitation for PASP estimation). At the time of the examination, the blood pressure measured was 130 x 80 mmHg, showing new parameters: GLS of -07%, global MW index of 614 mmHg%, constructive MW of 839 mmHg%, wasted MW of 152 mmHg% and efficiency of the MW of 80%.

Keywords

Heart Failure; Ventricular Dysfunction, Left; Echocardiography

Mailing Address: Alexandre Costa Souza •
Hospital São Rafael, Ecocardiografia. Avenida São Rafael. Postal code: 41253-190. Salvador, BA – Brazil
E-mail: alexandrecostahsr@gmail.com
Manuscript received January 19, 2023; revised manuscript February 10, 2023; accepted February 11, 2023
Editor responsible for the review: Daniela do Carmo Rassi Frota

DOI: https://doi.org/10.36660/abcimg.20230008i

Discussion

In the context of assessing ventricular performance in patients with HFrHF, the GLS has become a tool with prognostic information for the follow-up of this population.[3] Nevertheless, one of the limitations of the Longitudinal Strain is the dependency on pre- and post-load, whose variations can lead to alterations in its values with subsequent interference in the results.[3] Usually, the WM can allow an in-depth evaluation of the systolic performance of the myocardium through a wide range of physiological and pathological conditions in addition to traditional echocardiographic techniques.[5] In this context, a recent study using MW in HFrEF showed greater sensitivity in the assessment of ventricular systolic function when using speckle tracking analysis of myocardial deformation combined with the measurement of non- invasively, LV ventricular pressure, reducing load-dependent limitation on myocardial contraction.[4,6]

The quantification of cardiac work occurs through the following indexes: global MW index (GWI), constructive MW (GCW), wasted MW (GWW) and global efficiency (GWE).[4] There is growing evidence about the evaluation of constructive work (GCW) after optimization of therapy in heart failure, suggesting the identification of patients at increased risk of major cardiovascular events, as well as good correlation with conventional laboratory prognostic parameters, such as NT pro-BNP and troponin values.[5] Nevertheless, reference values for patients with HFrEF have not been described, so comparative analysis of parameters before and after decongestion therapy was used. Some studies also suggest a greater sensitivity of global MW index values related to functional improvement, demonstrated by the increase in the distance covered in 6 minutes without changes in LVEF and GLS.[5]

Comparatively in the case described, there was clinical improvement, reduction in the value of NT pro-BNP, improvement in all ventricular performance parameters analyzed, as well as an increase in GLS after decongestion therapy. In the analysis of the area of the deformity-pressure curve, there was an increase in the area correlated with the improvement in metabolism and the total amount of work performed by the LV, expressed through the reduction of global wasted work and increase of global constructive work (Figure 1). Additionally, there was an increase in overall efficiency of MW from 65% to 85%, with a reduction in overall wasted work from 359 mmHg% to 152 mmHg% (Figure 2), findings in line with published studies.[3,5] The described report demonstrates the use of this tool, through the recognition of the increase in GCW and GWE with a reduction in the rate of wasted MW, which can detect early markers of the effectiveness of therapy for decompensated HFrEF.

In the context of acute decompensation of heart failure, non-invasive dynamic assessment using MW is more sensitive than GLS in characterizing myocardial performance, adding prognostic value to other parameters already established.[3,5] Additionally, the joint assessment of WM with the patient's clinical condition and laboratory tests, such as NT pro-BNP and troponin values, can help in decisions regarding the adjustment of pharmacological therapy, diuretic conversion, evaluation of hospital discharge and even in the follow-up clinical.[5]

Although it is a technique with encouraging applicability in this scenario of assessing ventricular performance in HFrEF, there are intrinsic limitations to the method that must be considered. The measurement of myocardial deformation depends on the quality of the 2D image and the frame rate, and may generate inaccurate results in the presence of limited acoustic windows as well as in the presence of non-sinusal rhythm. The software for MW analysis is owned by a single company, with low reproducibility so far; alterations in ventricular geometry, as well as the presence of aortic stenosis are conditions in which the measurement of wall stress should be included in the assessment of WM instead of, exclusively, the non-invasive estimation of LV pressure.[4] In addition, the technique does not allow the performance evaluation, combined with the speckle tracking analysis, of

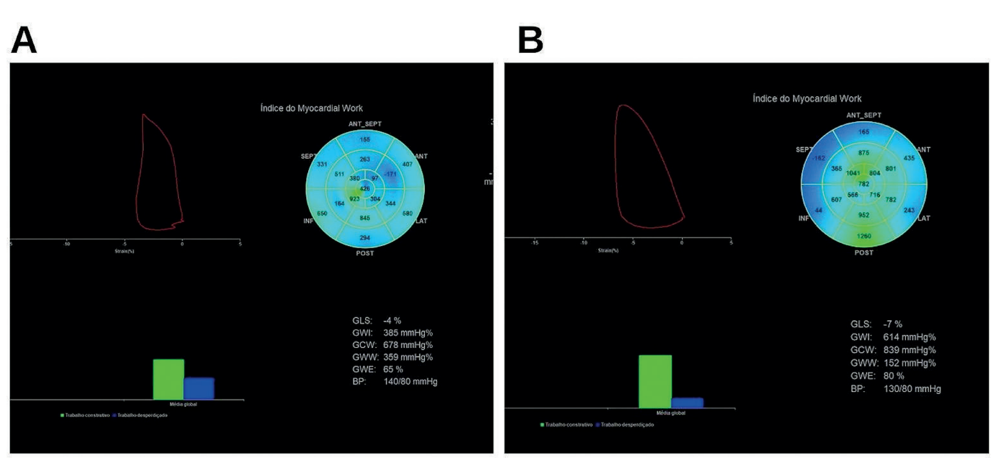

Figure 1 – *Comparative analysis of MW before and after decongestion therapy. Evaluation of the pressure-deformity curve of the left ventricle and bull's eye of the 17 segments in patients with dilated cardiomyopathy with severe ventricular dysfunction before (A) and after (B) decongestion therapy.*

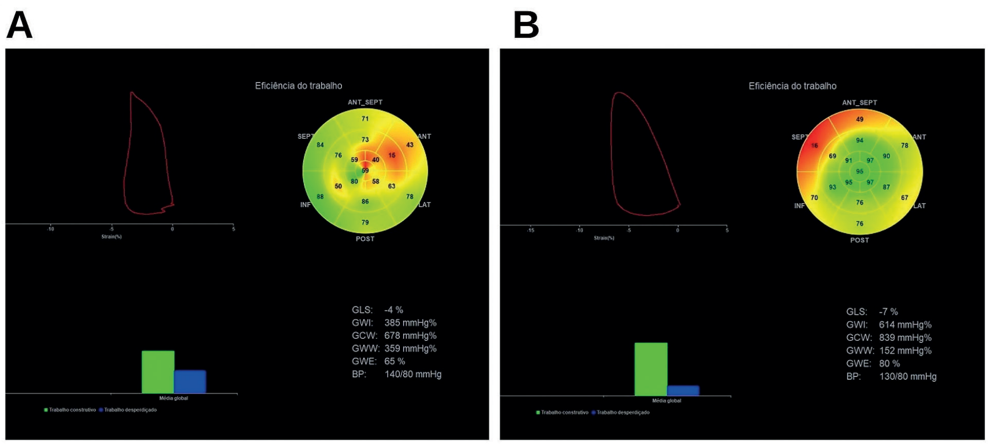

Figure 2 – *Comparative analysis of MW before and after decongestion therapy. Evaluation of the pressure-deformity curve of the left ventricle and bull's eye of the 17 segments in patients with dilated cardiomyopathy with severe ventricular dysfunction before (A) and after (B) decongestion therapy.*

other chambers, such as the right ventricle and left atrium, which are important for the global evaluation of the prognosis of patients with HFrHF.[4,5]

Additional studies are required to validate these parameters and their correlation with clinical and laboratory markers, with the possibility of adding prognostic value to this patient profile, being able to identify patients at greater risk of readmissions, as well as monitoring the response to clinical therapy.[5]

Author Contributions

Conception and design of the research: Costa A; acquisition of data: Drubi S, Chaves A; writing of the manuscript: Drubi S, Junqueira B; critical revision of the manuscript for intellectual content: Macedo CT, Guedes R.

Potential Conflict of Interest

No potential conflict of interest relevant to this article was reported.

Sources of Funding

There were no external funding sources for this study.

Study Association

This study is not associated with any thesis or dissertation work.

Ethics Approval and Consent to Participate

This article does not contain any studies with human participants or animals performed by any of the authors.

References

1. Albuquerque DC, Souza JD Neto, Bacal F, Rohde LE, Bernardez-Pereira S, Berwanger O, et al. I Brazilian Registry of Heart Failure - Clinical Aspects, Care Quality and Hospitalization Outcomes. Arq Bras Cardiol. 2015;104(6):433-42. doi: 10.5935/abc.20150031.

2. Park JJ, Park JB, Park JH, Cho GY. Global Longitudinal Strain to Predict Mortality in Patients with Acute Heart Failure. J Am Coll Cardiol. 2018;71(18):1947-57. doi: 10.1016/j.jacc.2018.02.064.

3. Wang CL, Chan YH, Wu VC, Lee HF, Hsiao FC, Chu PH. Incremental Prognostic Value of Global Myocardial Work Over Ejection Fraction and Global Longitudinal Strain in Patients with Heart Failure and Reduced Ejection Fraction. Eur Heart J Cardiovasc Imaging. 2021;22(3):348-56. doi: 10.1093/ehjci/jeaa162.

4. Roemer S, Jaglan A, Santos D, Umland M, Jain R, Tajik AJ, et al. The Utility of Myocardial Work in Clinical Practice. J Am Soc Echocardiogr. 2021;34(8):807-18. doi: 10.1016/j.echo.2021.04.013.

5. Ilardi F, D'Andrea A, D'Ascenzi F, Bandera F, Benfari G, Esposito R, et al. Myocardial Work by Echocardiography: Principles and Applications in Clinical Practice. J Clin Med. 2021;10(19):4521. doi: 10.3390/jcm10194521.

6. Boe E, Skulstad H, Smiseth OA. Myocardial Work by Echocardiography: A Novel Method Ready for Clinical Testing. Eur Heart J Cardiovasc Imaging. 2019;20(1):18-20. doi: 10.1093/ehjci/jey156.

Case Report

Acute Coronary Syndrome Followed by Pulmonary Thromboembolism and Identification of a Large Fixed Thrombus between Atria in a Patient with Severe COVID-19: A Case Report

Alice Mirane Malta Carrijo[1] *Veronica Perius de Brito,*[1] *Gabriel Alvarenga Santos,*[1] *Samuel Gomes Tomaz da Silva,*[1] *João Lucas O'Connell*[1]

Universidade Federal de Uberlândia (UFU),[1] *Uberlândia, MG – Brazil*

Introduction

Patent foramen ovale (PFO) is a relatively frequent congenital heart defect; however, the identification of large thrombi between the atria through a PFO is a rare condition.[1] When visualized, they represent a major clinical challenge and require emergency treatment.[2]

The severity of this condition becomes even more accentuated when associated with other thrombotic events, such as pulmonary embolism.[3] In turn, these events may have their genesis in hyperinflammatory states with high thrombogenic and angiopathic potential, as in the case of severe acute respiratory syndrome coronavirus 2 (SARS-CoV-2) infection.[4]

This study reports a rare case of a large fixed thrombus between the atria in a patient with severe condition caused by COVID-19, associated with the diagnosis of pulmonary embolism, which occurred days after an acute coronary syndrome (ACS) event.

Case description

We report the case of a 69-year-old female patient with grade III obesity, history of hypertension, hypothyroidism, and chronic venous insufficiency. On the sixth day of COVID-19 symptoms, the patient was hospitalized due to dyspnea and desaturation. At that time, isolation, bed rest, prophylactic anticoagulation with enoxaparin, supplemental oxygen, and non-invasive ventilatory support were required.

On the sixteenth day of evolution, the patient presented sudden-onset chest pain with tightness, radiating to the left upper limb, associated with sudden worsening of dyspnea. The electrocardiogram revealed an ST-segment elevation in the inferior wall, compatible with evolving acute myocardial infarction. The patient was referred to a tertiary hospital for diagnostic coronary angiography, which was performed more than 12 hours after the onset of symptoms, due to persistent chest pain, dyspnea and dependence on oxygen therapy. Coronary angiography showed tortuosity of the proximal segment of the right coronary artery (RCA) associated with a subocclusive stenosis of its middle segment, with an image suggestive of intracoronary thrombus (Figure 1A, 1B). No other coronary injury was observed. Primary angioplasty was carried out with drug-eluting stent implantation in the RCA, with satisfactory clinical and angiographic results (Figure 1C).

The patient was maintained on dual antiplatelet therapy with acetylsalicylic acid (ASA) and clopidogrel. On the day after angioplasty, she underwent a transthoracic echocardiogram that showed preserved cardiac chambers, left ventricular inferior wall hypokinesia, and preserved global ventricular systolic function. Moreover, the presence of a hypoechoic image with hypermobility in the left atrial cavity, measured at 60 mm × 10 mm, extending to the left ventricle, and a hypoechoic image with hypermobility in the right atrial cavity, measured at 55 mm × 10 mm, extending to the right ventricle were identified (Figure 2, Figure 3A, Video 1, Video 2), both suggestive of large intracavitary thrombi. In the diagnostic complementation by transesophageal echocardiography, a large filament image was confirmed, straddling the PFO, with mobile segments in the right and left atria (Video 3, Video 4, Video 5). No signs of pulmonary hypertension or right chamber overload suggestive of pulmonary embolism were identified.

Due to the risk of thrombus fragmentation and possible pulmonary or arterial embolization, the option of fibrinolysis was not considered. Once the characteristics and dimensions of the thrombus, the risk of pulmonary and systemic embolism, the recent infection status, the use of dual antiplatelet therapy and the increased risk of bleeding were known, surgical embolectomy was scheduled for the following days. Full anticoagulation with subcutaneous enoxaparin was initiated, and ASA was maintained.

In order to perform the embolectomy surgery, we opted to use tirofiban instead of clopidogrel, maintaining the triple therapy with enoxaparin, ASA, and tirofiban for 5 days before surgery. However, on the day immediately before surgery, a new control transthoracic echocardiogram showed that the interatrial thrombus was no longer present (Figure 3B). The presence of PFO was visualized, without associated thrombi, with left-right shunt. In view of this finding, surgical embolectomy was suspended.

Keywords

Patent Oval Foramen; Pulmonary Embolism; Case Reports

Mailing Address: João Lucas O'Connell •
Rua da Carioca, 2005, casa 852. Postal Code: 38.411-151. Morada da Colina, Uberlândia, MG – Brazil
E-mail: oconnelljl@me.com
Manuscript received October 11,2022; revised September 18, 2022; accepted March 3, 2023
Editor responsible for the review: Daniela do Carmo Rassi Frota

DOI: https://doi.org/10.36660/abcimg.2023351i

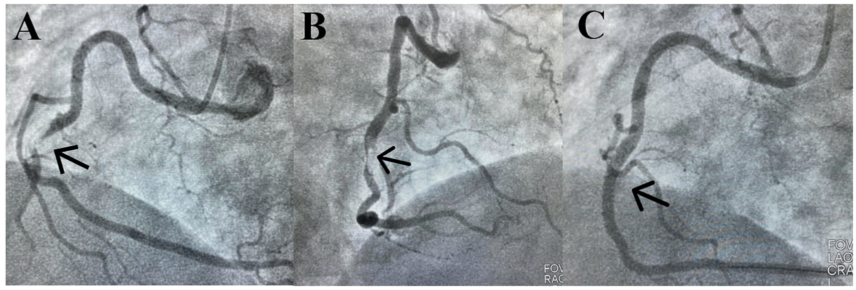

Figure 1 – *Coronary angiography. A and B: Tortuosity of the proximal segment of the RCA associated with a subocclusive stenosis of its middle segment, with an image suggestive of intracoronary thrombus; C: RCA after drug-eluting stent implantation with good angiographic result after angioplasty.*

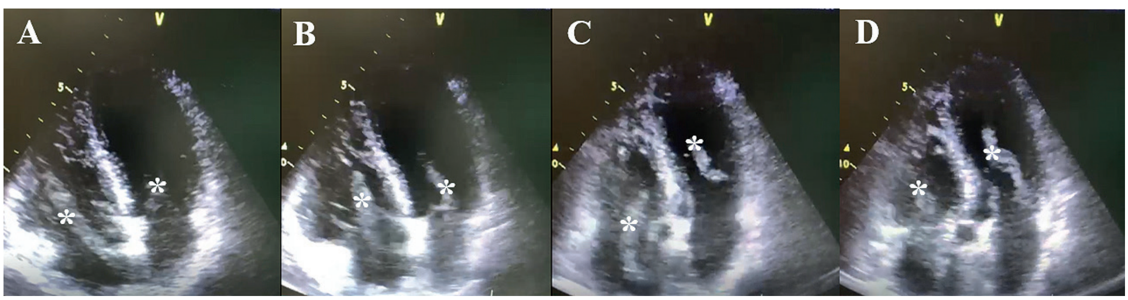

Figure 2 – **Transthoracic echocardiogram with hypoechoic image in the left and right atrial cavity extending to the left and right ventricles, respectively.*

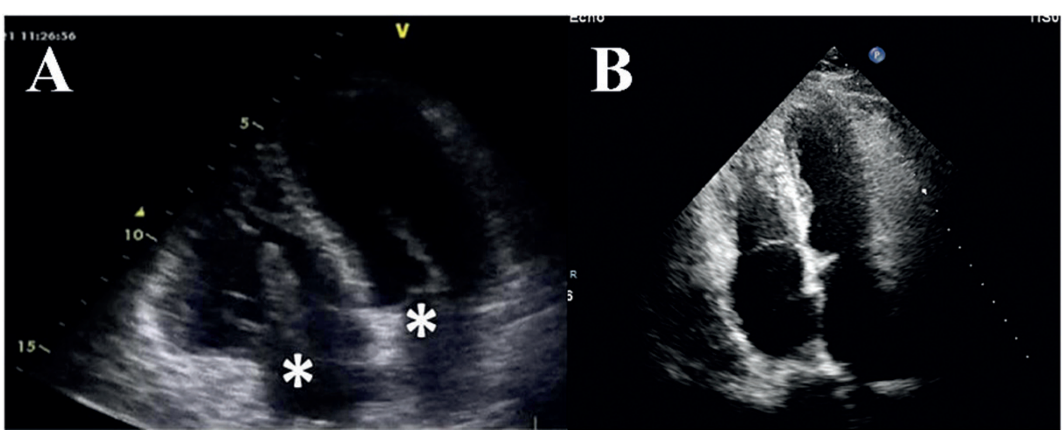

Figure 3 – **A: *Transthoracic echocardiogram with hypoechoic image in the left and right atrial cavity extending to the left and right ventricles, respectively; B: Absence of interatrial thrombus after drug therapy.*

To investigate possible thrombus fragmentation and secondary embolization, the patient underwent a pulmonary artery computed tomography angiography with iodinated contrast in cross-section. The exam demonstrated filling defects in the left pulmonary artery trunk and in segmental arterial branches to the left lower lobe, suggestive of acute pulmonary thromboembolism (Figure 4), in addition to lung parenchyma with sequelae of COVID-19. Carotid and venous Doppler results of lower limbs did not show significant changes.

Due to complete remission of the thrombus associated with PFO and clinical compensation, the patient was discharged from the hospital on day 33 of COVID-19 diagnosis, without requiring oxygen. Triple therapy (ASA, clopidogrel, and rivaroxaban) was indicated for 30 days due

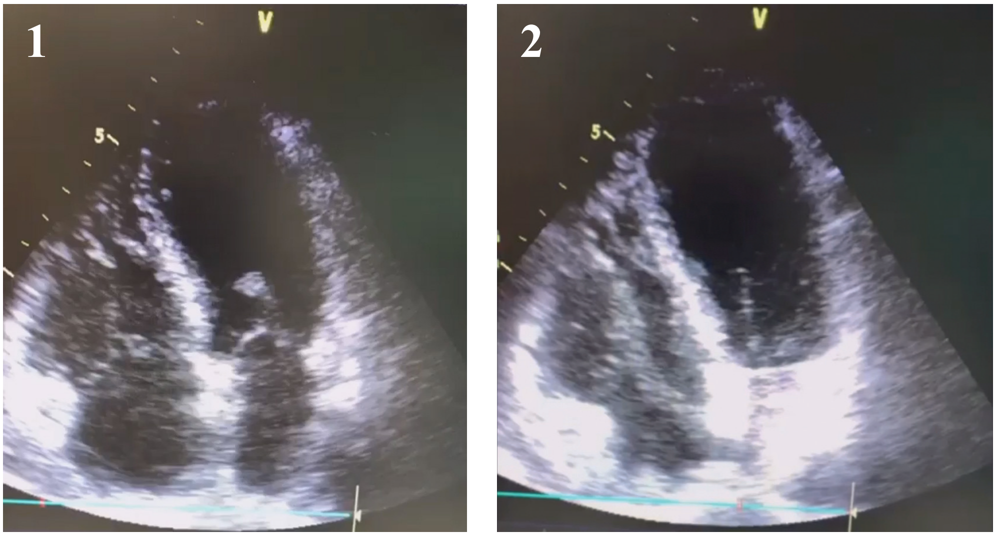

Videos 1 and 2 – *Transthoracic echocardiogram with hypoechoic image with hypermobility in the left and right atrial cavity extending to the left and right ventricles, respectively.*
Link video 1: http://abcimaging.org/supplementary-material/2023/3601/ABC 351_RC_Video1.mp4
Link video 2: http://abcimaging.org/supplementary-material/2023/3601/ABC 351_RC_Video2.mp4

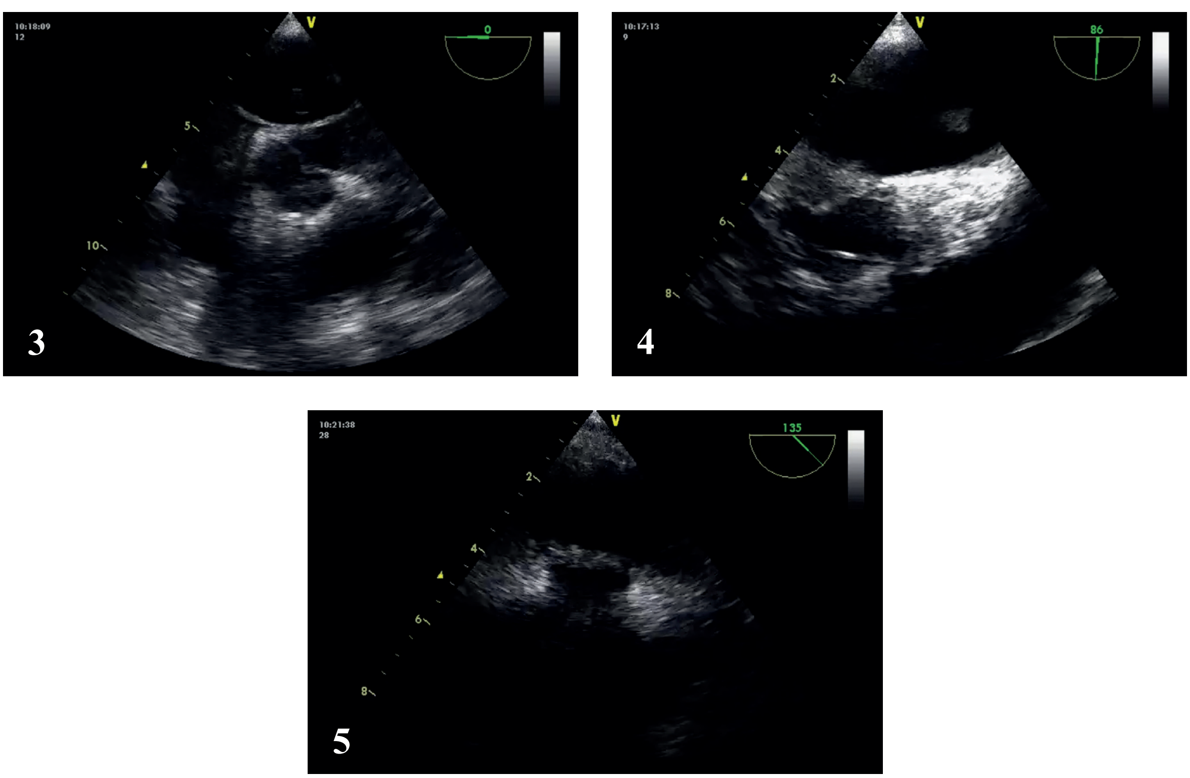

Videos 3, 4 and 5 – *Transesophageal echocardiography with hypoechoic large filament image, straddling the PFO, with mobile segments in the right and left atria.*
Link video 3: http://abcimaging.org/supplementary-material/2023/3601/ABC 351_RC_Video3.mp4
Link video 4: http://abcimaging.org/supplementary-material/2023/3601/ABC 351_RC_Video4.mp4
Link video 5: http://abcimaging.org/supplementary-material/2023/3601/ABC 351_RC_Video5.mp4

to the high thrombotic risk, in addition to beta-blocker and statin therapy for coronary artery disease. After this period, ASA was suspended, and rivaroxaban and clopidogrel were administered for at least another 6 months, to optimize the risk-benefit ratio of prophylaxis of thromboembolic events versus prevention of bleeding events.

Discussion

The case reported here exemplifies an association between COVID-19 and ACS, already observed in some patients in recent years.[5] Notably, it is not possible to state whether ACS occurred due to the classic rupture of an atherosclerotic plaque in the RCA or due to an embolus originating from the thrombus through the PFO, identified one day after the coronary event. Numerous recent reports in the literature indicate that, even without a previous atherosclerotic event,[6] the pro-inflammatory and prothrombotic state related to COVID-19 may act as triggering factors for coronary thrombosis.[5]

The increased metabolic demand caused by a viral infection can induce hypoxemia, hypotension, instability of atherosclerotic plaques, or some stress on the vascular system, thereby leading to the development of an occlusive thrombus and, consequently, ACS.[6] Furthermore, the inflammatory injury caused by SARS-CoV-2 in vascular and cardiac cells is also capable of causing ischemia or myocardial infarction.[5]

Another previously documented hypothesis is related to coagulation abnormalities, including increased prothrombin time, elevated D-dimer levels, platelet activation, and endothelial dysfunction[7] during severe cases of COVID-19. This scenario favors thrombogenesis and corroborates the occurrence of thromboembolic complications. Besides that, immobilization secondary to prolonged hospitalization also contributes to the hypercoagulable state, given the thrombogenic potential of blood stasis.[8] Additionally, obesity and chronic venous insufficiency are also risk factors for the occurrence of thromboembolic events, especially in patients with PFO.[7]

Another relevant aspect was the visualization of a thrombus trapped in the PFO during the transthoracic echocardiogram, which is a rare event.[9] Its identification requires immediate and timely treatment, especially due to the possible outcome of pulmonary or paradoxical systemic embolism.[2] If that occurs, the brain is the most frequently affected organ, followed by the coronary arteries.[1] It is not possible to state whether the identified interatrial thrombus was formed from the progression of a thrombus formed at the site or whether it was secondary to the expansion of an embolus from the lower limb or pelvis to the pulmonary artery, eventually "captured" by the PFO.

It is noteworthy that the transit of the thrombus in the interatrial septum, through the PFO, occurs when right atrial pressure exceeds left atrial pressure. This can happen in cases of acute pulmonary embolism and pulmonary hypertension.[9] In this case, the patient underwent an angiotomography of the pulmonary arteries, which showed filling failures compatible with pulmonary thromboembolism, but it was not possible to confirm the date of its occurrence.

Treatment strategy of thrombus in transit is challenging and controversial,[1,2] but three possible approaches include anticoagulation, fibrinolysis or cardiac surgery, which have particular benefits and risks.[1,2] It is worth emphasizing that anticoagulation alone is primarily used in patients with comorbidities or patients who refuse invasive therapy.[1]

Fibrinolysis should be considered in hemodynamically unstable patients with high surgical risk.[1] In view of the stability of the patient, this therapeutic option was not considered. Furthermore, this approach may cause thrombus fragmentation with subsequent pulmonary and/or systemic embolization.[1,2]

Currently, the treatment associated with a lower overall incidence of post-therapy embolic events and lower mortality is cardiac surgery for thrombus extraction.[2,3] The recommended treatment is surgical embolectomy with exploration of the right heart and closure of the PFO using cardiopulmonary bypass.[2] This was the conduct of choice for the patient in the reported case. However, surprisingly, the prescribed pre-surgical drug therapy (ASA, enoxaparin, and tirofiban for 5 days) resulted in complete disappearance of the thrombus.

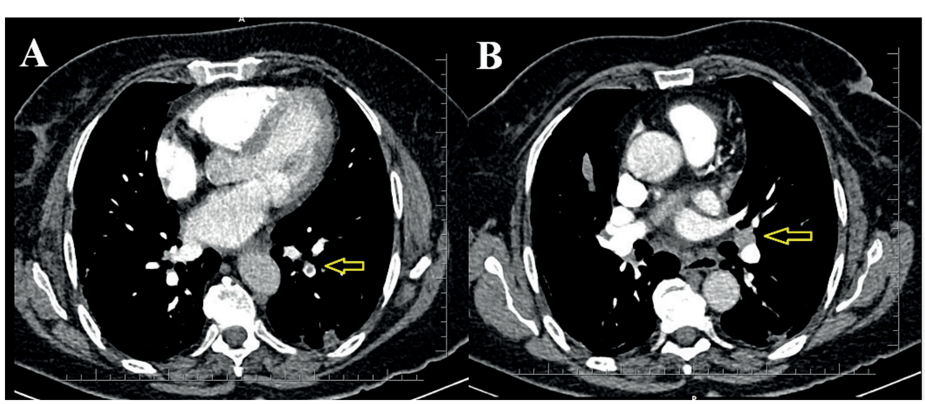

Figure 4 – *Pulmonary artery CT angiography. A: Filling defects in segmental arterial branches to the left lower lobe; B: Filling defects in the left pulmonary artery trunk.*

Considering the disappearance of the image of the interatrial thrombus and a possible pulmonary and systemic embolization,[1,2] carotid, vertebral, and lower limb Doppler scans were performed, with normal results. Nevertheless, an angiotomography of the pulmonary arteries revealed an acute pulmonary thromboembolism. It is not possible to state whether the patient had already had an episode of pulmonary embolism before the occurrence of ACS. On the one hand, the previous occurrence of pulmonary thromboembolism could facilitate the understanding of the thrombus in transit through a PFO due to the increase in right atrial pressure.[9] However, the absence of signs of pulmonary hypertension and right chamber overload on the first echocardiogram makes it difficult to defend this thesis to explain the pathophysiological mechanism. Thus, the occurrence of pulmonary embolism as a consequence of the dissolution of the interatrial thrombus through drug therapy used seems more plausible.

The uniqueness of the case reported, as a limitation of the study, makes it difficult to generalize the results and conclusions obtained in our analysis; furthermore, it supports the replication of the procedures used.

Author Contributions

Conception and design of the research and acquisition of data: Carrijo AMM, Brito VP, Santos GA, Silva SGT; analysis and interpretation of the data and writing of the manuscript: Carrijo AMM, Brito VP, Santos GA, Silva SGT, O'Connell JL; critical revision of the manuscript for intellectual content: O'Connell JL.

Potential Conflict of Interest

No potential conflict of interest relevant to this article was reported.

Sources of Funding

There were no external funding sources for this study.

Study Association

This study is not associated with any thesis or dissertation work.

Ethics Approval and Consent to Participate

This study was approved by the Ethics Committee of the Universidade Federal de Uberlândia under the protocol number 5.455.568. All the procedures in this study were in accordance with the 1975 Helsinki Declaration, updated in 2013. Informed consent was obtained from all participants included in the study.

References

1. Pires MIFB, Almeida I, Santos JM, Correia M. Thrombus in Transit Through a Patent Foramen Ovale: Catch it if You Can-a Case Report. Eur Heart J Case Rep. 2021;5(10):ytab382. doi: 10.1093/ehjcr/ytab382.
2. Cakir C, Duygu H, Eren NK, Akyildiz ZI, Nazli C, Ergene O. Witnessing a Rare Event - Thrombus Seeking its Route in the Right Atrium: 'Thrombus-In-Transit'. J Cardiovasc Med. 2008;9(11):1166-8. doi: 10.2459/JCM.0b013e328311eed8.
3. Seo WW, Kim SE, Park MS, Lee JH, Park DG, Han KR, et al. Systematic Review of Treatment for Trapped Thrombus in Patent Foramen Ovale. Korean Circ J. 2017;47(5):776-85. doi: 10.4070/kcj.2016.0295.
4. Borges NH, Godoy TM, Pereira MRC, Stocco RB, Dias VMCH, Baena CP, et al. Pulmonary Thromboembolism in a Young Patient with Asymptomatic COVID-19. Arq Bras Cardiol. 2020;115(6):1205-7. doi: 10.36660/abc.20200957.
5. Kermani-Alghoraishi M. A Review of Coronary Artery Thrombosis: A New Challenging Finding in COVID-19 Patients and ST-elevation Myocardial Infarction. Curr Probl Cardiol. 2021;46(3):100744. doi: 10.1016/j.cpcardiol.2020.100744.
6. Kwong JC, Schwartz KL, Campitelli MA, Chung H, Crowcroft NS, Karnauchow T, et al. Acute Myocardial Infarction after Laboratory-Confirmed Influenza Infection. N Engl J Med. 2018;378(4):345-53. doi: 10.1056/NEJMoa1702090.
7. Zadow EK, Wundersitz DWT, Hughes DL, Adams MJ, Kingsley MIC, Blacklock HA, et al. Coronavirus (COVID-19), Coagulation, and Exercise: Interactions That May Influence Health Outcomes. Semin Thromb Hemost. 2020;46(7):807-14. doi: 10.1055/s-0040-1715094.
8. Engbers MJ, Blom JW, Cushman M, Rosendaal FR, van Hylckama Vlieg A. The Contribution of Immobility Risk Factors to the Incidence of Venous Thrombosis in an Older Population. J Thromb Haemost. 2014;12(3):290-6. doi: 10.1111/jth.12480.
9. Baydoun H, Barakat I, Hatem E, Chalhoub M, Mroueh A. Thrombus in Transit through Patent Foramen Ovale. Case Rep Cardiol. 2013;2013:395879. doi: 10.1155/2013/395879.

Expandable Airway Stents: Success in the Extrinsic Bronchial Compression Approach After Reconstruction of the Aortic Arch

Camila Magalhães Silva,[1] Adriana Furletti Machado Guimarães,[1] Ricardo Wang,[1] Carla Maria Silva e Alves,[1] Edmundo Clarindo Oliveira[1]
Hospital das Clínicas da Universidade Federal de Minas Gerais,[1] Belo Horizonte, MG – Brazil

Introduction

The interruption of the aortic arch is a rare congenital cardiopathy, whose surgical correction generally requires reconstruction of the aortic arch. This intervention can cause distortion of the aortopulmonary space and results in bronchial compression with a consequent pulmonary atelectasis and dependence on ventilatory assistance. The most commonly used therapeutic options for bronchial decompression are not always enough to make pulmonary expansion possible. Our study presents a case of the implant of an endoluminal stent in an infant who, in the post-operative stage of the correction of the interruption of the aortic arch, developed complete atelectasis of the left lung secondary to bronchial compression, with no response after posterior aortopexy

Case Report

Our study presents the case of a 3-year-old, preschool, female patient with a diagnosis of the interruption of the aortic arch and a major interventricular communication, submitted to the reconstruction of the aortic arch at 13 days of life, with end-to-side anastomosis of the descending aorta with the ascending aorta, due to the large distance from the stumps and difference in the diameter of the aortic extremities.

In post-op, the patient presented complete and persistent atelectasis of the left lung (Figure 1A) and was kept on mechanical ventilation with high-level parameters, with no possibility of extubation.

Bronchoscopy suggested an extrinsic compression of the proximal portion of the left bronchus, a hypothesis confirmed by angiotomography, which demonstrated an external vascular compression of the main left bronchus between the left atrium and the descending aorta (Figure 2A).

Despite the tracheostomy performed at two months of age and positive pressure ventilation, the child continued with a collapsed left lung and frequent episodes of hypoxia. At three months of age, she was submitted to aortopexy, which promoted an adequate distancing of the aorta from the bronchus, but this did not result in lung aeration, demonstrating damage to the bronchial structure. A resection of the altered tracheal segment was contraindicated due to technical difficulties and the severity of the ventilatory condition.

At four months, after a multidisciplinary discussion, an expandable mechanical stent (Cordis Palmaz® Blue™ 5x15 mm) was implanted in the left bronchus by the hemodynamic service team (Video 1). Hence, progressive aeration of the affected lung (Figure 1B) led to a decrease in the ventilatory parameters. The child evolved with refractory heart failure due to the drug treatment, and was thus submitted to surgical correction of the ventricular septal defect and an implant of a stent in the anastomosis region of the aorta (Video 1), which proved to be stenotic, with good results.

During bronchoscopy follow-up, an excessive proliferation of the granulation tissue was observed (Figure 3A), causing a progressive obstruction of the bronchial light, with no response to the three attempts of balloon dilatation and consequent total obstruction after three months of stent implant.

As the child presented a good respiratory pattern, using oxygen inhaled through the tracheostomy, she was released at eight months of life, with the proposal of the evaluation of the implant of a new bronchial stent *(Dynamic Renal®* 5x15 mm*)*.

At approximately one year of life, five months after bronchoscopic confirmation of the total obstruction of the stent, a chest X-ray, performed within an infectious context, showed left lung aeration (Figure 1c).

At one year and six months, the child was admitted to an intensive care unit (ICU) with a severe respiratory failure. The chest X-ray showed a diaphragmatic hernia on the right side and complete aeration of the left lung (Figure 1D), confirmed through chest computed tomography (CT) (Figure 2B) and bronchoscopy (Figure 3B, video 2). After having performed surgery to correct the Morgani hernia, the child was released in good condition, with planning to be gradually weaned off of the tracheostomy.

Discussion

Bronchial compression is a potentially severe complication described in both the pre-operative and post-operative stages of congenital cardiopathies with an obstruction of the aortic arch, such as the coarctation of the aorta, the interruption of the aortic arch, and left heart syndrome. The altered relation between the blood vessels of the arch and the tracheobronchial tree found in these pathologies causes

Keywords

Stents; Cardiology Service, Hospital; Pediatrics

Mailing Address: Camila Magalhães Silva •
Hospital das Clínicas da Universidade Federal de Minas Gerais. Avenida Alfredo Balena, 100. Postal code: 30130-100. Santa Efigênia, Belo Horizonte, MG – Brazil
E-mail: camila.magalhaes@live.com
Manuscript received March 6, 2023; revised manuscript April 12, 2023; accepted April 28, 2023
Editor responsible for the review: Karen Saori Shiraishi Sawamura

DOI: https://doi.org/10.36660/abcimg.20230023i

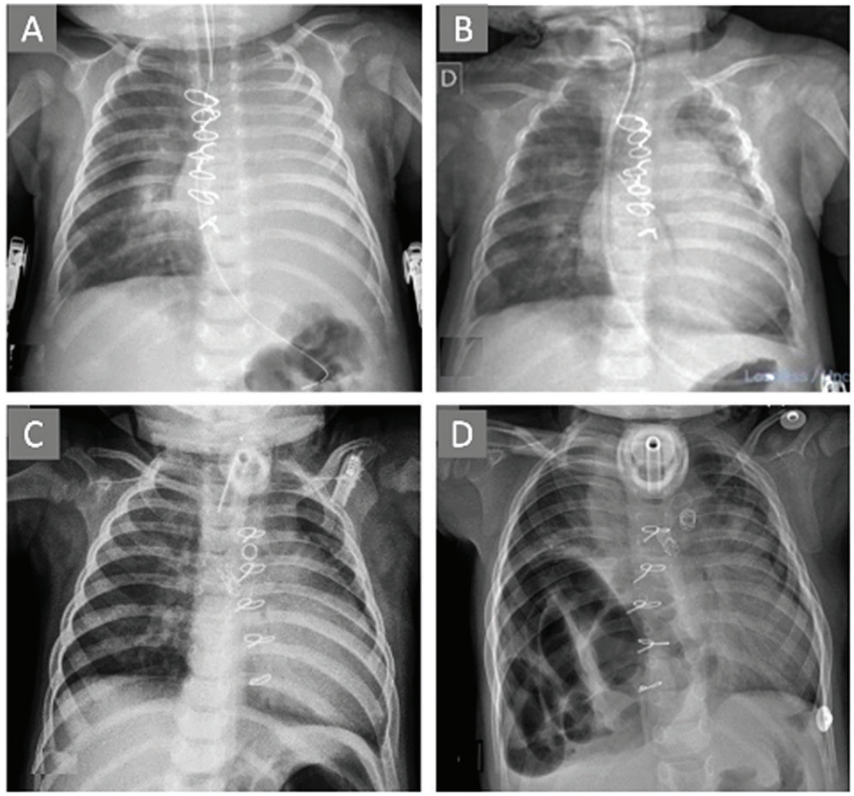

Figure 1 – *A) complete atelectasia of the left lung in the post-operative stage immediately after correction of the aortic arch; B) left lung aeration shortly after the endoluminal stent implant in the left bronchus; C) late aeration of the left lung after the spontaneous resolution of the obstruction of the stent; D) right diaphragmatic hernia, left lung aerated.*

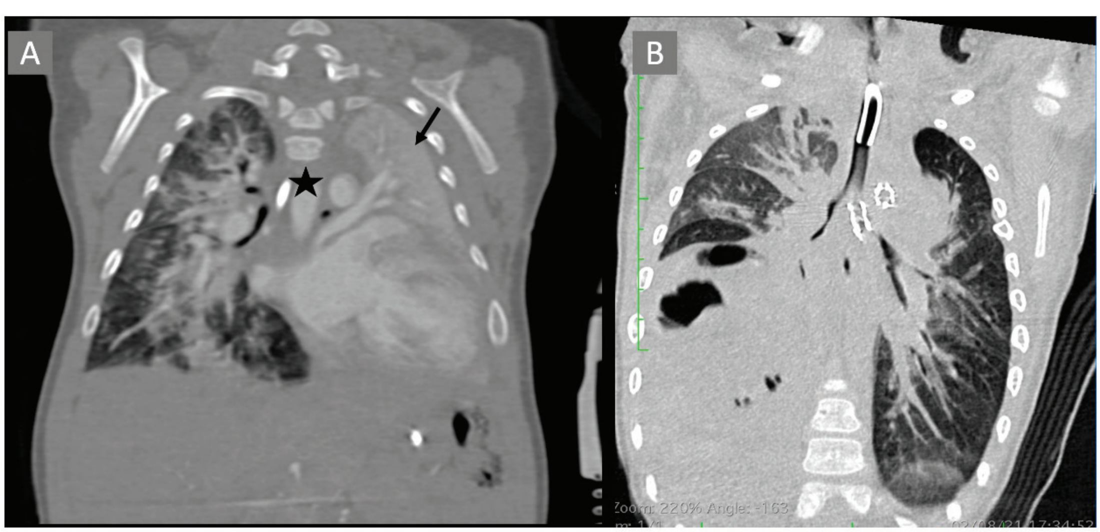

Figure 2 – *A) extrinsic compression of the main left bronchus (arrow: left lung without aeration; star: aorta compressing the bronchus); B) left lung aeration even in the face of a right diaphragmatic hernia.*

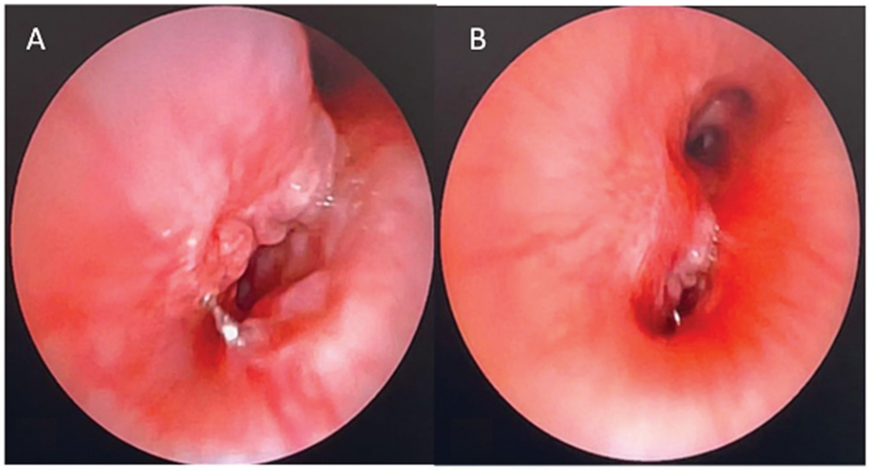

Figure 3 – *A) endoluminal stent in the left bronchus with proliferation of the granulation tissue; B) stent in the left bronchial light, causing progressive obstruction of the bronchial light, partial resolution.*

a distortion and straightening of the aortopulmonary space, and can lead to an extrinsic bronchial compression.[1,2] In this case, this alteration occurred in the geometry and position of the aortic arch after the surgical correction of the interruption.

The knowledge of a possible compression of the airways is of utmost importance, as its incidence can reach 27.2% in the pre-operative and 33.3% in the post-operative stages of cardiopathies that require the reconstruction of the aortic arch, according to findings from Jhang et al.[1]

The respiratory symptoms are generally unclear and may be absent in many cases.[2,3] In a study conducted by An et al., only 50% of the patients with airway compression found in CT images presented symptoms.[2] The bronchoscopy enabled the direct viewing of the compression of the tracheobronchial tree, while the CT enabled the evaluation of the spatial region between the airway and cardiovascular structures, and should therefore be considered, especially in patients with persistent atelectasis and failure to wean off of mechanical ventilation.[3-5]

The early diagnosis of this medical condition is essential, since a prolonged bronchial compression can cause significant functional involvement and tracheobronchomalacia, which can persist even after the release of extrinsic compression[2-5], as observed in the case described above.

If on the one hand the diagnosis of airway compression can be easily performed, the therapeutic handling can be challenging, especially in cases of severe residual malacia. The choice between a surgical option, such as posterior aortopexy, the remodeling of the aortic arch, and transverse extension of the aortic arch using an autograft of the pulmonary artery, as compared to a conservative conduct,[1,6] should be based on the severity of the obstruction and the clinical condition of the patient.[2,5] The tracheostomy with prolonged mechanical ventilation has been proposed when one considers the tracheomalacia to be self-limited, with progressive improvement during childhood.[5] In this case report, even if one had removed the bronchial compression, posterior aortopexy did not result in lung aeration, illustrating damage to the bronchial structure.

In recent years, attention has been geared toward placing the endoluminal stent in airways in severe cases of bronchomalacia that did not respond to the implemented therapy. Barnes et al. described the successful use of the stent in a case of severe bronchomalacia after stage I of the Norwood procedure, which was not reverted after posterior aortopexy.[7] Arcieri et al. also reported the use of the left bronchial stent in six patients with severe residual bronchomalacia after posterior aortopexy; however, these authors only analyzed the results of aortopexy.[4] In the study conducted by Serio et al., the stent implant restored the spontaneous respiration in 20 patients with severe residual malacia after surgery.[8] Based on these descriptions and faced with the complexity of the case and absence of new surgical proposals, we chose the endobronchial stent implant.

Although the stent implant in airways is a tempting conduct, as it can quickly restore the permeability of the bronchus and enable pulmonary aeration, it is not free of complications, such as migration, fracture, obstruction caused by mucus and granulation tissue, the rupture of the airways, and infection.[9,10] The formation of the granulation tissue is a constant, since the airway stent did not become epithelated like the endovascular stent.[5] In the case described herein, we detected the proliferation of serial dilatations with a balloon catheter, but with a partial and spontaneous resolution after nearly five months, most likely after a decrease in the reactional inflammatory process.

Therefore, a recommendation must first undergo a detailed analysis, since the stents are easy to implant, but difficult to remove, especially metallic stents, which should be considered permanent.[5]

Complication related to the use of the stent indicate the need for protocols to maintain the permeability of the lumen[9] and for regular follow-up by bronchoscopy and/or CT in order to achieve an early identification of the complications.[9,10]

Conclusions

Bronchial compression after the reconstruction of the aortic arch is a severe complication, which one may not be able to solve with available surgical interventions. In these cases, the stent implant in the location where the bronchial light is tapered can represent a successful alternative, though reserved for children in a critical condition, whose airway decompression surgery did not result in affective lung aeration.

Author Contributions

Conception and design of the research: Guimarães AFM; acquisition of data: Silva CM, Guimarães AFM, Wang R, Alves CMS, Oliveira EC; analysis and interpretation of the data: Wang R, Alves CMS, Oliveira EC; writing of the manuscript: Silva CM, Guimarães AFM; critical revision of the manuscript for intellectual content: Guimarães AFM, Oliveira EC.

Potential Conflict of Interest

No potential conflict of interest relevant to this article was reported.

Sources of Funding

There were no external funding sources for this study.

Study Association

This study is not associated with any thesis or dissertation work.

Ethics Approval and Consent to Participate

This article does not contain any studies with human participants or animals performed by any of the authors.

References

1. Jhang WK, Park JJ, Seo DM, Goo HW, Gwak M. Perioperative Evaluation of Airways in Patients with Arch Obstruction and Intracardiac Defects. Ann Thorac Surg. 2008;85(5):1753-8. doi: 10.1016/j.athoracsur.2008.01.059.
2. An HS, Choi EY, Kwon BS, Kim GB, Bae EJ, Noh CI, et al. Airway Compression in Children with Congenital Heart Disease Evaluated Using Computed Tomography. Ann Thorac Surg. 2013;96(6):2192-7. doi: 10.1016/j.athoracsur.2013.07.016.
3. Kim YM, Yoo SJ, Kim WH, Kim TH, Joh JH, Kim SJ. Bronchial Compression by Posteriorly Displaced Ascending Aorta in Patients with Congenital Heart Disease. Ann Thorac Surg. 2002;73(3):881-6. doi: 10.1016/s0003-4975(01)03405-1.
4. Arcieri L, Serio P, Nenna R, Di Maurizio M, Baggi R, Assanta N, et al. The Role of Posterior Aortopexy in the Treatment of Left Mainstem Bronchus Compression. Interact Cardiovasc Thorac Surg. 2016;23(5):699-704. doi: 10.1093/icvts/ivw209.
5. McNamara VM, Crabbe DC. Tracheomalacia. Paediatr Respir Rev. 2004;5(2):147-54. doi: 10.1016/j.prrv.2004.01.010.
6. Maddali MM, Kandachar PS, Al-Hanshi S, Al Ghafri M, Valliattu J. Mechanical Cause for Acute Left Lung Atelectasis after Neonatal Aortic Arch Repair with Arterial Switch Operation: Conservative Management. Ann Card Anaesth. 2017;20(2):252-5. doi: 10.4103/aca.ACA_197_16.
7. Barnes JH, Boesch RP, Balakrishnan K, Said SM, van Dorn CS. Temporary Bronchial Stenting for Airway Compression in the Interstage Palliation of Functional Single Ventricle. Ann Pediatr Cardiol. 2019;12(3):308-11. doi: 10.4103/apc.APC_94_18.
8. Serio P, Nenna R, Fainardi V, Grisotto L, Biggeri A, Leone R, et al. Residual Tracheobronchial Malacia after Surgery for Vascular Compression in Children: Treatment with Stenting. Eur J Cardiothorac Surg. 2017;51(2):211-7. doi: 10.1093/ejcts/ezw299.
9. Liu L, Kong J, George C. Recent Advances in Airway Stenting. Shanghai Chest. 2020;4:1-14. doi: 10.21037/shc.2019.11.02.
10. Folch E, Keyes C. Airway Stents. Ann Cardiothorac Surg. 2018;7(2):273-83. doi: 10.21037/acs.2018.03.08.

*Supplemental Materials

For supplementary figure, please click here.
For supplementary tables, please click here.
See the Supplemental Video 1, please click here.
See the Supplemental Video 2, please click here.

Patent Forame Ovale: Contribution of Transcranial Doppler in Patient Diagnosis

Eliza de Almeida Gripp,[1,2] Ana Carolina de Freitas Portela,[1] Flávio Luis da Costa Junior,[1] Rafael Rabishoffsky,[1] Jéssica Rizkalla Corrêa Medeiros,[1] Arnaldo Rabischoffsky[1]

Hospital Pró-cardíaco,[1] Rio de Janeiro, RJ – Brazil

Universidade Federal Fluminense,[2] Niterói, RJ – Brazil

Introduction

Patent forame ovale (PFO) is the most common type of interatrial shunt, with a prevalence between 25% and 27% of the adult population. It has a flap-like functioning and is generally asymptomatic. In some cases, it can be associated with clinical complications, such as brain strokes, paradoxical embolism, platypnea-orthodeoxia syndrome, and obstructive sleep apnea. The diagnosis is mainly found in young patients who present brain strokes, with no other apparent risk factor.[1]

The evaluation of PFO is commonly performed by means of transthoracic echocardiogram (TTE) and transesophageal echocardiogram (TEE). However, another important method of evaluation that is rarely used in our area is the Transcranial Doppler (TCD), which evaluates the presence of an indirect shunt in an awake patient and with high sensitivity.[2]

This article reports on two cases and demonstrates the TCD value in the initial screening in patients suspected of PFO.

Case 1

M.C., male, 57 years of age, with systemic arterial hypertension presented amaurosis fugax of the right eye. The patient underwent a cranial tomography, which presented a stroke in the region of the cerebellum. The 24-hr Holter showed no atrial fibrillation. The patient was referred to a reference center to undergo TCD, TTE, and TEE, sequentially, for etiological investigation. The TCD study was performed, following important steps. First, peripheral venous access was obtained in the right upper membrane (Figure 1A) for the injection of agitated saline solution (microbubbles), enabling the analysis in real time of the presence of high intense temporary signal (HITS) in the middle cerebral artery (MCA) directly through the transtemporal window. Next, the patient was asked to undergo the Valsalva maneuver (strain phase), and finally, shortly after the injection of microbubbles, the patient was asked to undergo the release phase. Through the Spectral Doppler of the MCA, HITS was visualized, defining the presence of the R-L shunt during the first three cardiac cycles. The image was easily acquired through the TCD resulting from the Valsalva maneuver, a situation commonly faced in the TTE. Once the presence of the shunt had been defined, the next step was to confirm its cardiac origin (Figure 1B and C).

After, the patient underwent a TTE with microbubbles, associated with the Valsalva maneuver, which showed, with the passage of the microbubbles from the right to the left atrium in the first three cycles in the apical plane, four chambers through the fossa ovalis, suggestive of PFO. Three injections of saline solution were necessary, since during the release phase of the Valsalva maneuver, there was a loss of the echocardiographic window (Figure 1C).

The TTE was conducted to adequately visualize the characteristics of the interatrial septum and PFO, focused on percutaneous closure, with no observation of an interatrial septum aneurysm, redundant Eustachian valve, or other interatrial septum defects (Figure 2).

Case 2

V.L.O.M., female, 32 years of age, with no comorbidities, but with a report of ischemic stroke. The patient was referred for echocardiographic study to evaluate the cardioembolic source. The 24-hr Holter showed atrial fibrillation. The same previous sequence of exams was carried out in this patient. During the TCD, the number of HITS was significant, suggesting a R-L shunt when compared to the previous patient (Figure 3A). The TTE (Figure 3B) and the TEE (Figure 4A and 4B) showed an interatrial septum aneurysm associated with PFO and a large shunt. It is important to highlight that, in this case, to visualize the flow through the PFO, some injections of saline solution were made due to the difficulty to conduct an effective Valsalva maneuver in a sedated patient.

Discussion

The brain stroke is the main cause of morbidity in the Brazilian population and its socioeconomic impact is highly significant, especially among young individuals, considered to be a portion of the active population of the country.[3]

The cryptogenic brain stroke (with no defined cause) occurs in a significant number of patients; however, 3% – 40% of the cases present PFO as the cause.

Keywords

Echocardiography, Doppler; Patente; Foramen Ovale; Ultrasonography, Doppler, Transcranial

Mailing Address: Eliza de Almeida Gripp •
Hospital Pró-cardíaco. Rua General Polidoro, 192. Postal Code: 22280-003. Botafogo, Rio de Janeiro, RJ – Brasil
E-mail: elizagripp@yahoo.com.br
Manuscript received February 26, 2023; revised manuscript May 7, 2023; accepted May 11, 2023
Editor responsible for the review: Daniela do Carmo Rassi Frota

DOI: https://doi.org/10.36660/abcimg.20230020i

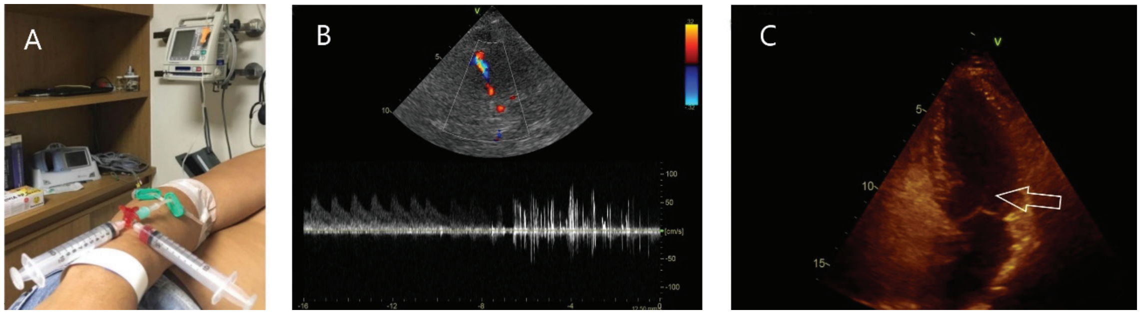

Figure 1 – *A) Illustation of the system set up for the infusion of agitated saline solution. First, the peripheral venous access is acquired in the right upper membrane, with a 24g caliber intravenouos catheter. The dual-valve short polifix is then connected to the catheter, attached to a three-valve tap: in one of the entrance valves of the polifix and in the other valve, a salinized vial with 100 ml of saline solution (this should fill the entire vial, making innumerous injections possible). Connect the two syringes of 10ml in the tap and aspirate 9ml of saline solution and 1ml of air to mix the content of the syringes until a whitish coloration is obtained. If necessary, aspirate a small quantity of blood to obtain a greater contrast. It is important to maintain the plunger of the syringe positioned upwards when introducing into the patient so as not to inject air through the syringe. B) TCD showing a flow in the MCA with the presence of HITS after the injection of saline solution. C) 4-chamber apical plane of the TTE, showing the passage of microbubbles (arrow) through the PFO, in the first three cycles after the injection of agitated saline.*

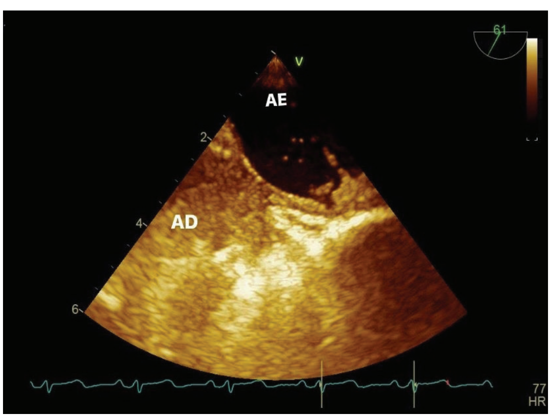

Figure 2 – *TEE showing the passage of microbubbles from the right atrium to the left atrium. LA: left atrium; RA: right atrium.*

PFO is a well-known cause of brain strokes, found in 27% of all autopsies, and the diagnosis is mainly found in young individuals with no risk factor.[4,5]

During the fetal period, the PFO is an embryonic structure resulting from an incomplete fusion of the septum primum and septum secundum, which work as a single valve, enabling the passage of oxygenated blood to the left atrium, to the left ventricle, and for systemic circulation, without passing through pulmonary circulation. After birth, PFO closure occurs, since the right atrial pressure decreases and the blood passes through pulmonary circulation. The complete fusion occurs in 75% of the cases. In those in which it remains, the PFO works as an intermittent valve, and the occurrence of the R-L shunt can lead to an embolic event.[6]

The Valsalva maneuver was described by Dr. Antonio Valsalva in 1704 in Bolonha. It is performed by asking the patient to cough, or to make an effort, such as that of

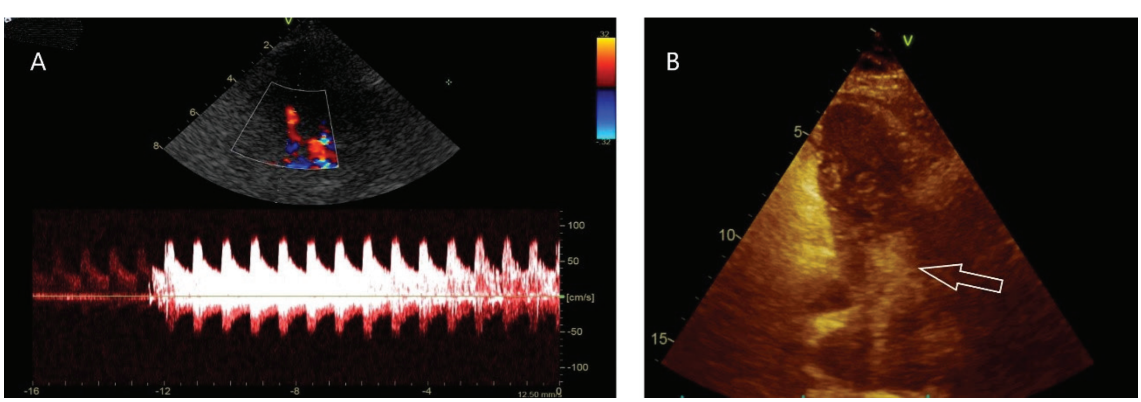

Figure 3 – *A) TCD demonstrating the presence of a significant number of HITS in the Spectral Doppler of the MCA. B) 4-chamber apical plane of the TTE with passage in the first three cardiac cycles of innumerous microbubbles through the PFO.*

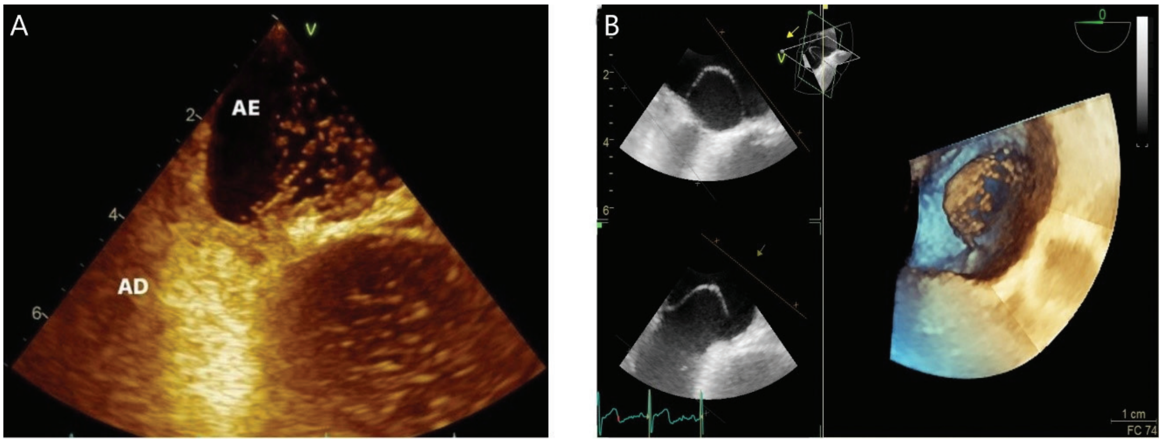

Figura 4 – *A) ETE demonstrando passagem de microbolhas do átrio direito para o átrio esquerdo. B) Imagem tridimensional do septo interatrial pela perspectiva do átrio esquerdo, evidenciando o aneurisma do septo e microbolhas em sua parede. AE: átrio esquerdo; AD: átrio direito.*

defecating or blowing in an instrument, causing an acute increase in the intrathoracic and abdominal pressure. During the strain phase, a decrease in the venous return occurs from the left to the right side, while during the release phase, the right atrium abruptly receives a large volume of blood, greater than the volume of blood through the pulmonary veins to the left atrium. The right atrial pressure in relation to the left atrium favors the appearance of PFO. One piece of data suggests that the Valsalva maneuver was effective, as was the bulge of the right atrium with agitated saline solution.[7] As these two findings are not always present in the echocardiographic studies, it is recommended that the patient receive a greater number of injections in order to increase the sensitivity of the exam. The Valsalva maneuver is, therefore, essential to detect it, since in the case of the PFO, the shunt can be transitory and is not always detected. Another piece of data that demonstrates that the maneuver was adequate is the decrease in speed of the E wave in the mitral flow by 20 cm/s, shown through the pulsed Doppler.[1,8]

The TTE with microbubbles associated with the Valsalva maneuver is the most commonly used due to its broad availability, not requiring sedation or an invasive procedure, only needing peripheral access (antecubital). The mixture of the agitated saline solution with a small quantity of blood increases the sensitivity of the exam. The study is considered positive for the R-L shunt through PFO when the passage of microbubbles occurs in the first three cardiac cycles. In this case, it is paramount that the electrocardiogram of the heart be firmly attached to the patient. The exam should perform a recording with a high number of cardiac cycles in order to safely check when the passage of the microbubbles occurs. It is important to highlight the differential diagnosis of PFO with arteriovenous pulmonary fistulas. In this pathology, a R-L shunt will occur after the fourth cardiac cycle. However, the TTE presents a low resolution and a low sensitivity when compared to the TEE with microbubbles.[2] The loss of the image in the apical plane of the four chambers is common with the Valsalva maneuver, thus hindering the diagnosis.

The TEE with microbubbles is considered to be the method of choice, as it confirms the presence of the PFO and studies the anatomy of the interatrial septum, classifying it as simple or complex, using the following variables: tunnel size (>8 mm), presence of the redundant Chiari network, fenestrations, and interatrial septum aneurysm. These data are important for the recommendation of the percutaneous closure of the PFO.[9] In addition, the TEE evaluates other sources of embolism, such as thrombi in the left atrial appendix or in the atriums, the presence of an atrial appendage, or atheromatous plaques in the thoracic aorta. In the cases in which it is difficult to conduct the Valsalva maneuver due to sedation, abdominal or inferior vena cava compression can be used to increase its sensitivity to detect the passage of the R-L flow through the PFO.[2,8]

The TCD is considered to be highly sensitive to the detection and quantification of the R-L shunt. It is a non-invasive, economical, and safe exam, which does not require sedation. However, it does have the limitation of the incapacity to define the origin of the shunt. The exam can be conducted through the transtemporal window, with the transducer index pointed to the right of the patient. The Spectral Doppler of the MCA shows the presence of HITS after the injection of microbubbles associated with the Valsalva maneuver, which does not hinder the capture of the image of the flow through the MCA. The diagnosis of the shunt is defined by the presence of one or more HITS. The intensity of the shunt can be quantified using the Spencer logarithmic scale. This can be graded from degree 0 – absence of HITS; degree 1 – 1 to 10 HITS; degree 2 – 11 to 30 HITS; degree 3 – 31 to 100 HITS; degree 4 – 101 to 300 HITS; and degree 5 – > 300 HITS ("curtain effect").[10] In a meta-analysis of 27 prospective studies, with 1,968 patients, which compared the TCD and the TEE with microbubbles, presented a 97% sensitivity and a 93% specificity to detect right-left intracardiac shunts, as compared to the TEE, which presented sensitivity values of 91-100% and specificity values of 88-97%.[2] This study shows how the TCD is an important tool that can be used in the initial screening of patients suspected of PFO.

In sum, the TCD is a diagnostic tool that should be used in the initial investigation of patients with brain strokes, especially in those in which the detection of a R-L shunt through the PFO is important for therapeutic handling.

Acknowledgements

We wish to thank Laryssa da Silva Siqueira's nursing team for their contribution to the write-up of this article.

Author Contributions

Writing of the manuscript: Gripp EA, Portela ACF, Rabischoffsky A; critical revision of the manuscript for intellectual content: Gripp EA, Costa Júnior FL, Rabishoffsky R, Medeiros JRC, Rabischoffsky A.

Potential Conflict of Interest

No potential conflict of interest relevant to this article was reported.

Sources of Funding

There were no external funding sources for this study.

Study Association

This study is not associated with any thesis or dissertation work.

Ethics Approval and Consent to Participate

This article does not contain any studies with human participants or animals performed by any of the authors.

References

1. Johansson MC, Eriksson P, Guron CW, Dellborg M. Pitfalls in Diagnosing PFO: Characteristics of False-Negative Contrast Injections During Transesophageal Echocardiography in Patients with Patent Foramen Ovales. J Am Soc Echocardiogr. 2010;23(11):1136-42. doi: 10.1016/j.echo.2010.08.004.
2. Mahmoud AN, Elgendy IY, Agarwal N, Tobis JM, Mojadidi MK. Identification and Quantification of Patent Foramen Ovale-Mediated Shunts: Echocardiography and Transcranial Doppler. Interv Cardiol Clin. 2017;6(4):495-504. doi: 10.1016/j.iccl.2017.05.002.
3. Brasil. Ministério da Saúde. Anuário Estatístico de Saúde no Brasil. Brasília: Ministério da Saúde; 2001.
4. Lechat P, Mas JL, Lascault G, Loron P, Theard M, Klimczac M, et al. Prevalence of Patent Foramen Ovale in Patients with Stroke. N Engl J Med. 1988;318(18):1148-52. doi: 10.1056/NEJM198805053181802.
5. Hagen PT, Scholz DG, Edwards WD. Incidence and Size of Patent Foramen Ovale During the First 10 Decades of Life: An Autopsy Study of 965 Normal Hearts. Mayo Clin Proc. 1984;59(1):17-20. doi: 10.1016/s0025-6196(12)60336-x.
6. Wechsler LR. PFO and Stroke: What are the Data? Cardiol Rev. 2008;16(1):53-7. doi: 10.1097/CRD.0b013e31815771e4.
7. Thiagaraj AK, Hughes-Doichev R, Biederman RWW. Provocative Maneuvers to Improve Patent Foramen Ovale Detection: A Brief Review of the Literature. Echocardiography. 2019;36(4):783-6. doi: 10.1111/echo.14297.
8. Rodrigues AC, Picard MH, Carbone A, Arruda AL, Flores T, Klohn J, et al. Importance of Adequately Performed Valsalva Maneuver to Detect Patent Foramen Ovale During Transesophageal Echocardiography. J Am Soc Echocardiogr. 2013;26(11):1337-43. doi: 10.1016/j.echo.2013.07.016.
9. Vitarelli A, Mangieri E, Capotosto L, Tanzilli G, D'Angeli I, Toni D, et al. Echocardiographic Findings in Simple and Complex Patent Foramen Ovale Before and after Transcatheter Closure. Eur Heart J Cardiovasc Imaging. 2014;15(12):1377-85. doi: 10.1093/ehjci/jeu143.
10. Santos SN, Alcantara ML, Freire CMV, Cantisano AL, Teodoro JAR, Carmen CLL, et al. Vascular Ultrasound Statement from the Department of Cardiovascular Imaging of the Brazilian Society of Cardiology – 2019. Arq Bras Cardiol. 2019;112(6):809-8. doi: 10.5935/abc.20190106.

Case Report

Transesophageal Echocardiogram in the Diagnosis of Superior Vena Cava Syndrome in a Patient With a Long-Term Catheter

Marcus Vinicius Silva Freire de Carvalho,[1,2] Endy de Santana Alves,[1,2] Laila Caroline Gomes,[1,2] Carolina Thé Macêdo,[1,2] Marco André Moraes Sales,[1,2] Alexandre Costa Souza,[1,2]

Hospital São Rafael, Rede D'Or,[1] Salvador, BA – Brazil

Instituto D'Or de Pesquisa e Educação (IDOR),[2] Salvador, BA – Brazil

Introduction

The superior vena cava syndrome (SVCS) is caused by the obstruction or severe occlusion of the superior vena cava (SVC) and can result in significant morbidity or mortality.[1,2] Malignancy is the most common cause of this obstruction, corresponding to approximately 70% of the cases.[3] However, more recently, the incidence of SVCS related to devices, such as central venous catheters and electrodes of a pacemaker or defibrillator, have increased.[4,5]

These devices, together with states of hypercoagulability, can precipitate the formation of thrombi.[4] In extreme situations, in the context of bacteremia, these can lead to the formation of a complex thrombus-vegetation association.

The traditional clinical findings include: facial, periorbital, cervical, and upper limb edemas, followed by venous dilations of the anterior thoracic wall, illustrating collateral circulation.[1-3] Although it generally does not represent an imminent risk, SVCS is often associated with symptoms of high morbidity-mortality, such as dyspnea, dysphagia, and even intracranial hypertension, which can result in a coma.[1,2]

To diagnose this condition, the transesophageal echocardiogram (TEE) plays a complementary role in a bedside multimodal image to demonstrate the presence of thrombus in SVC topography.[6] New tools, such as the real-time three-dimensional TEE (3D TEE), has enabled a greater quantification of the lesions in the right atrium and the SVC, with the risk of evolving into SVCS.

Case Report

A 52-year-old male patient, who was hypertensive, diabetic, and diagnosed with prior coronary artery disease and chronic dialytic kidney disease, underwent a kidney transplant in 2021, evolving with graft loss. The patient was hospitalized in February 2022 due to a fungal endocarditis and remained hospitalized during antifungal treatment. After six months, he developed a new medical condition of fever and chills associated with the use of the dialysis catheter and the poor functioning of this device, in addition to redness and facial edema, dysphagia, and dyspnea. The blood cultures showed the growth of *S. epidermidis*, and the patient had been taking vancomycin, staggered with teicoplanin and meropenem, and continued to use fluconazole. The two-dimensional (2D) TEE showed the presence of a large hyperechogenic image within the right atrium, protruding to the SVC, measuring approximately 40 x 08 mm (Figure 1). A 3D technique was used, which allowed for a better characterization of the lesion and its extension, occupying approximately 67% of the circumferential diameter of the SVC, associated with the presence of a mobile filament image in its outer portions, which can correspond to a thrombus or to vegetation (Figure 2). An angiotomography of the cervical and thoracic blood vessels was conducted, with signs of a partial thrombosis of the internal jugular veins, the left subclavian vein, the brachiocephalic veins, and the SVC. The dialysis catheter was moved by the vascular surgery team to the left femoral vein, and anticoagulation was begun.

Keywords

Transesophageal echocardiography; diagnosis; syndrome, vein.

Mailing Address: Marcus Vinicius Silva Freire de Carvalho •
Hospital São Rafael, Ecocardiografia, Cardiologia. Avenida São Rafael, 2.152. Postal Code 41253-190. São Marcos, Salvador, BA – Brazil
E-mail: marcusviniciusfrc@hotmail.com
Manuscript received March 12,2023; revised March 19, 2023; accepted April 12, 2023.
Editor responsible for the review: Simone Nascimento dos Santos

DOI: https://doi.org/10.36660/abcimg.20230028i

Discussion

The incidence of SVCS related to devices has increased considerably due to the increased use of catheters, pacemakers, and defibrillators.[1,2] In a recent study, 28% of all SVCS were related to devices.[3] Venous thrombosis, which is normally clinically silent, occurred in nearly 30% of all patients using pacemaker electrodes.[3] However, the obstruction of the SVC is rare and observed in only 0.1% to 3.3% of all patients.[2,3] The stenosis in the SVC-atrial junction occurs due to the deposit of fibrin on the surface of the stimulating electrodes and their incorporation in a person's reproductive organs, followed by the inflammation of the blood vessel wall, fibrosis, the formation of thrombosis, and stenosis.[3] The chronic mechanical irritation and reaction of the foreign body are the main mechanisms of the formation of thrombi and vegetations in this location. The extraction of devices and posterior re-implant also caused mechanical trauma and can be considered additional risk factors for the emergence of thrombi and venous occlusion.[4]

The diagnosis of this complication can be difficult. Although the computed tomography can show the location of the catheter, it is quite limited in revealing the structural details concerning the implanted device itself.[5] The proximal portion of the SCV can be viewed in the TEE through the subcostal window. However, the views are generally quite limited in many patients.[6] The TEE in this scenario is an excellent diagnostic approach as it is minimally invasive

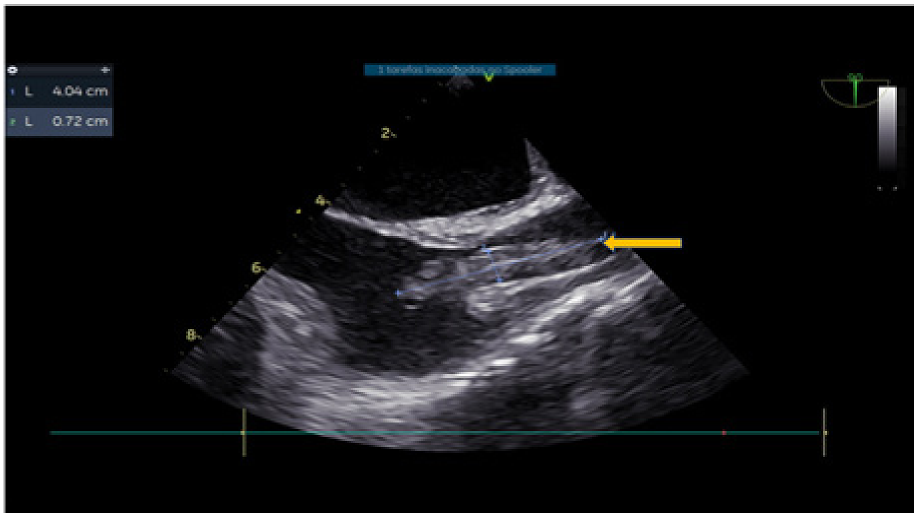

Figure 1 – *TEE showing a hyperechogenic image in the inner portion of the right atrium, projecting to the superior vena cava (yellow arrow).*

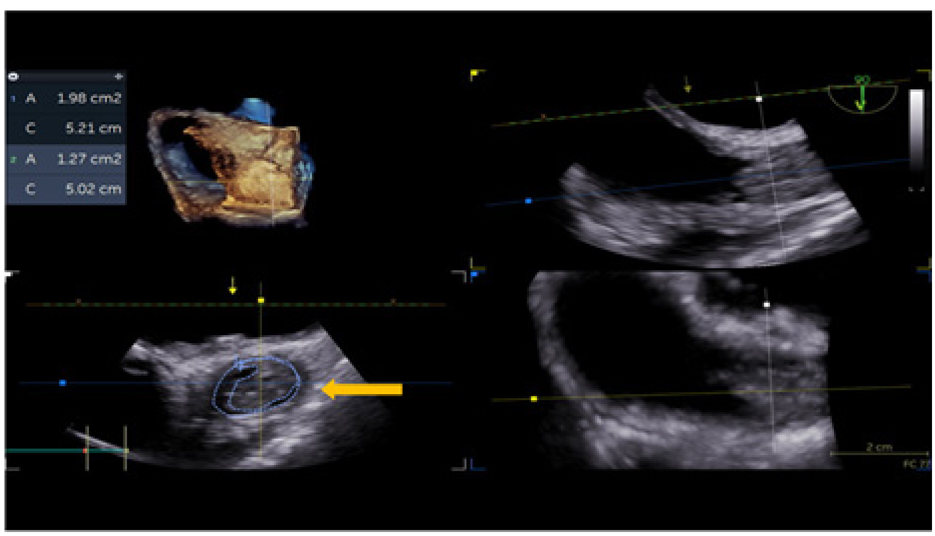

Figure 2 – *TEE with 3D reconstruction of the superior vena cava: Hyperechogenic image occupying approximately 67% of the circumference diameter of the superior vena cava (yellow arrow).*

and has few contra-indications.[6,7] The SVC can be easily observed, as demonstrated in our case, especially through the transesophageal acoustic window in a medium esophagus with an angulation of about 90° (bicaval incidence). The good spatial resolution of the echocardiographic images allows for an adequate definition of the catheter and associated pathology. In addition, follow-up using this imaging method is feasible, presents a low morbidity-mortality, and can guide additional treatment.[8]

A prior study evaluated the role of the TEE in the diagnosis of central venous thrombi associated with the implant of intracardiac devices (pacemaker electrodes), using the TEE and venography. After 06 months, the transesophageal method enabled the detection of most of the episodes of thrombosis in the intracardiac devices. By contrast, the venogram detected only thrombi in the subclavian vein and/or innominate vein. The main finding of this prospective study was that the thrombosis associated with the pacemaker electrode in the right atrium and with SVC is not uncommon six months after the implant, and that the 3D TEE was superior in the diagnosis of these thrombi when compared to the venogram with peripheral intravenous contrast and the TEE.[4]

The study of these emboligenic sources is essential, as it can reduce the rate of pulmonary embolism, the emergence of infectious endocarditis, and even rare cases of the SVCS due to the subtotal/total occlusion of this blood vessel, as seen in the present case report. In this context, the TEE is extremely useful, as it is a semi-invasive method, which is readily available, inexpensive, and capable of detecting thrombi in devices and/or long-term catheters, even in asymptomatic patients.[4,5]

The venogram by digital subtraction, by contrast, represents the gold standard in this syndrome, defining the severity of the obstruction and enabling the interventionist to develop the strategy for revascularization.[3,9,10] However, the viewing of the superior right vena cava is still a challenge due to the acoustic shadow imposed by the ribs and the lungs. In this context, it is important to perform not only the fluoroscopy, but also the TEE, which has the power to evaluate the insertion of the SVC in the right atrium.[6,7] The inadequate observation of the SVC junction – right atrium by the fluoroscopy enhances the accuracy of the TEE, making it an excellent ally in the visualization of this portion through the image obtained in the bicaval acoustic window, which is a quick, safe, and technically precise method for the differential diagnosis of SVCS.[7]

In the spectrum of the TEE, the use of the 3D TEE is an additional tool capable of bringing relevant information provided by an adequate spatial relationship.[7,8] In this sense, the 3D TEE allows for an improved evaluation of the SVC and its relation with the thrombus area, determining the occupation rate and the respective hemodynamic effects resulting from this obstruction, characterizing lesions with a greater risk of developing SVCS.[7,8]

Conclusion

The incidence of SVCS related to devices, such as central venous catheters and electrodes from pacemakers and defibrillators, have increased progressively. In this light, the echocardiogram, especially the transesophageal analysis, emerges as a quick, safe, and technically precise method to evaluate the presence of thrombi and/or vegetations that may well be related to SVCS, as seen in the present case report. The good spatial relation of the 3D TEE allows for an additional value in the topographical evaluation of the lesion in relation to the adjacent planes and a better evaluation of its dimensions.

Author Contributions

Conception and design of the research: De Carvalho MVSF, Souza AC; acquisition of data: De Santana EA, Souza AC; analysis and interpretation of the data: De Carvalho MVSF; writing of the manuscript: De Carvalho MVSF, De Santana EA, Gomes LC; critical revision of the manuscript for intellectual content: De Carvalho MVSF, Gomes LC, Sales MAM, Macedo CT, Souza AC.

Potential Conflict of Interest

No potential conflict of interest relevant to this article was reported.

Sources of Funding

There were no external funding sources for this study.

Study Association

This study is not associated with any thesis or dissertation work.

Ethics Approval and Consent to Participate

This article does not contain any studies with human participants or animals performed by any of the authors.

References

1. Rice TW, Rodriguez RM, Light RW. The Superior Vena Cava Syndrome: Clinical Characteristics and Evolving Etiology. Medicine. 2006;85(1):37-42. doi: 10.1097/01.md.0000198474.99876.f0.
2. Wilson LD, Detterbeck FC, Yahalom J. Clinical Practice. Superior Vena Cava Syndrome with Malignant Causes. N Engl J Med. 2007;356(18):1862-9. doi: 10.1056/NEJMcp067190.
3. Straka C, Ying J, Kong FM, Willey CD, Kaminski J, Kim DW. Review of Evolving Etiologies, Implications and Treatment Strategies for the Superior Vena Cava Syndrome. Springerplus. 2016;5:229. doi: 10.1186/s40064-016-1900-7.
4. Korkeila P, Nyman K, Ylitalo A, Koistinen J, Karjalainen P, Lund J, et al. Venous Obstruction after Pacemaker Implantation. Pacing Clin Electrophysiol. 2007;30(2):199-206. doi: 10.1111/j.1540-8159.2007.00650.x.
5. Sonavane SK, Milner DM, Singh SP, Aal AKA, Shahir KS, Chaturvedi A. Comprehensive Imaging Review of the Superior Vena Cava. Radiographics. 2015;35(7):1873-92. doi: 10.1148/rg.2015150056.
6. Ayala K, Chandrasekaran K, Karalis DG, Parris TM, Ross JJ Jr. Diagnosis of Superior Vena Caval Obstruction by Transesophageal Echocardiography. Chest. 1992;101(3):874-6. doi: 10.1378/chest.101.3.874.
7. Grote J, Lufft V, Nikutta P, van der Lieth H, Bahlmann J, Daniel WG. Transesophageal Echocardiographic Assessment of Superior Vena Cava Thrombosis in Patients with Long-Term Central Venous Hemodialysis Catheters. Clin Nephrol. 1994;42(3):183-8.
8. Azizi AH, Shafi I, Shah N, Rosenfield K, Schainfeld R, Sista A, et al. Superior Vena Cava Syndrome. JACC Cardiovasc Interv. 2020;13(24):2896-2910. doi: 10.1016/j.jcin.2020.08.038.
9. Yu JB, Wilson LD, Detterbeck FC. Superior Vena Cava Syndrome--A Proposed Classification System and Algorithm for Management. J Thorac Oncol. 2008;3(8):811-4. doi: 10.1097/JTO.0b013e3181804791.
10. Sfyroeras GS, Antonopoulos CN, Mantas G, Moulakakis KG, Kakisis JD, Brountzos E, et al. A Review of Open and Endovascular Treatment of Superior Vena Cava Syndrome of Benign Aetiology. Eur J Vasc Endovasc Surg. 2017;53(2):238-54. doi: 10.1016/j.ejvs.2016.11.013.

Case Report

Takayasu's Arteritis: Ascending Aortic Aneurysm and Coronary Artery Disease in a 19-year-old Young Adult

Iuri Betuel Gomes António,[1] Adnaldo da Silveira Maia,[1] Janayna Rabelato,[1] Aloysio Abdo Silva Campos,[1] Marilia Prudente Menezes,[1] Mário Issa[1]

Instituto Dante Pazzanese de Cardiologia,[1] São Paulo, SP – Brazil

Abstract

Takayasu's Arteritis (TA) is a disease of multiple presentation, which can involve many different systems and mainly affects women in the first decades of life. The present case reports on a 19-year-old patient with TA, with a diagnosis of ascending aortic aneurysm and severe coronary artery disease in the right coronary artery (RCA) and left coronary trunk (LCT), who underwent an implant of a supracoronary Dacron graft in the ascending aorta and myocardial revascularization with a double internal thoracic artery. The patient evolved satisfactorily in post-op and is today undergoing clinical follow-up in our medical services.

Introduction

Takayasu's Arteritis (TA) is a rare disease,[1] described for this first time in 1908 by Mikito Takayasu as a case of retinal vasculitis with the absence of a pulse in a young adult.[2] In an overall perspective, this disease is more common in women (80-90% of the cases), between the 2nd and 4th decades of life.[1] Its incidence varies and, according to statistical data from Japan, Europe, and the USA, around 1-3 new cases/one million inhabitants, are diagnosed each year.[3]

TA is defined as a progressive and granulomatous chronic inflammatory disease of the large blood vessels (aorta and its main supra-aortic branches, as well as the mid-sized pulmonary and coronary arteries), characterized by stenosis, occlusion, and/or dilation/aneurysm.[4,5] Of unknown etiology and poorly understood pathogenesis, it is presumed that genetic factors and infectious agents can play key roles in the origin of the disease.[6]

There are no specific laboratory exams for the diagnosis and follow-up of the disease's activity. Angiotomography (Angio-CT) and the magnetic resonance angiography (MRA) represent the gold standards for the diagnosis of TA.[7,8] According to angiographic findings, TA has been classified in 6 types of alterations, based on the affected region, which is useful for surgical planning.[9]

Keywords

Coronary Disease; Aneurysm; Takayasu Arteritis.

Mailing Address: Iuri Betuel Gomes António •
Instituto Dante Pazzanese de Cardiologia. Avenida Dante Pazzanese. Postal code: 04012-909. São Paulo, SP – Brazil
E-mail: adsm.ccv@gmail.com
Manuscript received March 18, 2023; revised manuscript April 17, 2023; accepted April 19, 2023
Editor responsible for the review: Daniela do Carmo Rassi Frota

DOI: https://doi.org/10.36660/abcimg.20230032i

The clinical treatment of this entity can be found in the guidelines, whose objective is the control of active inflammation and the prevention of new vascular damage. However, when in the presence of critical stenotic lesions, dilation, and/or aneurysm, percutaneous angioplasty and surgical treatment are recommended, on a case by case basis.[8] In this context, this work aims to describe a rare clinical manifestation of TA

Case report

Our study reports on a 19-year-old female patient, weighing 57 kg, with TA diagnosed at 3 years of age, who was medicated with applications of pulse therapy and methotrexate until 12 years of age, at which time she ceased to continue her medical follow-up until she was 18 years of age. The patient resumed her follow-up treatment one year ago at the same medical institution, at which time she was diagnosed with ectasia of the ascending aorta, with 35 x 34 mm in the transthoracic echocardiogram (TEE). The patient was then sent to the medical reference service.

She underwent an MRA, which revealed a thickening of the artic wall and dilation of the ascending aorta of 37x35 mm (Figure 1). Six months later, she returned to the outpatient clinic, reporting a medical condition of typical chest pain lasting 30 minutes, followed by syncope, but she did not go to the hospital on that occasion. An Angio-CT of the aorta and coronary arteries was requested, which revealed an aneurysm of the ascending aorta, 46 x 44 mm, with signs of circumferential parietal thickening and parietal calcification along its entire extension, as well as severe coronary artery involvement by extrinsic compression related to the parietal thickening of the aorta (Figure 2).

The coronary cineangiography showed severe lesions in the right coronary artery (RCA), 80% proximal and 80% proximal of the left coronary trunk (LCT). The case was discussed with the aorta Heart Team, and it was decided that the patient should be hospitalized for surgical treatment. The patient was asymptomatic at the time of hospitalization.

Upon physical exam, a systolic murmur appeared at a II/IV aortic focus. Laboratory data presented no significant alterations. During the pre-operative period, the patient's routine medication was maintained. Given the evidence of disease progression, the patient underwent a supracoronary Dacron graft implant in the ascending aorta and myocardial revascularization with double internal thoracic artery (ATIE-DA and ATID-CD, in Portuguese) (Figure 2). With no complications during hospitalization, the patient was released on the 8th post-operative day. She is currently undergoing optimized clinical treatment and is taking medicine to control the base disease, as advised by the healthcare team.

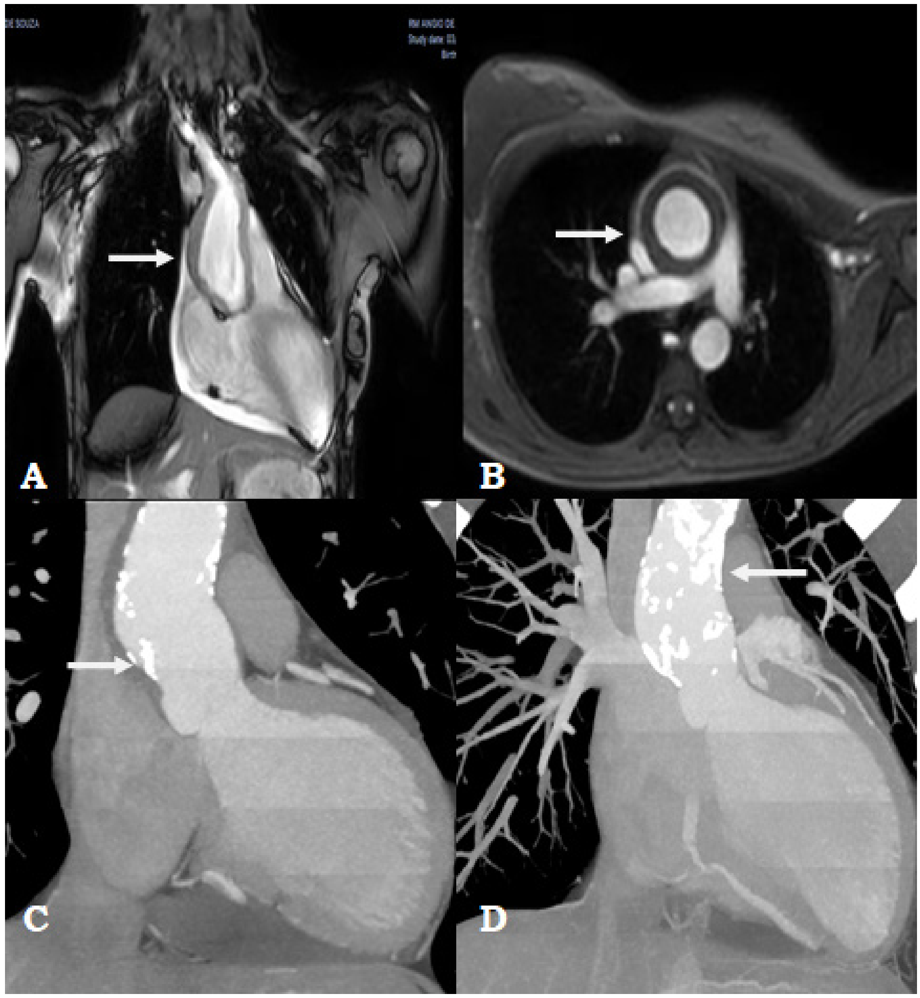

Figure 1 – A and B) CMR illustrating circumferential parietal thickening with dilation of the ascending aorta of 37x35 mm; C and D) Ascending aortic aneurysm by CT, measuring 46x44 mm, with signs of thickening and parietal calcification along its entire extension.

Discussion

The description of this case refers to the severity of TA, as well as to its complexity in the diagnostic approach and treatment. TA is a rare disease, most commonly found in women before 50 years of age, but many studies also show a high prevalence at more advanced ages.[10]

The diagnosis is based on diagnostic criteria from EULAR/PRINTO/PRES.[11] In this case, the clinical means of presentation was of coronary artery disease. Coronary artery involvement is uncommon, showing only a 9% incidence.[12] Although it is rare, myocardial ischemia is one of the main causes of death. The inflammatory process of the aorta has been identified as being responsible for these lesions, in which the occlusion of the ostium of the coronary arteries occurs more often, though there are many cases in the literature that describe coronary arteritis with no occlusion of the ostium.[13,14] Coronary artery involvement in this patient is similar to that described by Endo et al., in which 24 patients presented coronary artery stenosis, of whom 83.3% were women.[12]

According to angiographic findings, the TA was classified in six types of alterations based on the affected region, which is useful for surgical planning.[7,8] The decision of when to use an endovascular approach or open surgery can be influenced by a series of factors.[15] Percutaneous coronary interventions (PCI) have been used in the initial treatment of the obstructive lesions, presenting uncertain results and a long-term survival that is still not fully understood.[16]

Due to a serious chance of intra-stent restenosis, cardiac magnetic resonance (CMR) is the procedure of choice to treat coronary artery lesions.[14] In a retrospective case series involving 106 Japanese patients, Miyata et al.[17] observed a 15-year increase in the survival rate, rising from 43% (among those treated with medical therapy) to 67.5% after the addition of surgical intervention.

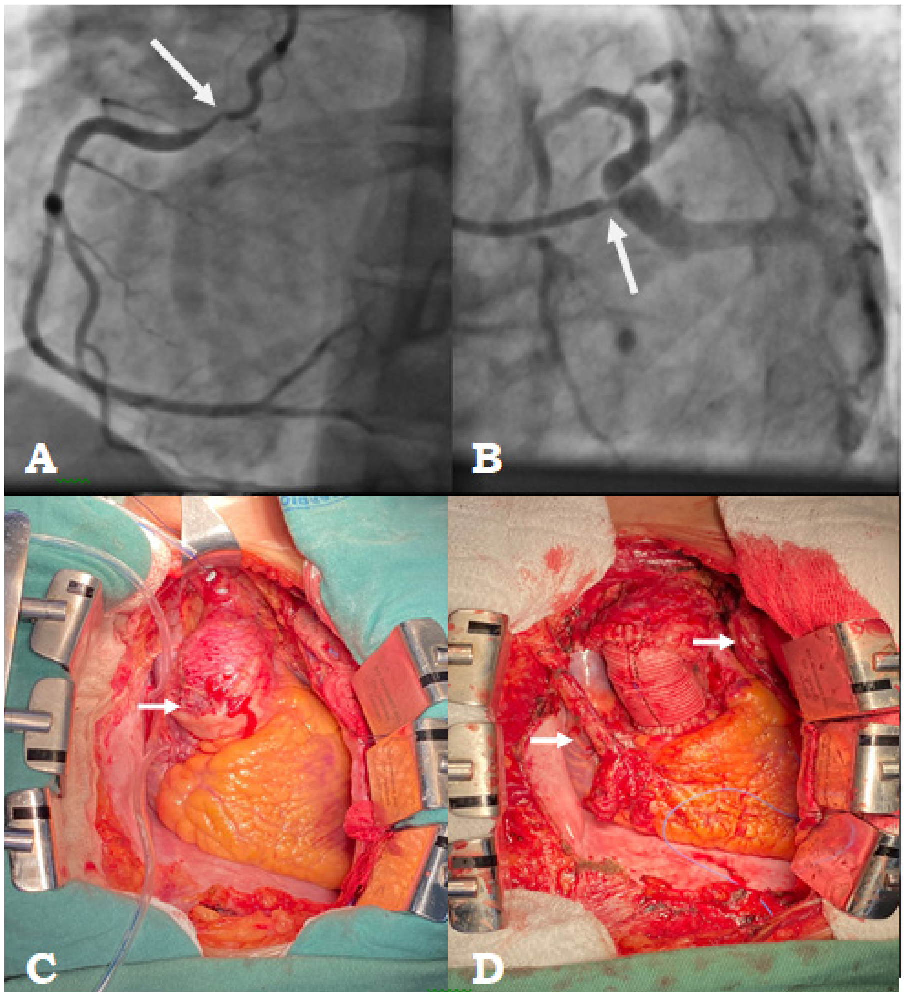

Figure 2 – A and B) Coronary angiography, showing severe lesions in the RCA and LCT; C and D) Final aspect of the surgery after myocardial revascularization and Dacron graft implant.

Yang et al.,[18] in an analysis of 31 patients with TA who underwent revascularization by CMR (12) and PCI (19), in an average follow-up of 101 months, observed higher restenosis rates in the percutaneous group. The inflammatory process can affect different parts of the coronary artery, but with a greater prevalence of ostial/proximal lesions, in accordance with that reported in the present study. The authors also highlight that the myocardial ischemia resulting from coronary artery involvement constitutes the main cause of death among TA patients. In this sense, the importance of studying the coronary arteries of these patients when there is a clinical suspicion is crucial.

Huang et al.,[19] in a study involving 90 patients comparing medicine vs. revascularization treatments in TA patients (CMR and PCI) were unable to identify any difference in mortality due to cardiovascular causes among the groups. Nevertheless, in the analysis of the subgroup through a revascularization strategy, the findings corroborated with those reported by Yang et al.[18] with higher restenosis rates in the percutaneous approach. Moreover, in this study, heart failure was an independent predictor of mortality.

Modalities of revascularization were also the focus of the study published by Wang et al.,[20] in an analysis of 46 patients with TA and coronary artery involvement. The authors found that the MACE rates (all-causes mortality, myocardial infarction, and revascularization) were greater in the group submitted to PCI. The multivariate analysis for the MACE outcome viewed the disease activity and the type of revascularization (CMR vs. PCI) as predictive factors. Such data reinforce the individualized indication and the importance of the Heart Team in these patients' medical evaluations.

Conclusion

Coronary artery lesions vary from patient to patient, especially proximal involvement, and therefore careful planning in all stages of the treatment through revascularization, be it percutaneous or surgical, is of utmost importance. The data point to higher restenosis rates after the percutaneous approach, with the CMR being the preferred method when no contraindications were presented, such as the availability of grafts and the possibility of using the internal thoracic artery.

The adequate suppression of the inflammatory activity from the pre-operative stage and the choice of technique to be used guarantee better end results. Thus, the evaluation of the patient's stage of the disease is essential, given that it is a factor associated with higher MACE rates, as well as the shared decision on the case. The rigorous and specialized clinical follow-up in a reference center should be encouraged.

Author Contributions

Conception and design of the research, acquisition of data, analysis and interpretation of the data, statistical analysis, writing of the manuscript and critical revision of the manuscript for intellectual content: António IBG, Maia AS, Rabelato J, Campos AAS, Menezes MP, Issa M.

Potential Conflict of Interest

No potential conflict of interest relevant to this article was reported.

Sources of Funding

There were no external funding sources for this study.

Study Association

This study is not associated with any thesis or dissertation work.

Ethics Approval and Consent to Participate

This study was approved by the Ethics Committee of the Instituto Dante Pazzanese de Cardiologia, CAAE: 60291322.8.0000.5462, Protocol Number: 5.629.949, All the procedures in this study were in accordance with the 1975 Helsinki Declaration, updated in 2013. Informed consent was obtained from all participants included in the study.

References

1. Lupi-Herrera E, Sánchez-Torres G, Marcushamer J, Mispireta J, Horwitz S, Vela JE. Takayasu's Arteritis. Clinical Study of 107 Cases. Am Heart J. 1977;93(1):94-103. doi: 10.1016/s0002-8703(77)80178-6.
2. Numano F. The Story of Takayasu Arteritis. Rheumatology. 2002;41(1):103-6. doi: 10.1093/rheumatology/41.1.103.
3. Dabague J, Reyes PA. Takayasu Arteritis in Mexico: A 38-Year Clinical Perspective Through Literature Review. Int J Cardiol. 1996;54 Suppl:S103-9. doi: 10.1016/s0167-5273(96)88779-1.
4. Judge RD, Currier RD, Gracie WA, Figley MM. Takayasu's Arteritis and the Aortic Arch Syndrome. Am J Med. 1962;32:379-92. doi: 10.1016/0002-9343(62)90128-6.
5. Keser G, Aksu K, Direskeneli H. Takayasu Arteritis: An Update. Turk J Med Sci. 2018;48(4):681-97. doi: 10.3906/sag-1804-136.
6. Villon MLFZ, de la Rocha JAL, Espinoza LR. Takayasu Arteritis: Recent Developments. Curr Rheumatol Rep. 2019;21(9):45. doi: 10.1007/s11926-019-0848-3.
7. Hata A, Numano F. Magnetic Resonance Imaging of Vascular Changes in Takayasu Arteritis. Int J Cardiol. 1995;52(1):45-52. doi: 10.1016/0167-5273(95)02438-3.
8. Russo RAG, Katsicas MM. Takayasu Arteritis. Front Pediatr. 2018;6:265. doi: 10.3389/fped.2018.00265.
9. Hata A, Noda M, Moriwaki R, Numano F. Angiographic Findings of Takayasu Arteritis: New Classification. Int J Cardiol. 1996;54 Suppl:S155-63. doi: 10.1016/s0167-5273(96)02813-6.
10. Richards BL, March L, Gabriel SE. Epidemiology of Large-Vessel Vasculidities. Best Pract Res Clin Rheumatol. 2010;24(6):871-83. doi: 10.1016/j.berh.2010.10.008.
11. Ozen S, Pistorio A, Iusan SM, Bakkaloglu A, Herlin T, Brik R, et al. EULAR/PRINTO/PRES Criteria for Henoch-Schönlein Purpura, Childhood Polyarteritis Nodosa, Childhood Wegener Granulomatosis and Childhood Takayasu Arteritis: Ankara 2008. Part II: Final Classification Criteria. Ann Rheum Dis. 2010;69(5):798-806. doi: 10.1136/ard.2009.116657.
12. Endo M, Tomizawa Y, Nishida H, Aomi S, Nakazawa M, Tsurumi Y, et al. Angiographic Findings and Surgical Treatments of Coronary Artery Involvement in Takayasu Arteritis. J Thorac Cardiovasc Surg. 2003;125(3):570-7. doi: 10.1067/mtc.2003.39.
13. Yokota K, Shimpo M, Iwata T, Hirose M, Ikemoto T, Ohya K, et al. A Case of Takayasu Arteritis with Repeated Coronary Artery Restenosis after Drug-Eluting Stent Implantation Successfully Treated with a Combination of Steroids. Intern Med. 2012;51(7):739-43. doi: 10.2169/internalmedicine.51.6344.
14. Gelape CL, Alvarenga FC, Figueroa CCS, Ribeiro ALP. Successful Treatment of Left Main Coronary Stenosis in Takayasus Arteritis. Rev Bras Reum. 2007;47(5):390-3. doi: 10.1590/S0482-50042007000500017.
15. Mason JC. Surgical Intervention and Its Role in Takayasu Arteritis. Best Pract Res Clin Rheumatol. 2018;32(1):112-24. doi: 10.1016/j.berh.2018.07.008.
16. Kang WC, Han SH, Ahn TH, Shin EK. Successful Management of Left Main Coronary Artery Stenosis with a Paclitaxel-Eluting Stent in Takayasu's Arteritis. Int J Cardiol. 2006;108(1):120-3. doi: 10.1016/j.ijcard.2005.02.024.
17. Miyata T, Sato O, Koyama H, Shigematsu H, Tada Y. Long-Term Survival after Surgical Treatment of Patients with Takayasu's Arteritis. Circulation. 2003;108(12):1474-80. doi: 10.1161/01.CIR.0000089089.42153.5E.
18. Yang Y, Tian T, Yang K, Zhang Y, Meng X, Fan P, et al. Outcomes of Percutaneous Coronary Intervention and Coronary Artery Bypass Grafting in Patients with Takayasu Arteritis. Int J Cardiol. 2017;241:64-9. doi: 10.1016/j.ijcard.2017.02.041.
19. Huang Z, Zhang H, Wang M, Yang W, Qiao S, Hu F. Revascularization Versus Medical Therapy in Takayasu's Arteritis Patients with Coronary Artery Involvement. Rheumatol Ther. 2021;8(1):119-33. doi: 10.1007/s40744-020-00251-2.
20. Wang X, Dang A, Lv N, Cheng N, Cheng X, Yang Y, et al. Long-Term Outcomes of Coronary Artery Bypass Grafting Versus Percutaneous Coronary Intervention for Takayasu Arteritis Patients with Coronary Artery Involvement. Semin Arthritis Rheum. 2017;47(2):247-52. doi: 10.1016/j.semarthrit.2017.03.009.

Case Report

Takotsubo Syndrome After Mitral Valve Surgery: Multimedia Presentation of a Rare Diagnosis

Adnaldo da Silveira Maia,[1] Germano de Sousa Leão,[1] Jhonathan Gouveia da Mota,[1] Dante Togeiro Bastos Filgueiras,[1] Verônica Noronha Rodrigues,[1] Luiz Minuzzo,[1] Mario Issa[1]

Instituto Dante Pazzanese de Cardiologia (IDPC),[1] São Paulo, SP – Brazil

Introduction

The Takotsubo Syndrome, also known as "broken heart syndrome", is characterized by a severe and transitory left ventricular dysfunction, with the presence of alterations in the contraction of the basal, medial, or apical segments of the left ventricular walls.[1] The syndrome can be caused by an emotional or physical trigger, or by a combination of both; however, this is not a mandatory criterion for its diagnosis.[2]

This study describes a case of Takotsubo Syndrome after mitral valve surgery to replace the valve with a mechanical prosthesis.

Case report

A 56-year-old, female patient, with a history of smoking, atrial fibrillation, rheumatoid arthritis, and mitral stenosis, underwent a percutaneous mitral valvuloplasty in 2007, using warfarin, atenolol, digoxin, amiodarone, prednisone (intermittent), hydroxychloroquine, and leflunomide. The patient was hospitalized to undergo elective mitral valve replacement surgery.

The transthoracic echocardiogram showed an ejection fraction of 64%, with an increase in the left atrium (indexed volume of 122ml/m^2) and eccentric left ventricular hypertrophy. The mitral vale presented thickened cusps, with the posterior leaflet fixed and the anterior with a cup-shaped opening. The Doppler imaging showed an important reflux with a maximum and average gradient of 14 and 4 mmHg, respectively. The planimetry indicated a valve area of 1.9 cm^2. The previously conducted cinecoronariography showed a 40% obstruction in the anterior descending artery (Figure 1).

The patient underwent mitral valve surgery to replace the valve with a mechanical prosthesis, and to close the left atrial auricle, without complications. On the second post-operative day, the patient evolved with a hypertensive acute pulmonary edema and atrial fibrillation with a good ventricular response, introducing a treatment with intravenous amiodarone, nitroglycerin, and furosemide. The electrocardiogram presented a T-wave inversion in the V2-V4 derivations (Figure 2). A transthoracic echocardiogram was performed, which presented hypercontractility of the basal segments and akinesia of the medial, apical, and apex segments (standard suggestive of Takotsubo cardiomyopathy), as well as a high-degree systolic dysfunction of the left ventricle (ejection fraction of the left ventricle = 22% by the Simpson method). The mitral mechanical prosthesis showed a normal function, with no obstruction of the left ventricle outflow (Figure 3 and 4, Videos 1 and 2). Due to a suspected coronary complications resulting from the heart surgery, a dose of troponin was applied, which showed a value of 3,305 ng/L (reference: < 11 ng/L). However, the patient's coronary anatomy was only understood after the decision by the clinical-surgical team, along with the results from the imaging exams (echocardiographic standard) and the given surgical context. For this reason, we opted to manage this situation clinically.

Due to the worsening of her medical condition, the patient underwent orotracheal intubation and therapy with noradrenaline (0.25 mcg/kg/min), and dobutamine (8 mcg/kg/min) was applied in the context cardiogenic shock. After 96 horas, The patient's medical condition improved to a hemodynamic state, leading to the gradual suspension of the support measures. The echocardiogram showed a recovery of the systolic function of the left ventricle, with a left ventricle ejection fraction of 61%, with anomalous movement of the intraventricular septum and myocardial contractility preserved in the other segments of the left ventricle. The mechanical prosthesis was in the mitral position, with a good excursion of its mobile elements.

After an excellent clinical evolution, the patient was released from the ICU, with subsequent outpatient follow-up.

Discussion

The Takotsubo Syndrome has been described in some cases of patients submitted to gynecological, urological, and abdominal surgeries.[3] The cardiovascular procedures are also reported as triggers of the Takotsubo Syndrome, including stress tests with dobutamine, pericardiocentesis, cardioversion of atrial fibrillation, insertion of a pacemaker, electrophysiological tests, ablation and valve replacement surgery, and the use of a transcatheter.[4]

Takotsubo cardiomyopathy in the perioperative period has

Keywords

Mitral Valve; Takotsubo Cardiomyopathy; Ventricular Dysfunction

Correspondência: Adnaldo da Silveira Maia •
Departamento de Cirurgia Cardiovascular, Instituto Dante Pazzanese. Av. Dr. Dante Pazzanese, 500, III, 2. andar, Postal Code: 04011-061. São Paulo, SP – Brasil
E-mail: adsm.ccv@gmail.com

Manuscript received November 10, 2022; revised manuscript February 16, 2023; accepted February 18, 2023
Editor responsible for the review: Daniela do Carmo Rassi Frota

DOI: https://doi.org/10.36660/abcimg.2023362i

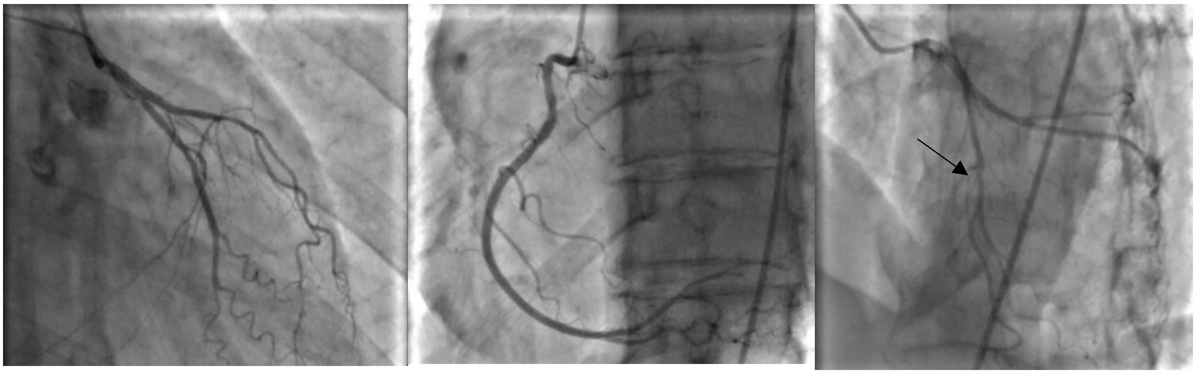

Figure 1 – *Preoperative cinecoronariography showing a lesion of 40% in the descending artery.*

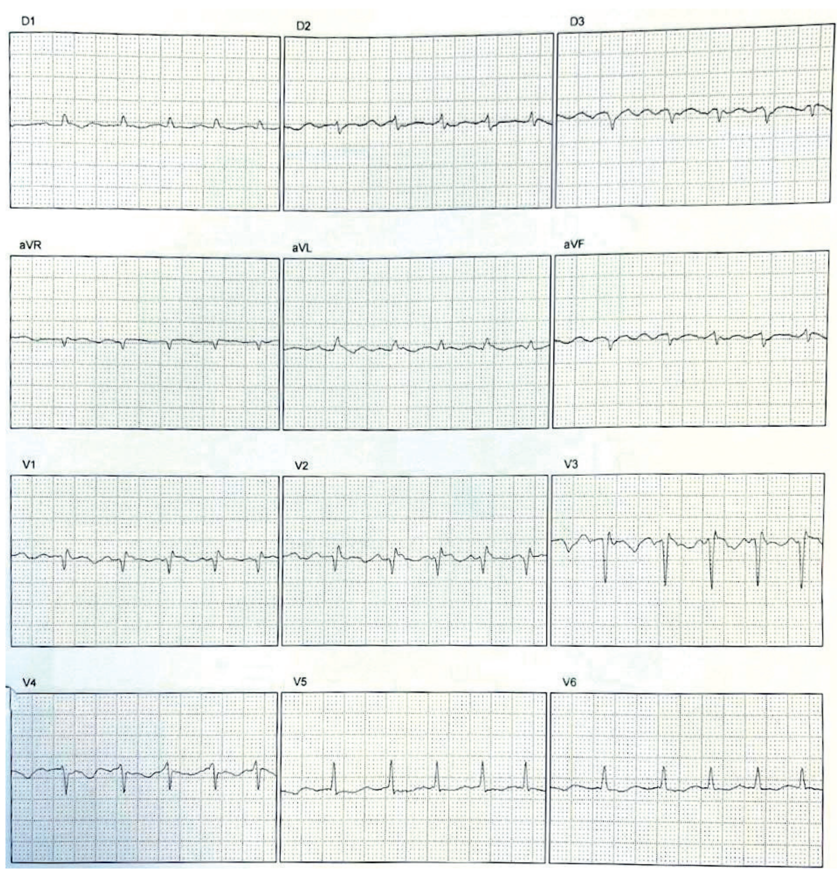

Figure 2 – *Electrocardiogram taken in the Intensive Care Unit, showing atrial fibrillation associated with T-wave inversion on the anterior wall.*

gained recognition, but its association with heart surgery is, to a great extent, mostly unknown and rarely described.[5] There are insufficient data in the literature on which to base the hypothesis of the prevalence of a cardiothoracic procedure or other procedure concerning the increased risk of the development of the syndrome. However, what is important to note here is the increase in the number of cases that describe the development of Takotsubo Syndrome after heart surgery.[5]

The possible mechanisms associated with the event in patients submitted to heart surgery are likely multiple, such as a coronary vasospasm (epicardial and microvascular ischemia), toxicity mediated by catecholamine, and excessive sympathetic activation.[6]

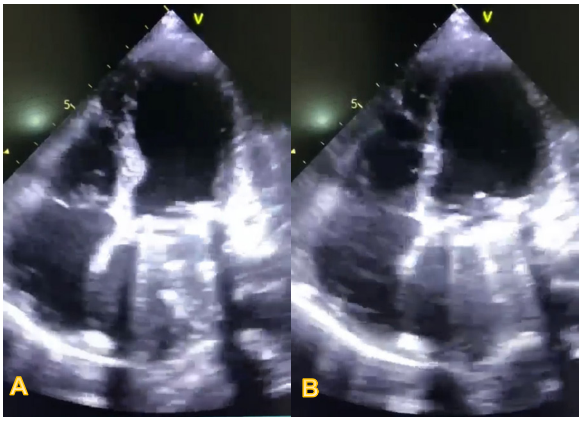

Figure 3 – *Transthoracic Echocardiogram, showing, during the systole (A) and the diastole (B), respectively, movement of the basal segment and akinesia of the medial and apical segments.*

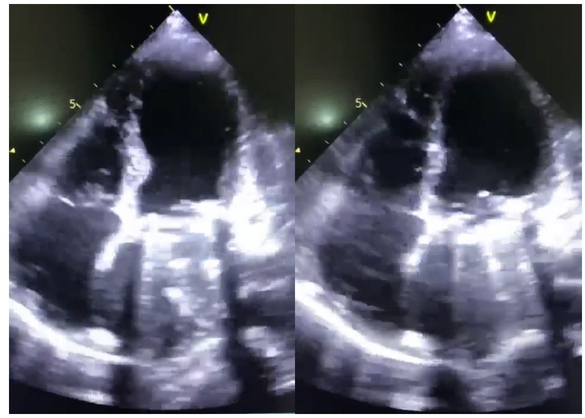

Figure 4 – *Transthoracic Echocardiogram, showing, during the systole (A) and the diastole (B), respectively, movement of the basal segment.*

Video 1 – *Link: http://abcimaging.org/supplementary-material/2023/3601/ABC 362_RC_video-01.mp4*

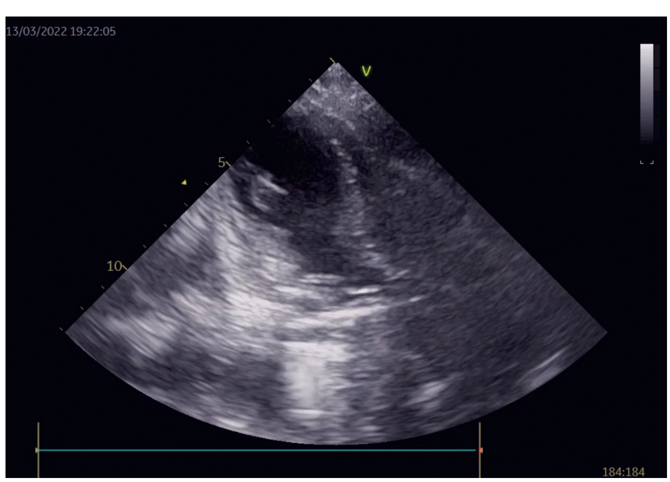

Video 2 – *Link: http://abcimaging.org/supplementary-material/2023/3601/ABC 362_RC_video-02.mp4*

Lyon et al.,[7] in a review of the physical-pathological mechanisms involved in the genesis of this syndrome, highlight the intense sympathetic activation, as well as the high levels of catecholamines, as central **triggers**. These findings are related to micro and macrovascular dysfunctions and, consequently, to the dysfunction of the cardiomyocytes and their respective consequences evidenced in the manifestation of the syndrome.

Thus, the development of electrocardiographic abnormalities, circumferential dysfunction of the ventricular contraction, clinical signs/symptoms (precordial pain and/or hypotension/circulatory shock) in the postoperative period of cardiovascular surgery are possible manifestations of the Takotsubo Syndrome, likely caused by extracorporeal circulation and surgical trauma, factors associated with the rise in catecholamines in this post-procedural period. Fundao et al., in their study, showed that these patients represented 10.4% of the cases.[8]

Many entities around the world have created diagnostic criteria to recognize this syndrome.[6] In an attempt to define a consensus, a new group of diagnostic criteria (InterTAK criteria) was proposed by specialists in 2018, including:

- *The patients show a transitory left ventricular dysfunction (hypokinesia, akinesia, or dyskinesia), appearing with an apical or medial ventricular ballooning, basal, or focal abnormalities of wall movement. The involvement of the right ventricle may appear;*
- *An emotional, physical, or combined trigger can precede the Takotsubo Syndrome event, but this is not a mandatory factor;*
- *New abnormalities in the ECG are present (ST-segment elevation, ST-segment depression, T-wave inversion, and QTc extension); however, there are rare cases with no alterations in the ECG.*

The InterTAK criteria mention the occurrence of the syndrome in the postoperative period of heart surgery, that is, they do not confirm nor exclude the diagnosis of the Takotsubo Syndrome in this case; however, with the increase in the number of cases reported in the literature, these criteria have been used for diagnoses in these groups of patients.[8] Findings from Fundao et al. suggest that, for future updates of the diagnostic criteria, one should consider the inclusion of heart surgery as a trigger for Takotsubo Syndrome.[8]

The differential diagnosis should mainly include acute coronary syndromes, since cardiomyopathies caused by stress overlap with acute coronary syndromes in their clinical and electrocardiographic manifestations.[3] In this scenario, in which the patient develops a cardiogenic shock in the postoperative period of heart surgery with acute alterations in the electrocardiogram and a left ventricle dysfunction with an anomalous movement of the wall, the first possibility to be discarded is coronary disease.[9]

In myocardiopathy caused by stress, the left ventricular function returns to normal within a few weeks; however, some complications can occur before fully recovering the ventricular systolic function. The main complications include: cardiogenic shock, obstruction of the left ventricular outflow, arrhythmias, systemic thromboembolism, and intramyocardial rupture.[3]

Treatment of the Takotsubo Syndrome is controversial, since no randomized prospective clinical trials have been conducted on the theme. Thus, the treatments are based on clinical experience and the consensus of specialists. One of the main questions in the treatment is to determine the presence or absence of the obstruction of the left ventricular outflow, which can change the therapeutic approach. The detection of the obstruction of left ventricular outflow is generally achieved through echocardiography or hemodynamic measures during the cardiac catheterization.[2] In the case reported here, the obstruction of the left ventricular outflow was discarded, and treatment using inotropics was implemented. Another possibility would be the temporary use of the intra-aortic balloon to minimize the use of inotropics, which was not necessary in the present case.

Conclusion

The Takotsubo Syndrome should be remembered as a rare complication in the context of cardiogenic shock during the postoperative period of cardiovascular surgery. This syndrome stems from conditions directly related to stress factors, with an abrupt rise in catecholamine levels. The characteristic echocardiographic standard, associated with the clinical scenario presented above, can aid in the diagnostic definition.

There are still many aspects concerning Takotsubo Syndrome that are still not fully understood. Clinical research is necessary to evaluate the treatment strategies in the acute stage and their impacts upon the patients' recovery of their ventricular function.

Author Contributions

Conception and design of the research, acquisition of data, analysis and interpretation of the data, writing of the manuscript and critical revision of the manuscript for intellectual content: Maia AS, Leão GS, da Mota JG, Filgueiras DTB, Rodrigues VN, Minuzzo L, Issa M.

Potential Conflict of Interest

No potential conflict of interest relevant to this article was reported.

Sources of Funding

There were no external funding sources for this study.

Study Association

This study is not associated with any thesis or dissertation work.

Ethics Approval and Consent to Participate

This article does not contain any studies with human participants or animals performed by any of the authors.

References

1. Gariboldi V, Jop B, Grisoli D, Jaussaud N, Kerbaul F, Collart F. Takotsubo Syndrome after Mitral Valve Replacement for Acute Endocarditis. Ann Thorac Surg. 2011;91(3):e31-2. doi: 10.1016/j.athoracsur.2010.10.085.

2. Ghadri JR, Wittstein IS, Prasad A, Sharkey S, Dote K, Akashi YJ, et al. International Expert Consensus Document on Takotsubo Syndrome (Part I): Clinical Characteristics, Diagnostic Criteria, and Pathophysiology. Eur Heart J. 2018;39(22):2032-46. doi: 10.1093/eurheartj/ehy076.

3. Devesa A, Hernández-Estefanía R, Tuñón J, Aceña Á. Takotsubo Syndrome after Mitral Valve Surgery: A Case Report. Eur Heart J Case Rep. 2020;4(6):1-5. doi: 10.1093/ehjcr/ytaa327.

4. Dias A, Núñez Gil IJ, Santoro F, Madias JE, Pelliccia F, Brunetti ND, et al. Takotsubo Syndrome: State-of-the-art Review by an Expert Panel - Part 1. Cardiovasc Revasc Med. 2019;20(1):70-9. doi: 10.1016/j.carrev.2018.11.015.

5. Chiariello GA, Bruno P, Colizzi C, Crea F, Massetti M. Takotsubo Cardiomyopathy Following Cardiac Surgery. J Card Surg. 2016;31(2):89-95. doi: 10.1111/jocs.12675.

6. Blázquez JA, González JM, Dalmau MJ, López J. Takotsubo Cardiomyopathy after Elective Mitral Valve Replacement. Interact Cardiovasc Thorac Surg. 2010;11(1):117-9. doi: 10.1510/icvts.2010.234013.

7. Lyon AR, Citro R, Schneider B, Morel O, Ghadri JR, Templin C, et al. Pathophysiology of Takotsubo Syndrome: JACC State-of-the-Art Review. J Am Coll Cardiol. 2021;77(7):902-21. doi: 10.1016/j.jacc.2020.10.060.

8. Fundão NHF, Ribeiro HB, Campos CM, Seleme VB, Soeiro AM, Vieira MLC, et al. The Clinical Course of Takotsubo Syndrome Diagnosed According to the InterTAK Criteria. Int J Cardiovasc Sci. 2020;33(6):637-4. doi: 10.36660/ijcs.20190133.

9. Husain A, Alsanei A, Tahir M, Dahdouh Z, AlHalees Z, AlMasood A. Left Circumflex Artery Injury Postmitral Valve Surgery, Single Center Experience. J Saudi Heart Assoc. 2019;31(2):94-9. doi: 10.1016/j.jsha.2018.12.003.

The Value of Vascular Ultrasonography in Defining Inflammatory Activity in Takayasu Arteritis: Case Reports

Fanilda Souto Barros,[1] Simone Nascimento dos Santos,[2] Joana Storino,[3] Cláudia Maria Vilas Freire,[4] Felipe Souto Barros,[5] Valquiria Garcia Dinis[6]

Laboratório Vascular Angiolab,[1] Vitória, ES – Brazil
ECCOS Diagnóstico Cardiovascular,[2] Brasília, DF – Brazil
Faculdade de Ciências Médicas de Minas Gerais,[3] Belo Horizonte, MG – Brazil
Universidade Federal de Minas Gerais,[4] Belo Horizonte, MG – Brazil
Hospital Santa Rita de Cássia,[5] Vitória, ES – Brazil
Escola Superior de Ciências, Santa Casa de Misericórdia de Vitória,[6] Vitória, ES – Brazil

Introduction

Takayasu arteritis (TA) is a rare large-vessel arteritis that primarily affects the aorta and its major branches.[1] The greatest challenge is to identify disease activity, since therapeutic measures modify the clinical course of the disease.

Vascular ultrasonography (VUS) is a promising tool for characterizing vessel wall inflammation and monitoring hemodynamic changes in response to therapy.[2]

We present 2 case reports that demonstrate the importance of VUS in identifying inflammatory activity in TA. The cases reflect the differences in thickened intima-media complex (IMC) between patients in active and non-active phases of the disease.

Case reports

First case: A 6-year-old boy who was suffering headaches but had no previous comorbidities was brought to a pediatrician. Clinical examination detected arterial hypertension (140 x 90 mmHg), and laboratory tests and VUS were scheduled to assess the renal arteries.

VUS revealed: 1) stenosis > 80% in the proximal segment of the left renal artery, and 2) thickened IMC of the abdominal aorta, with a lumen reduction of approximately 40% in the segment adjacent to the origin of the mesenteric vessels (Figure 1 B.C). Magnetic resonance angiography of the abdominal aorta and its branches was then performed (Figure 1D), with the findings confirming the VUS results.

Keywords

Vascular ultrasound; Takayasu's arteritis; vasculitis; intima-media thickness

Mailing Address: Fanilda Souto Barros •
Angiolab Laboratório Vascular. Rua José Teixeira, 290. Postal Code: 29055-310. Praia do Canto, Vitória, ES – Brasil
E-mail: fanildas@gmail.com
Manuscript received February 28, 2023; revised March 2, 2023; accepted March 3, 2023.
Editor responsible for the review: Simone Nascimento dos Santos

DOI: https://doi.org/10.36660/abcimg.20230021i

Examination of the carotid arteries was indicated, and significant thickening of the IMC was detected in both common carotid arteries, although the internal carotid artery was preserved, which is suggestive of TA (Figures 2 A-C).

VUS can be used to characterize vascular tissue as hypo- or hyperechogenic, and is validated by the adventitial layer or adjacent muscle. In this case, the IMC was characterized as hyperechogenic, suggesting fibrosis with no apparent disease activity.[3] The laboratory results showed no changes, with a C-reactive protein level of 0.1 mg/L and an erythrocyte sedimentation rate of 7 mm/h.

Clinical course: The patient was treated with antihypertensive drugs; the renal artery lesion was not treated with angioplasty due to his age. Ultrasound follow-up of the carotid arteries, aorta, and renal arteries 1 year after the initial examination showed no significant changes.

Second case: A 22-year-old woman presented with neck and axillary pain for the last 2 months, which worsened with movement and palpation. This was initially attributed to her physical activity. However, her neck and axillary pain worsened, and she progressed to fever and fatigue during light activity. She was evaluated by a rheumatologist, who requested laboratory tests and VUS of the carotid arteries, axillary vessels, and subclavian artery, in addition to magnetic resonance angiography of the cervical vessels.

VUS of the brachiocephalic trunk, the right common carotid artery, and the right supraclavicular region of the subclavian artery revealed increased diameters at the expense of significant intima-media thickening, causing subocclusion of these vessels (Figure 3A-C). The movement of the vessels was blocked, representing a drop in pulsatility, and the presence of hypoechoic areas probably represented vascularization of the wall of the right common carotid artery, which was detected by B-mode, color flow mapping, and amplitude Doppler imaging (Figure 4A-C). Retrograde flow in the external carotid artery flow was filling the internal carotid artery, which kept the flow at low speed, but in a cephalad direction. The caliber of both carotid branches was reduced, with no IMC involvement. The right vertebral artery was occluded (Figure 4D). The caliber of the infraclavicular region of the subclavian artery

Contents

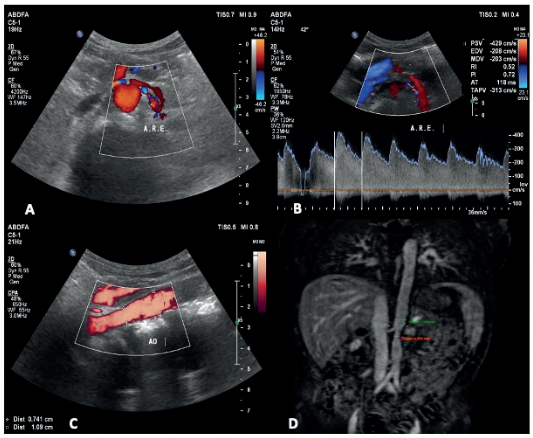

Figure 1 – *A) Color flow mapping shows lumen narrowing in the proximal course of the renal artery with flow turbulence; B) spectral Doppler analysis with PSV = 429cm/s and EDV = 208cm/s; C) measurement of the caliber of the abdominal aorta in the path with narrowing = 7.4mm, compared to the most distal path = 10.9mm; D) magnetic angioresonance of the abdominal aorta showing narrowing of the aorta in the path close to the origin of the mesenteric vessels.*

and the axillary artery was reduced due to IMC thickening, with low-amplitude single-phase flow.

Ultrasound imaging of the left carotid, subclavian, and axillary arteries showed no abnormalities.

In maximum intensity projection reconstruction, magnetic resonance angiography of the intracranial vessels showed no opacification of the right internal carotid artery, suggesting chronic occlusion or subocclusion, and the right middle cerebral and right anterior cerebral arteries were visualized through the right anterior and posterior communicating arteries (Figure 5A). However, contrasted axial sections showed diffuse parietal thickening and thread-like flow in the right internal carotid artery (Figure 5B).

The patient's laboratory results showed increased inflammatory response, with a C-reactive protein level of 97 mg/L and an erythrocyte sedimentation rate of 114 mm/h.

Clinical course: Treatment consisted of prednisone 1 mg/kg and methylprednisolone pulse therapy 1000 mg for 3 consecutive days, associated with 6 monthly pulses of cyclophosphamide. Approximately 1 month after treatment began, the clinical picture improved and new VUS of the cervical arteries showed reduced arterial caliber and no signs of artery wall vascularization, but arterial obstruction had not reduced.

Discussion

TA is a chronic granulomatous panarteritis of unclear etiology that involves the large vessels, primarily the aorta and its major branches. The vast majority of cases (75% to 97%) occur women < 40 years of age.[1] There is no gold standard imaging or laboratory test with adequate sensitivity or specificity to diagnose TA. The diagnostic criteria for TA are a combination of physical examination, laboratory findings, and imaging studies.

Several authors have demonstrated the importance of VUS in diagnosis and follow-up of giant cell arteritis, suggesting that it should be included as a complementary exam in both TA and temporal arteritis.[3-5]

The recommended technique for evaluating IMC in patients with suspected arteritis is longitudinal ultrasound section imaging in B-mode with a high-frequency linear transducer. Measurement is made from the inner edge of the IMC to the outer edge of the adventitial layer of the vessel. Diffuse, homogeneous, and concentric increase in IMC, associated or not with loss of pulsatility, are considered positive criteria. The degree of echogenicity depends on disease stage. Vascularization in the arterial wall indicates

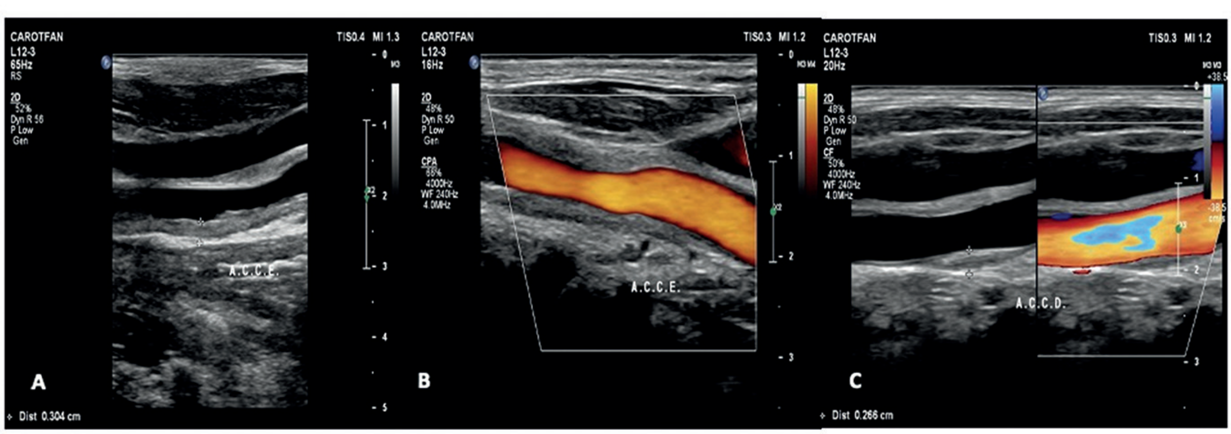

Figure 2 – *A) Diffuse and hyperechogenic thickening of the intima-media complex of the left common carotid artery; B) a reduction of the vascular lumen is observed as a result of the intima-media thickening; C) diffuse and hyperechoic thickening of the intima-media complex of the right common carotid artery.*

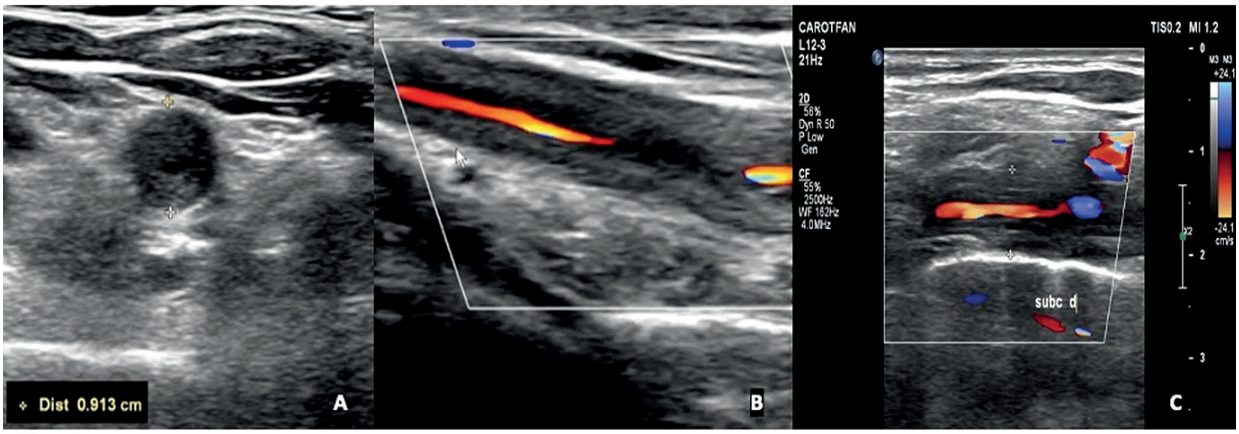

Figure 3 – *A) Transverse section of the right common carotid artery with increased anteroposterior diameter (9.13mm); B) Longitudinal section of the right common carotid artery, with marked thickening of the intima-media complex, with color flow mapping showing significant reduction of the vascular lumen; C) right subclavian artery, in its supraclavicular course, with increased diameters and accentuated intima-media thickening.*

disease activity, which can be further investigated through ultrasound with contrast-enhancing agents.[6]

After the creation of fast-track clinics, which provide clinical and laboratory tests and VUS within 24 hours, the importance of ultrasound assessment for patients with suspected arteritis has become clear. The decreased number of patients with permanent vision loss and the reduced number of biopsies in patients with suspected temporal arteritis, which have been demonstrated in 2 important studies, reinforce the value of VUS in the rapid diagnosis of this disease, as well as arteritis in general.[7,8]

Increased IMC thickness, which is identified through B-mode VUS, reflects inflammation in the vessel wall due to the mobilization and migration of myofibroblasts to the IMC.[9] This increase in mural thickness can cause stenosis, occlusion and, consequently, ischemia and damage to the target organ tissue.[10]

In ultrasound assessment, an arteritic IMC will be concentrically and homogeneously arranged, which must be differentiated from non-homogeneous, asymmetrical, and partially calcified alterations of the arterial wall, which are typically observed in atherosclerosis.[11]

IMC thickening, which is associated with vessel caliber > 10 mm and neovascularization, has been described as a sign of disease activity.[12] As has been described in the diagnosis of temporal arteritis, an inflammatory halo, representing low IMC echogenicity, may be a sign of disease activity in a thickened IMC in TA. The opposite is also true, ie, hyperechogenic areas in a thickened IMC indicate the presence of fibrotic material, characterizing a more chronic stage of the disease.[13]

Svensson et al.[14] compared IMC characteristics in patients with and without disease activity, characterizing the different stages into five grades. Grades I, II and V are considered disease activity:

Grade I: - Increased IMC, low-to-medium echogenicity and hypoechoic areas in the IMC

- Increased IMC, low-to-medium echogenicity and neovascularization
- Increased IMC, low-to-medium echogenicity, and increased vessel diameter

Grade II: Increased IMC, medium echogenicity (no increase in diameter or hypoechoic areas)

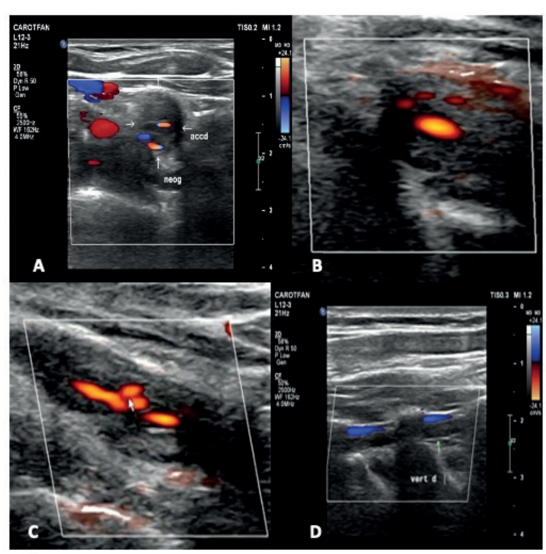

Figure 4 – *A) Transverse section of the right common carotid artery with color flow mapping showing areas of neovascularization intermingled in the thickened mediointimal complex; B) areas of vascularization in the arterial wall evidenced by amplitude Doppler in the transverse section; C) longitudinal section of the common carotid artery; D) absence of flow on color flow mapping in the right vertebral artery (occlusion).*

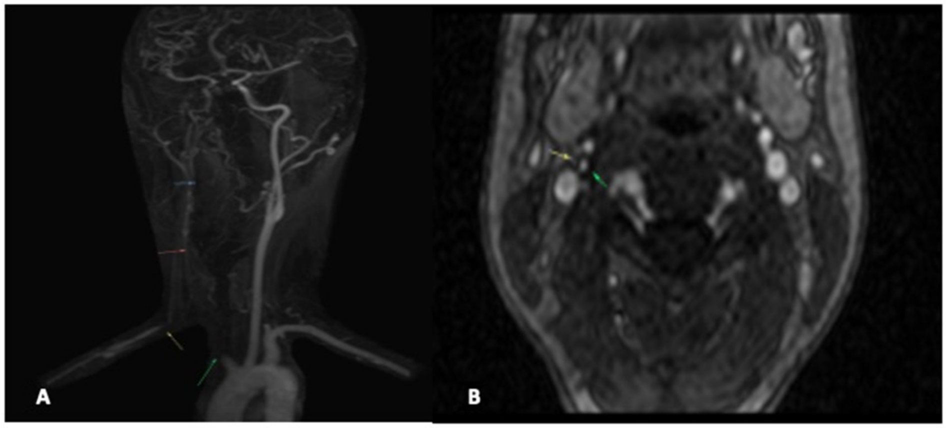

Figure 5 – *AngioRM of intracranial vessels. A) MIP reconstruction of cervical AngioMR: absence of flow in the right brachiocephalic trunk, right subclavian artery, ACCD and in most of the ACID; B) Axial section of MRA, with contrast: ACID with diffuse parietal thickening and marked luminal reduction, with threadlike flow inside it.*

Grade III: Increased IMC, medium echogenicity and fibrotic areas

Grade IV: Increased IMC, high echogenicity and fibrotic areas

Grade V: Grade III or IV with any signs of grade I

Conclusions

VUS is a non-invasive method that can aid in the diagnosis and monitoring of inflammatory changes in the vessel wall of patients with TA. Increased artery diameter at the expense of a thickened hypoechoic IMC or with signs of increased vascularization of the arterial wall are suggestive of disease activity. Thickening of the IMC, which is characterized by greater echogenicity and the appearance of fibrotic elements in the wall, suggests disease stability and a lack of inflammation.

Author Contributions

Conception and design of the research, acquisition of data and analysis and interpretation of the data: Barros FS; writing of the manuscript and critical revision of the manuscript for intellectual content: Barros FS, dos Santos SN, Storino J, Freire CMV, Barros FS.

Potential Conflict of Interest

No potential conflict of interest relevant to this article was reported.

Sources of Funding

There were no external funding sources for this study.

Study Association

This study is not associated with any thesis or dissertation work.

Ethics Approval and Consent to Participate

This article does not contain any studies with human participants or animals performed by any of the authors.

References

1. Gornik HL, Creager MA. Aortitis. Circulation. 2008;117(23):3039-51. doi: 10.1161/CIRCULATIONAHA.107.760686.
2. Czihal M, Lottspeich C, Hoffmann U. Ultrasound Imaging in the Diagnosis of Large Vessel Vasculitis. Vasa. 2017;46(4):241-53. doi: 10.1024/0301-1526/a000625.
3. Brkic A, Terslev L, Døhn UM, Torp-Pedersen S, Schmidt WA, Diamantopoulos AP. Clinical Applicability of Ultrasound in Systemic Large Vessel Vasculitides. Arthritis Rheumatol. 2019;71(11):1780-7. doi: 10.1002/art.41039.
4. Kim ESH, Beckman J. Takayasu Arteritis: Challenges in Diagnosis and Management. Heart. 2018;104(7):558-65. doi: 10.1136/heartjnl-2016-310848.
5. Germanò G, Monti S, Ponte C, Possemato N, Caporali R, Salvarani C, et al. The Role of Ultrasound in the Diagnosis and Follow-Up of Large-Vessel Vasculitis: An Update. Clin Exp Rheumatol. 2017;35 Suppl 103(1):194-8.
6. Germanò G, Macchioni P, Possemato N, Boiardi L, Nicolini A, Casali M, et al. Contrast-Enhanced Ultrasound of the Carotid Artery in Patients with Large Vessel Vasculitis: Correlation with Positron Emission Tomography Findings. Arthritis Care Res. 2017;69(1):143-9. doi: 10.1002/acr.22906.
7. Diamantopoulos AP, Haugeberg G, Lindland A, Myklebust G. The Fast-Track Ultrasound Clinic for Early Diagnosis of giant Cell Arteritis Significantly Reduces Permanent Visual Impairment: Towards a More Effective Strategy to Improve Clinical Outcome in Giant Cell Arteritis? Rheumatology. 2016;55(1):66-70. doi: 10.1093/rheumatology/kev289.

8. Patil P, Williams M, Maw WW, Achilleos K, Elsideeg S, Dejaco C, et al. Fast Track Pathway Reduces Sight Loss in Giant Cell Arteritis: Results of a Longitudinal Observational Cohort Study. Clin Exp Rheumatol. 2015;33(2 Suppl 89):S-103-6.

9. Weyand CM, Goronzy JJ. Medium- and Large-Vessel Vasculitis. N Engl J Med. 2003;349(2):160-9. doi: 10.1056/NEJMra022694.

10. Weyand CM, Goronzy JJ. Immune Mechanisms in Medium and Large-Vessel Vasculitis. Nat Rev Rheumatol. 2013;9(12):731-40. doi: 10.1038/nrrheum.2013.161.

11. Czihal M, Zanker S, Rademacher A, Tatò F, Kuhlencordt PJ, Schulze-Koops H, et al. Sonographic and Clinical Pattern of Extracranial and Cranial Giant Cell Arteritis. Scand J Rheumatol. 2012;41(3):231-6. doi: 10.3109/03009742.2011.641581.

12. Park SH, Chung JW, Lee JW, Han MH, Park JH. Carotid Artery Involvement in Takayasu's Arteritis: Evaluation of the Activity by Ultrasonography. J Ultrasound Med. 2001;20(4):371-8. doi: 10.7863/jum.2001.20.4.371.

13. Schmidt WA, Gromnica-Ihle E. What is the Best Approach to Diagnosing Large-Vessel Vasculitis? Best Pract Res Clin Rheumatol. 2005;19(2):223-42. doi: 10.1016/j.berh.2005.01.006.

14. Svensson C, Eriksson P, Zachrisson H. Vascular Ultrasound for Monitoring of Inflammatory Activity in Takayasu Arteritis. Clin Physiol Funct Imaging. 2020;40(1):37-45. doi: 10.1111/cpf.12601.

Transient Perivascular Inflammation of the Carotid Artery (TIPIC): Vascular Ultrasonography Role

Fanilda Souto Barros,[1] Simone Nascimento dos Santos,[2] Daniela Souto Barros,[3,4] Sérgio Salles Cunha,[5] Ana Lopes Albricker,[6] Ana Cláudia Gomes Petisco[3]

Angiolab Laboratório Vascular,[1] Vitório, ES – Brazil
ECCOS Diagnóstico Cardiovascular,[2] Brasília, DF – Brazil
Instituto Dante Pazzanese de Cardiologia,[3] São Paulo, SP – Brazil
Hospital Nossa Senhora das Graças,[4] Curitiba, PR – Brazil
Society of Vascular Ultrasound,[5] Jacksonville, FL – United States
Instituto Imede de Ultrassom,[6] Belo Horizonte, MG – Brazil

Transient Perivascular Inflammation of the Carotid Artery (TIPIC syndrome) is a rare and underdiagnosed condition. In this article, we describe a case of TIPIC syndrome, including topics such as clinical evaluation, indication and findings of vascular ultrasonography (VUS), treatment and follow-up, with a brief review of the literature.

Case Report

Male patient, 53 years old, complaining of progressive unilateral neck pain, which appeared spontaneously, in association with edema, local redness, and great sensitivity to palpation. The patient's past history included radiotherapy for about 5 years in the neck and face region, on the opposite side of the current complaint. The patient was a non-smoker and had no other significant risk factors for atherosclerotic disease. One year before the current clinical picture, the patient had undergone VUS of the carotid arteries, in a routine evaluation for follow-up after radiotherapy, the result was within normal limits.

Given the clinical picture, a new VUS examination was requested, which included the standard protocol for evaluating the extracranial common, external, and internal carotid arteries (ACC, ICA and ACE). Special attention was given to extracarotid (perivascular) tissues due to the history of radiotherapy. The B-mode US showed extensive hypoechoic and homogeneous involvement of the tissues, including the arterial wall at the level of the carotid bifurcation, expanding to the proximal ICA (Figure 1A). The peak systolic velocity and end-diastolic velocity (PSV/EDV) were high: PSV/EDV = 288/129 cm/s (Figure 1B). Local stenosis measured in the transverse plane of the image was estimated at 74% (Figure 1C), consistent with the Doppler velocity data. The extent of the affected area was 5.57 mm compared to a lumen of 1.96 mm. Magnetic resonance imaging (MRI) and angioresonance (MRA) showed irregular thickening, with contrast enhancement, in the proximal ICA and bifurcation, corroborating the VUS findings (Figures 2A and 2B).

The patient underwent drug treatment with corticosteroids for 2 weeks with significant improvement in symptoms.

The VUS of the carotid arteries was repeated after 4 months, this second exam being essential for the diagnostic conclusion. Ultrasound examination showed that, after treatment, there was a reduction in the degree of stenosis to approximately 50% (Figures 3A and 3B). The ICA luminal diameter increased from 1.96 mm to 3.19 mm. PSV decreased from 288 cm/s to 132 cm/s and EDV decreased from 129 cm/s to 62 cm/s (Figure 3C).

Due to clinical improvement and VUS data after treatment, the diagnosis of TIPIC syndrome was considered.

Discussion

TIPIC syndrome is a rare and underdiagnosed disease, supposedly of an inflammatory nature.[1] Its etiology and pathophysiology are unknown, and it may be part of an autoimmune process that has not yet been clarified. Prevalence was estimated at 2.8%, in individuals with acute onset neck pain, with a slight male predominance [(1,5,1)] and a mean age of 48 years. Its evolution suggests that it is benign, with resolution of the symptoms in approximately 2 weeks, either spontaneously or with the use of drugs such as non-hormonal anti-inflammatory drugs, corticosteroids and acetylsalicylic acid.[1-3]

Laboratory tests can be normal or nonspecific, and the diagnosis is made by clinical presentation and imaging tests.[1] VUS is capable of identifying vascular and perivascular alterations in TIPIC syndrome, in which one of the characteristic alterations is the diffuse and homogeneous increase in the echogenicity of the perivascular fatty tissue at the site of pain, causing attenuation of the sound beam, as well as the presence of a self-limited intimal soft plaque could be related to the carotid inflammatory process.[1,2] Other imaging methods that can also be used for the

Keywords

TIPIC; Carotid artery; arteritis

Mailing Address: Fanilda Souto Barros •
Angiolab Laboratório Vascular. Rua José Teixeira, 290. Postal code: 29055-310. Praia do Canto, Vitória, ES – Brazil
E-mail: fanildas@gmail.com
Manuscript received February 20,2023; revised March 2, 2023; accepted March 3, 2023
Editor responsible for the review: Simone Nascimento dos Santos

DOI: https://doi.org/10.36660/abcimg.20230019i

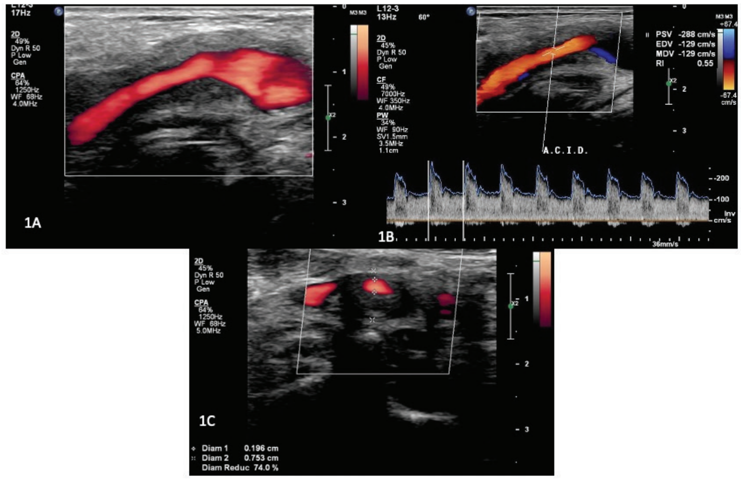

Figure 1 – *Transient Perivascular Inflammation of the Carotid Artery (TIPIC syndrome) is a rare and underdiagnosed condition. In this article, we describe a case of TIPIC syndrome, including topics such as clinical evaluation, indication and findings of vascular ultrasonography (VUS), treatment and follow-up, with a brief review of the literature.*

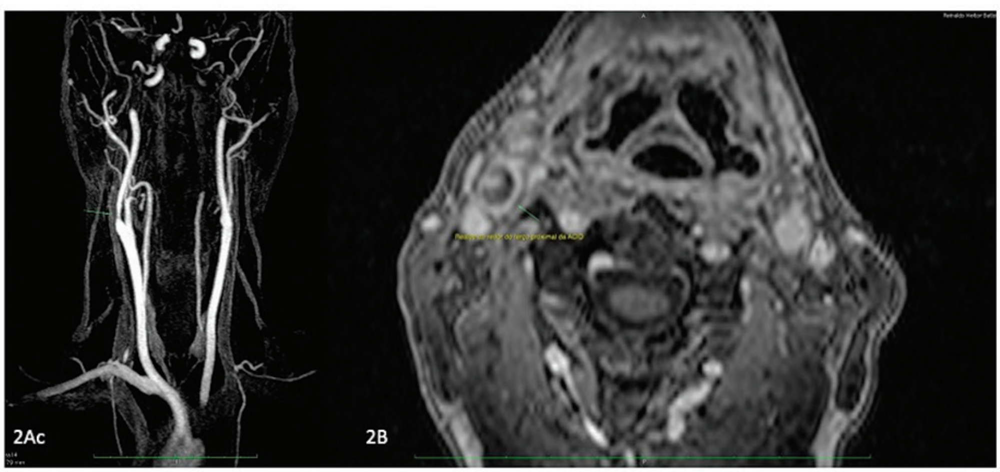

Figure 2 – *MRI and magnetic resonance angiography (NMR). A) MRA showing a 70% reduction in the lumen of the proximal ICA; B) Irregular thickening with contrast enhancement in the periphery of the ICA. Cortesy: Fernando Santos Emerick Gomes M.D. Federal University of Espírito Santo.*

diagnosis of TIPIC and that contribute to the sonographic findings are computed tomography (CT), MRI and NMR.[2-4]

A retrospective multinational observational study, involving 72 patients, discussed findings such as thickness and longitudinal extent of the disease in ultrasound images, with the purpose of evaluating the clinical behavior and characteristics at VUS in the TIPIC syndrome.[2] The authors reaffirmed the use of the previously proposed term TIPIC, replacing the term "carotidynia" for cases such as the one described in this article.[1,2]

Lecler et al.[1] proposed 4 major diagnostic criteria for TIPIC: 1) presence of acute pain along the course of the carotid artery, which may radiate to the head; 2) eccentric perivascular infiltration on imaging; 3) exclusion of another diagnosis, whether vascular or non-vascular; 4) improvement in 14 days with anti-inflammatory treatment or spontaneous. And yet a minor criterion: presence of self-limited intimal soft plaque.

Potential differential diagnoses include acute carotid artery dissection, Takayasu arteritis, giant cell arteritis, other vasculitis (including radiation-induced arteritis), jugular vein thrombosis, lymphadenitis, submandibular gland disorder, and tumors.[1,2]

Lately, two case reports were published that presented similar clinical characteristics, however, one of them was affected by COVID-19. Both were male individuals, 38

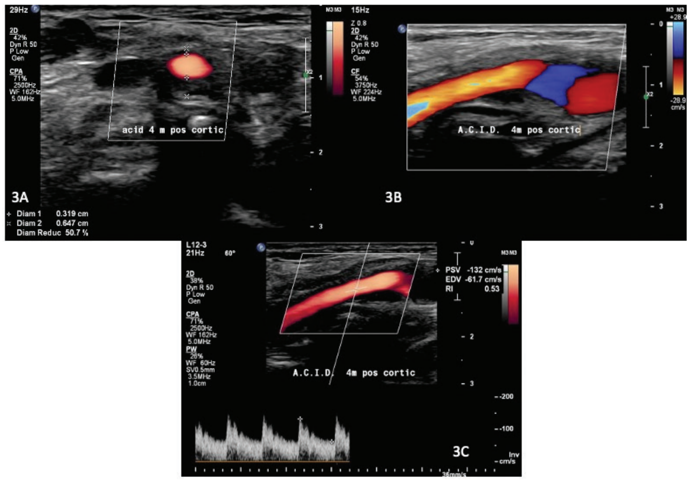

Figure 3 – *VUS findings of the TIPIC case, 4 months after diagnosis and treatment. A) Cross-sectional image in B-mode and power Doppler, with measurement of the degree of stenosis in the proximal ICA; B) Thickening reduction covering the wall of the proximal ICA, from the carotid bifurcation, with color Doppler flow; C) Pulsed Doppler of the proximal ICA demonstrating a reduction in flow velocity values.*

and 45 years old, with thickening of the arterial wall of the ACC and carotid bifurcation on VUS. B-mode VUS imaging demonstrated hypoechogenic homogeneous tissue, without significant arterial stenosis, and the findings were corroborated by CT and magnetic resonance.[3,4] As in our case, local signs and symptoms in the neck region improved within two weeks after treatment.

The VUS performed 4 months after the beginning of the condition in our patient showed a substantial improvement in the alterations, compared with the alterations detected in the diagnostic ultrasound examination. Such findings are consistent with the data described in the literature, and there may be complete remission of the ultrasonographic alterations, although there may be residual lesions.[1-3] One explanation, according to the histopathological study, would be the early development of fibrosis associated with chronic and low-grade inflammatory activity.[1]

Ultrasound Tissue Characterization Analysis can use tissue brightness to identify cases of TIPIC.[5] The technique used by Lal et al.[5] stratifies the B-mode image using reference points between 0-190 in differentiating blood -adventitia. Adventitia may not be clear in TIPIC cases, but tissue characterization can separate homogeneous TIPIC findings from heterogeneous findings suggestive of atherosclerotic plaque. There is also the prospect of using contrast-enhanced ultrasound (CEUS) to investigate TIPIC findings, just as CEUS has been promising for the detection of flow on Doppler arising from neovascularization within carotid plaques[2,6] and also in cases of carotid membranes.[7]

Conclusion

VUS, clinical history and physical examination documented a rare case of TIPIC, which was confirmed by MRI. Treatment results were consistent with literature data. The etiology of the TIPIC syndrome still requires further investigation for its better elucidation.

Author Contributions

Conception and design of the research: Barros FS, dos Santos SN, Cunha SS; Acquisition of data and analysis and interpretation of the data: Barros FS; Writing of the manuscript and critical revision of the manuscript for intellectual content: Barros FS, dos Santos SN, Barros DS, Cunha SS, Albriker ACL, Petisco ACGP.

Potential Conflict of Interest

No potential conflict of interest relevant to this article was reported.

Sources of Funding

There were no external funding sources for this study.

Study Association

This study is not associated with any thesis or dissertation work.

Ethics Approval and Consent to Participate

This article does not contain any studies with human participants or animals performed by any of the authors.

References

1. Lecler A, Obadia M, Savatovsky J, Picard H, Charbonneau F, Champfleur NM, et al. TIPIC Syndrome: Beyond the Myth of Carotidynia, a New Distinct Unclassified Entity. AJNR Am J Neuroradiol. 2017;38(7):1391-8. doi: 10.3174/ajnr.A5214.

2. Micieli E, Voci D, Mumoli N, Mastroiacovo D, Grigorean A, Obadia M, et al. Transient Perivascular Inflammation of the Carotid Artery (TIPIC) Syndrome. Vasa. 2022;51(2):71-7. doi: 10.1024/0301-1526/a000989.

3. Maggialetti N, De Marco I, Sasso S, Farchi G, Ianora AAS, Lucarelli NM, et al. "Translent Perivascular Inflammation of the Carotid Artery (TIPIC) Syndrome" as a Rare Case of Laterocervical Pain: Multimodal Diagnosis. Radiol Case Rep. 2022;17(7):2378-82. doi: 10.1016/j.radcr.2022.04.021.

4. Venetis E, Konopnicki D, Jissendi Tchofo P. Multimodal Imaging Features of Transient Perivascular Inflammation of the Carotid Artery (TIPIC) Syndrome in a Patient with Covid-19. Radiol Case Rep. 2022;17(3):902-6. doi: 10.1016/j.radcr.2021.12.005.

5. Lal BK, Hobson RW 2nd, Pappas PJ, Kubicka R, Hameed M, Chakhtoura EY, et al. Pixel Distribution Analysis of B-Mode Ultrasound Scan Images Predicts Histologic Features of Atherosclerotic Carotid Plaques. J Vasc Surg. 2002;35(6):1210-7. doi: 10.1067/mva.2002.122888.

6. Dong S, Hou J, Zhang C, Lu G, Qin W, Huang L, et al. Diagnostic Performance of Atherosclerotic Carotid Plaque Neovascularization with Contrast-Enhanced Ultrasound: A Meta-Analysis. Comput Math Methods Med. 2022;2022:7531624. doi: 10.1155/2022/7531624.

7. Zhou Q, Li R, Feng S, Qu F, Tao C, Hu W, et al. The Value of Contrast-Enhanced Ultrasound in the Evaluation of Carotid Web. Front Neurol. 2022;13:860979. doi: 10.3389/fneur.2022.860979.

Case Report

New Application of FFRCT in Clinical Practice: Evaluation of Interarterial Anomalous Coronary Course

Fábio Bordin Trindade,[1] Thamara Carvalho Morais,[1,2] Roberto Nery Dantas Junior,[1,2] Roberto Vitor Almeida Torres,[1,2] Clarice Santos Parreira Soares,[1] José Rodrigues Parga Filho[1,2]

Hospital Sírio-Libanês,[1] São Paulo, SP – Brazil

Instituto do Coração da Faculdade de Medicina, Universidade de São Paulo (InCor/FMUSP),[2] São Paulo, SP – Brazil

A 58-year-old male patient, who worked as an airline pilot, sought emergency cardiology care due to palpitations and ill-defined chest discomfort, which had onset at rest 1 hour before admission, without irradiation or associated symptoms. He had personal history of diabetes mellitus, obesity, generalized anxiety disorder, and a mild COVID-19 episode 3 months prior (not requiring hospitalization), in addition to family history of early coronary artery disease (his father had an infarction at 40 years of age). Physical examination showed no relevant alterations. The electrocardiogram showed only sinus tachycardia and nonspecific ventricular repolarization changes. Serial troponin testing was performed, and all results were within normal limits. Echocardiogram showed preserved left ventricular ejection fraction (71%), absence of alterations in segmental contractility, and discreet diastolic dysfunction (altered relaxation). Following the institutional chest pain protocol, the patient was referred for computed tomography angiography (CTA) of the coronary arteries, which showed right coronary artery with an anomalous origin in the left coronary sinus and an interarterial (suprapulmonary) course, with significant luminal reduction (> 50%) in the ostium and proximal segment (Figure 1). After the diagnostic finding, the patient was recruited in a research protocol for evaluation of myocardial ischemia by tomography by means of non-invasive quantification of the myocardial fractional flow reserve (FFRCT). Software based on artificial intelligence (cFFR, version 3.0.0) available on a research platform (Syngovia Frontier Platform, Siemens Healthineers) was used. The calculation of FFRCT demonstrated ischemia in the right coronary artery territory (Figure 2; FFRCT 0.63 [reference values: FFRCT ≤ 0.75 = indicates ischemia; between 0.76 and 0.80 = borderline zone; > 0.80 = excludes ischemia]).[1] The patient continued investigation with coronary angiography with invasive FFR (iFFR), which confirmed flow limitation in the anomalous right coronary artery (Figure 3A; iFFR 0.68 [reference values: iFFR ≤ 0.8 indicates ischemia; > 0.8 excludes ischemia]).[2] At that moment, treatment with drug-eluting stent implantation was chosen (Figure 3B), with good angiographic results and no complications. After 6 months, the patient was asymptomatic, with no recurrence of symptoms.

Keywords

Fractional Flow Reserve, Myocardial; Congenital Abnormalities; Tomography, X-Ray Computed; Myocardial Ischemia; Machine Learning.

Mailing Address: Fábio Bordin Trindade •
Hospital Sírio-Libânes. Rua Adma Jafet, 115. CEP: 01308-050. Bela Vista. São Paulo, SP – Brazil
E-mail: fabio.trindade@hsl.org.br
Manuscript received November 8, 2022; revised manuscript February 16, 2023; accepted February 17, 2023
Editor responsible for the review: Leonardo Sara da Silva

DOI: https://doi.org/10.36660/abcimg.2023361i

Discussion

Anomalous origin and course of coronary arteries are rare congenital heart diseases, affecting less than 1% of the general population.[3,4] Anomalous coronary origin with an interarterial (suprapulmonary) course is characterized by the course of the coronary artery between the ascending aorta and the pulmonary artery trunk, most commonly involving the right coronary artery.[3,5] Most individuals are asymptomatic, but, among symptomatic patients, chest pain and dyspnea on exertion are the most prevalent complaints. There is also an increase in rates of arrhythmia, sudden death, and acute myocardial infarction.[4,6] Sudden death is the main complication of this anatomical variant, occurring in approximately 30% of patients.[3,4,6] In these cases, the narrowing and stretching of the anomalous ostium, mainly during physical exercise and in stressful situations, with consequent reduction in coronary flow, is the substrate for potentially fatal ischemic alterations.[3,4,6] Since electrocardiogram, in most cases, does not reveal ischemic alterations, diagnosis is generally made through an incidental finding on imaging exams.[4] These exams are of great importance, especially coronary CTA, which, in addition to being a non-invasive exam with high negative predictive value, allows detailed anatomical visualization (angle of the origin, presence of intramural trajectory in the aorta, degree of ostial/proximal luminal reduction) and the correct classification in relation to the pulmonary valve plane (suprapulmonary versus subpulmonary).[2,6,7]

Recent studies have demonstrated that coronary CTA is an accurate test for identifying myocardial ischemia through FFRCT, when compared to invasive measurement (iFFR) by coronary angiography.[1,2,7,8] The detection of ischemia in coronary CTA is of great importance in decision-making, mainly in plaques considered moderate (50% to 69% luminal reduction) or when there is diagnostic doubt, reducing the number of unnecessary referrals to coronary angiography in cases without ischemia on FFRct.[1,2,8] Due to the excellent accuracy between

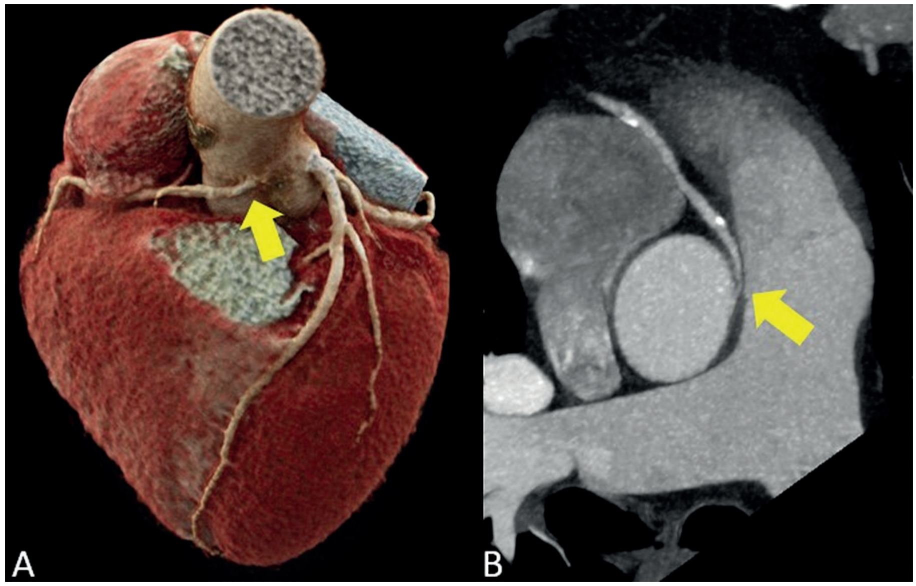

Figure 1 – *Three-dimensional reconstruction of the coronary tree with origin of the anomalous right coronary artery (arrow) in the left coronary sinus and interarterial course (A); two-dimensional curved planar reconstruction of the anomalous right coronary artery (arrow) with significant luminal reduction (> 50%) of the ostium and proximal segment (B).*

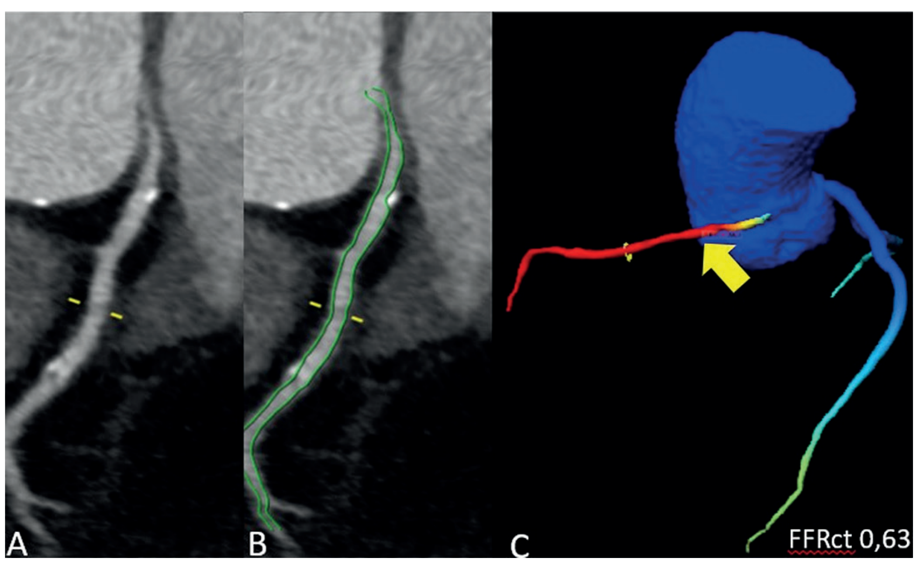

Figure 2 – *Two-dimensional curved planar reformatting (A), with delimitation of the coronary lumen (B) of the anomalous right coronary artery. Three-dimensional reconstruction with representation of FFRCT values throughout the entire coronary tree (C). FFRCT demonstrates coronary flow limitation, calculated approximately 1 cm after the luminal reduction in the ostium/proximal third of the anomalous right coronary artery (arrow).*

the methods in the analysis of a coronary tree without anomaly, the applicability of the method in the context of coronary anomaly has been extrapolated.[5,7] Our group applied the most current version of a tool for calculating FFRCT currently available only on a research platform developed by Siemens Healthineers (cFRR, version 3.0.0) in the clinical case described. This research tool is available for installation on standard configuration computers, and it uses artificial intelligence tools, with reduced processing time.[8] Currently, commercially available options require the step of sending images in DICOM format for processing in specific centers, with delivery of results at least 24 hours

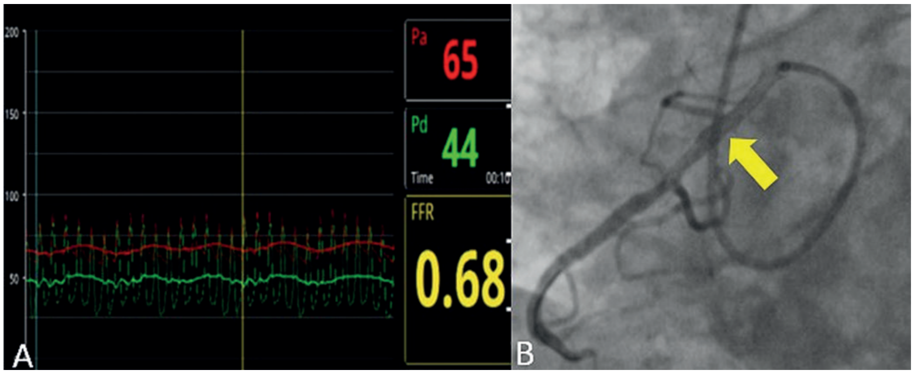

Figure 3 – *Ischemia in the right coronary artery confirmed by iFFR (reference value for ischemia ≤ 0.8) (A); invasive coronary angiography demonstrating the final result after drug-eluting stent implantation (arrow) in the proximal segment of the anomalous pathway (B).*

after the images have been sent.[1,2] The research tool used in this clinical case has advantages, such as fast processing time on standard configuration computers in the analysis room and use of tomographic images from the standard routine protocol, without requiring the addition of a specific protocol or a higher dose of radiation, without the use of stressors.[2,8] This tool, in general, has some limitations, such as difficulty in defining the coronary borders in the presence of excessive calcification, and the need for high-quality images, without movement artifacts, for adequate automatic detection of the central luminal line and the lines that delimit the coronary borders, allowing adequate calculation of FFRct.[8] It is important to emphasize that this tool distinguishes the interarterial pathways associated with ischemia, considering only the flow obstacle during rest, without estimating the risk of ischemic events associated with dynamic changes secondary to intense exercise. Use of this tool is scarce in the literature,[5] and it still does not have a robust body of evidence. Nevertheless, in the clinical case described, the FFRCT tool was applied in a context different than what is usual, where luminal reduction was not determined by coronary atheromatosis, but by ostial angulation and compression of the proximal segment of the anomalous interarterial pathway. The ischemic response was considered a parameter of poor prognosis; subsequently, the confirmatory invasive functional test (iFFR) was indicated to assist in the therapeutic decision.

Treatment of coronary anomalies involves the following two strategies: conservative treatment with clinical follow-up of patients in asymptomatic cases; or invasive (surgical or percutaneous) treatment, myocardial revascularization surgery being the preferred technique in symptomatic patients under 30 years of age.[4,6,7] Percutaneous coronary intervention with drug-eluting stent implantation, as in the clinical case described, has emerged more recently as a promising alternative therapy.[4]

Conclusion

Considered a rare anatomical variation, interarterial course is a potentially fatal coronary anomaly, even in asymptomatic patients. In the case described, the novel application of FFRCT based on artificial intelligence proved to be an excellent diagnostic alternative in this anatomical context, given that it is a non-invasive method capable of detecting ischemic coronary luminal reductions in accordance with iFFR, with future potential to guide planning and decision-making in myocardial revascularization interventions.

Author Contributions

Conception and design of the research: Trindade FB; writing of the manuscript: Trindade FB, Soares CSP; critical revision of the manuscript for intellectual content: Morais TC, Dantas Júnior ND, Parga Filho JR; literature review: Trindade FB, Morais TC, Dantas Júnior ND; realization of the FFRct: Morais TC; obtaining and reconstructing 2D and 3D images: Torres RVA.

Potential Conflict of Interest

No potential conflict of interest relevant to this article was reported.

Sources of Funding

There were no external funding sources for this study.

Study Association

This study is not associated with any thesis or dissertation work.

Ethics Approval and Consent to Participate

This article does not contain any studies with human participants or animals performed by any of the authors.

References

1. Rajiah P, Cummings KW, Williamson E, Young PM. CT Fractional Flow Reserve: A Practical Guide to Application, Interpretation, and Problem Solving. Radiographics. 2022;42(2):340-58. doi: 10.1148/rg.210097.

2. Morais TC, Assunção NA Jr, Dantas RN Jr, Silva CFGD, Paula CB, Torres RA, et al. Diagnostic Performance of a Machine Learning-Based CT-Derived FFR in Detecting Flow-Limiting Stenosis. Arq Bras Cardiol. 2021;116(6):1091-8. doi: 10.36660/abc.20190329.

3. Ferreira AFP, Rosemberg S, Oliveira DS, Araujo-Filho JAB, Nomura CH. Anomalous Origin of Coronary Arteries with an Interarterial Course: Pictorial Essay. Radiol Bras. 2019;52(3):193-7. doi: 10.1590/0100-3984.2017.0203.

4. Suryanarayana P, Lee JZ, Abidov A, Lotun K. Anomalous Right Coronary Artery: Case Series and Review of Literature. Cardiovasc Revasc Med. 2015;16(6):362-6. doi: 10.1016/j.carrev.2015.03.006.

5. Ferrag W, Scalbert F, Adjedj J, Dupouy P, Ou P, Juliard JM, et al F. Role of FFR-CT for the Evaluation of Patients with Anomalous Aortic Origin of Coronary Artery. JACC Cardiovasc Imaging. 2021;14(5):1074-6. doi: 10.1016/j.jcmg.2020.10.003.

6. Saleem S, Syed M, Elzanaty AM, Nazir S, Changal K, Gul S, et al. Interarterial Course of Anomalous Right Coronary Artery: Role of Symptoms and Surgical Outcomes. Coron Artery Dis. 2020;31(6):538-44. doi: 10.1097/MCA.0000000000000893.

7. Adjedj J, Hyafil F, Fretay XH, Dupouy P, Juliard JM, Ou P, et al. Physiological Evaluation of Anomalous Aortic Origin of a Coronary Artery Using Computed Tomography-Derived Fractional Flow Reserve. J Am Heart Assoc. 2021;10(7):e018593. doi: 10.1161/JAHA.120.018593.

8. Röther J, Moshage M, Dey D, Schwemmer C, Tröbs M, Blachutzik F, et al. Comparison of Invasively Measured FFR with FFR Derived from Coronary CT Angiography for Detection of Lesion-Specific Ischemia: Results from a PC-Based Prototype Algorithm. J Cardiovasc Comput Tomogr. 2018;12(2):101-7. doi: 10.1016/j.jcct.2018.01.012.

Case Report

Important Constrictive Pericarditis in a Patient with Schistosomiasis: A Case Report

Djair Brindeiro Filho,[1] José Maria Del Castillo,[1] Fábio Antonio Amando Granja[2]
Escola de Ecografia de Pernambuco,[1] Recife, PE – Brazil
Hospital de Clínicas da UFPE,[2] Recife, PE – Brazil

Introduction

Schistosomiasis mansoni (SM) is one of the most common causes of pulmonary hypertension and is often associated with the hepatosplenic form of the disease. However, constrictive pericarditis (CP) is not cited in the medical literature as a consequence of SM.[1,2] One single case report, published in 1979, associating CP with schistosomiasis, presented the etiologic agent of *Schistosoma haematobium*.[3] The present study described a rare case of CP in a patient with chronic hepatosplenic SM, with a significant improvement in the parameters of ventricular filling and myocardial deformation after surgery, illustrating the importance of the echocardiogram in the detection of complications caused by this disease.

Case report

A 47-year-old, female patient, diagnosed with schistosomiasis 10 years ago, presented signs of right heart failure (jugular ingurgitation, hepatomegaly, edema of the lower limbs) and left heart failure (exhaustion with minimum/maximum effort, hypotension). The precordium examination showed no abnormalities and upon auscultation of the heart, one could hear a third sound and a discrete systolic murmur on the left sternal border.

The preliminary echocardiogram showed a major biatrial dilation, signs of mild pulmonary hypertension (41 mmHg), major thickening of the pericardium with no stroke, and the interventricular septum with an altered movement, with a "*septal bounce* " pattern (Figure 1). The spectral Doppler showed a mitral flow with a left ventricular restrictive pattern, and the Tissue Doppler (TD) of the mitral ring with a septal-lateral inversion in an *Annulus reversus* pattern (Figure 2). The speed of left ventricle (LV) outflow was above 100 cm/s and the LV's longitudinal global strain (LGS) was discretely reduced (-14.7%), with an accentuated decrease in the inferolateral and anterolateral walls (Figure 3). Taking these data into account, the CP diagnostic hypothesis was conducted, together with x-ray. A partial surgical pericardiectomy was recommended, revealing an important calcification and adherence of the pericardial layers; the material was sent to the pathological anatomy department (Figure 4).

Eight months after the surgery, there was a clear improvement in the systolic function and the LV filling pattern, diminishing the atrial volumes and increasing the speed of the e´ wave of the lateral ring in relation to the speed of the LV, which increased to -20.7% strain, with the disappearance of the alterations in the inferolateral and anterolateral walls (Figure 5).

Keywords

Constrictive pericarditis; schistosomiais; echocardiography; strain; pericardiectomy

Mailing Address: Djair Brindeiro Filho •
Av. Bernardo Vieira de Melo 2965, apto 1201. Postal Code 54410-010. Piedade, Jaboatão dos Guararapes, PE - Brazil.
E-mail: brindeirofilho@gmail.com
Manuscript received January 1,2023; revised February 10, 2023; accepted March 9, 2023
Editor responsible for the review: Daniela do Carmo Rassi Frota

DOI: https://doi.org/10.36660/abcimg.2023378i

Discussion

Chronic CP is associated with a wide range of possible causes. The disease develops in an insidious manner and, in many cases, the etiology remains undefined.[4] The diagnosis of CP is based on symptoms and signs of heart failure due to the constriction of the pericardium associated with one or more imaging methods. Transthoracic echocardiography (TTE) is recommended in all patients suspected of CP.[5] Schistosomiasis, a tropical endemic parasitosis, can lead to pulmonary hypertension due to the occlusion of the pulmonary arterioles by the SM eggs. The myocardial and pericardial involvement of SM species is rare and can occur due to the accumulation of SM eggs, which induce a local granulomatous response.[6] In the only case published in the medical literature,[3] the histopathological study of the pericardium showed a fibrous thickening with an increase in the connective tissue and identified the presence of *Schistosoma haematobium* eggs. In the present case, the anatomopathological study of pericardial fragments showed fibrous connective tissue, showing extensive dystrophic calcification, but no SM eggs were identified. Two possibilities can be suggested: the absence of eggs in the analyzed fragments and/or the disintegration of the eggs. In any case, the etiological possibility cannot be discarded, since there was no medical history or other concomitant disease that could be attributed as a cause of CP. The TTE identified various parameters of CP, which normalized in the exams performed about eight months after the excellent result of the surgical procedure (Figure 5). The analysis of the myocardial strain can aid in providing a more precise detection of the adherence of the pericardium to the myocardium along the free wall of the LV, aiding in the diagnosis of CP, as illustrated the present case.

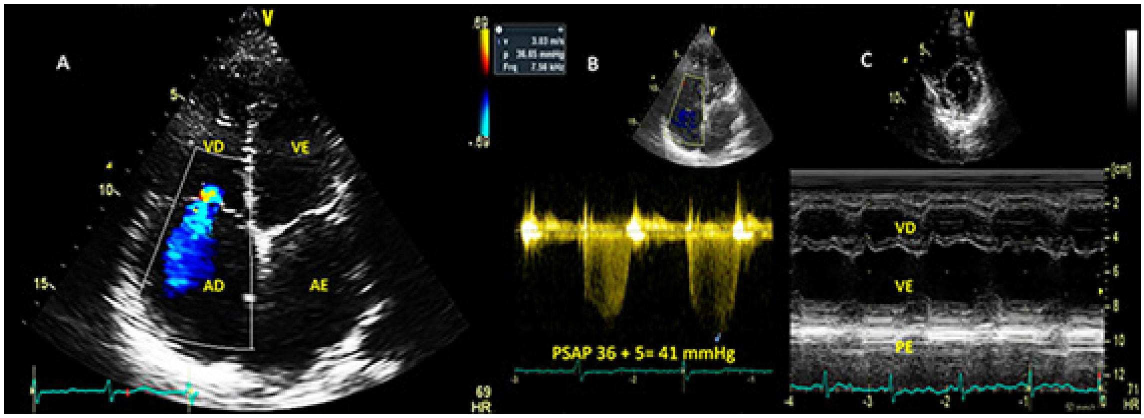

Figure 1 – *Eco 2D 4C showing the dilation of the atriums and tricuspid regurgitation; B) Estimation of pulmonary systolic blood pressure using the continuous Doppler; C) Mode M "septal bounce" and pericardial thickening. PSAP: Pulmonary Systolic Arterial Pressure.*

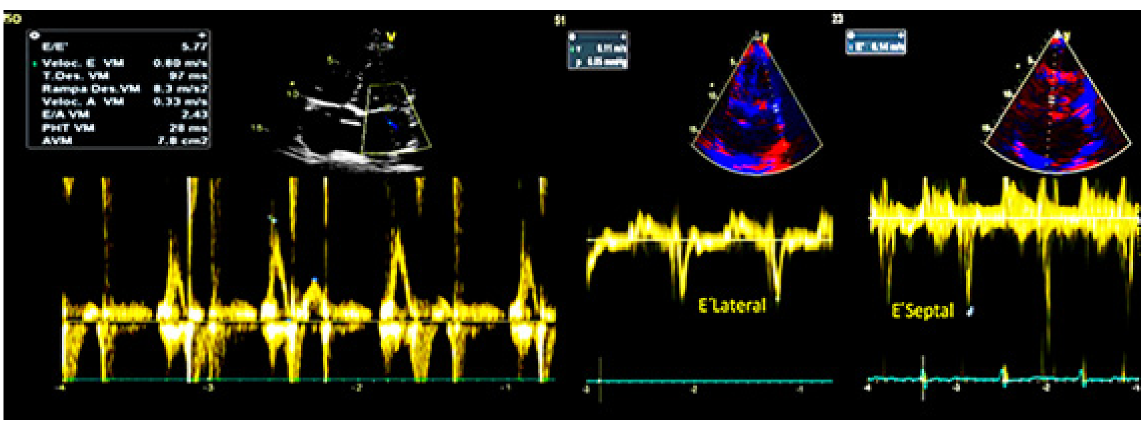

Figure 2 – *Mitral flow with restrictive pattern (Left); TD showing lateral E´ < septal E´ speed (Right).*

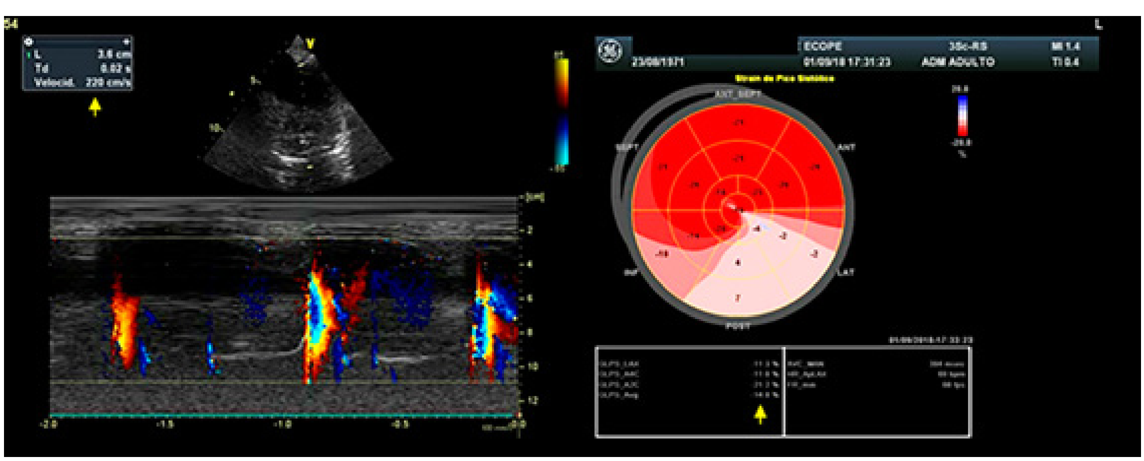

Figure 3 – *Left: Colored Mode M; Speed of outflow with 220 cm/s (arrow photo); Right: LGS, 14.8% (arrow photo) with evident decrease in the inferolateral and anterolateral walls.*

Case Report

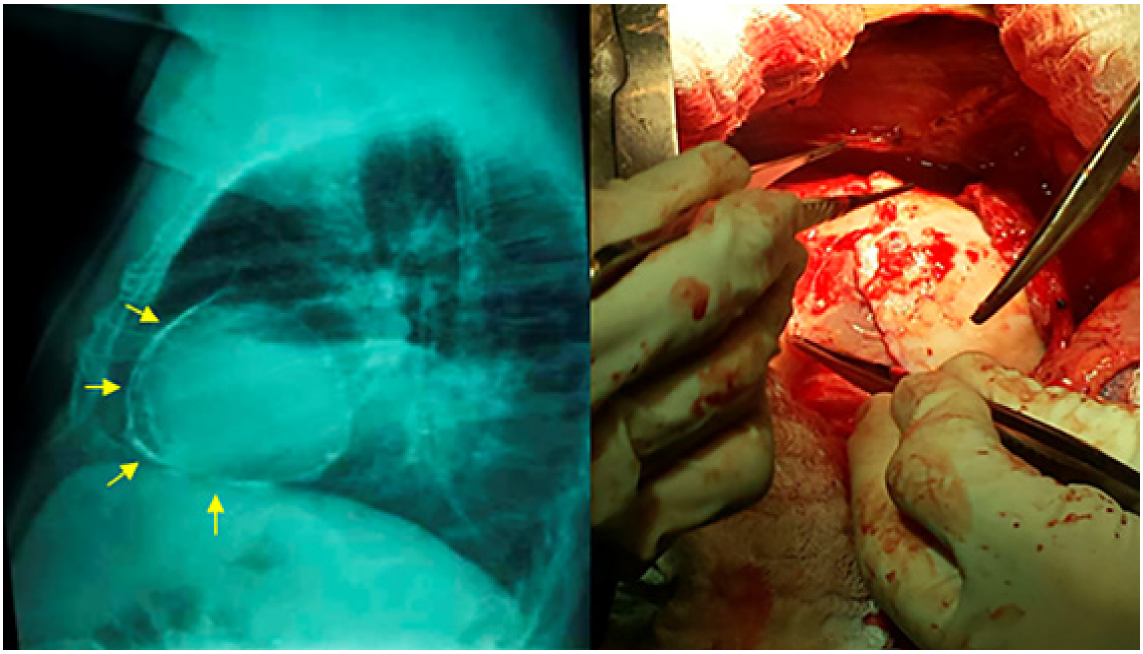

Figure 4 – *Intense pericardial thickening observed in the chest X-ray (left) and during surgery (right)*

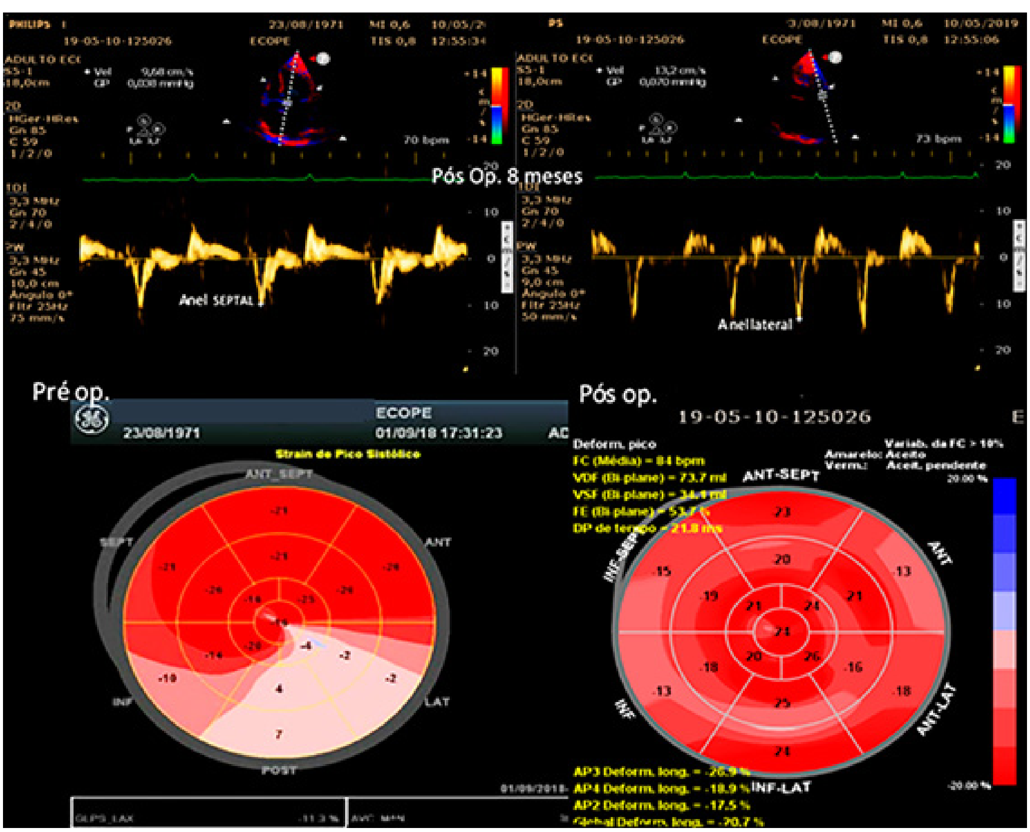

Figure 5 – *Above (TD). Normalization of the speed of the lateral ring (lateral ring E´ wave > septal). Below (LGS). Normalization of the deformity in the inferolateral and anterolateral walls.*

Author Contributions

Conception and design of the research and acquisition of data Brindeiro Filho D, Granja FAA; analysis and interpretation of the data Brindeiro Filho D, Del Castillo JM; writing of the manuscript Brindeiro Filho D; critical revision of the manuscript for intellectual content Del Castillo JM. Granja FAA.

Potential Conflict of Interest

No potential conflict of interest relevant to this article was reported.

Sources of Funding

There were no external funding sources for this study.

Study Association

This study is not associated with any thesis or dissertation work.

Ethics Approval and Consent to Participate

This article does not contain any studies with human participants or animals performed by any of the authors.

References

1. Nunes MC, Guimarães MH Jr, Diamantino AC, Gelape CL, Ferrari TC. Cardiac Manifestations of Parasitic Diseases. Heart. 2017;103(9):651-8. doi: 10.1136/heartjnl-2016-309870.
2. Posada-Martínez EL, Gonzalez-Barrera LG, Liblik K, Gomez-Mesa JE, Saldarriaga C, Farina JM, et al. Schistosomiasis & Heart - On Behalf of the Neglected Tropical Diseases and other Infectious Diseases Affecting the Heart (The NET-Heart Project). Arq Bras Cardiol. 2022;118(5):885-93. doi: 10.36660/abc.20201384.
3. van der Horst R. Schistosomiasis of the Pericardium. Trans R Soc Trop Med Hyg. 1979;73(2):243-4. doi: 10.1016/0035-9203(79)90227-x.
4. Edwards WM, O'Brien T. Constrictive Pericarditis [Internet]. New York: Medscape; 2021 [cited 2023 Apr 24]. Available from: https://emedicine.medscape.com/article/157096-print.
5. Adler Y, Charron P, Imazio M, Badano L, Barón-Esquivias G, Bogaert J, et al. 2015 ESC Guidelines for the Diagnosis and Management of Pericardial Diseases: The Task Force for the Diagnosis and Management of Pericardial Diseases of the European Society of Cardiology (ESC) Endorsed by: The European Association for Cardio-Thoracic Surgery (EACTS). Eur Heart J. 2015;36(42):2921-64. doi: 10.1093/eurheartj/ehv318.
6. Albakri A. Parasitic (Helminthic) Cardiomyopathy: A Review and Pooled Analysis Of pathophysiology, Diagnosis and Clinical Management. Med Clin Arch. 2019;3:1-13. doi: 10.15761/MCA.100 153.

Case Report

Behcet's Disease with Vascular Involvement: Case Report

Isabela Rodrigues Tavares,[1] Maria Cristina Miranda,[1] Ana Claudia Gomes Pereira Petisco,[1] Daniela Souto Barros,[1] Caio Buscatti Folino,[1] Vitor Leonidas Boher Dornas,[1] Mohamed Hassan Saleh,[1] Fábio Henrique Rossi,[1] Raquel Peres Sousa,[1] Larissa Chaves Nunes Carvalho[1]

Instituto Dante Pazzanese de Cardiologia,[1] São Paulo, SP – Brazil

Behçet's disease is an inflammatory, multisystemic, relapsing syndrome of unknown etiology. It involves heterogeneous clinical manifestations such as: recurrent oral ulcers, ocular inflammation, genital ulcers, and skin lesions. More severe manifestations may occur due to vasculitis of small and large arteries and/or veins with formation of arterial aneurysms or thrombosis, in addition to neurological or gastrointestinal involvement. Diagnosis is clinical and mainly symptomatic, and treatment may include corticosteroids with or without immunosuppressants and, eventually, other interventions for more severe manifestations.

Clinical case

Male patient, 34 years of age, previously healthy, admitted to the Emergency Room (ER) of *Instituto Dante Pazzanese de Cardiologia* reporting a 3-month history of pain in the right lower limb (RLL) and limping for distances of 100 meters in the 3 weeks prior to admission. The patient evolved with worsening pain in the right calf and spontaneous pulsatile bulging a week before admission. He mentioned the use of Rivaroxaban for deep venous thrombosis (DVT) in the RLL five months before, weight loss (15kg in 6 months), and appearance of aphthous lesions in the oropharyngeal region. He had a vascular ultrasound image from another service, with signs of DVT in a partially recanalized right popliteal vein.

On the occasion of admission, physical examination indicated: posteromedial pulsatile mass on the right leg and present pulses, except posterior tibial. Heart, lungs, abdomen, and left lower limb (LLL) without alterations.

A new vascular echography with Doppler of the RLL was performed, which showed a pseudoaneurysm of the tibioperoneal trunk (TPT), measuring 4.5 cm x 5.7 cm [anteroposterior (AP) X laterolateral (LL)] (Figures 1A and 1B), in addition to chronic post-thrombotic changes in the ipsilateral femoral and popliteal veins. An echocardiogram was also performed with patterns within normal limits. Endovascular treatment by bilateral puncture of the common femoral arteries was the elected therapeutics. TPT angioplasty was performed with a V12 tubular endoprosthesis (5 mm x 38 mm) and successful embolization of the D peroneal artery with an Interlock 2D occlusion system (4 mm x 8 cm – 2 units) was performed (Figure 1C). The patient was discharged with a prescription for Clopidogrel (75mg/day) and ASA (100mg/day); the use of Rivaroxaban was discontinued.

At the outpatient follow-up, after two weeks, the patient reported improvement in pain in the RLL, however accompanied by worsening of pain in the right foot, associated with paresthesia, coldness, and stable oral lesions. RLL pulses were present, except for the tibialis posterior with a slight thermal gradient in the right foot. A new vascular ultrasound examination showed occlusion of the TPT endoprosthesis (Figure 1D). Clinical follow-up and reintroduction of Rivaroxaban 20mg plus maintenance of ASA were carried out.

After 3 weeks, the patient was readmitted to the ER reporting a new, spontaneous, pulsating bulge in the right thigh, with progressive increase associated with significant pain at the site and impaired walking. The complaint of paresthesia in the right foot persisted. He also reported worsening of the aphthous lesions in the oral cavity and the appearance of ulcerated lesions in the scrotal region (Figures 2A and 2B). Physical examination indicated a large pulsating bulge in the distal right thigh and loss of pedal pulse. A new vascular echography with RLL Doppler was performed, which showed, in the right superficial femoral artery (RSFA), the presence of a pseudoaneurysm of the posterior wall, in the distal segment, measuring approximately 3.06 cm x 4.01 cm (AP x LL), in addition to another pseudoaneurysm measuring approximately 0.5 cm x 0.8 cm, 2.5 cm away from the femoral bifurcation, and two bulges in the posterior wall with apparent intimal rupture, maintaining the integrity of the adventitia. Images of partially thrombosed pseudoaneurysms were observed in the right (RCFA) and left common femoral arteries (LCFA) measuring approximately 1.1 cm and 1.0 cm, respectively. He also presented intraluminal hypoechoic material in the right femoral vein (RFV) and right popliteal vein (RPV), compatible with acute DVT. Ultrasound findings are shown in Figures 3A–F.

Laboratory tests: normal white blood cell count, hypochromic and microcytic anemia — Hemoglobin (Hb) = 10.9 g/dL, Mean Corpuscular Volume (MCV) = 75.9, Mean Corpuscular Hemoglobin Concentration (MCHC) = 31.5 —, C-reactive protein (CRP), erythrocyte sedimentation rate (ESR) and high fibrinogen (CRP = 25.2 mg/dL, ESR = 44mm/h, and fibrinogen= 636mg/dL); high values of oxaloacetic transaminase (TGO) = 233 U/L, pyruvic transaminase (TGP) = 153 U/L, gamma glutamyl transferase (GGT) = 490 U/L; and alkaline phosphatase (FA) = 264 U/L; negative serologies for hepatitis and syphilis.

Keywords

Behçet disease; Doppler ultrasonography; vasculitis.

Mailing Address: Ana Claudia Gomes Pereira Petisco •
Instituto Dante Pazzanese de Cardiologia. Rua Dr. Dante Pazzanese, 500. Postal code: 04012-909. São Paulo, SP – Brazil.
E-mail: anapetisco@outlook.com
Manuscript received February 6, 2023; revised manuscript February 11, 2023; accepted February 14, 2023
Editor responsible for the review: Simone Nascimento dos Santos

DOI: https://doi.org/10.36660/abcimg.20230014i

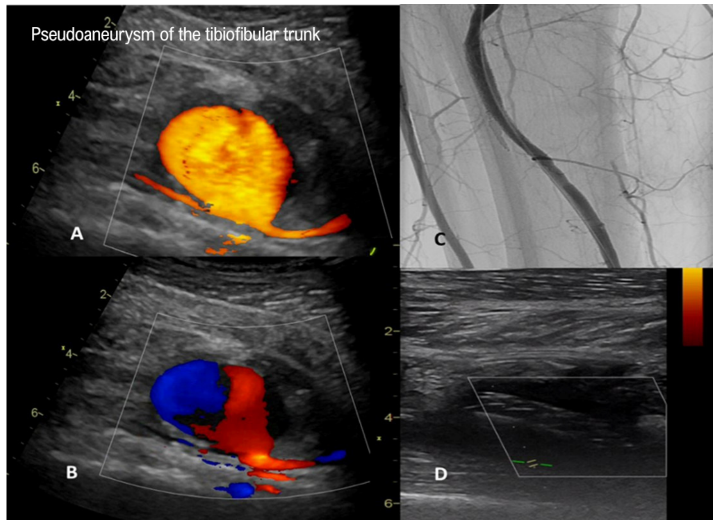

Figure 1 – *Pseudoaneurysm of the tibiofibular trunk. A) Power Doppler; B) Color flow mapping; C) Angiographic control after correction of the tibiofibular trunk pseudoaneurysm with endoprosthesis; D) Endoprosthesis occluded at USV in Power Doppler mode (two weeks later).*

Figure 2 – *A) Oral ulcerated lesions; B) Genital ulcerated lesions; C) Improvement of oral lesions after treatment with pulse therapy.*

The hypothesis of autoimmune vasculitis was suggested. Given the disease activity, no invasive investigation was performed at that time and a rheumatological evaluation was requested. Considering the arterial and venous involvement — arterial pseudoaneurysms and venous thrombosis, elevated inflammatory tests, and oral and genital ulcers —, the diagnosis of Behçet's disease was concluded. Pulse therapy with methylprednisolone and cyclophosphamide was onset. There was a reduction in symptoms, oral and genital ulcers, and inflammatory evidence after the first session (Figure 2C). In reassessment, after the second session of pulse therapy (30 days), a new intervention in RLL was indicated.

Endovascular treatment of the RSFA pseudoaneurysm was then performed with Viabahn Gore (7 mm x 100 mm), with good therapeutic results (Figures 4A-D). The patient had an uneventful postoperative period and was discharged from the hospital.

Discussion

Behçet's disease consists of a multisystem inflammatory process of unknown etiology characterized by recurrent episodes of oral and genital ulcers, other skin lesions, and ocular lesions. It was first described by Hulûsi Behçet in 1937 as a triad of oral, genital, and uveitis ulcers.[1]

Currently, it is known that the involvement goes beyond this triad and extends to several systems, including neurological, pulmonary, gastrointestinal, cardiac, articular, and vascular. Manifestations are not the same in all patients, clinical phenotypes are very heterogeneous and disease progression varies according to ethnicity, geography, and individual differences.[2]

The increase in evidence indicating the possibility of immunological mechanisms in the pathogenesis of the disease suggests an autoimmune etiology. Vascular alterations, for example, result from endothelial cell dysfunction caused by a probable immune-mediated reaction. Vasculitis appears to be the pathogenic basis of the various systemic manifestations.[3]

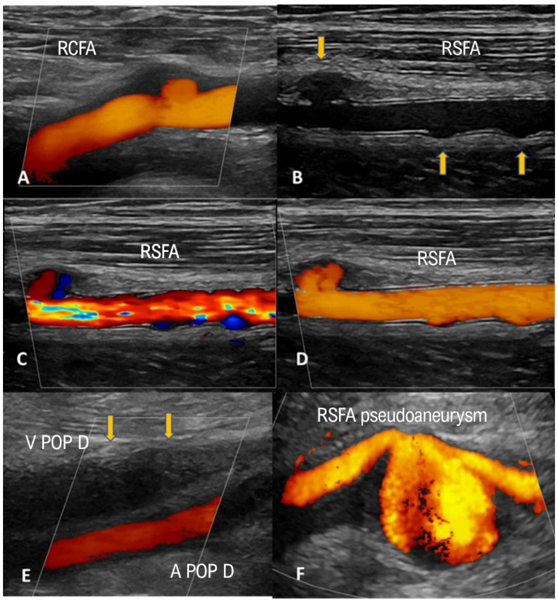

Figure 3 – *A) Pseudoaneurysm in RCFA; B, C and D) Small pseudoaneurysm on the anterior wall of the RSFA and two bulges on the posterior wall, with apparent intimal rupture; E) deep venous thrombosis of the right popliteal vein; F) Large pseudoaneurysm in RSFA. RCFA: right common femoral arteries; RSFA: right superficial femoral artery*

Series of patients confirmed that young men are more prone to vascular involvement of the disease.[2] Large vessel disease is one of the manifestations associated with systemic symptoms and laboratory evidence of acute phase response.[4] There is no specific laboratory test for Behçet's disease, but the presence of the HLAB-51 gene is suggestive of the disease.[2,4-6]

The arteries most affected by the formation of aneurysms are the pulmonary, femoral, iliac, aorta, and popliteal arteries. The main pathological findings in the aneurysm wall are: thickening of the adventitia, fibrosis, perivascular lymphocytic infiltration, decrease in muscle and elastic fibers in the media layer, and increase in spongy cells and fibroblasts in the intimal layer.[7] The inflammatory process is acute and causes destruction of the arterial wall, resulting in rapid formation of aneurysms or pseudoaneurysms, increasing the incidence of rupture and bleeding.[4]

Venous involvement is the most frequent (88%), while arterial involvement is responsible for a smaller number of cases (12%).[8] Venous thrombosis is the most common finding, which can occur in different territories and progress despite anticoagulation.[8] Thrombi, aneurysms or pseudoaneurysms can occur as complications of surgery or invasive procedures.[4]

Treatment is based on immunosuppression. Anticoagulants are used in the treatment and prevention of thromboembolic phenomena[9] and surgical or endovascular procedures may be necessary.

The use of endovascular repair has been increasing in Behçet's disease, with the aim of reducing complications resulting from surgical trauma. Surgical treatment in the acute phase of the disease is associated with higher rates of thrombosis and suture dehiscence.[5] It is suggested that the combined use of corticosteroids and immunosuppressants, and possibly the use of antiplatelet agents or anticoagulants, may be effective in reducing complications associated to the procedures.[4]

Aneurysms and pseudoaneurysms of the distal arteries are infrequent in these patients and each case must be evaluated individually. The literature describes few cases of

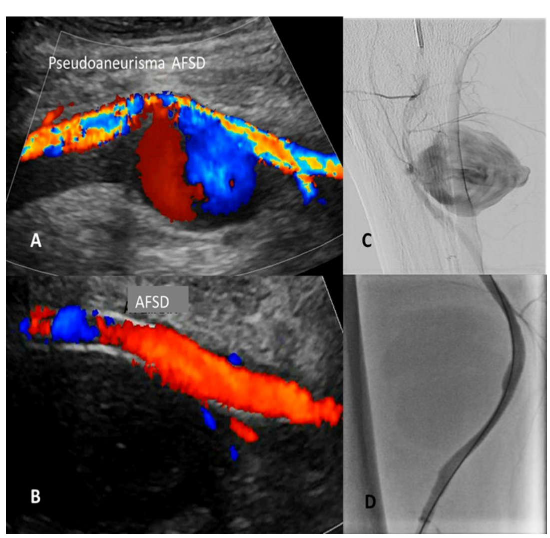

Figure 4 – *A) RSFA pseudoaneurysm on color flow mapping; B) Control vascular ultrasound (VUS) after endovascular treatment of the RSFA pseudoaneurysm; C) Angiography demonstrates RSFA pseudoaneurysm; D) Control angiography after endovascular treatment of the RSFA pseudoaneurysm.*

TPT involvement in Behçet's disease. The main advantage of the endovascular technique is that it is less invasive and allows access to the affected area from a different site, without direct manipulation.

Author Contributions

Conception and design of the research: Tavares IR, Petisco ACGP, Folino CB, Dornas VLBL, Saleh MH, Rossi FH, de Sousa RP; acquisition of data: Tavares IR, Miranda MC, Petisco ACGP, Barros DS, Folino CB, Dornas VLBL, de Sousa RP, de Carvalho LCN; analysis and interpretation of the data: Miranda MC, Petisco ACGP, de Carvalho LCN; statistical analysis: Tavares IR; writing of the manuscript: Tavares IR, Miranda MC, Petisco ACGP, Barros DS; critical revision of the manuscript for intellectual content: Petisco ACGP, Saleh MH, Rossi FH.

Potential Conflict of Interest

No potential conflict of interest relevant to this article was reported.

Sources of Funding

There were no external funding sources for this study.

Study Association

This study is not associated with any thesis or dissertation work.

Ethics Approval and Consent to Participate

This article does not contain any studies with human participants or animals performed by any of the authors.

References

1. Behcet H. Uber Rezidivierende Aphthose, Durch ein Virus Verursachte Geschwure am Mund, am Auge Und an Den Genitalien. Dermatologische Wochenschrift. 1937;105:1152-7.
2. Kokturk A. Clinical and Pathological Manifestations with Differential Diagnosis in Behçet's Disease. Patholog Res Int. 2012;2012:690390. doi: 10.1155/2012/690390.
3. Gürler A, Boyvat A, Türsen U. Clinical Manifestations of Behçet's Disease: An Analysis of 2147 Patients. Yonsei Med J. 1997;38(6):423-7. doi: 10.3349/ymj.1997.38.6.423.
4. Calamia KT, Schirmer M, Melikoglu M. Major Vessel Involvement in Behçet's Disease: An Update. Curr Opin Rheumatol. 2011;23(1):24-31. doi: 10.1097/BOR.0b013e3283410088.
5. Rico JV, Pedrajas FG, González IC, Iglesias RJS. Urgent Endovascular Treatment of a Ruptured Tibioperoneal Pseudoaneurysm in Behçet's Disease. Ann Vasc Surg. 2011;25(3):385.e11-4. doi: 10.1016/j.avsg.2010.10.012.
6. Brito C. Cirurgia Vascular - Cirurgia Endovascular: Angiologia. 4th ed. Rio de Janeiro: Revinter; 2020.
7. Alhan C, Çamur G. Pseudoaneurysm Repair in a Behçet Case Having Multiple Arterial Invasions. Turk J Thorac Cardiovasc Surg. 1999;7:344-6.
8. Akpolat T, Danaci M, Belet U, Erkan ML, Akar H. MR Imaging and MR Angiography in Vascular Behçet's Disease. Magn Reson Imaging. 2000;18(9):1089-96. doi: 10.1016/s0730-725x(00)00215-0.
9. Koo BK, Shim WH, Yoon YS, Lee BK, Choi D, Jang Y, et al. Endovascular Therapy Combined with Immunosuppressive Treatment for Pseudoaneurysms in Patients with Behçet's Disease. J Endovasc Ther. 2003;10(1):75-80. doi: 10.1177/152660280301000116

Aortocaval Fistula: A Rare Complication of Ruptured Abdominal Aortic Aneurysm

Karoline Evelyn Barbosa Gomes,[1] Eduardo Koltun Sanvesso,[1] Edwaldo Edner Joviliano,[1] Maurício Serra Ribeiro,[1] Elisa Helena Subtil Zampieri[1]

Departamento de Cirurgia Vascular e Endovascular, Hospital das Clínicas da Faculdade de Medicina, Universidade de São Paulo,[1] Ribeirão Preto, SP – Brazil

Aortocaval fistula is a rare complication of aortic aneurysm, occurring in approximately 0.2% to 6.04% of all abdominal aortic aneurysms.[1] It may occur in the context of aortic aneurysm rupture, aortitis, Ehlers-Danlos syndrome, Marfan syndrome, or penetrating abdominal trauma.[1,2] The classic clinical signs are abdominal pain, abdominal thrill, and symptoms of decompensated heart failure.[1] It is usually diagnosed via computed tomography angiography, and typical findings include early contrast enhancement of the inferior vena cava (prior to contrast of the renal and hepatic parenchyma) and retrograde enhancement of the renal or iliac veins.[1] Open surgical treatment has high associated morbidity and mortality, with reported rates of approximately 30%. With the advent of endovascular therapy, these rates have been reduced, with success rates as high as 96%.[3]

An 85-year-old male patient, with hypertension and history of tobacco use, was admitted to the emergency unit with a history of sudden onset of abdominal pain four days prior, associated with a pulsating abdominal mass in the hypogastric region. Tomography angiography of the total aorta was performed, showing a pararenal abdominal aortic aneurysm with a diameter of 11.5 cm, extending from the right renal artery to the aortic bifurcation, with signs of tamponade rupture into the retroperitoneum (Figure 1A), associated with an aortocaval fistula with a point of communication at the level of the iliac veins. In the tomography image, retrograde and early enhancement of the iliac veins was observed in the arterial phase (Figure 1B and 1C). During clinical evaluation, the patient presented hemodynamic instability, and an emergency surgical procedure was indicated. Intraoperatively (Figure 2), an aneurysm with signs of rupture was found, showing thrill on palpation. The patient evolved with refractory hypotension and died.

Aortocaval fistula is a rare complication of abdominal aortic aneurysm, and it is associated with high morbidity and mortality rates. Knowledge about it is highly important for suspected diagnosis, in order to improve patients' survival results.

Keywords

Arteriovenous Fistula; Aortic Rupture; Vascular Surgical Procedures

Mailing Address: Karoline Evelyn Barbosa Gomes •
Rua Tenente Catão Roxo, 3900, Vila Monte Alegre. Postal Code 14015-010. Ribeirão Preto, SP – Brasil
E-mail: karolineevelyn@gmail.com
Manuscript received December 6, 2022; revised December 14, 2022; accepted December 17, 2022.
Editor responsible for the review: Daniela do Carmo Rassi Frota

DOI: https://doi.org/10.36660/abcimg.2023369i

Author Contributions

Conception and design of the research and analysis and interpretation of the data: Gomes KEB, Sanvesso EK, Joviliano EE, Ribeiro MS, Zampieri EHS; acquisition of data: Gomes KEB, Sanvesso EK, Zampieri EHS; writing of the manuscript: Gomes KEB, Sanvesso EK; critical revision of the manuscript for intellectual content: Gomes KEB, Joviliano EE, Ribeiro MS, Zampieri EHS.

Potential Conflict of Interest

No potential conflict of interest relevant to this article was reported.

Sources of Funding

There were no external funding sources for this study.

Study Association

This study is not associated with any thesis or dissertation work.

Ethics Approval and Consent to Participate

This study was approved by the Ethics Committee of the HCFMRP-USP under the protocol number 68048223.7.0000.5440. All the procedures in this study were in accordance with the 1975 Helsinki Declaration, updated in 2013. Informed consent was obtained from all participants included in the study.

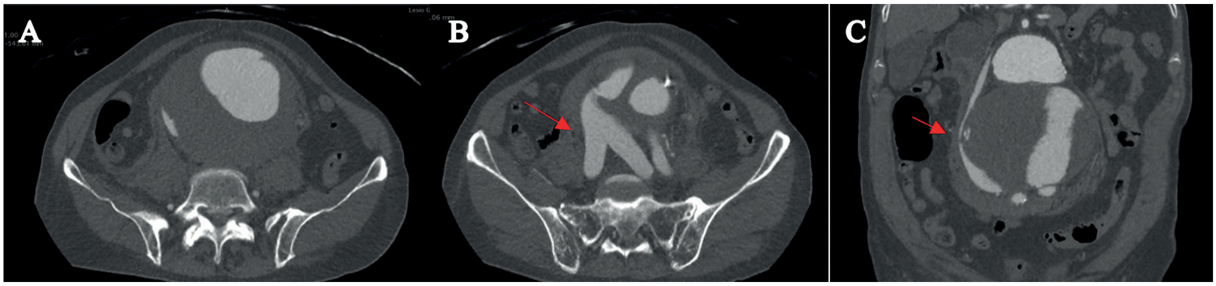

Figure 1 – *A) Abdominal aortic aneurysm with signs of tamponade rupture; B) retrograde and early enhancement of the iliac veins (arrow) in the arterial phase; C) abdominal aortic aneurysm compressing the inferior vena cava (arrow) showing early enhancement in the arterial phase due to an aortocaval fistula.*

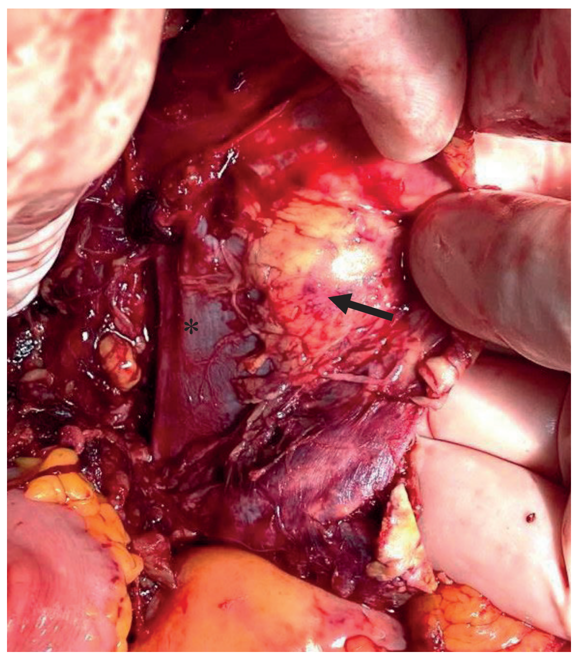

Figure 2 – *Intraoperative finding showing inferior vena cava (*) and aortic wall (arrow) in close contact with an area of aortocaval fistula.*

References

1. Lorenzati B, Perotto M, Bottone S, Tenconi G, Gazzina G, Cataldi W. Aortocaval Fistula. Intern Emerg Med. 2014;9(8):895-6. doi: 10.1007/s11739-014-1076-5.

2. Kashyap VS, Kumar A, Atallah PC, Warner C. Aortocaval Fistula. J Am Coll Surg. 2006;203(5):780. doi: 10.1016/j.jamcollsurg.2006.03.024.

3. Brightwell RE, Pegna V, Boyne N. Aortocaval Fistula: Current Management Strategies. ANZ J Surg. 2013;83(1-2):31-5. doi: 10.1111/j.1445-2197.2012.06294.x.

Review Article

My Approach To: Vascular Ultrasonography in Dolichoarteriopathies of the Carotid Arteries

Armando Luis Cantisano,[1] Catarina Schiavo Grubert[1]
Hospital Barra D'Or, Ecocardiograma,[1] Rio de Janeiro, RJ – Brazil

Abstract

This article provides step-by-step guidance on how I investigate, classify and evaluate dolichoarteriopathies anatomically and hemodynamically, often found in the carotid and vertebral arteries. Dolichoarteriopathies may be present in children, disappearing during growth and reappearing with increasing age. Previously considered benign anatomic variations (AVs), discussion has arisen on the topic in view of new implications due to associations with cardiovascular events, risk factors, and various pathologies.

Introduction

The internal carotid artery (ICA) usually runs a straight extracranial course in the parapharyngeal space to the base of the skull, without branching. It runs posterolaterally to the pharyngeal wall and the external carotid artery and medial to the internal jugular vein. However, the vessel may elongate to form tortuosity, coils, loops, and kinks. These anatomic variations (AVs), also called dolichoarteriopathies, are frequently found in the general population, ranging from 10% to 45%, with 5% of them being pronounced aberrations.[1-3]

Among AVs, kinking is the most prevalent. Women are predominantly affected by kinking and coiling, while both men and women are equally affected by tortuosity. The incidence rate of AVs increases with age and is particularly high in people over the age of 70 years. The peak prevalence has a bimodal characteristic, occurring in the youngest and oldest extremities, with a lower incidence between 21 and 60 years of age (Table 1).[3,4]

In children, AVs are often the reason for reduced cognitive and neuropsychological capacity, with developmental delay and presence of focal seizures or status epilepticus.[3,5,6] It is a sporadic congenital condition that, apparently, decreases and/or disappears with increasing age and body growth due to stretching of the aorta and supra-aortic trunk. In older people, however, dolichoarteriopathies may manifest due to senile crushing (eg, osteoporotic vertebral compression).[3,4]

Different hypotheses for the development of AVs include embryological and genetic causes and the presence of fibromuscular dysplasia (more closely related to coiling), as well as the process of atherosclerosis in patients with hypertension, diabetes and smokers (more closely related to kinking and tortuosity).[5-8] The ICA is normally coiled during intrauterine development, and straightening occurs as the fetal heart and great vessels descend into the mediastinum. If the descent is incomplete, coiling of the ICA occurs.[9]

There is an increased prevalence of kinking in patients with arterial hypertension, probably due to increased endoluminal pressure and parietal tension, favoring endothelial thickening and deformation. A more severe alteration in vessel wall elasticity may also be related to postmenopause in women due to the hormonal process, without excluding a bias associated with the larger number of comorbidities in men. This might explain the higher overall prevalence of AVs in women than in men aged 60 years or older.[10,11]

The carotid ultrasound study assesses ICA's morphological and atherothrombotic risk by observing alterations in arterial wall thickness and hemodynamic disturbance due to luminal narrowing, which may lead to turbulent blood flow, thus predisposing patients to stroke.[3] However, not all AVs lead to stroke, which occurs in 11% to 33% of cases with AVs.[6] Coiling and tortuosity cannot be considered risk factors for ischemic events due to their weak association

Table 1 – Prevalence of coils and kinks stratified by age decades

Age groups (years)	Patients undergoing ECD of ICA (2856) (n)	Patients with ICCK (284) (n)	Prevalence, % (ratio)	
0–10	208	39	18.8	15.2% (57/374)
11–20	166	18	10.8	
21–30	55	2	3.6	4.4 % (5/113)
31–40	58	3	5.2	
41–50	228	18	7.9	5.3% (36/682)
51–60	454	18	4	
61–70	777	59	7.6	11% (186/1687)
71–80	680	90	13.2	
> 80	230	37	16.1	

ECD : echo-color Doppler; ICA: internal carotid artery; ICCK: internal carotid coiling and kinking.
Table adapted from Luigi Di Pino et al.[3]

Keywords

Anatomic Variation; Carotid Arteries; Ultrasonography, Carotid Arteries

Mailing Address: Armando Luis Cantisano •
Hospital Barra D'Or, Ecocardiograma. Av. Ayrton Senna, 3079. Postal Code: 22775-002. Rio de Janeiro, RJ – Brazil
E-mail: alcantisano@gmail.com
Manuscript received April 7, 2023; revised May 9, 2023; accepted May 22, 2023
Editor responsible for the review: Simone Nascimento dos Santos

DOI: https://doi.org/10.36660/abcimg.20230034i

with cerebrovascular events. Kinking, however, even in the absence of atherosclerotic plaques, is more closely associated with the onset of events, being aggravated when combined with carotid stenosis.[4]

Cerebral ischemia occurs by two mechanisms: thromboembolic mechanism, resulting from endothelial lesions associated with blood flow stasis at the kink level and the occurrence of microembolization; and hemodynamic mechanism, which plays a role in both neutral and dynamic conditions. The smaller the angle formed between the kinked carotid segments, the greater the resistance to blood flow, which can worsen in conditions such as hypotension during sleep or flexion and/or extension of the head. Altogether, these situations may lead to vessel collapse at the point of greatest narrowing.[3,5,6]

Dolichoarteriopathies can be classified into 3 types, as shown in Figure 1:[2,6]

- Type 1: S- or C-shaped tortuosity of a non-rectilinear artery segment with an angulation > 90°;
- Type 2: a 360° angulation of an artery on its transverse axis in a circular or spiral shape (coil);
- Type 3: torsion of the inflection of 2 or more segments of an artery with an internal angle of ≤ 90° (kinking).

While Type 2 or coiling is attributed to embryological causes, the other two types are generally caused by the aging process with progression of atherosclerosis or by fibromuscular dysplasia.[11-13]

The anatomic classification of kinks using the Metz criteria is performed as follows (Figure 2):[6,8,13]

- Mild kinking: acute ICA angle between the two segments forming the kink, ≥ 60°;
- Moderate kinking: acute ICA angle between the two segments forming the kink, between 30° and 60°;
- Severe kinking: acute ICA angle between the two segments forming the kink, < 30°.

Kinks are common among patients with ischemic stroke, affecting both the intracranial and extracranial vasculature. The unfavorable anatomy of these vessels has been identified as an impediment to several types of endovascular treatment, such as ICA catheterization, leading to worse outcomes with increased revascularization time during thrombectomy. Alternative procedures include vessel resection and bypass grafting. Carotid stenting may also have its outcome quite impaired, since this device will further stretch the carotid artery, making a distal kink to become even more kinked. Twists and spirals are a contraindication to endovascular interventions because of the danger associated with passing a wire through an angled segment.[3,9,12,14] Carotid ultrasound is the gold standard for assessing extracranial circulation, has replaced carotid arteriography as a screening test for carotid artery occlusive disease, and has low cost, minimal risk, and good diagnostic accuracy.[4]

The use of intraoperative duplex ultrasonography in carotid endarterectomy has allowed the identification and repair of intraluminal residual defects, which may arise from the arterial reconstruction at the distal end of the repair and

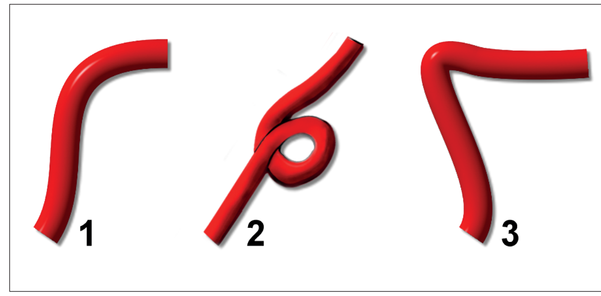

Figure 1 – *Classification of dolichoarteriopathies: Type 1, Type 2, and Type 3.*

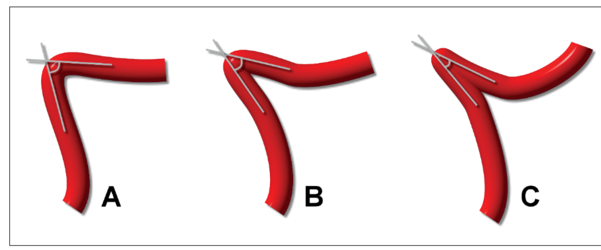

Figure 2 – *Anatomic classification of kinks. Mild kinking, angle between 60° and 90° (A); moderate kinking, angle between 30° and 60° (B); severe kinking, angle <30° (C).*

appear to result from hydrodynamic forces seen after primary closure of the arteriotomy.[15] The specificity of the method for predicting small ICA diameter, high carotid bifurcation, and a coiled or kinked carotid artery was 56%, 100%, and 100%, respectively. The presence of severe tortuosity of an artery, high carotid bifurcation, obesity or arterial calcification will reduce the accuracy of the ultrasound. This method can be improved with the use of high-frequency combined with low-frequency probes. This combination can provide an intuitive interface with a complete anatomic image of the artery for surgeons.

As it is a simple method that does not add risk or increase cost or discomfort for patients, the use of a convex probe is suggested as a complement to conventional ultrasound if necessary.[6,16,17] It is a noninvasive and effective method to easily detect vascular dysfunctions that allows us to assess the presence of AV-related submucosal masses in the posterior pharyngeal wall, which may be at risk for surgical injury to the oropharynx and laryngopharynx. Thus, it is possible try to predict cardiovascular events and complications during surgical procedures, both vascular and non-vascular, such as tonsillectomy, treatment of peritonsillar abscess, and adenoid surgery. Hence the great importance of careful and accurate examination prior to the procedure.[5,6,18]

Vascular ultrasound image acquisition technique with color flow mapping – "how I do it" step by step

1. Use a device with a multifrequency linear array transducer with frequencies greater than 7 MHz and color and power Doppler capability. Not infrequently, we need to use of a convex probe with frequencies ranging from 2 to 5 MHz in order to obtain an image

of the complete extent of the carotid alteration and reach a greater depth;

2. Lay the patient in the supine position with the head slightly hyperextended and rotated 45° away from the side to be examined;
3. Perform an axial and longitudinal scan from the origin of the common carotid artery to the most distal visible portion of the ICA, looking for any tortuosity;
4. Using pulse Doppler, color Doppler and power Doppler, detect blood flow and determine its direction, velocity, spectral waveform, and morphology;
5. Using spectral or pulse Doppler, record the peak systolic velocity (PSV), end-diastolic velocity (EDV), and resistance index in the common carotid artery, proximal ICA, and proximal external carotid artery;
6. Once an AV is identified, still using pulse Doppler, record the velocities before, inside, and after the curved portion, keeping the angle correction at 0° (Figures 3 and 4):

   a) PSV > 140 cm/s – hemodynamically significant parameter, suggestive of an approximately 50% diameter stenosis;

   b) PSV > 140 cm/s with EDV < 70 cm/s – hemodynamically significant parameters, suggestive of 50% to 69% diameter stenosis;

   c) PSV > 140 cm/s with EDV > 70 cm/s – parameter suggestive of 70% to 99% diameter stenosis.

7. Calculate the PSV ratio between two carotid segments (velocity at the kinking level divided by the velocity obtained at 2 cm proximal to the internal branch before the lesion).[3]

   If:

   a) Ratio < 1.5 → physiological or stenosis < 50%

   b) Ratio > 3.2 → stenosis > 60%

   c) Ratio > 3.3 → stenosis > 70%

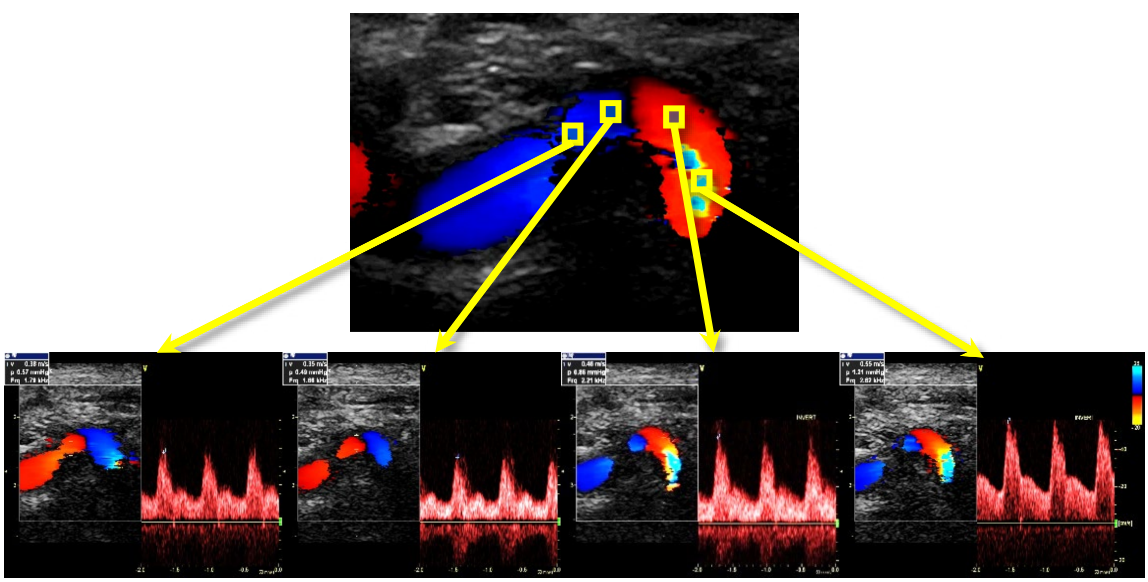

Figure 3 – *Mapping of velocities along the kinked segment, without angle correction in the region of kinking.*

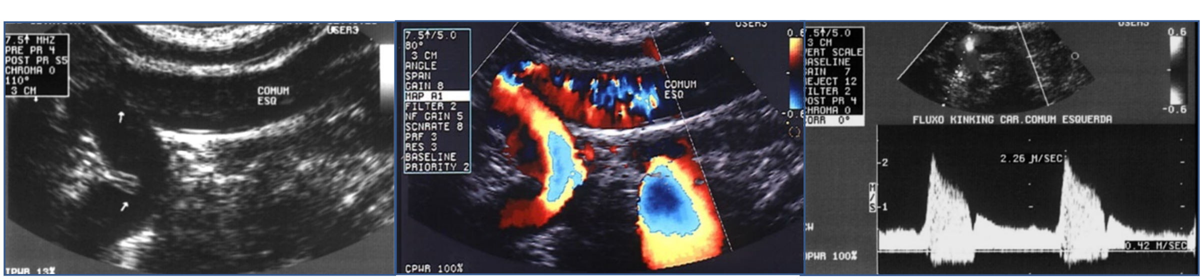

Figure 4 – *Stenotic kinking with a peak velocity of 2.26 m/s. The common carotid artery velocity before the kinked segment was 0.68 m/s. Ratio = 3.3.*

Technical pitfalls

In our service, we usually use a ratio of 2.5 for kinks with significant stenosis (above 60%), a criterion used for the serial assessment of the severity of peripheral arterial occlusion. It is important to note that a kink is considered occlusive only when it presents a significant increase in pulse Doppler velocities. The degree of kinking is not necessarily related to major occlusion (even with angles close to 0°). Also, the presence of turbulent flow on Doppler does not reflect the degree of stenosis, as it is found in all kinks, whether occlusive or not.

Dolichoarteriopathies can be located at the very beginning of the common carotid artery or at a great distance from the carotid bifurcation in the internal branch, requiring a scan of the entire length of the carotid artery from the base of the neck until it is no longer visible in the skull vault. Approximately 75% of the abnormalities are found at 2-4 cm proximal to the carotid bifurcation, but they are also seen more distally, as shown in Figure 5.[5,6] A possible presence of distal kinking in the internal branch should be considered when the opening angle between the internal and external carotid arteries is greater than 60° (Figure 6).

Coils can be found in different planes, requiring a "3D mental" map, with image acquisition in different axes, planes and angles of the neck for their composition and evaluation (Figure 7).

When associated with aneurysms, dilations, atheromatous plaques or thrombi in dolichoarteriopathies, the quantification of possible stenosis is even more difficult (Figure 8).

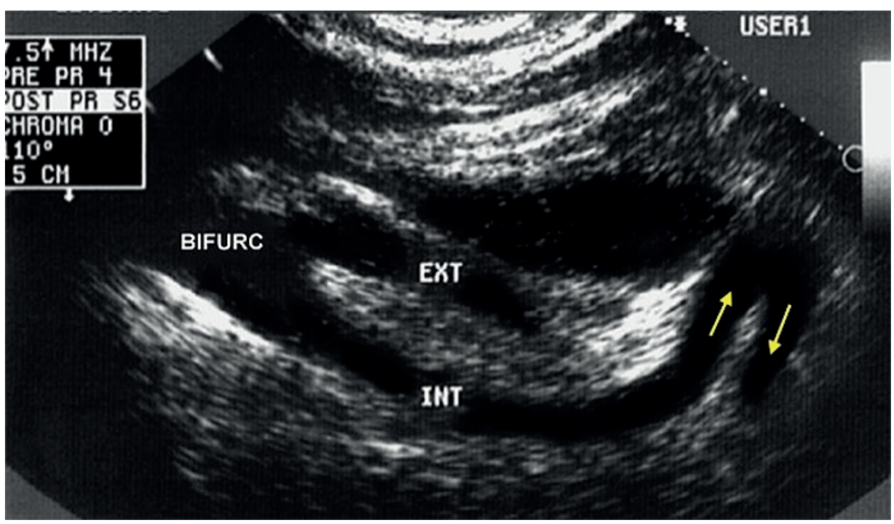

Figure 5 – *Kinking far from the bifurcation. Bifurc: carotid bifurcation; Ext: external carotid artery; Int: internal carotid.*

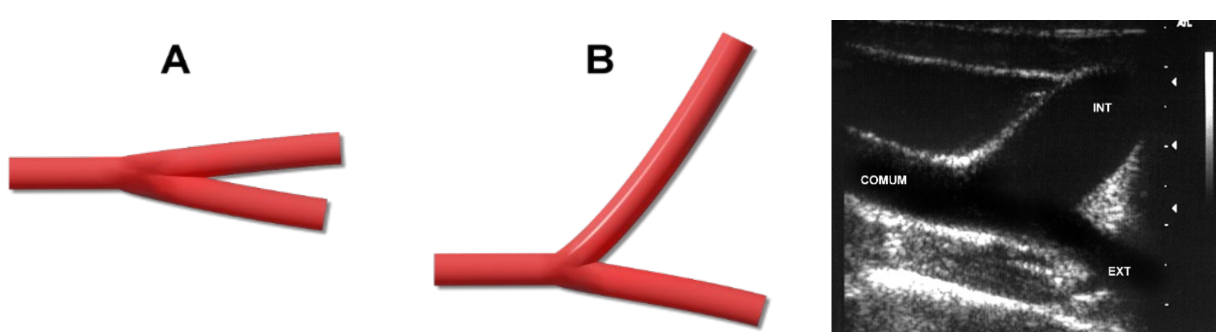

Figure 6 – *In the illustration, the angle formed between the carotid branches. A: small angle between the branches, which is more common; B: there is a greater probability of kinking, as the angle between them is >60°, as shown in the image on the right. Comun: common carotid; Ext: external carotid artery; Int: internal carotid.*

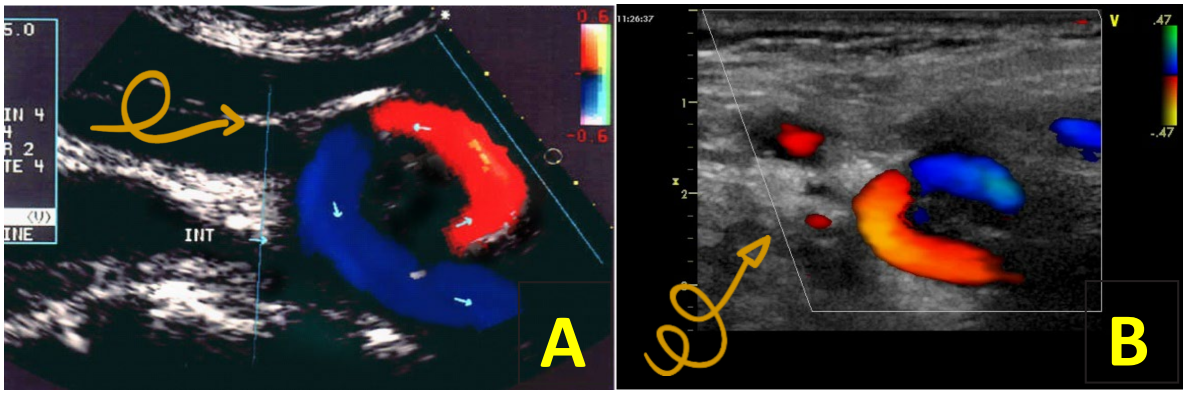

Figure 7 – Coil being built in two ways. A) circular, it appears entirely in the same plane; B) spiral, where its complete tracing is observed in several planes, requiring a scan with the transducer. Int: internal carotid.

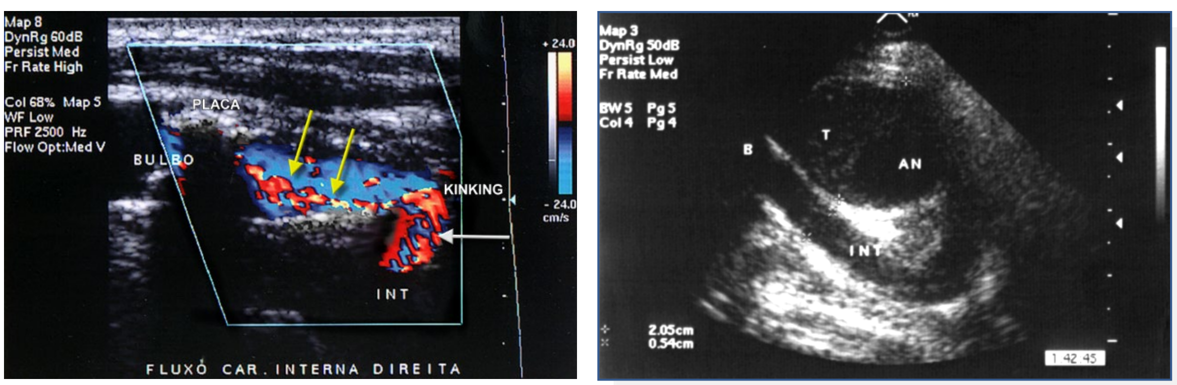

Figure 8 – *Associated conditions. A) occlusive atheromatous plaque preceding kinking (plaque turbulence, yellow arrows, mixes with kinking, white arrow); B) large internal branch aneurysm after kinking. Int: internal carotid artery; B: carotid bifurcation; T: thrombus; An: Aneurysm.*

Conclusion

Dolichoarteriopathies are frequently found in our clinical practice, whether in preoperative patients with non-vascular or vascular diseases, patients with stroke, and those with genetic diseases or in children with seizures, who require a detailed study of the entire course of the vessel in the search for anatomic abnormalities with turbulent flows and increased velocities.

Faced with a patient with a cerebrovascular condition, using the appropriate technique, we must actively search for these abnormalities, which may be responsible for the event and, thus, guide our decision on the optimal approach and treatment.

Author Contributions

Conception and design of the research, acquisition of data and critical revision of the manuscript for intellectual content: Cantisano AL; analysis and interpretation of the data and writing of the manuscript: Cantisano AL, Grubert CS.

Potential Conflict of Interest

No potential conflict of interest relevant to this article was reported.

Sources of Funding

There were no external funding sources for this study.

Study Association

This study is not associated with any thesis or dissertation work.

Ethics Approval and Consent to Participate

This article does not contain any studies with human participants or animals performed by any of the authors.

References

1. Pfeiffer J, Becker C, Ridder GJ. Aberrant Extracranial Internal Carotid Arteries: New Insights, Implications, and Demand for a Clinical Grading System. Head Neck. 2016;38(Suppl 1):E687-93. doi: 10.1002/hed.24071.

2. Beigelman R, Izaguirre AM, Robles M, Grana DR, Ambrosio G, Milei J. Are Kinking and Coiling of Carotid Artery Congenital or Acquired? Angiology. 2010;61(1):107-12. doi: 10.1177/0003319709336417.

3. Di Pino L, Franchina AG, Costa S, Gangi S, Strano F, Ragusa M, et al. Prevalence and Morphological Changes of Carotid Kinking and Coiling in Growth: An Echo-Color Doppler Study of 2856 Subjects between Aged 0 to 96 Years. Int J Cardiovasc Imaging. 2021;37(2):479-84. doi: 10.1007/s10554-020-02014-0.

4. Wain RA, Lyon RT, Veith FJ, Berdejo GL, Yuan JG, Suggs WD, et al. Accuracy of Duplex Ultrasound in Evaluating Carotid Artery Anatomy Before Endarterectomy. J Vasc Surg. 1998;27(2):235-42. doi: 10.1016/s0741-5214(98)70354-4.

5. Radak D, Babić S, Tanasković S, Matić P, Sotirović V, Stevanović P, et al. Are the Carotid Kinking and Coiling Underestimated Entities? Vojnosanit Pregl. 2012;69(7):616-9. doi: 10.2298/vsp110722001r.

6. Zenteno M, Viñuela F, Moscote-Salazar L, Alvis-Miranda H, Zavaleta R, Flores A, et al. Clinical Implications of Internal Carotid Artery Tortuosity, Kinking and Coiling: A Systematic Review. Romanian Neurosurgery. 2014;21(1)50-9.

7. Mercado MDCH, Mercado MDNH, Ceballos MDML. Role of Doppler Ultrasound in Carotid Kinking and Coiling: A Pictorial Essay and Brief Review. Int J Med Sci Clin Res. 2022;2(6):451-7. doi: 10.47191/ijmscrs/v2-i6-02.

8. Metz H, Murray-Leslie RM, Bannister RG, Bull JW, Marshall J. Kinking of the Internal Carotid Artery. Lancet. 1961;1(7174):424-6. doi: 10.1016/s0140-6736(61)90004-6.

9. Kayssi A, Mukherjee D. Fibromuscular Dysplasia, Carotid Kinks, and Other Rare Lesions. In: Hans SS, editor. Extracranial Carotid and Vertebral Artery Disease: Contemporary Management. Cham: Springer International Publishing; 2018. p. 225-39.

10. Martins HFG, Mayer A, Batista P, Soares F, Almeida V, Pedro AJ, et al. Morphological Changes of the Internal Carotid Artery: Prevalence and Characteristics. A Clinical and Ultrasonographic Study in a Series of 19 804 Patients Over 25 Years Old. Eur J Neurol. 2018;25(1):171-7. doi: 10.1111/ene.13491.

11. Sacco S, Totaro R, Baldassarre M, Carolei A. Morphological Variations of the Internal Carotid Artery: Prevalence, Characteristics and Association with Cerebrovascular Disease. Int J Angiol. 2007;16(2):59-61. doi: 10.1055/s-0031-1278249.

12. Benson JC, Brinjikji W, Messina SA, Lanzino G, Kallmes DF. Cervical Internal Carotid Artery Tortuosity: A Morphologic Analysis of Patients with Acute Ischemic Stroke. Interv Neuroradiol. 2020;26(2):216-21. doi: 10.1177/1591019919891295.

13. Iwai-Takano M, Watanabe T, Ohira T. Common Carotid Artery Kinking is a Predictor of Cardiovascular Events: A Long-Term Follow-Up Study Using Carotid Ultrasonography. Echocardiography. 2019;36(12):2227-33. doi: 10.1111/echo.14536.

14. Yu J, Qu L, Xu B, Wang S, Li C, Xu X, et al. Current Understanding of Dolichoarteriopathies of the Internal Carotid Artery: A Review. Int J Med Sci. 2017;14(8):772-84. doi: 10.7150/ijms.19229.

15. Yuan JY, Durward QJ, Pary JK, Vasgaard JE, Coggins PK. Use of Intraoperative Duplex Ultrasonography for Identification and Patch Repair of Kinking Stenosis after Carotid Endarterectomy: A Single-Surgeon Retrospective Experience. World Neurosurg. 2014;81(2):334-43. doi: 10.1016/j.wneu.2012.11.055.

16. Xiong JQ, Yu C, Shi YW, Li YH. Morphological Features of the Internal Carotid Artery: Advantages of Combining Linear and Convex Probes in Duplex Ultrasonography. Acad Radiol. 2013;20(10):1240-6. doi: 10.1016/j.acra.2012.08.018.

17. Murray CSG, Nahar T, Kalashyan H, Becher H, Nanda NC. Ultrasound Assessment of Carotid Arteries: Current Concepts, Methodologies, Diagnostic Criteria, and Technological Advancements. Echocardiography. 2018;35(12):2079-91. doi: 10.1111/echo.14197.

18. Kaplan ML, Bontsevich SV, Shilko SV. Role of Abnormalities at Pathologic Tortuosity of the Arteries in Development of Vascular Cerebral Insufficiency. Russ J Biom. 2015;19(1):5-19. 10.15593/RJBiomech/2015.1.01.